Pretensioned cable-strut roof

A study with parametric design and optimisation

Pic: iDNova

Xue Zhengyu
12-7-2016

TU Delft Delft University of Technology

octatube

BEM Next lab

Author

Name:	Xue Zhengyu
Student No.:	4403959
Telephone:	+31 617291483
Email:	xt92phoenix@gmail.com
University:	Delft University of Technology
Faculty:	Civil Engineering and Geosciences
Master Programme:	Building Engineering
Specialisation:	Structural Design
Company:	Octatube
Address:	Rotterdamseweg 200, 2628 AS, Delft, the Netherlands

Committee Information

Chairman

Name:	Prof.ir. R.Nijsse
Faculty:	Civil Engineering and Geosciences (TU Delft)
Section:	Building Engineering
Email:	R.Nijsse@tudelft.nl

Supervisor

Name:	Dr.ir. J.L.Coenders
Faculty:	Civil Engineering and Geosciences (TU Delft)
Section:	BEMNext Lab
Company:	White Lioness technologies
Email:	jeroencoenders@white-lioness.com

Name:	ir. S.Pasterkamp
Faculty:	Civil Engineering and Geosciences (TU Delft)
Section:	Building Engineering
Email:	S.Pasterkamp@tudelft.nl

Daily supervisor Octatube

Name:	L.A. Weber
Company:	Octatube
Address:	Rotterdamseweg 200, 2628 AS, Delft, the Netherlands
Section:	Design and Engineering
E-mail:	L.Weber@octatube.nl

Name:	M.V. van Telgen
Company:	Octatube
Address:	Rotterdamseweg 200, 2628 AS, Delft, the Netherlands
Section:	Design and Engineering
E-mail:	m.vantelgen@octatube.nl

谨以此书献给我的父亲母亲。

Preface

Presented here is the Master's thesis for the graduation work at the Faculty of Civil Engineering and Geosciences, in Delft University of Technology. The subject of the graduation project is:

Pretensioned cable-strut roof; A study with parametric design and optimisation.

Accomplishment of this graduation work and the final thesis means a completion of my two-year life overseas for pursuing the Master degree. Normally, I should be excited and thrilled, or be in blue and unwilling to say bye to this experience. Instead, I am very calm. Graduation is just a completion of this period of life. I'll soon come to the next stage of life, full of energy and with no fear. For the past two years, I have lived my life, I experienced a lot and gained far more than expected. When I was a student in university, I devoted myself to the study and projects. I finished all the mandatory courses and exams in the first year. For the second year I didn't waste a single day in Octatube. Looking back on the past, I am really grateful to many.

First of all, I would like to express my gratitude to my daily supervisor, Mr. Luis Weber, who offered me the opportunity of doing this research in Octatube and supervised me throughout my graduation. His trust and encouragement gave me great freedom to explore after my own instinct. He always gives me immediate and patient help both theoretically and technically with his vast knowledge on almost every aspects of steel structures. In China, we use the word "shifu" to describe the teacher who is like your father outside home. Luis is my shifu, friend and boss. Without him this work could not have been possible. I am also very thankful for my other supervisor in Octatube, Mr. Michael van Telgen. In the literature study, I've learned a lot about tensegrity from his Master's thesis. And during my design process, Michael offered me great help and support by guiding me through variable study with great patience.

My graduation committee in the university have to be thanked for the time and effort they spent. Among them, I would like to thank Prof. Rob Nijsse for his helpful advice on lifecycle assessment, for his guidance on every committee meeting, and for his support to me to finalize this thesis work. Dr. Jeroen Coenders is thanked for leading me into the world of programming and giving me instant reply to emails and remarks on my reports even in the evening. It is always great to meet and talk to him. Thanks also goes to Mr. Sander Pasterkamp, for the inspiring discussions during the committee meeting and for his valuable advice on the detailing part.

Outside the committee I am still in great debt to many genius. An exceptionally complex parametric model in the environment of Grasshopper has been made for this design work. Special thanks go to Mr. Peter Fotiadis, architect and CEO in Greece, for offering me reliable and brilliant support in scripting with C# in Grasshopper and also for some smart connections which has great adjustability. I would also appreciate the great help from Mr. Yarko Yurechko, SDC verifier in Ukraine, for technical support about programming with Vb in Femap. I had no basic about programming before the graduation project, without their help the completion of this graduation work should last months longer.

Appreciation also goes to my colleagues in Octatube. I want to thank Mr. Koos Fritzsche for his smart plug-in and for his guide in programming. I am very grateful for Mr. Peter van de Rotten. He has very rich

knowledge in pretensioned cable structures and taught me how to apply pretension in real construction with great patience. Also the big brother Mr. Wouter van der Sluis, for his care and all the shares during break. And Mr. Joey Janssen for his advice and for helping me read Dutch newspaper.

I also would like to thank Dr. Qingpeng Li, he cares a lot about my academic progress and always encourages me to behave better. And Dr. Roel Schipper has to be thanked for a lot of help during the past two years. And all my friends in TU Delft owns my sincere thanks. We experience the life here, share our joys and sorrows, and witness the progress of each other. You make my life here not only academic research. The thanks also goes to Tianqi Fei, for the piano and beers.

A special acknowledgement goes to Hsia, with whom I had the best moments in the Netherlands. Many people you meet overseas should be like the blinking stars, after intersection they cannot be found from then on afar. But something true never fades and shall exist eternal in the memory.

Last but the most important, I would like to give my greatest gratitude to my parents, for their endless and unconditional love through my life. All the work presented in this book is the fruit of their support. Therefore, I would like to dedicate this thesis to my father and mother.

Zhengyu Xue

July 1,2016

Delft, the Netherlands

Summary

Chapter 1 Introduction

Tensegrity corresponds to a structural principle consisting of discontinuous struts and continuous pretensioned cables forming a 3D system (*Jan De Boeck, 2013*). The impressive character of tensegrities like light-weight and transparency leads to the increasing popularity of its application in civil engineering and architecture. In this Master's thesis project, a roof system with a combination of tensegrity and beam structures has been designed for the opening of Het Gelders Huis (*Het Gelders Huis, 2015*), Arnhem, the Netherlands. The influences of the possible variables in the design of a tensegrity have been investigated and the results give a light-weight roof structure which satisfies both serviceability limit state (SLS) and ultimate limit state (ULS) check under large asymmetric loads. A parametric model has been built for this design work and the final model has been determined after optimisation.

Chapter 2 Methodology

To find out the influence of changing the variables in the design of this roof system and make a good design, a methodology has been set up. This chapter introduces the methods used in the design process in order to make the parametric model and do optimisation.

Chapter 3 Study of pretensioned structures

This chapter is based on the study of the existing theory and application of tensegrities. To find out the mechanical theory behind this complex 3D roof structure, the cable-strut system was simplified and investigated. In Chapter 3, the single element was analysed locally and then the matrix was transformed and combined to find the equation for the entire system. Case study and reference projects show how engineers have found solutions to apply pretensioned cable-strut system for a roof. All in all it is the factors determining the stiffness of the structure that matters to the structural performances. These factors are: material use, sectional size, shape of structure, element length, and amount of pretension.

Chapter 4 Preliminary design – Variable study

In the preliminary design, firstly the load combinations and boundary conditions have been defined. Within the boundary conditions the possible variables in this roof design have been chosen and classified into different orders with regards to their influences on the structure. Then a model which satisfies both SLS and ULS check has been designed and chosen as the standard model, based on which all the changes have been made. In this variable study, there are always three variables studied at the same time: the chosen variable, pretension, and cross section.

It is very complex to design such roof structures due to the interdependence of variables. In essence, it is the required minimum pretension that matters. Pretension is essential in guaranteeing stiffness and maintaining stability of the cable system. Increasing pretension from a low value may bring increase of stiffness to the tensegrity system. However, the higher pretension in cables requires larger cross sections for strut and hoop to resist axial stresses and the risk of buckling. In the variable study, the minimum pretension is controlled within 0kN to 10kN. The variable study gives indications in the following aspects:

- Increasing the number of branches does not necessarily lead to larger mass in a certain group of elements considering the application of smaller cross section.
- The model with vertical struts has better load transfer path thus smaller bending occurs which allows the application of smaller cross sections for strut and hoop beams.
- The model with shape of cable net from radial loads has the smallest total mass.
- Changing the depth of cable net brings almost no difference to the total mass. However, increasing the depth of cable net leads to a stiffer structure.

Chapter 5 Detailed design

In this chapter, Karamba and Galapagos have been used to optimise pretension and cross sections. The required cross sections from Karamba are similar to those from Femap, which proves the possibility to use programs to find the minimum required pretension and proper cross sections which satisfy unity check for this roof structure. Then buckling check has been done for the compression hoop. For the final model, additional load cases like 10kN test load and load from the climber due to maintenance have been taken into account. Also three failure modes have been simulated to evaluate the redundancy. The roof structure has been divided into pieces by considering the limit of transportation. Supports and connections have been designed with regards to increasing the possibility of reuse and recycling.

Chapter 6 Construction

For the construction of the roof structure, all the elements will be prefabricated in the factory and then assembled on site. The most important part is pretensioning of the cables. The possible factors that may result in loss of pretension should be considered carefully and the lost amount needs to be compensated to guarantee enough pretension. Hydraulic jacks will be used with the specially designed connection for cable and hoop. Pretension will be applied at the same time for all the cables and the hydraulic jack with pressure guage will ensure the right amount of preloading in cables. With cranes, the components will be lifted and placed on the right position. Sequences of construction have been defined in this chapter.

Chapter 7 Conclusions and Recommendations

At the end of the thesis an answer has been given to the research question in the beginning. With literature study, the theory behind and possible variables for the cable-strut system have been found. By means of parametric modeling it is possible to change the variables and find their influences on the structure. Optimisation with Femap and making loops with Karamba prove that it is possible to reduce mass of the structure without sacrificing the structural safety and stiffness.

For the design of a cable-strut roof system, future improvements can be made by making the structure asymmetric. Influence of fatigue and dynamic loading is also recommended to be considered to determine resilience of the structure. If the allowable maximum deflections for the tensegrity are given, the structural requirement could be updated and the cable-strut system can be made with less pretension thus possibly less material and thus mitigated impact on environment.

Table of Contents

Chapter 1 Introduction

Chapter 2 Methodology

Chapter 3 Study of pretensioned structures

Chapter 4 Preliminary design – Variable study

Chapter 5 Detailed design

Chapter 1

Introduction

1 Abstract

Since the appearance of the first tensegrity structure during the last century, many artists and engineers have tried to explain what a tensegrity exactly is. Precise boundaries have not been established (*Jan De Boeck, 2013*). All definitions however agree that it is a combination of tension and compression being in equilibrium and creating an ensemble (*Jan De Boeck, 2013*). A relatively sound definition of tensegrity given by René Motro (*Motro René, 2003*) is:

> "A tensegrity system is a system in a stable self-equilibrium state comprising a discontinuous set of compressed components inside a continuum of tensioned components."

Currently, the definition of tensegrity is subjected to controversies partially due to a large variety of forms developed. All these controversies ignored, tensegrity systems can be defined from structural point of view:

> "Tensegrity systems are free-standing pin-jointed networks in which an interconnected system of cables are stressed against a disconnected system of struts or extensively, any free-standing systems composed of tensegrity units satisfying the aforesaid definition. " (*Wang bin bing, 2004*)

In this research, the pretensioned cable-strut systems are taken as tensegrity systems under the above definition. Different system types of the tensegrity roof will be investigated. All the structures contain three main components: tension elements, compression elements, and ring systems.

The tensegrity roof structure has some major advantages:

- Large stiffness-to-mass ratio
  A compressive member loses stiffness as it is loaded, whereas a tensile member gains stiffness as it is loaded. Hence, a large stiffness-to-mass ratio can be achieved by increasing the use of tensile members (*R.E. Skelton, 2001*).
- The roof is light-weight with high efficiency of material use.
  Tensegrity structures use longitudinal members arranged in very unusual (and non-orthogonal) patterns to achieve strength with small mass.
- Aesthetics
  Tensegrity structures have special architectural aesthetics.

Recent years a lot of atriums, football stadia, and glass curtain walls have applied tensegrity as load-bearing structures. Examples of these types are:

- Canopy Prinsenhof (Delft,1997) (*Mick Eekhout, 1997*)
- Droogbak (Amsterdam,1999) (*J. van Stigt, 1999*)
- Bancopolis (Madrid,2005) (*Kevin Roche, 2005*)
- Headquarters Banco Santander (Madrid,2009) (*Alfonso Millanes, 2009*)

Due to the mentioned advantages of tensegrity structures, there is an increasing interest in this type of roof structure.

Key Words: Tensegrity, Form Finding, Parametric Design, Structural Optimisation, Pretension

1.1 Problem description

In this research, a structurally safe, light-weight and engineering practical cable-strut roof structure will be designed based on the opening in Het Gelders Huis, Arnhem, the Netherlands. The self-weight of steel structure, dead loads of roof cladding, connections, and other possible technical installations, and variable load from wind are all small compared to the relatively large snow load. In winter, the snow accumulates on three sides of the rectangular roof due to high walls around. Moreover, the suction from wind will also bring stability problem to the relatively light-weight roof structure.

The design of a light-weight but structurally safe tensegrity structure is quite a complex affair due to the large number of parameters, conditions and possibilities. Changing the parameters manually and evaluating the structural performances to find a better structure would be quite laborious and time-consuming. To build a parametric model helps the design and selection process, at the same time maintain the design freedom, has the practical significance to considerably decrease the time and cost needed for design, but also increase the quality of design.

Possible variables in the design of a tensegrity structure are:

Table 1 Variables in the tensegrity roof design(*M.V. van Telgen, 2012*)

Order	Variable	Choice/Domain
1st	Cable net shape	Rectangular or circular
2nd	Number of cables and struts	Depends on system type
3rd	Height above support Height below support	2000mm<D_{top}<2400mm 2000mm<D_{bottom}<2600mm
4th	Pretension	50kN<F_p<500kN
5th	Sectional size of elements	Depends on elements and locations

1.2 Aim of the research

The aim of the research is to find answers to the challenges described in the problem description. The main research question can be defined as:

> *How to design a high efficiency light-weight cable-strut roof structure which satisfies both SLS and ULS check under large asymmetrical snow load and upward wind suction load?*

Efficiency in this context is defined as: a cable-strut roof structure that requires the minimum amount of material, also the material should be highly reusable after the lifecycle of this roof structure.

To find an answer for this problem, a wide range of aspects need to be investigated. By dividing the research question into various sub-questions, it is clear where the effort should be devoted to.

The sub-questions that will be investigated are listed as follows:

1. What are the design variables? What are the influences of changing variables that may exist in the design of a given shaped cable-strut structure?
   There are different design variables that influence the final design of the structure. The influences will be investigated. A parametric design tool will be created to enable the variant studies.
2. Is it possible to use the software to find the minimum pretension and proper cross sections with high efficiency of material use? What will happen to the structure after optimisation?
   After the investigation of different variables, more optimisation options will be looked for. And see if it is possible to optimise the tensegrity structure automatically in order to find the minimum required pretension and proper cross sections without sacrificing the structural safety and stiffness. Here proper cross sections means the leading elements in each group (see Figure 45) have the utilisation between 0,7 and 1,0.
3. How does the supports and connections look like in this roof structure?
   The choice of type supports and connections influences the structural behaviour of the roof system. In real construction, the supports and connections should have the same DOF as in the FEM to guarantee enough stiffness and stability of the structure.
4. What is the construction and installation process of a pretensioned roof structure?
   The construction process could be labour-intensive because all the cables must be kept under tension to guarantee the stiffness and load path. The assembly sequence of this cable-strut roof system and how to apply prestress to the pretension cables will be investigated.
5. What is lifecycle assessment (LCA) and how to apply LCA into this roof system?
   By doing investigation into lifecycle assessment, methods can be found to reduce the environmental impacts of this structure during its whole life.

To provide a good answer, an efficient structural design of a cable-strut roof will be made. Through the research and design of such a structure, insight and knowledge will be gained about this type of roof structure. With the design and research of this pretensioned cable-strut roof structure, the sub-questions and eventually the main research question can be answered. The conclusions and recommendations can be used for the future design of a pretensioned cable-strut roof structure.

1.3 Boundary conditions

For the research project a design of a rectangular cable-strut roof structure will be studied in order to gain knowledge and insight about this structure. The roof is surrounded by higher walls on three sides. The dimension of the roof is about 34m*34m. Above the tensegrity there is a pneumatic ETFE cushion.

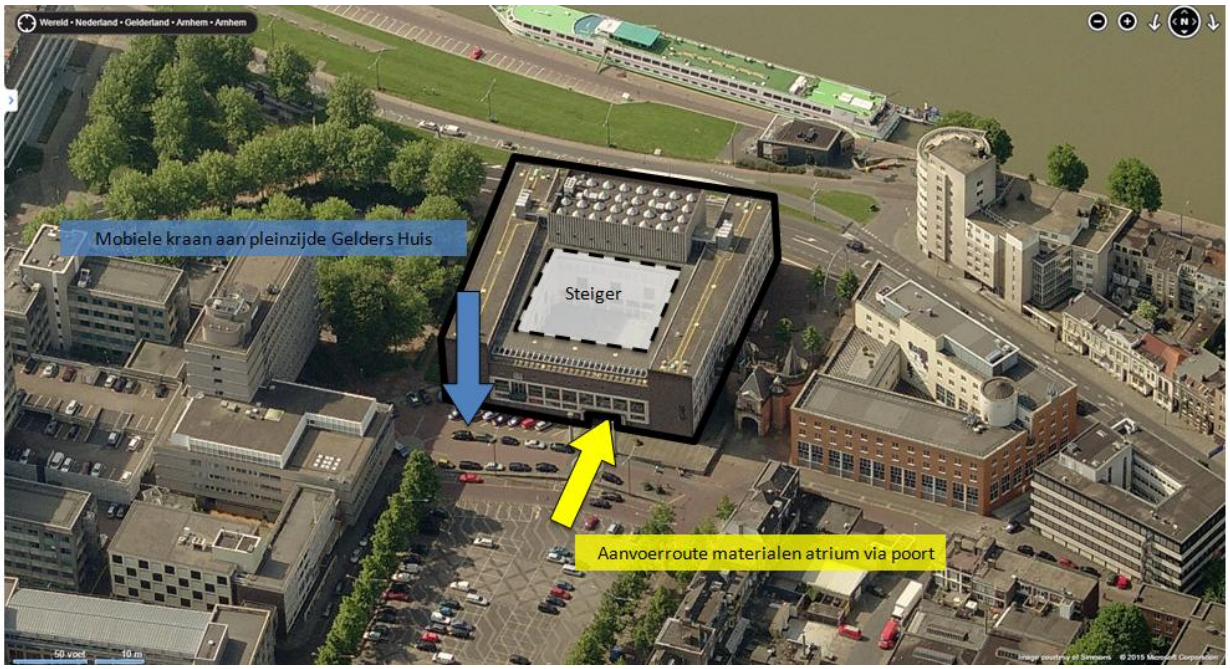

Figure 1 Het Gelder Huis (***Simmons, 2015***)

1.4 Motivation for the study

1) Parametric design can save significant time when changing variables in the design phase.
   By making the tensegrity model in Grasshopper and developing some GH components with Visual Basic or C#, the design variables are able to be modified in a parametric way, then the designer can find out what will happen to the structure by connecting the GH file with FEM software to do static analysis. This is much handy than deleting elements and rebuilding them in FEM software thus saves significant time.
2) In a real project, optimisation of the structure enables potential weight reduction and mitigated impacts on the environment.
   By performing unity checks, enough strength and high efficiency of material use will be guaranteed. Less material use means reduced self-weight and smaller impact on environment due to material manufacture and maintenance.
3) Through well-founded design considerations the structural safety and possibility of construction are guaranteed.
   There are a large quantity of variables in such a cable-strut roof structure. The aim of the variable study is to find the influences of the possible design variables and take the most influential ones into consideration in the structural design. Also the detailed design of connections makes it possible to assemble the steel elements on site.

1.5 Thesis outline

In this graduation work, first literature study has been performed to gain knowledge and insight about the roof structure. Second with the programming and scripting skills some design components based on the Grasshopper environment have been developed to build a parametric model. Based on the parametric model, a lot of FEM analysis have been performed. With the above steps a model which satisfies both SLS and ULS check has been designed and chosen as the standard model, based on this model the variable study has been conducted. Details of supports and connections have been designed with regards to lifecycle assessment. Methods for pretension and construction have been elaborated.

With all the design phases above, a final design of the pretensioned cable-strut roof has been accomplished with some conclusions and recommendation.

Study of pretensioned structure

This chapter gives the research about pretensioned structures. The theory of slender structures, the property and application of tensegrity as roof structures are described followed by the analysis of reference projects. The structural concept is determined last in this chapter.

Methodology

In order to translate the structural concept into a parametric model with its boundary conditions, form finding with Kangaroo is the starting point to determine the shape of the cable net. Also a plug-in is made to communicate between Grasshopper and Femap for easier FEM analysis. In the optimisation stage, Karamba is used to form a loop and optimise the cross sections and pretension.

Preliminary design – variable study

In this chapter, first the load combinations and other boundary conditions have been determined. Within the boundary conditions the possible variables of this roof design have been listed. Then a model which satisfies the SLS and ULS requirements has been designed and chosen as the standard model, based on which all the changes have been made. After the research on the possible design variables, the influences of each variable have been found.

Detailed design

After the preliminary design, Karamba and Galapagos have been used to build a loop to optimise pretension and cross sections. The hoop system has been designed with buckling taken into account. Then the final design has been made, and three failure modes have been simulated. In this chapter, also the supports and connections have been designed in detail with lifecycle assessment taken into account.

Construction

Construction is quite important for the pretensioned structure. This has already been taken into account in the connection design. In this chapter, the method for pretension and the assemble sequence have been investigated and depicted in detail.

Conclusion and recommendations

The last chapter gives conclusions and recommendations which answer the main question of this thesis.

Chapter 2

Methodology

2 Methodology

The methodology can be described as six steps:

1) Literature study of tensegrity structures and structural optimisation.
2) Mathematics, mechanics, and scripting studies are needed to develop the methods and tools.
3) Structural concept elaboration and variant study for a tensegrity roof structure.
4) Translation of the concept into a parametric model with its boundary conditions.
5) Combine the optimisation tool and the structural concept of the tensegrity roof.
6) FEM analysis of the design.

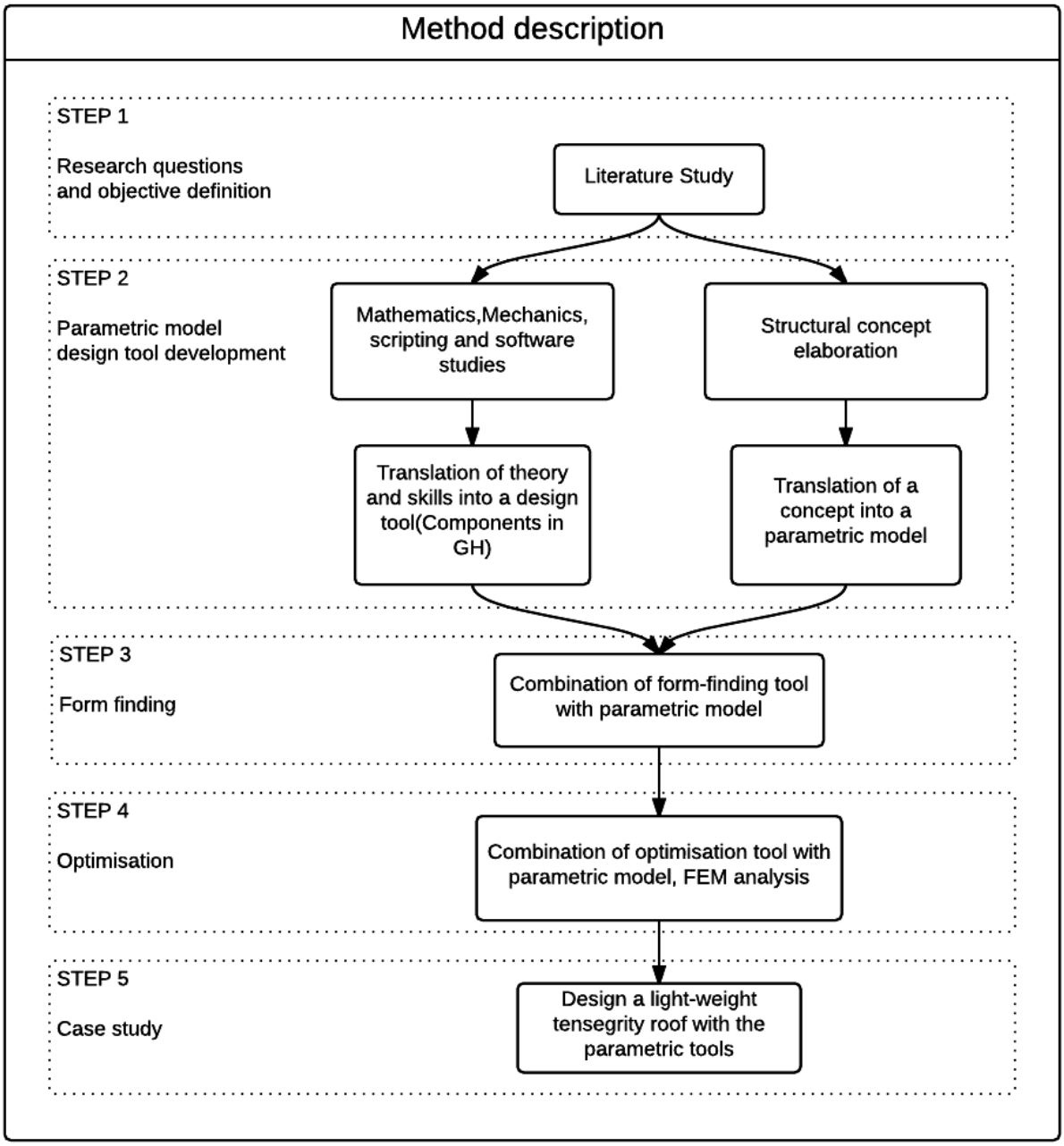

Figure 2 Method description

In this chapter, first the methods for form finding, parametric design and optimisation have been introduced in detail, then the Grasshopper components made by programming and scripting have been introduced with their functions in design.

2.1 Form finding

Performance of tensegrity depends largely on the shape and node locations. Before the designing of this roof structure, it is of great importance to find a shape with good structural performance (here good performance means certain amount of stiffness) under the specific external loads.

The most famous application of form finding in architecture is the Sagrada Familia (*Wikipedia, 2016*), designed by Antoni Gaudi. He used hanging models to predict the shape of his building with different loads from sand bags. By mirroring the tension model, he obtained a completely opposite shape, which is the shape of his brick structure under compression.

Figure 3 Sagrada Familia scale model (***Sophie's mazes, 2007***)

Nowadays the concept of form finding is universally used in structural engineering (*Wikipedia, 2016*). Form finding has become a generic term to describe the process that shapes the form of a structure under the defined load combinations and boundary conditions (*Piscitelli, G., 2015*). The goal for form finding is to get the optimal geometry of the structure.

Different ways for form finding will lead to different forms of the shape. Force density method (*Schek, H., 1974*) is used here to find the shape of the cable net.

Force density method (*Schek, H., 1974*)

Force density method is used for tensile structures based on the concept 'Form Follow Force'. The process starts with defining internal and external forces and all further structural constraints, then use the FEM to search for the equilibrium of all external and internal forces resulting in a form with minimal strain energy (*De Boeck, J., 2013*). The strain energy given by normal force acting on a cable is:

$$E_{C,N} = \frac{N^2 \times l}{2 \times E \times A} \tag{2.1}$$

Three types of forces are applied in this form finding process.

1) Gravity

Figure 4 Form finding by self weight

2) Vertical point load

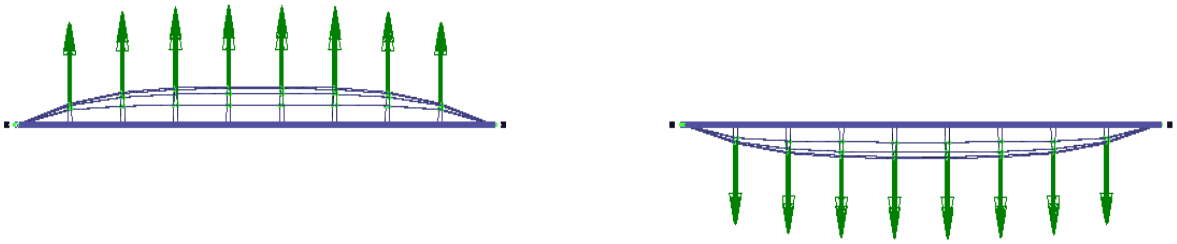

Figure 5 Form finding by vertical point load

3) Radial point load

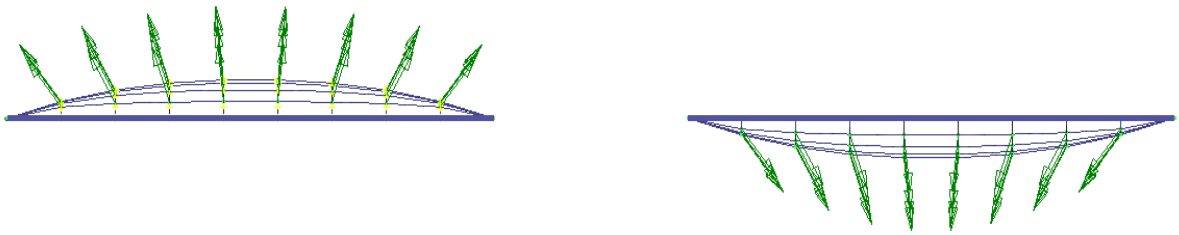

Figure 6 Form finding by radial point load

2.2 Parametric design

Parametric design, also known as parametric and associative design, is a set of concepts which occur in novel design systems, such as GenerativeComponents (*Computational Design Software, 2016*), Grasshopper (*Grasshopper, 2016*), of which parameters and associations are the two foremost concepts (*Coenders, J.L., 2011*). In parametric design, parameters or variables can be edited to manipulate or alter the end result of an equation or system (*Wikipedia, 2016*). To build a parametric model can save a lot of time in the design of this cable-strut roof. In every parametric design, the designer builds his models parametrically with his basic structural concepts and boundary conditions. After a working model is obtained, the designer is free to modify the predefined parameters or variables, and the model will immediately display the graphic output.

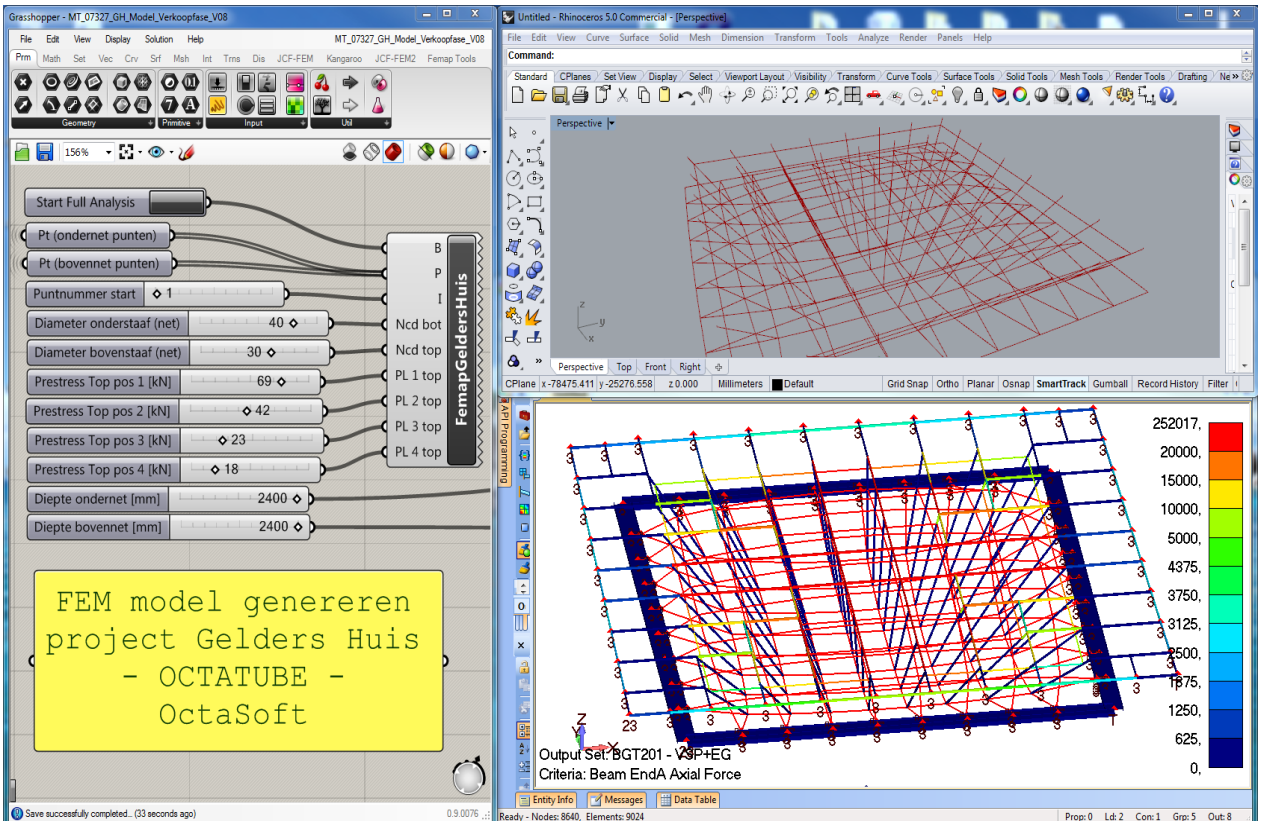

Figure 7 Parametric design (*M.V. van Telgen, 2015*)

In this research project, parametric design is defined into two parts, first part is to build a parametric model with geometry only in Grasshopper. Second is to export the geometric model from Grasshopper to the FEM software Femap to do static analysis. With some special components developed to accurately communicate between Grasshopper and Femap, not only the geometry, but also constraint, loads, and some other commands in Femap can be defined in Grasshopper environment.

Parametric design can save significant time due to some major advantages:

1) It is easier to detect errors in the parametric model thus mistakes can be avoided. In the parametric model, we can immediately see the graphic output when changing a possible variable or parameter. This helps tremendously in error detection.
2) Modifications and adaptations can be made at any time due to the flexible nature of parametric models. For this graduation work, the design of the cable-strut system first start with a model with fixed geometry. Then the possible variables are listed and made adjustable with defined boundaries in the parametric model. Therefore, a parametric design can start with a simple model, and then improvements can be added and make the model flexible with deeper insight of the structure.
3) FEM calculation is controlled by the parametric model and results can also be read and displayed in the interface of the parametric model. This means that the design and FEM analysis are conducted with separate software but the designer can manipulate within one interface, and some complex commands are combined into one with some special components developed by programming and scripting. This saves significant time for the analysis.

However, it is not easy to make the design properly modelled. First is that the designer need to have a clear idea about how to organize the algorithm. Second, the numerous components with different functions tend to confuse the designer. In the parametric model, errors can easily be detected because the designer can get immediate graphic output when changing the parameters, but it is very hard to find where the error is in a complex parametric model. Another disadvantage is that programming and scripting skills are required to make some components in Grasshopper with special functions.

All in all, comparing the advantages and disadvantages for parametric design in the long run, more preparation may quicken the speed in doing work. Alternatively, many more variants can be investigated in a short time, and the plug-in and scripted components can be used in the future design.

2.3 Optimisation

In optimisation (*Slobbe, G., 2015*) parameters of the variables that lead to an optimal value of the result are searched. Structural optimisation is usually categorized into three classes (*P.W. Christensen, 2009*): topology, shape, and size optimisation. It is common that optimisation fulfills multiple classes partially.

1) Topology optimisation: it searches for a structural shape within a given region. It is usually considered in the conceptual design phase. For a tensegrity, a topology optimisation searches for the optimal connectivity and node locations.
2) Shape optimisation: it tries to transform a given structural shape into a more optimal one. Especially parametrically designed shapes can be optimised by this technique. In this case, a shape optimisation changes the height of cable net above and below support.
3) Size optimisation: it looks for the optimal cross sections for a given design. If a structural shape is known and can be divided into several parts, a size optimisation can be used to optimise the individual cross sections for the benefit to the structure as a whole.

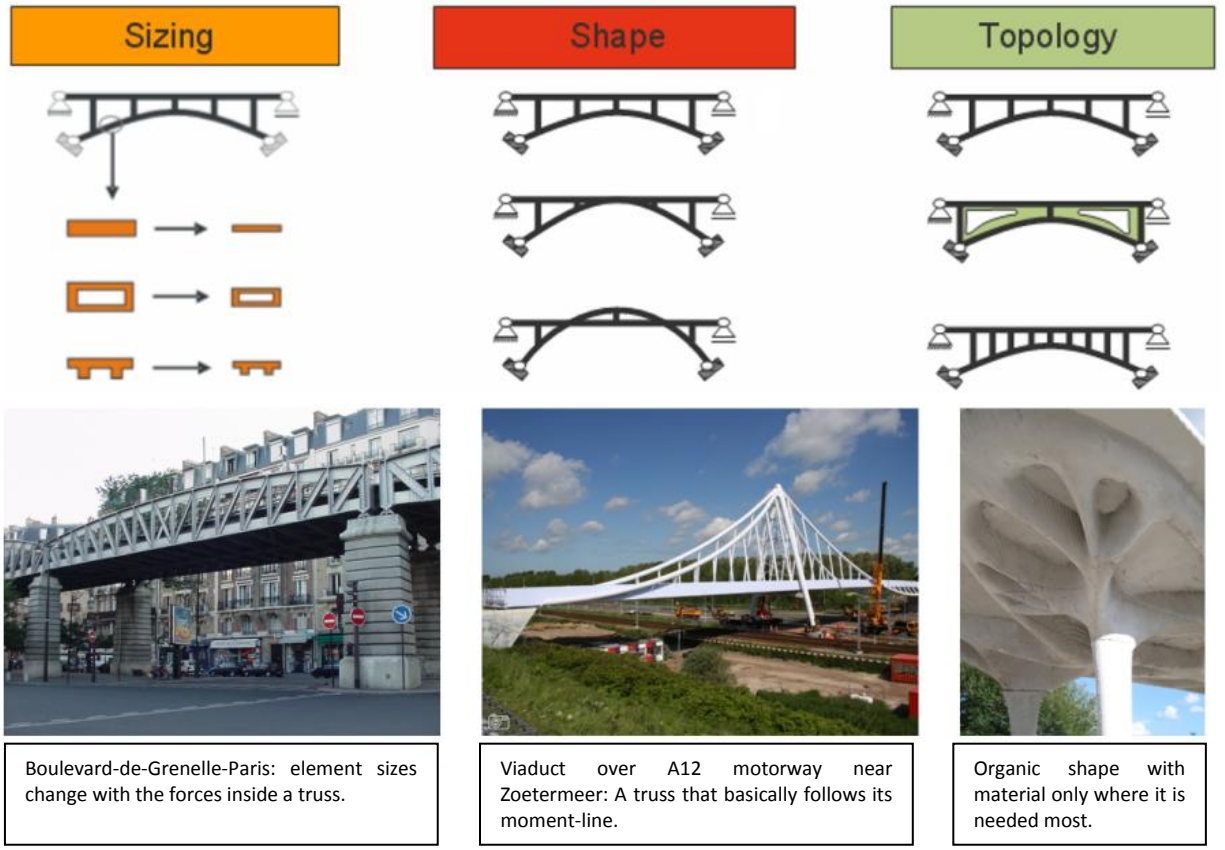

Boulevard-de-Grenelle-Paris: element sizes change with the forces inside a truss.

Viaduct over A12 motorway near Zoetermeer: A truss that basically follows its moment-line.

Organic shape with material only where it is needed most.

Figure 8 Three types of optimisation (*Slobbe, G., 2015*)

In this design, even when a parametric model is available for this cable-strut system, it is very difficult to do optimisation of the structure because of the interdependence both between variables and elements. To make the design as reliable as possible, manual optimisation with Femap and generic optimisation with Glapagos and Karamba based on the model decided from variable study are conducted and the results are compared.

2.4 Plug-in GH-FEM

For the parametric design, a special plug-in is required to communicate between the geometric modeling software Grasshopper and the FEM software Femap (*Femap*). It is also possible to simply export the geometry in Rhino (*Rhinoceros*) to AutoCAD (*AutoCAD*) , and then import the DXF file to Femap to do FEM. However, this takes several steps and cost pretty much time considering the large number of models to be analysed. With the special plug-in, all the geometric modeling and FEM calculations can be controlled in Grasshopper and the designer can get the results in a minute.

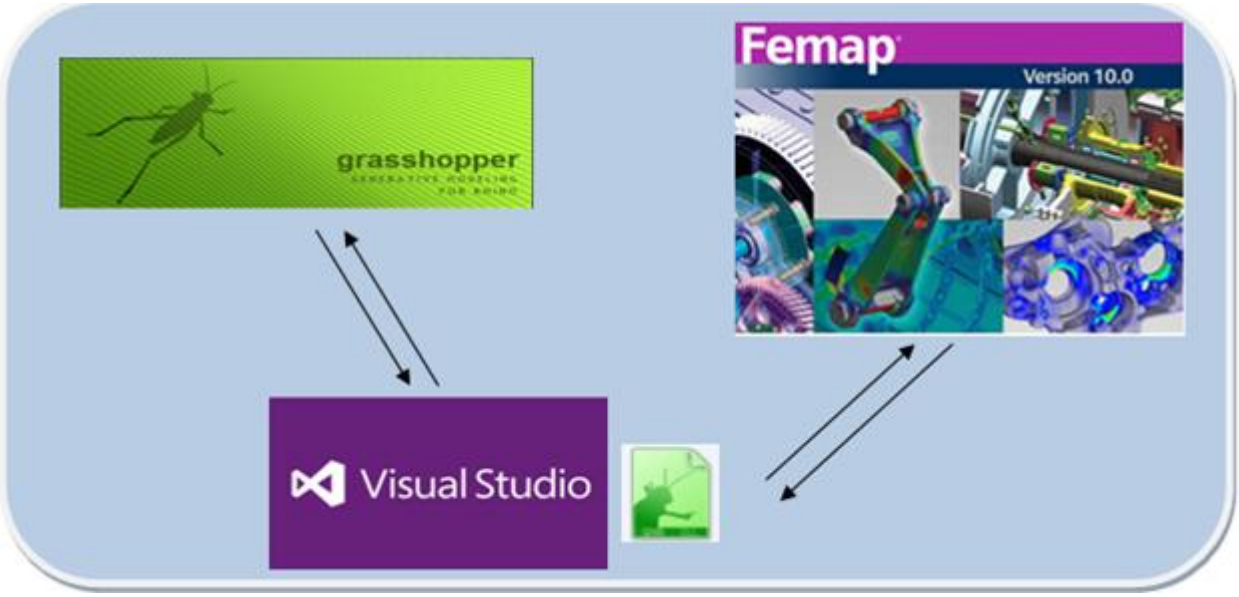

Figure 9 Plug-in between Grasshopper and Femap

The Grasshopper plug-in is developed in Visual Studio (*Visual Studio*) with the programming language Visual Basic (*Visual Basic*). Each plug-in contains a lot of Grasshopper components with different functions for specific design purposes. It is quite difficult to start learning programming with zero basis but tends to be easier with increasing understanding of the programming language.

Luckily, there is already such a plug-in FemGrassVBA (*Koos Fritzsche, 2015*) being developed by Octatube. Some components can be used in this research project. The specially developed plug-in GHToFem with additional components can be a supplement for the existing plug-in.

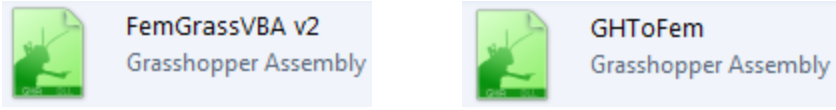

Figure 10 Grasshopper Assembly

The used components from the plug-ins are listed in Figure 11. The components marked with orange are used from FemGrassVBA, and those marked with grey are developed for this graduation work. The plug-in with different components aims to communicate between Grasshopper and Femap and can be used in any design with the mentioned software. The used components from plug-ins are:

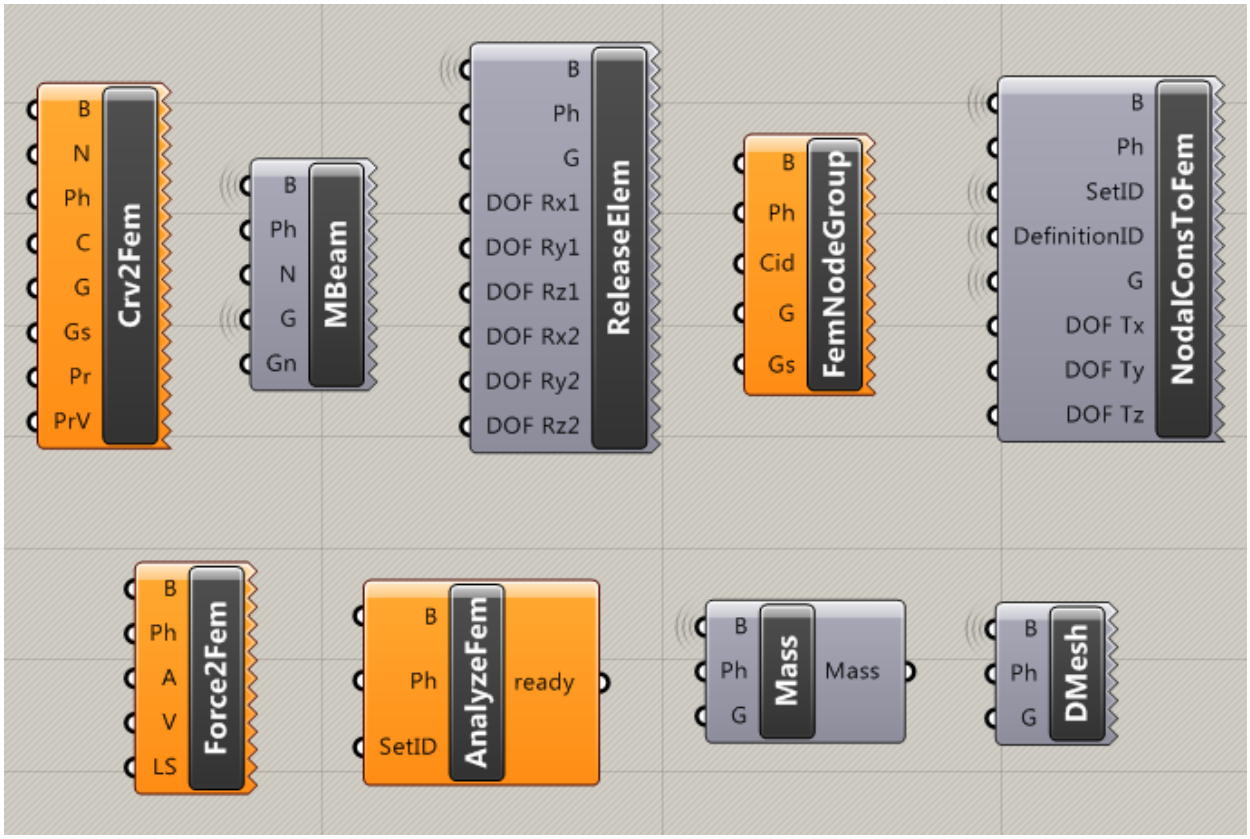

Figure 11 Components from plug-in

1) Crv2Fem

This component functions to export the geometric model from Grasshopper to Femap. At the same time, the designer can group the list of curves and give the same property and orientation to all the curves in the same group. Orientation means the direction of elements in FEM. The property should be predefined manually in Femap.

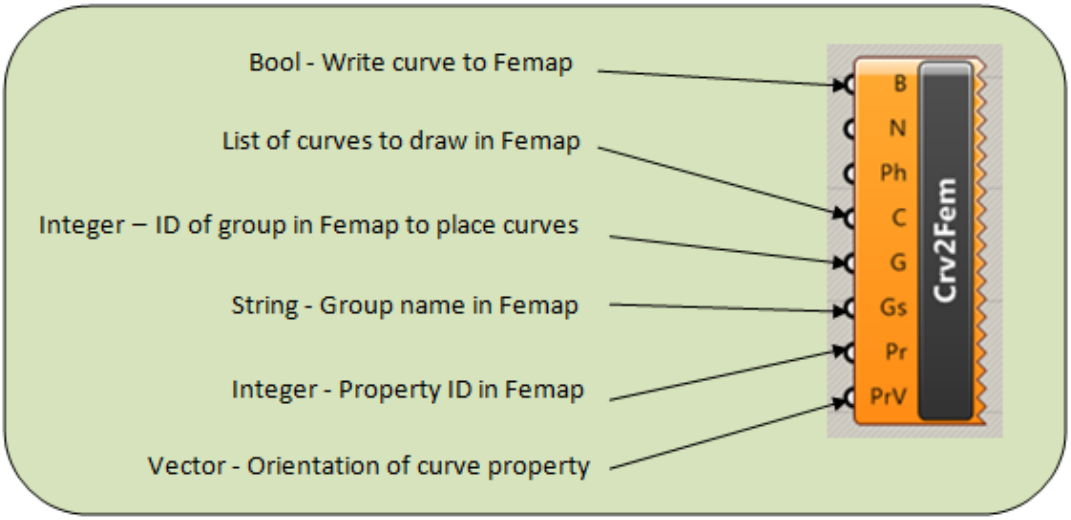

Figure 12 Component - Crv2Fem

2) MBeam

This component can control Femap to do mesh for the curves with defined number of elements for each curve. Mesh here means to generate finite elements in FEM with defined property and element length. The meshed elements can be put into the defined groups.

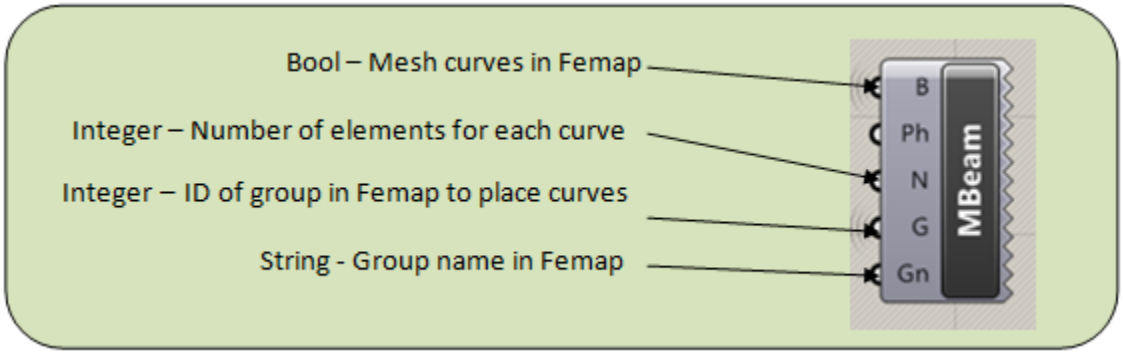

Figure 13 Component – Mbeam

3) ReleaseElem

In the Femap model, the connection of different elements are considered as fixed by default. The ReleaseElem component can make hinges in the model. This component has the function to release both ends of the elements in a defined group, and the designer can decide the DOF to release according to the design.

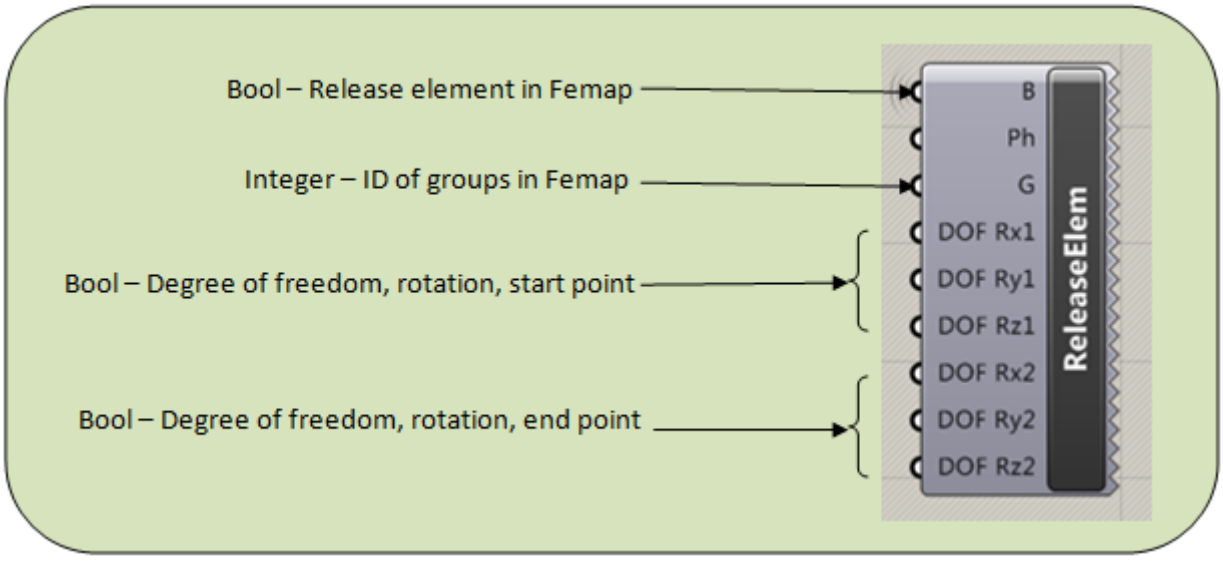

Figure 14 Component - ReleaseElem

4) FemNodeGroup

Nodes in Femap can be put into defined group with this component. In Femap, changes can be applied to a group of elements or nodes which saves lots of time.

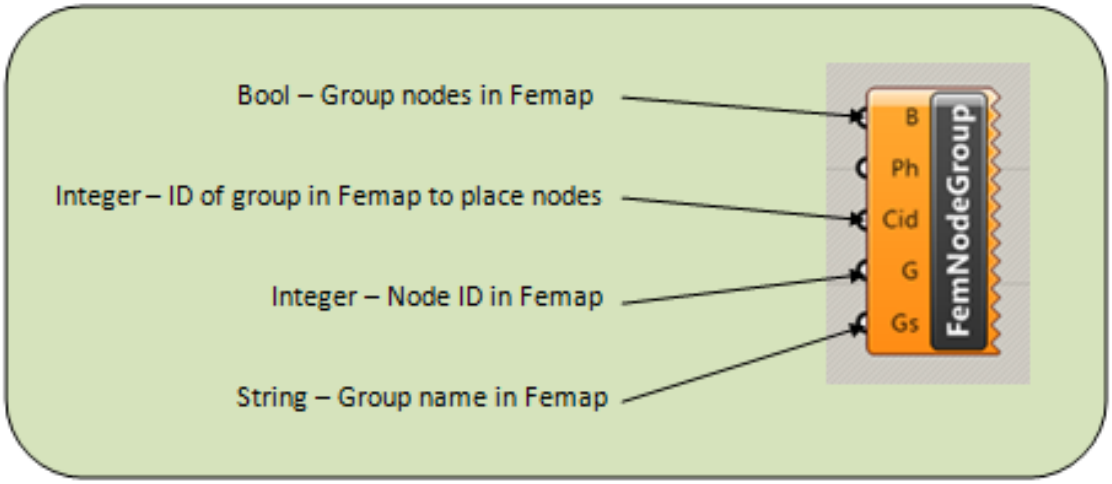

Figure 15 Component FemNodeGroup

5) NodalConsToFem

The component defines nodal constraints for all the nodes in the chosen group, the designer can decide the DOF of translation to restrict. In FEM, constraints are applied to nodes to restrict the movement of elements. The created constraints can be put into a defined group.

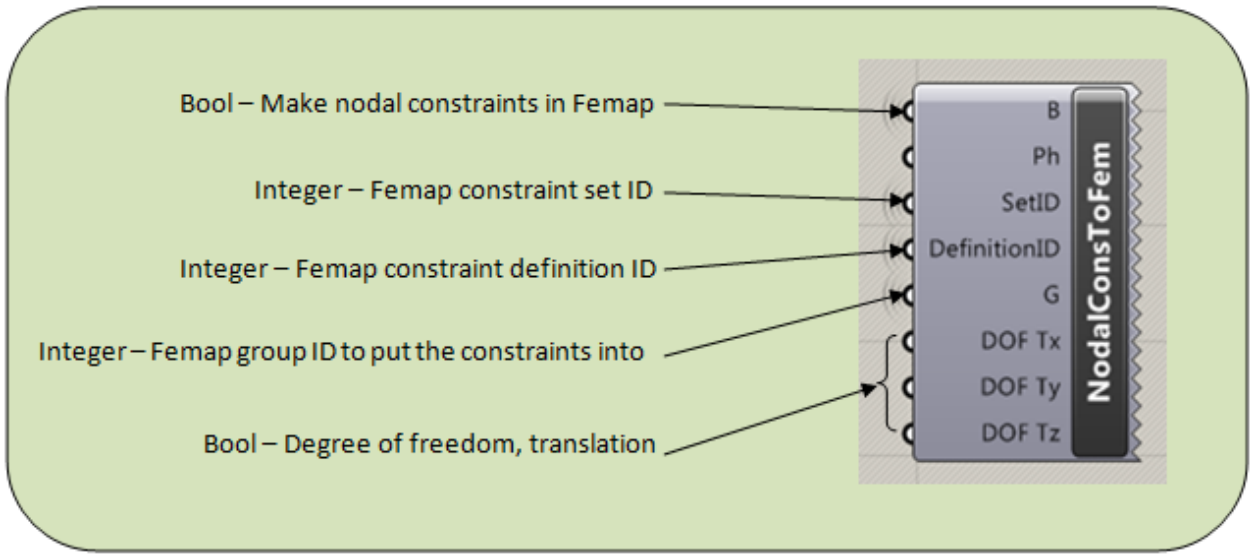

Figure 16 Component NodalConsToFem

6) Force2Fem

In the optimisation with Karamba (*Karamba 3d*) and Galapagos (*Galapagos*), the area load from snow and wind are transformed into point loads which are firstly taken by the connection points of the ETFE Beam grid. The component Force2Fem functions to define point loads in Grasshopper and write them to the model in Femap.

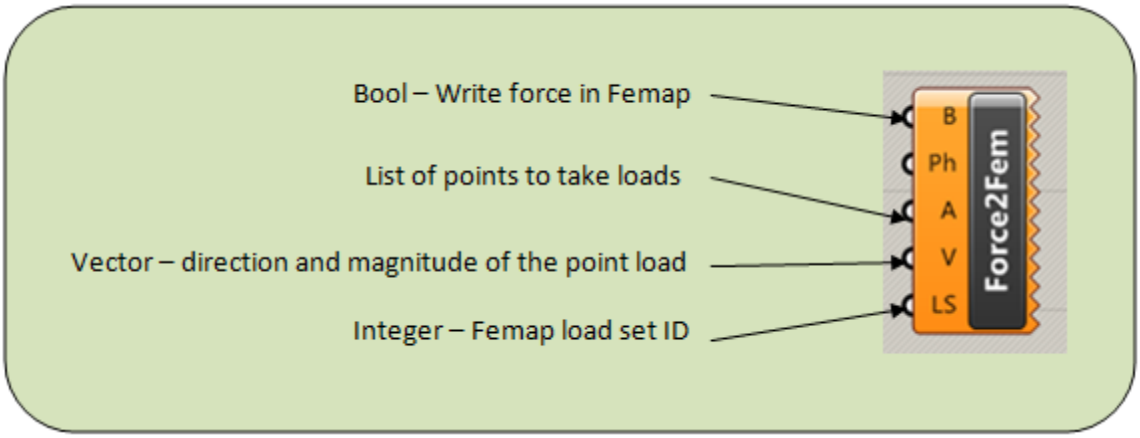

Figure 17 Component - Force2Fem

7) AnalyzeFem

The designer can choose the analysis type and boundary conditions in Femap, and then use the AnalyzeFem component to send command from Grasshopper to Femap to do analysis for the chosen analysis set.

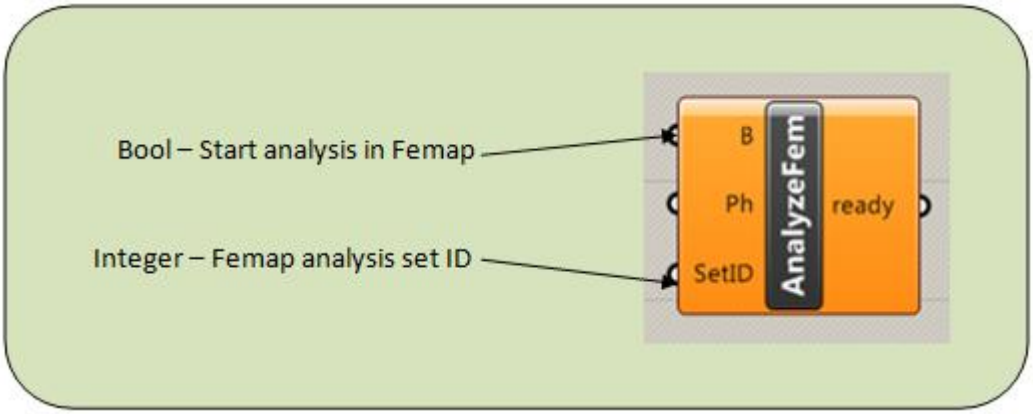

Figure 18 Component – AnalyzeFem

8) Mass

In Femap, the mass processor computes the mass properties of a finite element model. The designed component Mass can send command to Femap to calculate the mass of elements and display the results in Grasshopper.

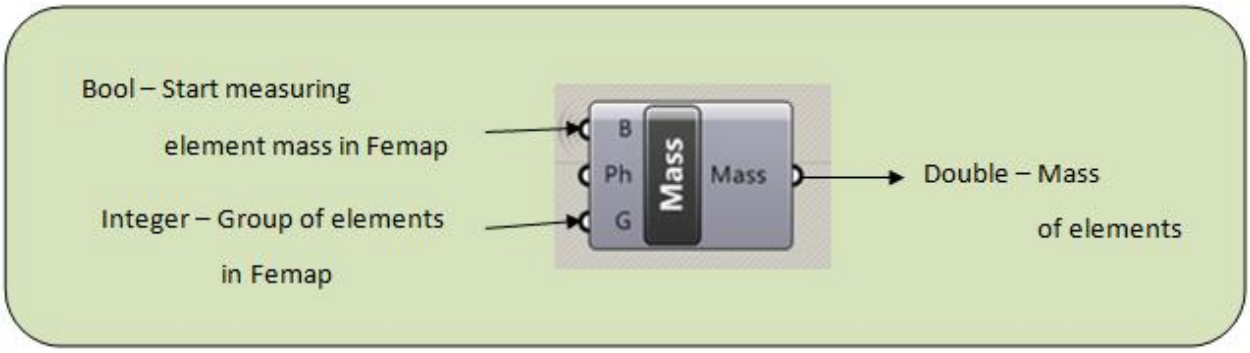

Figure 19 Component – Mass

9) DMesh

This component is used to delete the meshed elements in Femap. The mesh includes elements and nodes.

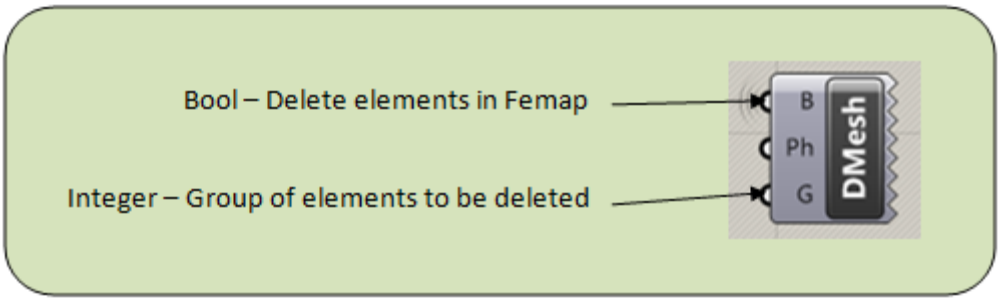

Figure 20 Component - DMesh

Above are the components used for communicating between Grasshopper and Femap. These components allow the designer to send commands to Femap and read results from Femap within the interface of Grasshopper. Developing the plug-in with these components is the fundamental step and also the starting point for parametric design of this cable-strut system. A lot of time has been devoted to developing this tool but more time has been saved in the later design and analysis work.

Related codes for the above components can be found in Appendix C.

2.5 Components

Grasshopper allows designers to build parametric models with existing components. And it is also possible to script personal commands within the same environment. In this parametric model, apart from the components developed in the plug-in, a lot of components have been made with scripting skills. The new components can better translate the mathematical concept into design thus able to achieve specific or more generic design requirements.

Designers can make customized components because Grasshopper is an open environment with the following features:

1) The default components are ready to be dragged onto the canvas and connected in order to create any kind of algorithm.
2) The scripting components can be dragged onto the canvas and be developed. The user can define the inputs, outputs, and the script connecting them with specific functions.
3) Group is a graphical way to organize a series of components. Normally the components forming a complex algorithm are put into the same group.
4) The clusters allow the user to combine a series of components into one. Thus components in the same group can be made into a cluster. Then the user can rename the input and output of the cluster with specific function.

All the mentioned features have been explored and applied in the parametric model.

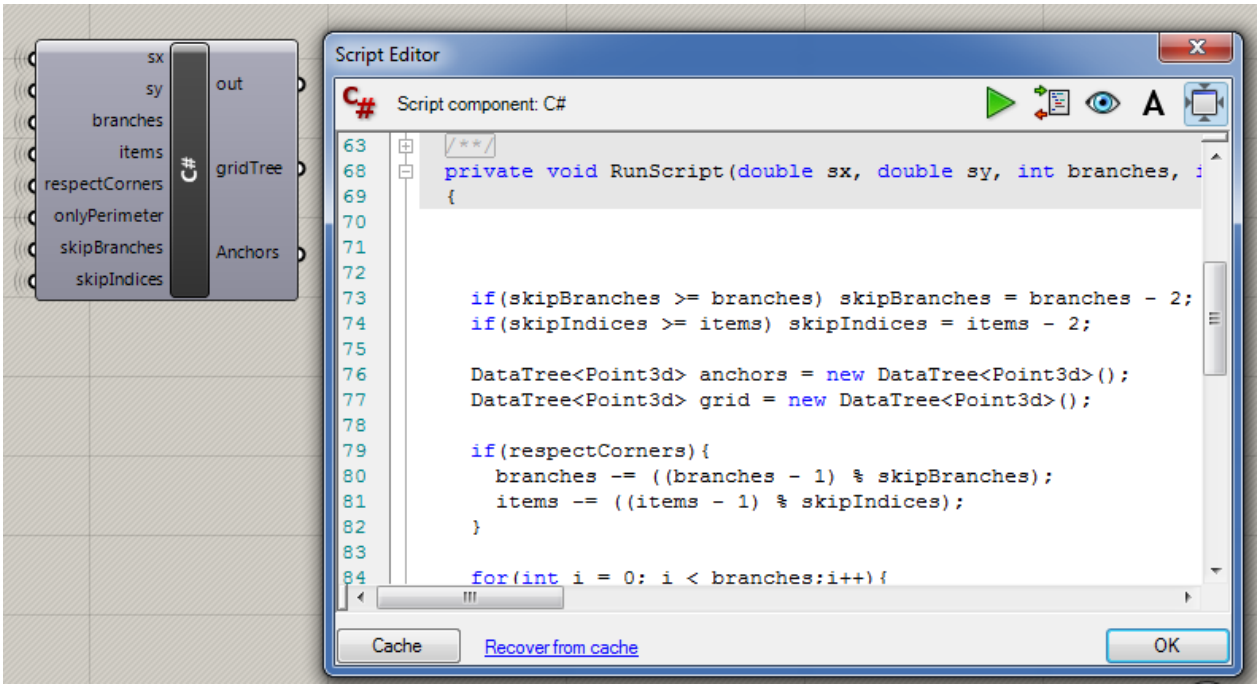

Figure 21 Scripting component

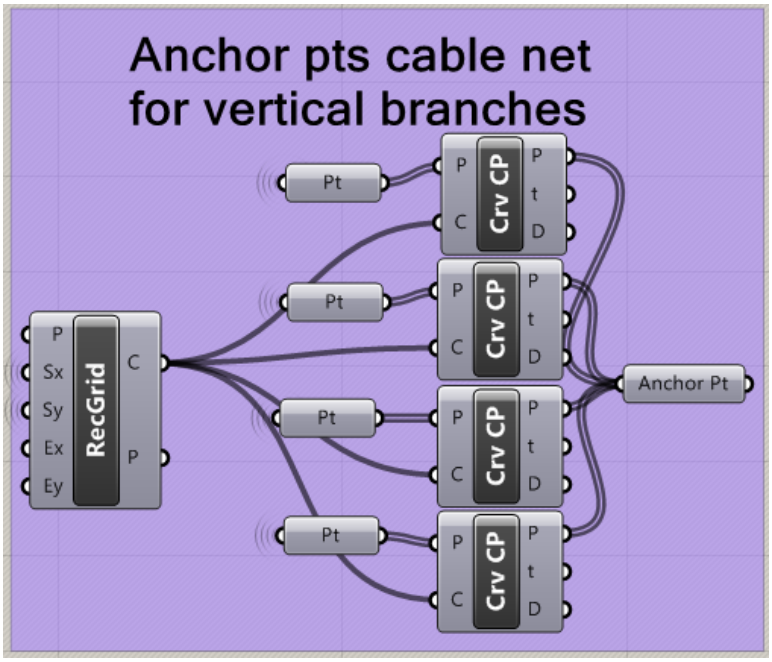

Figure 22 Group of components

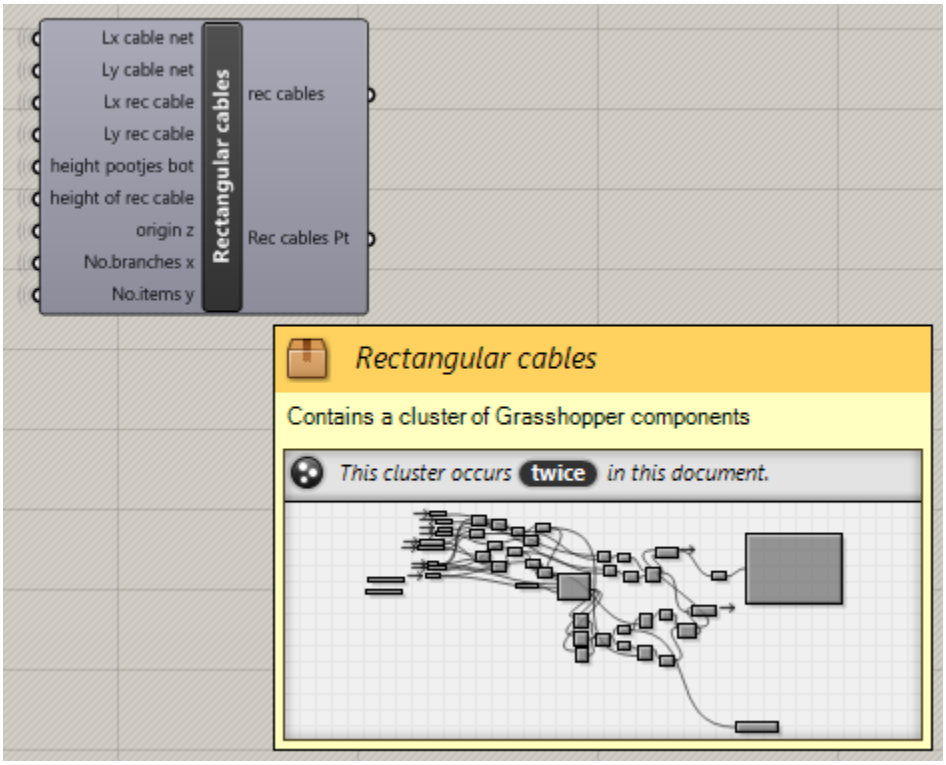

Figure 23 Make cluster of a group of components

With scripting, the customized components can be defined with various functions. By grouping the components with the same design purpose and make them into clusters the design interface can be more organized which makes it easier for error detection and model modification.

Chapter 3

Study of pretensioned structure

3 Introduction of tensegrity

The term tensegrity was coined by Buckminster Fuller in the 1960s as a portmanteau of "tensional integrity" (*V. Gómez-Jáuregui, 2010*). Since the appearance of the first tensegrity structure in the last century, there are no precise boundaries for the definition of tensegrity due to a large variety of forms developed.

In this thesis, tensegrity can be simply taken as a combination of discontinuous compression struts inside continuous tensioned cables, and any free-standing systems composed of tensegrity units satisfying the aforesaid definition.

This type of structure provides good lightness and transparency. In a tensegrity, the bars in compression are surrounded by a continuous net of tensioned cables, resulting in a 3-D system in a state of equilibrium. The struts are supported by the cables, creating an illusion of a floating structure in air.

3.1 Application

Eleanor Hartley points out visual transparency as an important aesthetic quality of these structures (*Eleanor Hartley, 2013*). Korkmaz et al. put forward that the concept of tensegrity is suitable for adaptive architecture thanks to lightweight characteristics (*Korkmaz et al, 2011*). Some examples include:

1) Snelson's sculptures (*Eleanor Hartley, 2013*)

Needle Tower is a public artwork by American sculptor Kenneth Snelson located outside of the Hirshhorn Museum and Sculpture Garden in Washington, DC, United States. This is a pure tensegrity structure with a height of 18m. Based on three-strut tensegrity modules superposed one on top of the other. Snelson built his Needle Tower two in 1971 which reaches 30 m high.

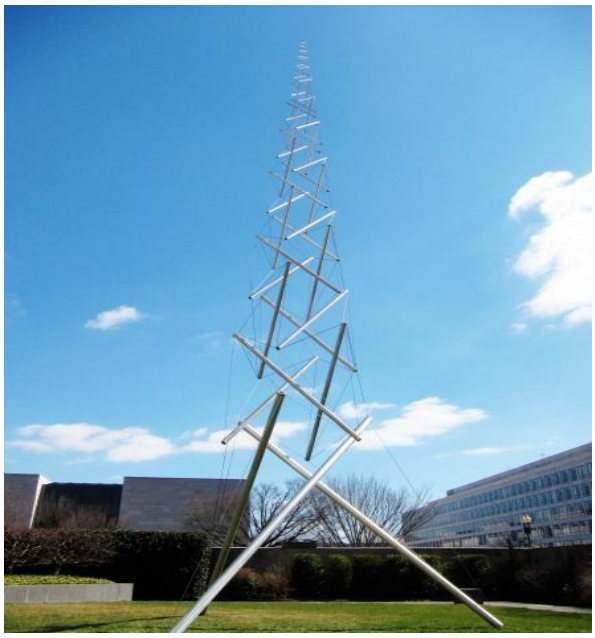

Figure 24 Snelson's needle tower (***Kenneth Snelson, 1968***)

2) Roof structures

In civil engineering tensegrity was not used until the first cable-dome structure, the Olympic Gymnastics Hall and the Fencing Hall in Seoul (*Geiger, D.H, 1986*),was built in 1988, Due to their innovative forms and lightweight features, cable domes have become popular as roofs for structures including arenas, stadiums and sport centers over the past two decades. All tensegrity structures are made from cable structures thus generally tensegrity is a subcategory of cable structures.

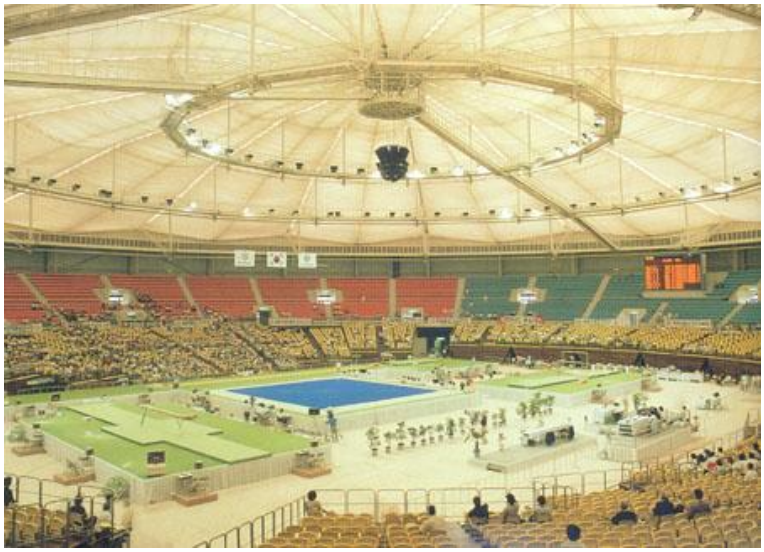

Figure 25 The Olympic Gymnatics Hall in Soul (***Geiger, D.H, 1986***)

3) Structure to support glass façade

Glass façade became popular because of its lightness and transparency. At the same time different supporting structures have been developed to guarantee that the façade stays in place. A tensegrity system with two tensioned cables kept apart by compression struts leads to an efficient bracing system to support the façade and to resist wind loads. Pre-stress is applied to make sure the cables stay under tension.

Figure 26 Support structure for glass (***Alfonso Millanes, 2009***)

4) Tensegrity bridges

The 'Bridge of Masts' in Purmerend was designed by architect Jord den Hollander with an idea to make the bridge float above water (*Jord den Hollander, 2000*). He developed a platform over the water with 18 spans of 4 m. Each mast is connected to three cables rather than the deck to make the bridge suspended.

Figure 27 The Bridge of Masts in Purmerend (***Jord den Hollander, 2000***)

3.2 Properties of tensegrity

1) Large strength-to-mass ratio

A compressive member loses stiffness as it is loaded, whereas a tensile member gains stiffness as it is loaded (*Yildirim Hurmuzlu, 2002*). Stiffness is lost in two ways in a compressive member:

- In the absence of any bending moments in the axially loaded members, the forces act exactly through the mass center. Under compression, the material spreads, increasing the diameter of the center cross section but decrease the element height; whereas the tensile member reduces its cross-section but increases the element length. Thus a compression member loses stiffness while a tensile member gains stiffness under loading.

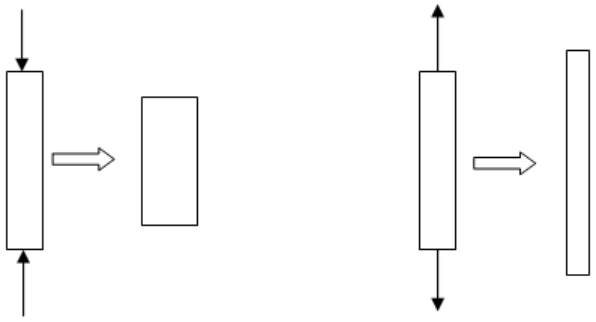

Figure 28 Deformation of bar elements under axial loading: left – compression, right - tension

- In the presence of bending moments due to offsets in the line of force application and the center of mass, the bar becomes softer due to the bending motion. For most materials, the tensile strength of a longitudinal member is larger than its buckling strength (Obviously, sand, masonry, and unreinforced concrete are exceptions to this rule).

Hence, a large strength-to-mass ratio can be achieved by increasing the use of tensile members.

2) Lightweight

The most outstanding characteristic of tensegrity is that it creates lightweight structures. Tensegrity structures resemble 3D trusses with all the struts in compression and all cables in tension. Geometry determines the equilibrium of each node. The strength relies largely on the relation between shape and load path. In pure tensegrity, forces are limited to normal force. Efficiency is maximized with every particle of the structure contributing to the load-bearing capacity, and having the majority of elements in tension being the most efficient way in material use, resulting in a high strength-to-weight ratio and relatively small cross section.

3) Geometric nonlinear

Tensegrity structures are geometric nonlinear. When a tensegrity is under loading, large initial displacement occurs and rearrangement of individual elements leads to the change of strength and stiffness of the structure. Generally speaking, tensegrities are self-stabilized, independent of gravity and the behavior of the global structure is not predictable by the behavior of local elements.

4) Prestress required

In tensegrity cables that have no tension become uncontrolled. Prestress makes sure that the cables remain in tension as long as the applied compression force is inferior to applied prestress. When tensile forces is eliminated in one cable, stiffness of the structure drops drastically. Increasing pretension from a low level may increase the stiffness. But for a structure with high level of pretension, a further increase of prestress may lead to an unstable structure. If all the cables stay in tension, geometry of the tensegrity and the use of materials and section size determine the stiffness. Prestress increase the load-bearing capacity mainly by assuring that load path stays unchanged.

3.3 Possible system types

1) Lens-shaped tensegrity

The tensegrity consists of a cable-strut system to transfer external loads from cladding and a ring system around to stabilize the structure. As is shown in the following picture, each part of the cable net system is inclined slightly from the vertical plane in such a way that the extension lines of all the compression struts coincide to the same central point (*SID STUDIO, 2015*).

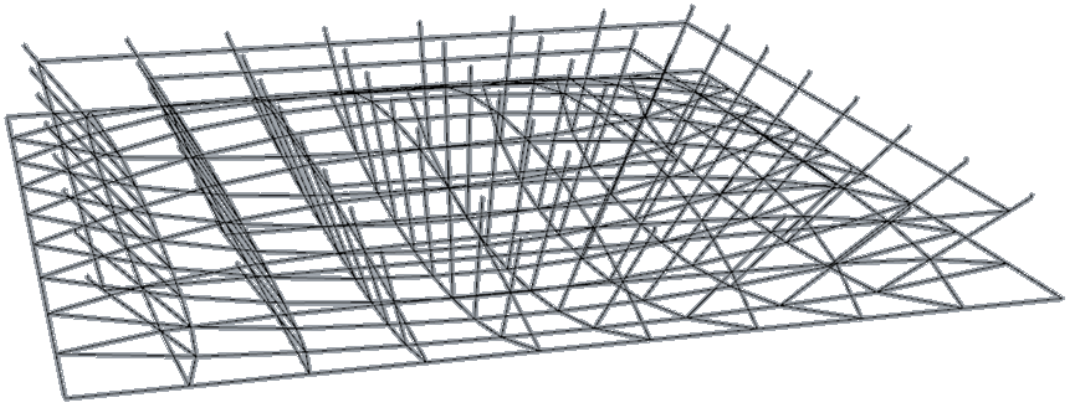

.

Figure 29 Lens-shaped tensegrity

2) Tensegrity truss system (*Dennis R. Holloway, 1975*)

In this structure a truss system is applied with a bottom cable net rather than beams. The top beams are in a flat surface taking compression and transferring forces to the ring and struts. All the cables are in tension.

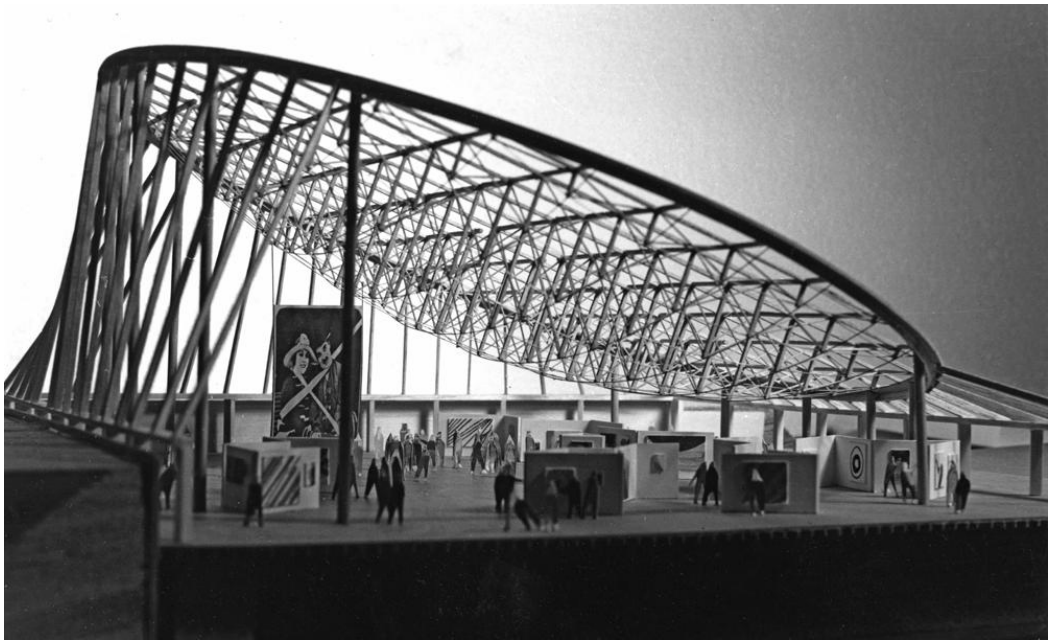

Figure 30 Tensegrity truss system (***Dennis R. Holloway, 1975***)

3) Spoke wheel roof (*Ivar. Boom, 2012*)

A spoke wheel consists of three elements: the rim, the hub and the spokes that connect the ring and hub. The strength and stiffness of the wheel depends on the amount of ring action of the structure. The higher the pre-tension in the spokes, the stronger and stiffer the wheel becomes.

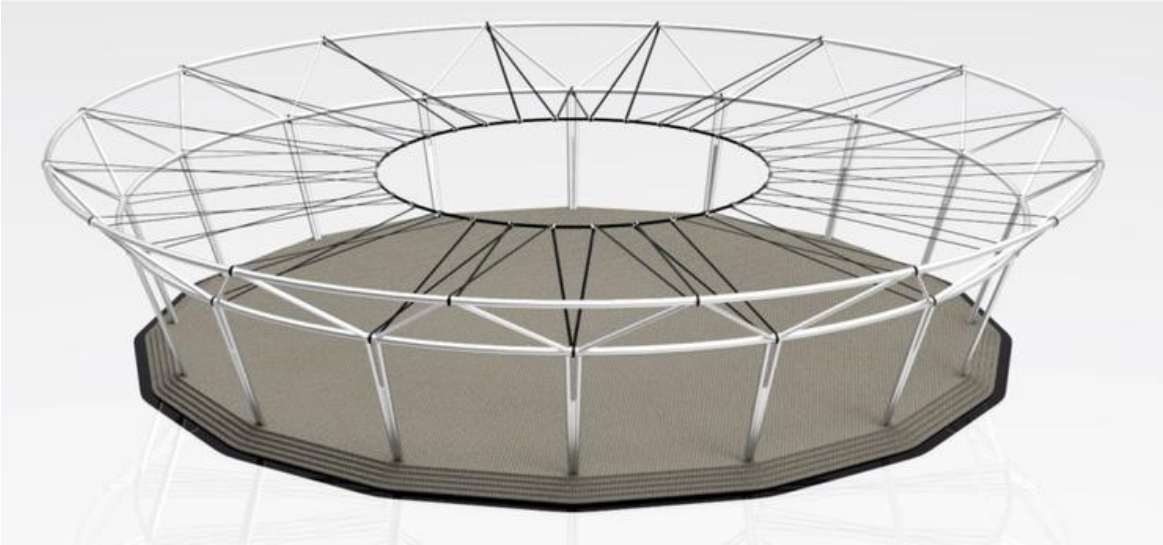

Figure 31 Spoke wheel roof (***Yue Liu, 2015***)

4) David Geiger tensegrity dome (*Geiger, D.H, 1986*)

The characteristics of this dome is the ridge cables spanning from the outer compression hoop to the inner tension hoop, connected to the hoop rings at the bottom layer by compression struts and diagonal cables.

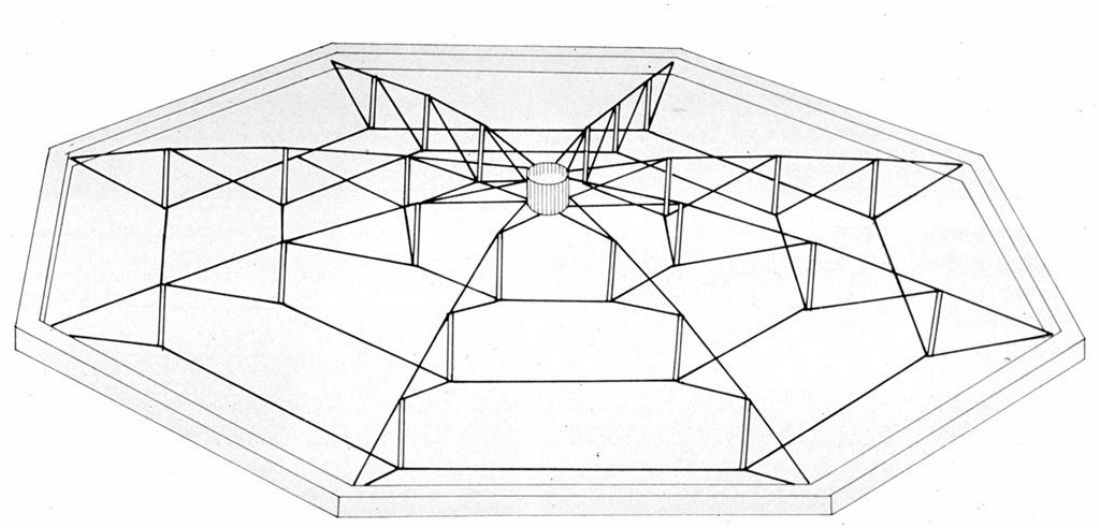

Figure 32 Geiger dome (***Geiger, D.H, 1986***)

4 Case study and reference projects

4.1 Case studies

There are a lot of tensegrity structures like roof structures for atrium and support structures for glass curtain walls realized by Octatube. Besides, many studies on the subject tensegrity have been conducted by Master students. Although not all the assumed system types can be referred to a found project, and none of the found projects aims to compare different types of tensegrity as a roof structure, a better understanding about the properties of tensegrity can be learned from other people's experiences and certain findings are definitely applicable to this research project.

Here two graduation projects are studied about three types of tensegrity roof : Geiger dome, Fuller dome and Spoke Wheel. Some tensegrity structures realized by Octatube are referred to.

Graduation Project ir. Michael van Telgen (*M.V. van Telgen, 2012*)

Since 2011, Michael van Telgen started to research the influence of variables in the design of circular tensegrity domes and compression hoops based on the prototypes of Geiger dome and Fuller dome. And then investigated the viability of the design of an elliptical tensegrity dome.

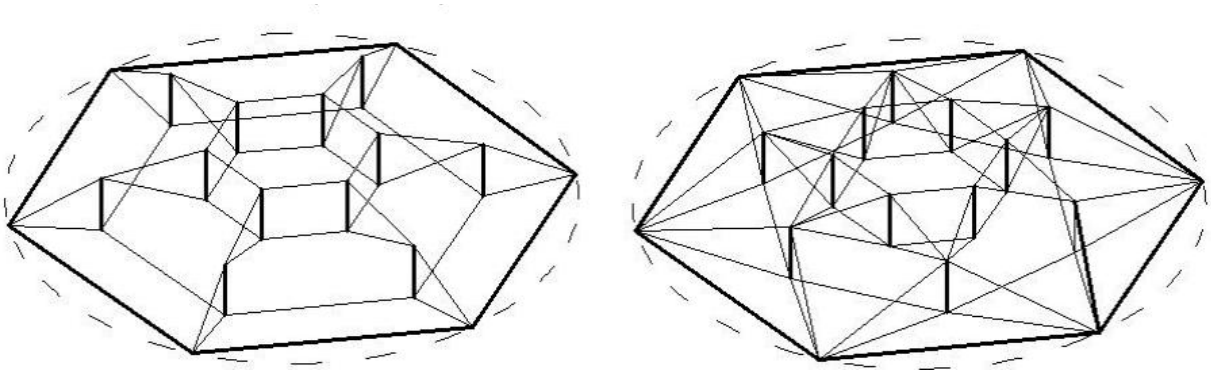

Figure 33 Tensegrity domes left: Geiger dome, right: Fuller dome (*M.V. van Telgen, 2012*)

For Geiger dome, in the top layer the ridge cables span from the outer compression hoop to the inner tension hoop. The ridge cables are connected to the ascending tension hoops by compression struts and diagonal cables. For the more complex Fuller dome, it has curved cables in two directions, which results in higher stiffness compared to Geiger dome.

Michael van Telgen first researched the design variables and classified them into five orders considering their influence to the dome structure. In general, the higher the order the more radically a tensegrity dome changes. These variables are:

- 1st. System type – David Geiger Dome or Buckminster Fuller Dome
- 2nd. Boundary conditions – compression hoop shape
- 3rd. Topology changes – number of tension hoops
- 4th. Global changes to geometry – diameter and height of the structure
- 5th. Local changes – angles and lengths of elements

It is difficult to analyse the influences of a change in a single parameter since most of the variables are related to each other, the change of one variable has a (large) consequent influence on the features of the tensegrity dome like heights and lengths. The interaction of these variables decides whether a design is efficient or not. In his study, only deliberate changes of variables are investigated, which means the consequent change of variables due to the adjustment of another variable is not considered here.

Three aspects are chosen to evaluate the performance of the tensegrity dome:

- The amount of pretension force,
- Mass of the tensegrity structure,
- The modified total mass (MGM).

He concluded that the needed pretension is determined by the mass of tensegrity and the geometry of the dome. In turn the amount of pretension affects mass of the structure. Low pretension forces need smaller cross sections, which means a low pretention force leads to a decreased mass of the tensegrity.

Then three methods to apply pretension is introduced:

- Applied node displacement at the supports
- Pretensioning the struts
- Temperature change in the struts

To find the needed amount of pretension , the node displacement method was applied. Support nodes are displaced outwardly until all the cables are in tension. The higher the pretension, the stiffer the tensegrity and the larger the mass. It is wiser to adjust the geometry of the dome if smaller deflections are desirable. The dome was analysed with and without a compression hoop.

Some conclusions from the research which are instructive for this research project are listed as follows:

1) The nodal displacement in the tensegrity is determined by the stiffness, which is influence by four factors: pretension force, geometry of the tensegrity, cross section of elements, and residual capacity in the elements.
2) Fuller domes are generally stiffer than Geiger domes due to two-direction spanning ridge cables but at the same time require more elements thus being more labor-intensive. The pretension is lower in Fuller dome cables and struts, so lighter equipment can be used to apply the pretension in the dome. It cannot be stated that which type of dome is qualitatively better since the evaluation depends on a lot of criteria like structural performance, cost, aesthetics, etc.
3) Geiger dome designs are almost always designed based on the maximum allowed additional displacement due to wind. The sensitivity of the tensegrity dome to this effect is determined by the stiffness of the dome.
4) Fuller dome designs are usually determined by the minimal required amount of pretension force in one of the elements. Failure under the influence of wind is seen the most, which has an unfortunate side effect. Due to the position and direction of some diagonals in the dome, the difference between the maximum and minimum normal force can be large, affecting required section sizes adversely.

5) Combining the properties of well performing tensegrity domes from different studies will not automatically result in better solutions. This is because the stiffness and the distribution of forces are largely influenced by these choices, and they may not be interchangeable.
6) Pretension and hoop angle influence the amount of normal force in the compression hoop. Bending moments occur when non-uniform load is applied. And bending moments make up only a small part of the unity check (about 5% to 10%) for the compression hoop.

Graduation Project ir. Ivar Boom (*Ivar Boom, 2012*)

The main research question for Ivar Boom in his MSc graduation work was "To what extent is the application of the spoke wheel principle feasible and efficient for football stadia roof structures?"

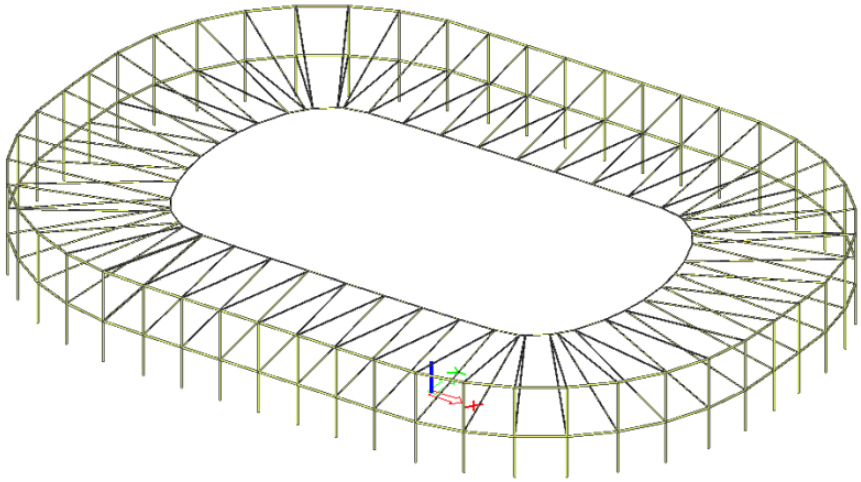

Figure 34 Shape of designed stadium (*Ivar Boom, 2012*)

He started with the analysis of the spoke wheel principle applied to a roof structure. From the theory of the spoke wheel principle (ring action) he found four key factors that influence the ring action, these are:

- Curvature
- Loads on the ring
- Extensional rigidity of the ring
- Translation of the ring

The design of a spoke wheel roof depends on certain design variables that influence the ring action in the roof. Based on the investigation of key factors and strength and stiffness of the roof, the design variables are determined:

- Shape of the roof
- Double inner/outer ring
- Pretension of the spokes
- Choice of profile and elements
- Supports and connections

Relation of the design variables to the key factors that influence the ring action are shown in the following figure:

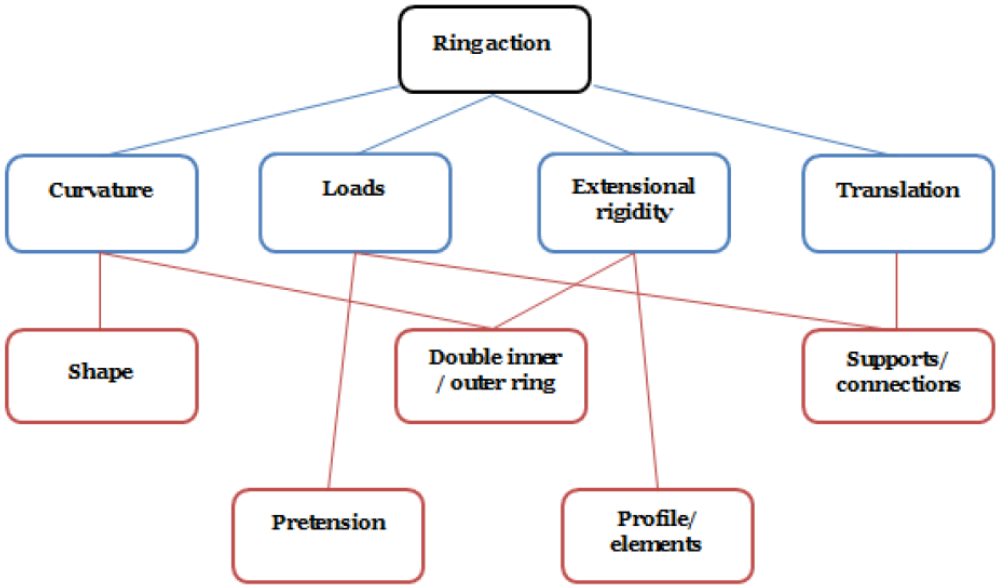

Figure 35 Relation between design variables and ring action (*Ivar Boom, 2012*)

In preliminary design, the shape of a reference stadium was investigated for structural problems and possibilities. Then design variables were studied to find their influence to the ring action. At the end of preliminary design phase, a question was raised if a pretensioned or non-pretensioned spoke wheel roof will provide a stable structure and which design will lead to the most efficient structure?

The above question was answered in the detailed design phase. A study was made for a spoke wheel roof that used a truss system and a cable system.

Based on the above design and research, he drew conclusions as follows:

1) The use of the spoke wheel principle has its limits. Less curvature results in less benefits from the strength of the spoke wheel principle.
2) The feasibility of the spoke wheel principle for stadia roof structures depends on the shape conditions. A spatial truss structure has the ability to use the spoke wheel principle even in case of stadium roofs with straight sides. Due to beam action it is still possible to design an efficient structure.
3) A cable structure heavily relies on the amount of the available curvature and can only provide stiffness by means of ring action. A cable structure is still feasible for roofs with straight sides in a structural manner. However, looking from a financial and durability perspective the cable structure is not attractive for owners and is very inefficient. It is advised to use a cable structure only for circular or oval shaped spoke wheel roofs.

4.2 Reference projects by Octatube

There are a lot of tensegrity structures realized by Octatube from design, engineering to construction. By looking at real-life projects we can have a better understanding about the structural performance and construction about tensegrity.

Canopy Prinsenhof, Delft (*Mick Eekhout, 1997*)

In 1997, The courtyard of the Museum Prinsenhof in Delft was renovated. The atrium offers a view on two churches in the surroundings: the Waalse Church and the Old Church. The project is an early example of the trend to place modern structures next to historical buildings (old versus new). The transparent and fully structurally glazed atrium provides an unobstructed view on the surrounding monumental buildings.

Figure 36 Canopy Prinsenhof, Delft (*Mick Eekhout, 1997*)

The main load-bearing structure is free from the surrounding buildings and consists of five meter high cylindrical steel columns and 2,5 meters high lenticular tensegrity trusses. The façade construction is built with steel columns and stainless steel 3D tensegrity trusses, in line with the medieval brickwork. Double glass units are glued on steel arms, cantilevering from the roof trusses. The coated façade glass panels are fixed to the pre-stressed stainless steel.

Droogbak, Amsterdam (*J. van Stigt, 1999*)

In the roof of the Droogbak building in Amsterdam, the atrium is covered of a similar size 26x30m^2 in a non-rectangular shape without columns. The tubular primary structure was reinforced by an additional structure of tensile elements below and short compression bars. The subdivision of the roof modules was stabilized by tensegrity structure.

Figure 37 Droogbak, Amsterdam (*J. van Stigt, 1999*)

The main load bearing construction of the roof over this atrium consists of a constructive grid of intersecting tubes in two directions. Maximal module size is eight by eight meters. These tubes are fitted with round tension trusses for vertical downward forces and vertical compression tubes on the intersection of the large tubes. Downward directed bars, anchored into the concrete attic floor, absorb the upward wind load. The roof modules are divided by a secondary stainless steel tensile structure system underneath. The double glazing panels are attached to the Quattro-nodes by glued disks.

Figure 38 Connection (*J. van Stigt, 1999*)

Bancopolis, Madrid (*Kevin Roche, 2005*)

The stainless steel tensegrity structure determines the overall image of this extraordinary and highly transparent circular glass roof, 31 meters in diameter and with a structural height of 3 meters. The layout is clear as a bicycle wheel: an outer ring that is permanently pre-stressed and an inner ring that is subjected to tension and functions as a hub. In between 36 compression studs and stainless steel tensile rods are spanned, without stabilizers for wind. To obtain stiffness the upper and lower tension bars of the tension trusses are pre-stretched. The curvature and design of the roof is a direct result of the optimal shape of the trusses and the distribution of forces in the pre-stretched structure. The roof is covered with structural and frameless glazing of which the stainless steel glass nodes are specially designed for this project. A 3,5 meters wide glass dome forms the crown of the roof.

Figure 39 Bancopolis, Madrid (*Kevin Roche, 2005*)

Headquarters of Bank SCH. Madrid (*Alfonso Millanes, 2009*)

In the year 2007, Octatube was awarded a tender to develop a Glass Cube for the headquarters of Bank SCH in Madrid, Spain.

The main construction of the Glass Cube is executed in mild steel with stainless steel tensegrity parts. The construction consists of steel beams and columns. These members are stiffened by stainless steel rods, working as a tensegrity construction. The overall stability of the glass cube is also guaranteed by diagonal stainless steel tension rods, that also works as supporting members of the glass panels.

In Figure 40 a 3D rendering of the construction can be seen.

Figure 40 Glass cube of Headquarters of Bank SCH, Madrid (***Alfonso Millanes, 2009***)

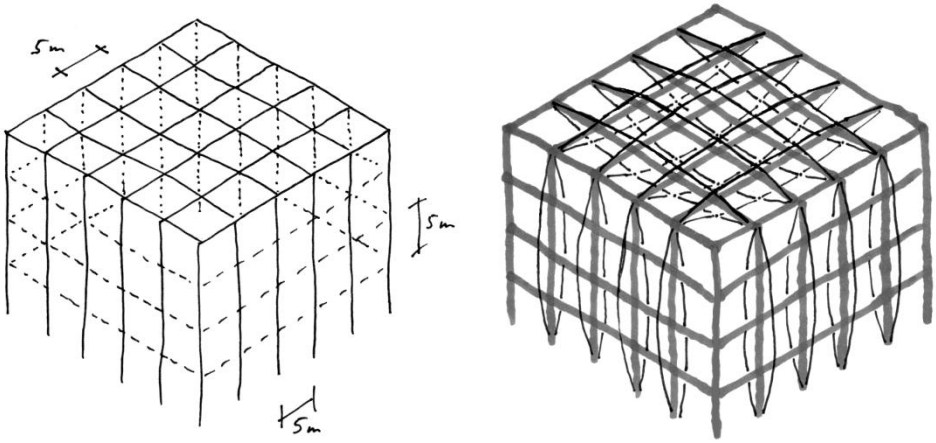

Figure 41 Main structure of the glass cube

The main beams are all stiffened by main tension rods that are kept at a fixed distance to the beams by compression members. In the roof these tension rods are placed above and below the main beams, in the facades the columns have tension rods on two sides, to the inside as well as to the outside of the facades. The corner columns do not have an extra tension rod system, as they are stiffened sufficiently by the rest of the façade construction.

The small tensegrity structure within the 5x5m spaces between the main structure is used for two main purposes in the structural system: first it transmits the forces acting on the glass plane via the glass nodes and the tension rods into the main structure; second it acts as bracing of the whole structure and transmits horizontal forces in the plane of the main steel frame to the supports on the bottom of the columns.

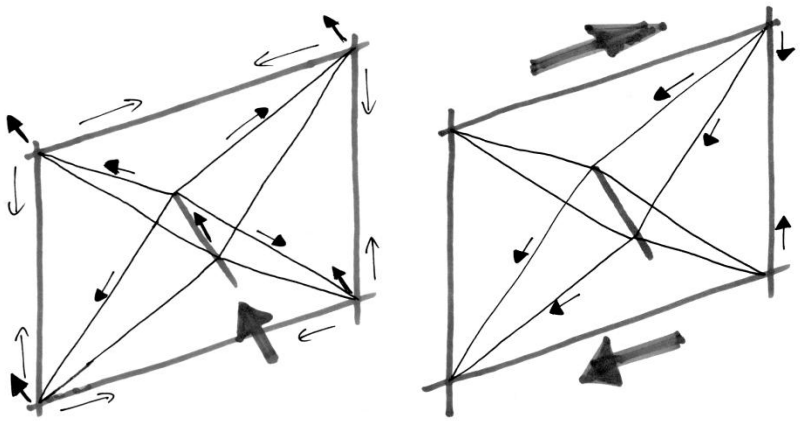

Figure 42 Load bearing path in tensegrity: left- normal force, right- shear force

The main stability of the building is guaranteed by the steel construction in the wind parallel sides. The wind pressure and the wind suction on the windward respectively. The downwind side is transmitted by the columns half to the bottom of these façades, and half to the roof. The forces that are transmitted to the roof are transmitted by the small tensegrity structures from the middle of the roof to the side, and from there via the small tensegrity structures to the supports at the bottom of the columns of these facades. The wind forces will therefore lead to shear forces at the supports, as well as considerable normal forces in the corner columns in the wind parallel sides.

In Figure 43, only the bracing of one wind parallel side is shown. The bracing of the roof as well as the bracing of the other wind parallel side is working in the same principle.

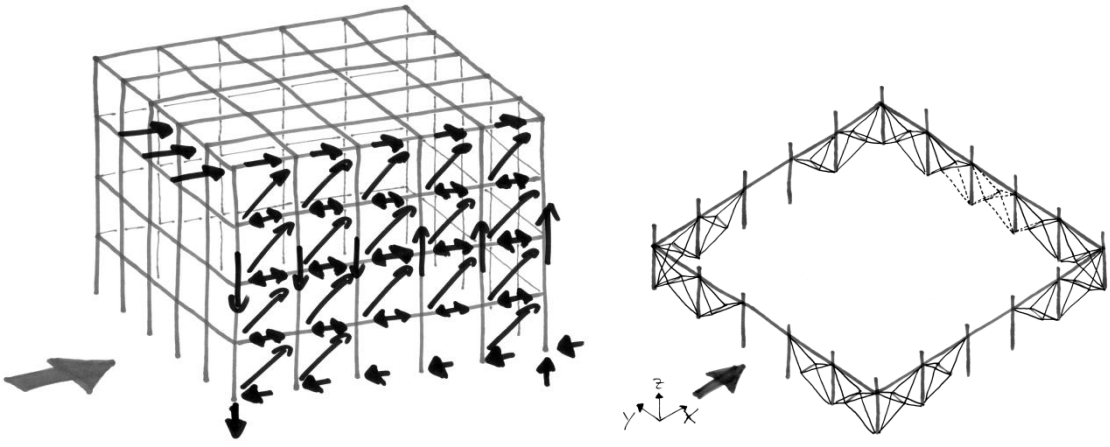

Figure 43 Bracing of the glass cube

5 Discussion

Tensegrities are stable and light-weight structures with compression struts and tension cables, being able to carry loads depending largely on stiffness properties of the system. There are four factors (see Appendix B) that determine the stiffness of the cable-strut system:

- Material use
- Sectional size
- Shape of structure
- Element length

In chapter 3, first an overview of tensegrity has been presented. Mechanism of slender structures gives an insight of the leading factors that influence the load-bearing capacity of a tensegrity. Case studies and reference projects show how engineers apply tensegrity in the real projects.

The conclusions from chapter 3 are briefly summarized for each section.

Section 3 Introduction of tensegrity

Tensegrity, also called tensional integrity, is a type of self-stabilised structure with a disconnected system of struts in between an interconnected system of cables. Tensegrity was first related to artwork and soon gained more and more popularity in civil engineering and architecture field due to its outstanding properties like light-weight and transparency. Some possible system types related to the application of tensegrity are listed and investigated which give inspiration about the roof structure.

Section 4 Case study and reference projects

The case study and reference projects show how engineers have found solutions to apply the pretensioned cable-strut system for a roof or for a glass curtain wall. For different types of pretensioned cable-strut system, there are three fundamental structural elements: the pretensioned cables, the compression struts, and the hoop structure which provides stability to the whole system. There are lots of variables in the design of a cable-strut roof system, all in all it is the factors determining the stiffness of the structure that matters to the structural performances.

In the following chapter, the impacts of the possible design variables are investigated and a cable-strut structure which satisfies both SLS and ULS check requirements is designed.

Chapter 4

Preliminary design – Variable study

6 Introduction to variable study

The roof is created in the form of ETFE cushion, supported by a lens-shaped tensegrity structure. The tensegrity consists of an interconnected system of cables which cross with each other orthogonally and a discontinuous system of struts in between the cables. The fish-belly girders are inclined slightly from the vertical plane in such a way that the extension line of all the struts may converge at the same central point. Around the tensegrity there is a compression hoop which functions to form a closed constructive system and to stabilize the whole structure.

To improve the structural performance of the preliminary design, in this chapter the design variables regarding the roof system have been investigated to find out the influences of changing variables that may exist in the design of this given shaped cable-strut roof system.

6.1 Geometry

Roof structure designed in this research is based on the opening in Het Gelders Huis, Arnhem, the Netherlands. The roof structure will be supported at two different layers to cover the opening. Dimension of the lower layer is about 29m x 29m, and the higher layer about 34m x 34m. The height of the highest point of the roof is about 16m.

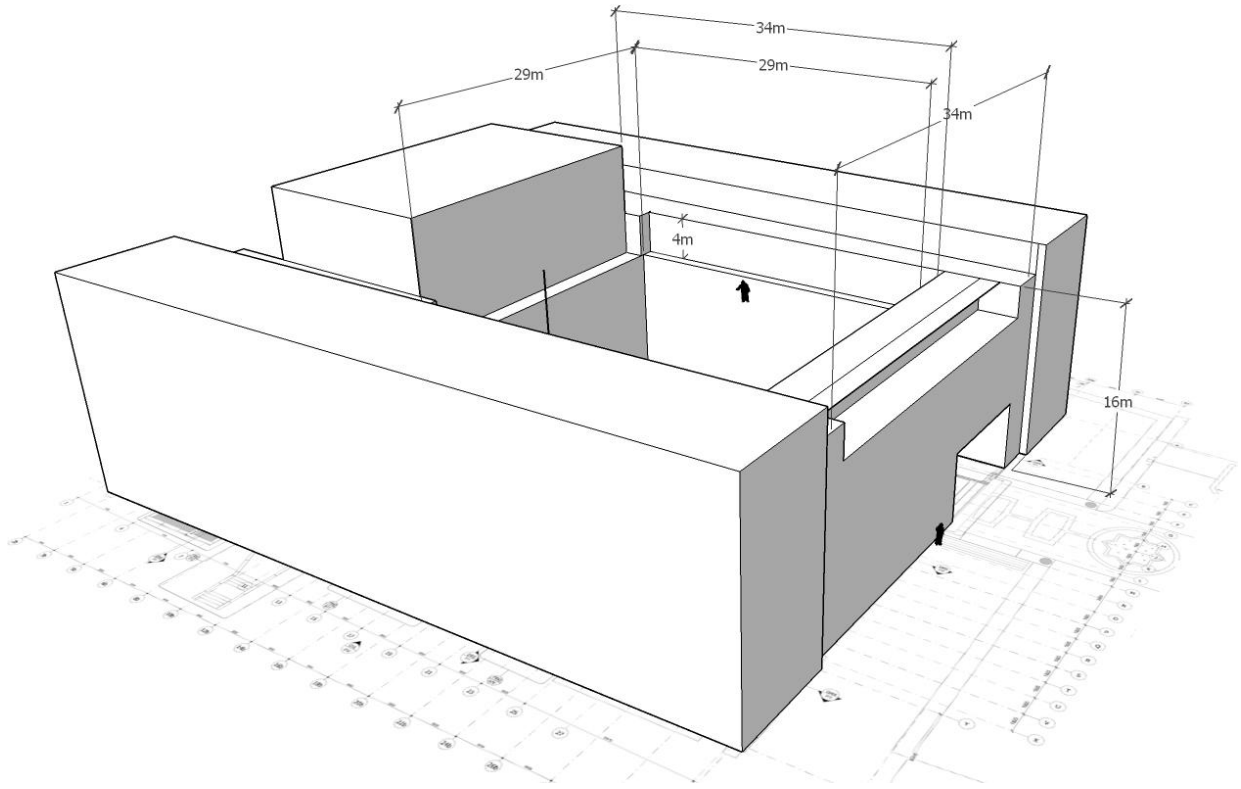

Figure 44 Dimension of the opening for Het Gelders Huis

There are seven groups of this steel structure: (a) ETFE beams, (b) Rods, (c) Rectangular cables, (d) Top cables, (e) Struts, (f) Bottom cables, (g) Hoop.

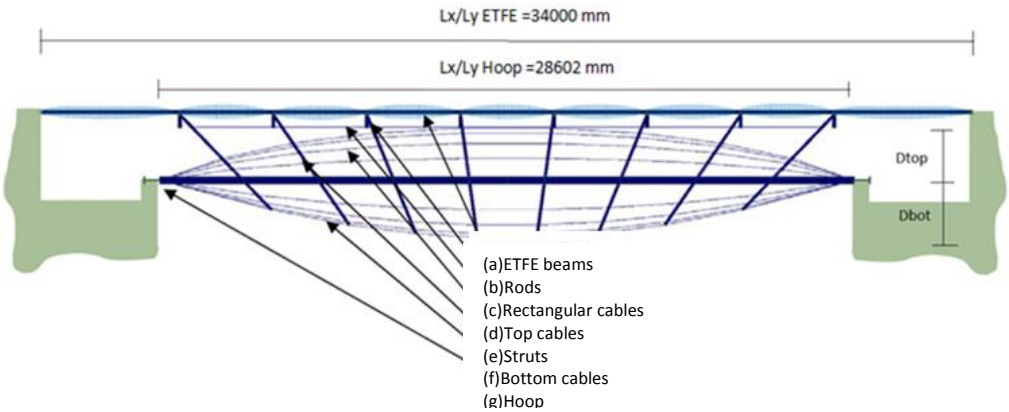

Figure 45 Front view of the roof structure

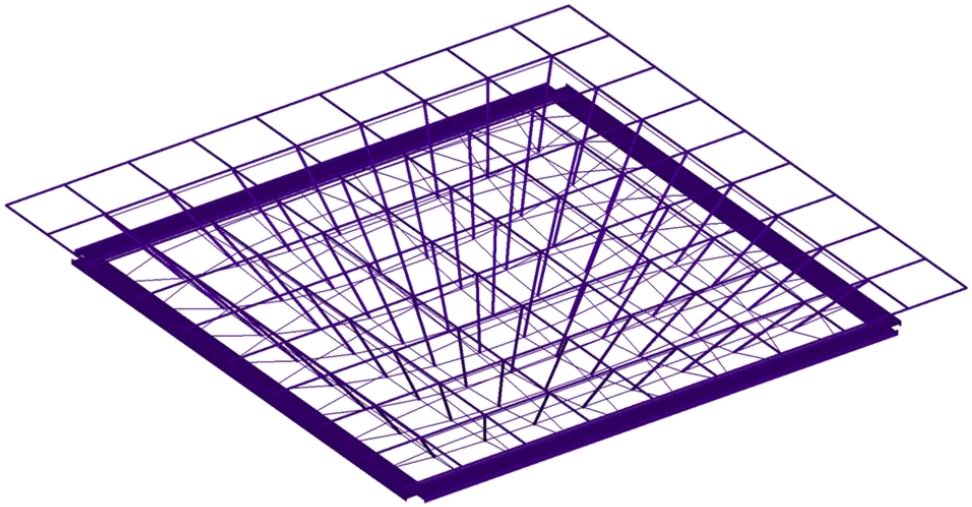

Figure 46 Roof model

In this study, the dimension of ETFE beam and the dimension of hoop are defined according to the on-site situation. The length of rods is predefined, the function of rods is to transfer all the loads from ETFE beam to the struts.

Table 2 Predefined geometry of the roof

Geometry	Choice
Dimension of ETFE Beam	34000mm x 34000mm
Dimension of hoop	28602mm x 28602mm
Length of rods	100mm

6.2 Supports and connections

The choice of type of supports and connections influences the structural behavior of the roof system by restricting translation and the load path.

supports

The roof structure will be supported at two floor levels, the upper ETFE beam grid and at the lower hoop beams. Connections at the outer ring of the ETFE beam can be made supports for the beam grid. For the hoop beams, the corner and the position in between two cables will be constrained. Therefore, the number of cable branches determines the total number of supports.

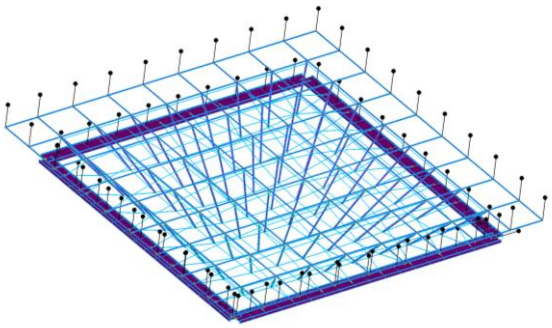

Figure 47 Position for support

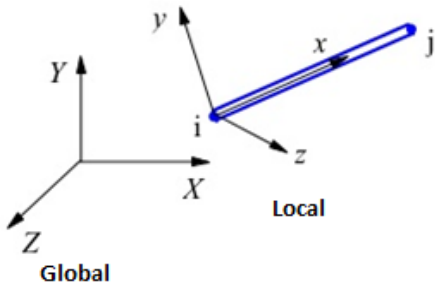

Figure 48 Global and Local axis of a single element

For a single beam element, the axis along the element length is defined as local x direction, the other two directions perpendicular to local x axis is defined as local y and local z direction respectively. In total the x, y, z axis compose the local 3D coordinate system.

In general there are four types of supports (*Chris H. Luebkeman, 1995*):

- Simple supports
  This is idealized as to put the structure simply on a frictionless surface which is not often found in building structures. The simple supports could only resist the downward translation.
- Roller supports
  Roller supports are free to rotate and translate along the surface upon which the roller sets. The resulting reaction force is always a single force that is perpendicular to, and away from the surface. Roller supports allow the structure to expand and contract with temperature change.
- Pinned supports
  A pinned support can resist both vertical and horizontal forces but not a moment. They will allow the structural member to rotate, but not to translate in any direction. Many connections are assumed to be pinned even though they might resist a small amount of moment in reality.
- Fixed supports
  Fixed supports can resist vertical and horizontal forces as well as moments. A structural member needs only one fixed support in order to be stable, all three equations of equilibrium can be satisfied.

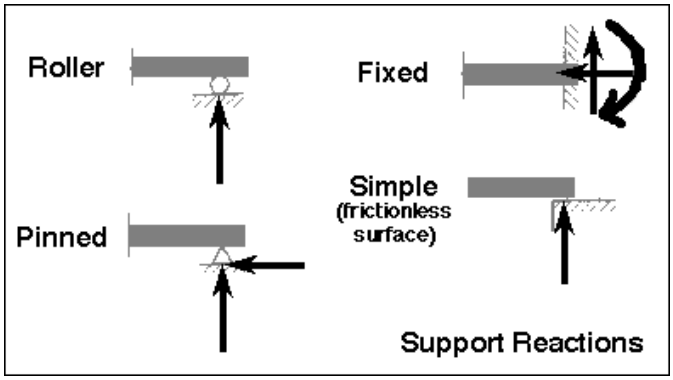

Figure 49 Supports and reactions

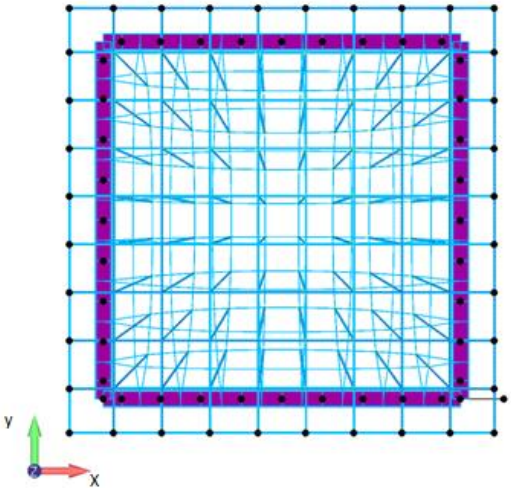

Figure 50 Top view of the model

With a fixed or hinged support, the translation in all directions is blocked. When applying hinged or fixed supports to the ring beam, the loads acting on the roof are taken up by the supporting structures, the ring system does not function to take the loads and becomes unnecessary. Thus the supports should be designed to stabilize the structure at the same time let the ring beam to work by translation. In this design, roller supports are applied.

The roof structure will be stable as long as the global z- and local x-direction translation are blocked. This can be achieved by applying a blocked translation in the local x-direction of a single support on each side of the hoop. In this case the hoop cannot rotate around its global z-axis and can only translate in its local y-direction. In this way, stability is guaranteed for the whole structure and the hoop beam functions to withstand compression and bending.

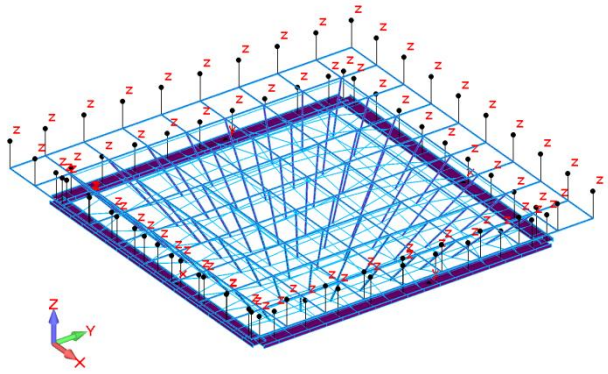

Figure 51 Support on this roof

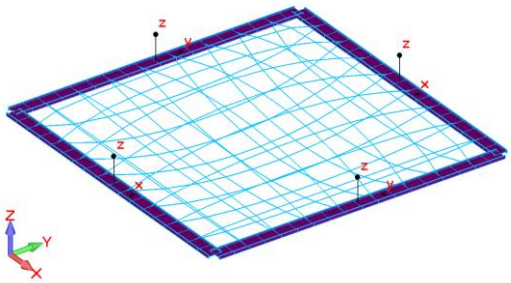

Figure 52 Place for rolled supports to block translation in local x-direction

Connections

Within the roof structure different connections can be applied. The choice of the type of connection will influence the deformation and resulting forces in the structure. The connection between elements can be either pinned or fixed connected.

- Pinned connections
  In contrast to pinned supports, pinned connections can restrict translation but a certain amount of movement would be permitted around the axis of each pin. Bending moment cannot be transferred by the pinned connections.
- Fixed connections
  Fixed connections can resist normal and shear forces as well as bending moments. Welded connections for steel elements, or cast-in-place concrete structure that is automatically monolithic and becomes a series of rigid connections are fixed connections.

However, whether a connection is pinned or fixed is determined by its stiffness compared to the elements to be connected. Not all the fixed connections must be welded or monolithic in nature, a connection composed of two screws can be considered as fixed as long as it provides enough resistance to vertical and lateral loads as well as to moments. And a fixed connection can become a pinned connection, this can be witnessed in steel structures when the connection yields and allows rotation in prior to the yielding of the connected elements. Fixed connections demand greater attention during construction and are often the source of building failure.

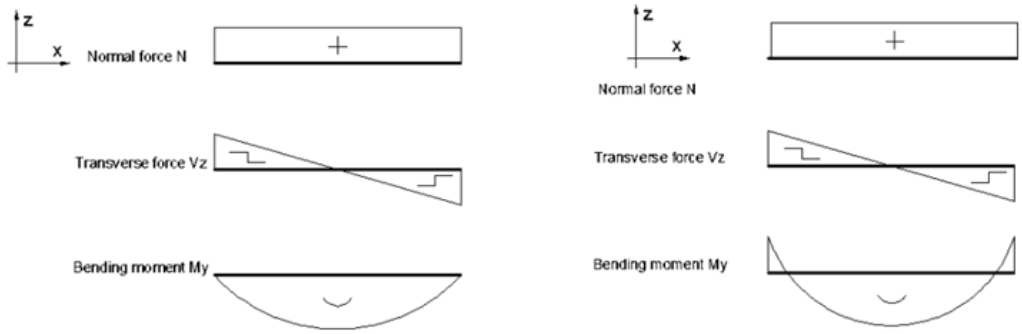

Figure 53 Force and moment distribution(left- pinned connection, right- fixed connection)

Choices of connection(see Section 15) type for this roof design are listed in the table below:

Table 3 Choice of connections

Position to apply connections	Type of connections
Connection for ETFE beam elements	Fixed – to transfer loads by bending
Connection between ETFE beam and rods	Fixed – to transfer loads by bending
Connection between rods and struts	Pinned – to allow rotation of struts
Connection for struts and cables	Pinned – to allow rotation of cables
Cable and hoop connection	Pinned – to allow rotation of cables
Hoop connection	Fixed – to transfer loads by bending

6.3 Materials and elements

The strength and stiffness of a single element are determined by the properties like material and cross section. The roof structure is composed of beams and cables, proper choices of materials and profiles need to be guaranteed in order to fulfill all structural requirements.

Material

For this roof structure, structural steel is applied to all the beam elements, cables are chosen from the producer Pfeifer (see Appendix A). General material characteristics are listed in the tables below:

Table 4 Mechanical properties of structural steel – S235, S355

Structural Steel Grade	Minimum Yield Strength (N/mm^2)	Tensile Strength (N/mm^2)
S235	235	360-510
S355	355	470-630

*Results of minimum yield strength are for steel with nominal thickness at 16mm.
*Results of tensile strength are for steel at nominal thickness between 3mm and 16mm.
*For steel the compression strength is equal to the tensile strength.

Table 5 Properties of PG cables

Cable Profile	Cross section(mm^2)	Limit tension(kN)	Breaking load(kN)
PG 40	237	222	367
PG 55	347	326	537
PG 75	467	438	722

*The breaking load for PG cable is about 1.65 times of the limit tension.

Elements

For the design different profiles are applied to different groups of elements with regards to the governing resulting force in elements.

Table 6 Choice of profiles for elements in different groups

Group	Profile	Advantage
ETFE beams	CHS	High moment of inertia, take large bending
Struts	CHS	High aesthetic value
Hoop	I profile	High moment of inertial, take large bending Easy connection
Rods	Circular bar	Take both normal force and bending
Top/ Bottom cable	PG cable	High tensile strength
Rectangular cables	PG cable	Light weight

7. Load combinations and Structural requirements

For any structural design, the load distribution is always a significant part as the structure reacts to the load cases. There are constant loads and variable loads, special attention needs to be paid to the later ones since the environmental loads tend to have random durations, magnitudes, and distributions. In this section, the possible load cases will be described first, then possible load combinations will be made to achieve high accuracy in the result from the structural analysis.

According to Eurocode NEN-EN 1990, actions on a structure are classified into three types with respect to their variation in time:

- Permanent action(G)
- Variable action(Q)
- Accidental action(A)

Permanent actions consist of self-weight of structures, pre-stress, and indirect actions caused by shrinkage and uneven settlements. Wind, snow and imposed loads on buildings are examples for variables loads, their magnitudes and distributions change over time. Accidental loads are loads caused by explosions, earthquakes and collisions from external objects. In this research project, considering the location of the building, accidental loads will not be taken into account due to their small occurrence rate.

7.1 Load cases

In total there are seven major load cases to be considered. These are pretension force, self weight from structural mass, dead load from installations, snow load, wind load, point load from Christmas tree (In Europe a big Christmas tree may be hang on the roof during Christmas), and point load from climbers due to maintenance. Pretension is applied to the cable net system to ensure that the cables are always under tension. Variable loads are applied to the ETFE beams as line loads. This means that the surface loads have to be converted to line loads. Point load from Christmas tree and from climbers can occur at any connection points of the bottom cable network. An approximation of the magnitude of each load case is given in this section.

Load Case 1: Pretension

Pre-stress results in a tensioned tie as long as the compression force is inferior to pre-stress level, which guarantees the stiffness and load path of the tensegrity structure.

There are two competing sources for a tensegrity's stiffness: the change of force carried by members as their length is changed, and the reorientation of forces as already stressed members are rotated. For any particular tensegrity, both sources of stiffness may have a critical role to play. The balance between these sources changes as the prestress varies. Research have shown that, for a particular 'stable' tensegrity, increasing a low level of prestress will increase the stiffness; while for a high level of prestress, a further increase in prestress may reduce the stiffness, and even lead to a structure with zero or negative stiffness (*S.D. Guest, 2010*).

If the prestress is too small, pretension could be insufficient to give the model enough stiffness thus the struts may displace sideways due to external loads. However, if too much prestress is added, the system may become inefficient. Therefore, pretension is defined differently for each model.

Load Case 2: Self weight

Self weight represents an additional load which sometimes could be of great influence due to the size of elements. It is determined by the property of materials, geometry and sections of the structure.

Self-weight: steel 78,5 kN/m^3

However, here it is very easy to take self-weight into account because Femap can calculate self-weight of the model by itself.

Load Case 3: Load from connections and installations

In this project, loads from installations mainly come from connection for ETFE beam elements, and from cable and strut connection. According to detailing of connections in Section 15 , the dead load of these connections are assumed as follows:

ETFE beam connection:	Steel box with holes, assume to be 150N/node
Cable-strut connection:	End fitting, 100N each *4=400N/node
	Connector, assume to be of the same mass of end fittings = 400N/node
ETFE cushion:	0,004kN/ m^2

Dead load from ETFE cushion is about 0.004kN/m^2, which is too small compared to other load cases thus not taken into account. Other loads like dead load from electricity wires, dead load from secondary structures are negligible compared to the relatively large load from connections.

Therefore, the dead load from connections and installations is assumed to be 150N per node for ETFE beam connection and 800N per node for the cable-strut connection.

Load Case 4: Snow load (*SID STUDIO, 2015*)

Snow load plays an important role in the structural design and can be the dominant load acting on a structure. Snow load is determined according Eurocode NEN-EN 1991-1-3, In this research, three of the four sides of the new roof are surrounded by higher buildings. On one side the elevation difference is 6,8m. The adjacent edges of the roof edge are 1,265 m higher. Due to height difference of adjacent roof edges, it is possible that snow may slip and accumulate on edges, resulting in large asymmetric snow loads.

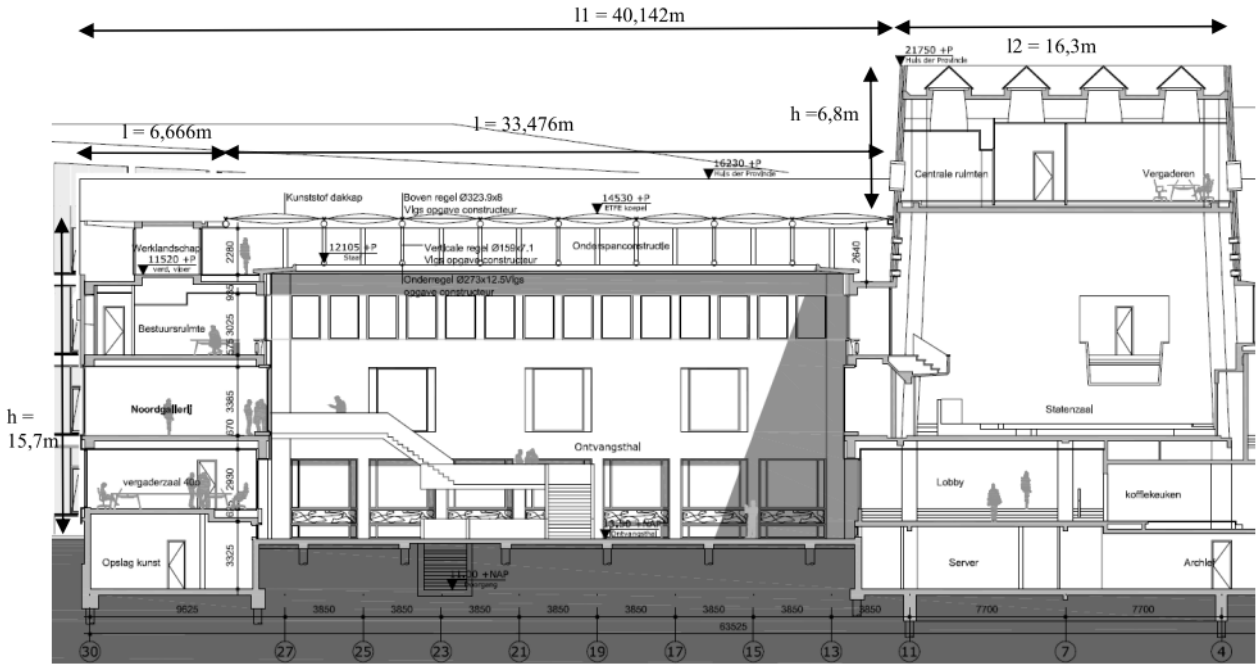

Figure 54 Section 1 - Right View

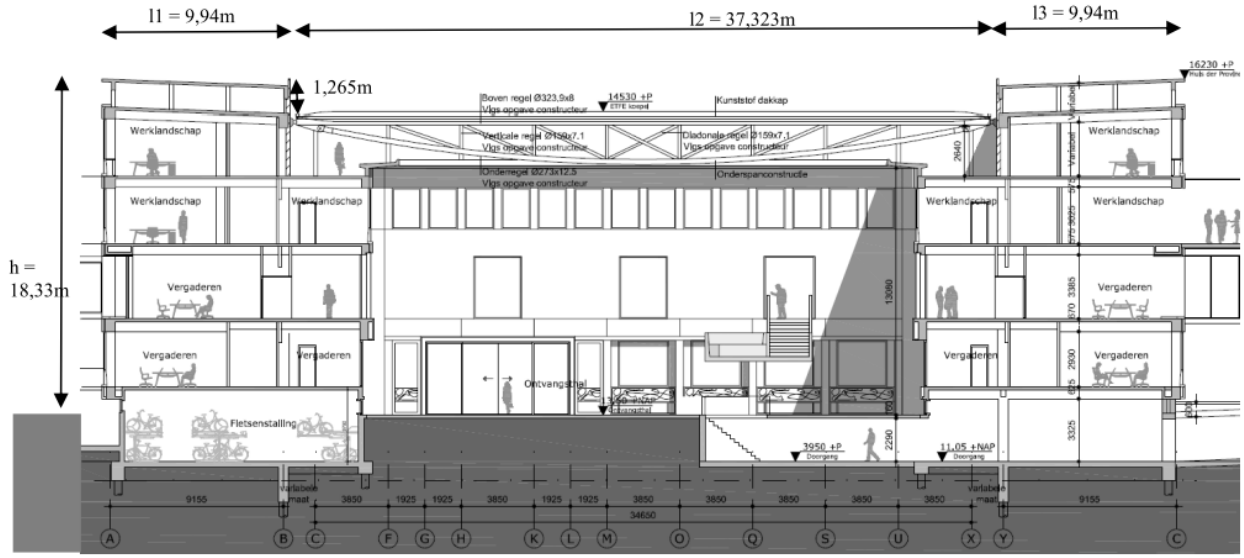

Figure 55 Section 2 - Front View

$$\text{Snow load } s_k = \mu_i \times c_e \times c_t \times s_k \qquad (7.1)$$

Where s_k = characteristic value of the snow load on the ground [kN/m^2], 0,7 kN/m^2 in the Netherlands

μ_i = shape coefficient, dependent on roof angle α, here take 0,8

c_e = exposure coefficient, 1,0 for most cases

c_t = thermal coefficient, 1,0 for most cases

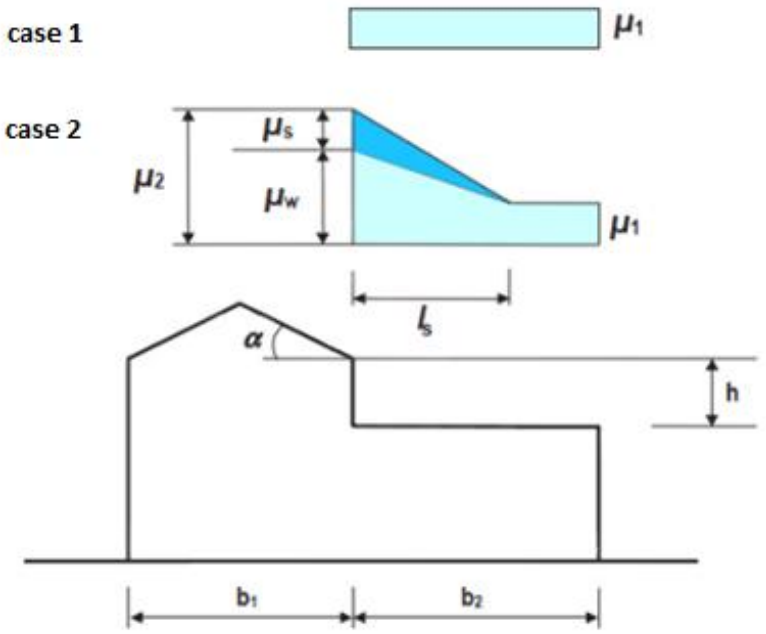

Figure 56 Snow load shape coefficient μ_i for roofs adjacent to higher buildings

Case 1

In case one snow load is considered as distributed to the entire roof at 0,56 kN/m^2 (μ_1 = 0,8).

Case 2

In Case snow accumulation on roof edges is taken into consideration. The accumulation of snow is partly caused by the wind (μ_w) and partly by the slide of snow from the upper roof (μ_s).

Table 7 Calculation for snow accumulation

Section 1	Section 2
b_1 = 16,3 m b_2 = 40,142 m h = 6,8 m L_s = 2 x h = 2 x 6,8 = 13,6m μ_w = (b 1 + b 2)/(2 x h) ≤ γ x h/s_k (with 0,8 ≤ μ_w ≤ 4,0) μ_w = (16,3+40)/(2 x 6,8) = 4,13 ≤ 2,0 x 6,8/0,7 = 19,4 ≤ 4,0 μ_w =4,0	b_1 = 9,94 m b_2 = 37,323 m h = 1,265 m L_s = 2 x h = 2 x 1,265 = 2,53 → min 5m μ_w = (b_1 + b_2)/(2 x h) ≤ γ x h/s_k (with 0,8 ≤ μ_w ≤ 4,0) μ_w = (9,8+37)/(2 x 1,7) = 18,7 ≤ 2,0 x 1,265/0,7 = 3,61 ≤ 4,0 μ_w =3,61
α < 15˚ → μ_s =0	α < 15˚ → μ_s =0

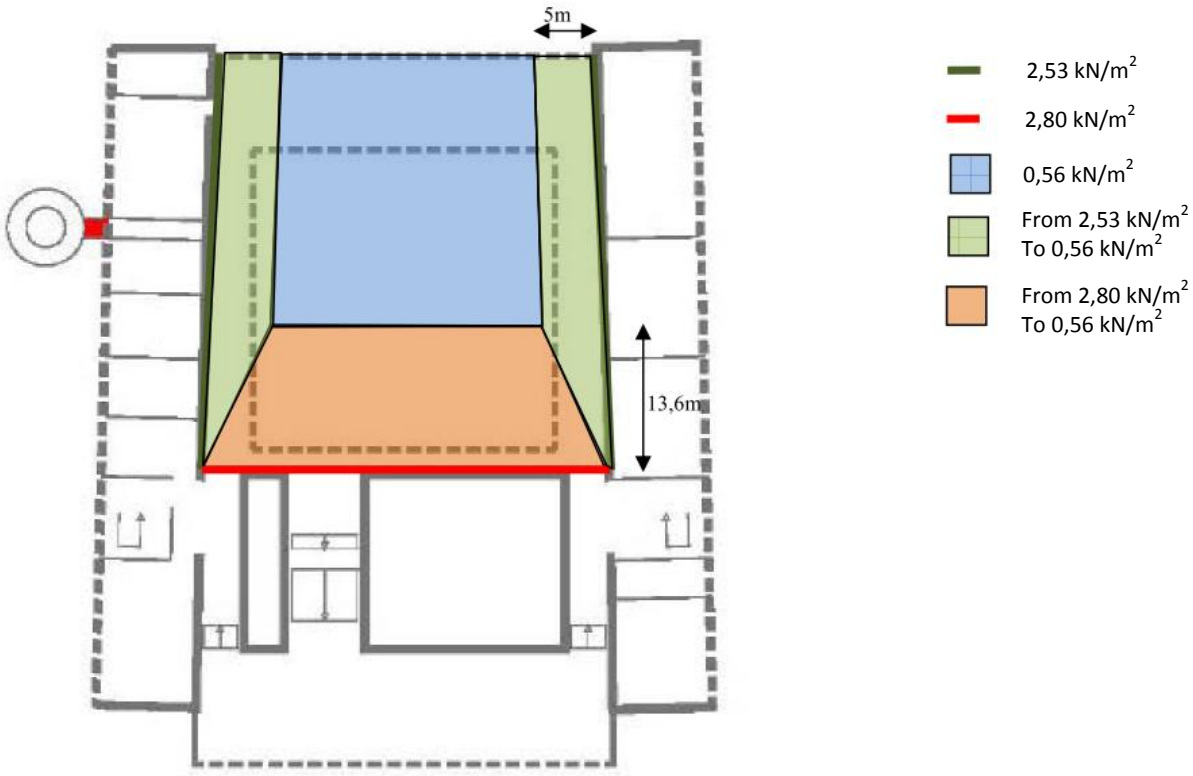

Figure 57 Snow load on the ETFE roof

This asymmetric snow load is considerably high and will be the decisive load for the roof.

Load Case 5: Wind load (*SID STUDIO, 2015*)

The wind load is determined according Eurocode NEN-EN 1991-1-4,It is dependent on the location, the environment, the dimensions and form of the structure. This applies to height, width and length.

$$\text{The wind pressure } w_e = q_{p(z)} \times c_f \times c_s c_d \qquad (7.2)$$

Where w_e = wind load on a structure or structural component [kN/m^2]

$q_{p\,(z)}$ = peak velocity pressure at reference height z_e, take 1,0 [kN/m^2]

c_f = force coefficient for structure or structural component [-], $c_f = c_{pe} - c_{pi}$

c_{pe} = external force coefficient for wind

c_{pi} = -0,3/+0,2 (negative means under pressure)

$c_s c_d$ =structural factor [-], here take 1,0

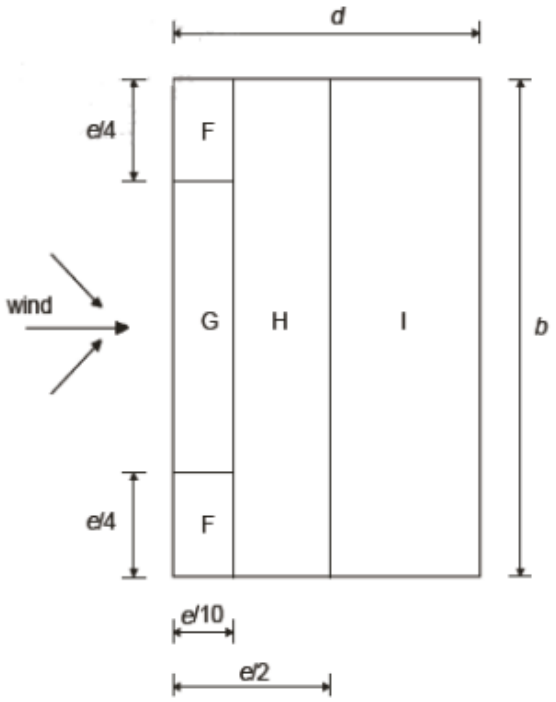

e= min{b,2h}

b= dimension in crosswind direction

d= dimension along wind direction

h= highest point of building

Figure 58 wind zones for flat roof

Table 8 External pressure coefficients c_{pe} for flat roofs

Flat roofs	c_{pe} For zone			
Type	F	G	H	I
Value	-1,8	-1,2	-0,7	+0,2/-0,2

*negative means suction

Wind comes from both longitudinal and transverse directions. For each direction, there are different wind cases depending on the geometry of the building.

Situation 1

In situation 1, wind comes from the transverse direction. If the roof and the neighbourhood higher walls act as a whole, geometry parameters of the structure are as follows :

b = 56m

h = 22m

d = 40,43m

e = b or 2h = 44m

Wind case 1

In wind case 1, the roof is loaded with wind comes from the left. Here assume that wind is moving over the higher wall. The wind load will mainly provide suction to the roof in the left part. The right part is loaded with pressure or suction at a very small magnitude.

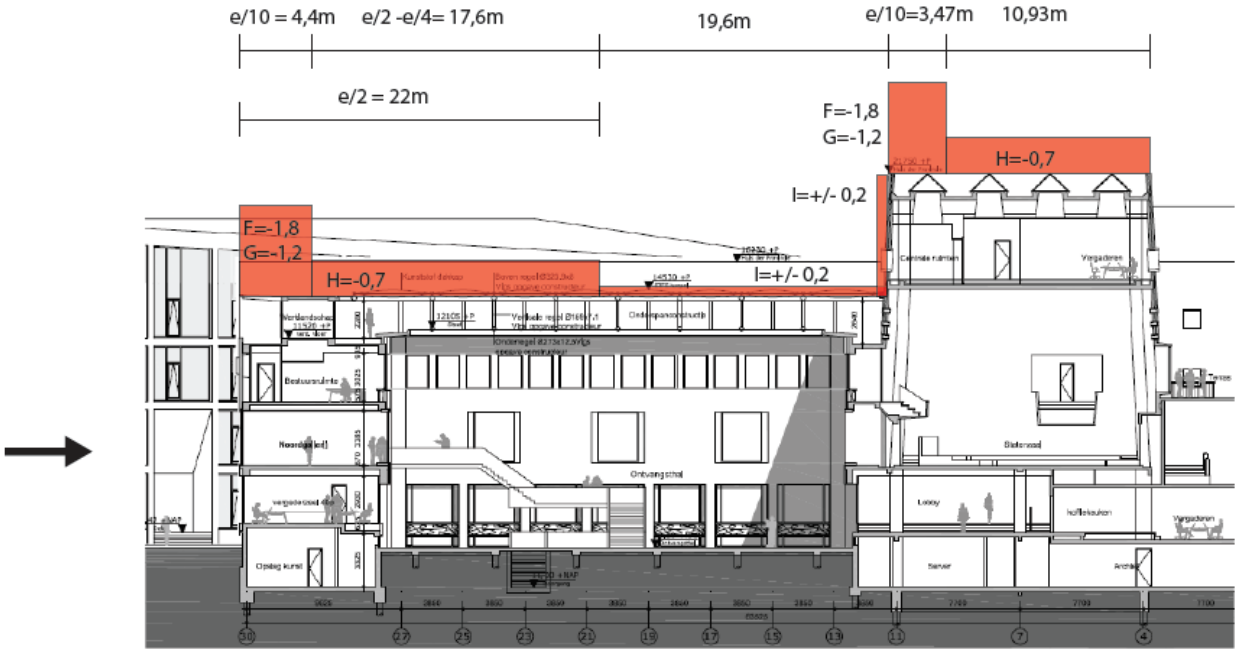

Figure 59 Wind case 1

Wind case 2

In wind case 2, wind still comes from the left part. However, it does not move over the higher building in the right side, but causes a pressure on the right part of the roof structure. The length of the roof structure subjected to pressure is taken equal to the height difference between the roof and the higher building.

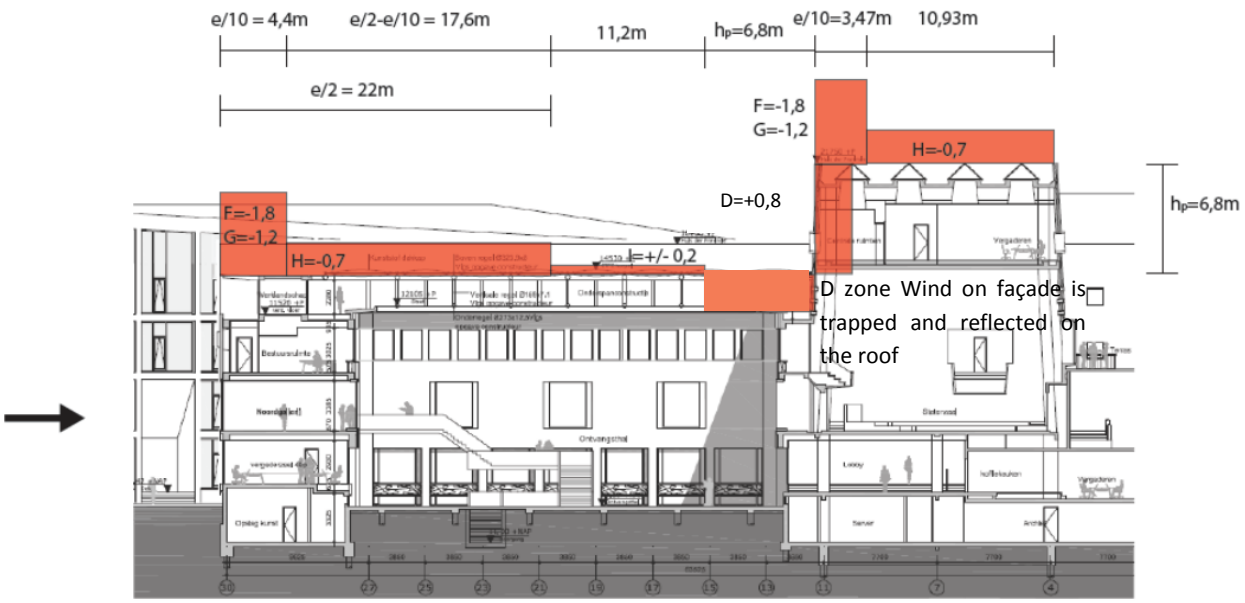

Figure 60 Wind case 2

Wind case 3

In wind case 3, the roof is loaded with wind from the right. Wind gives high local wind effects on the higher portion of the building. Suction occurs on the right part of the roof over a length equal to the height of the higher walls. The remainder of the roof is loaded in pressure or suction.

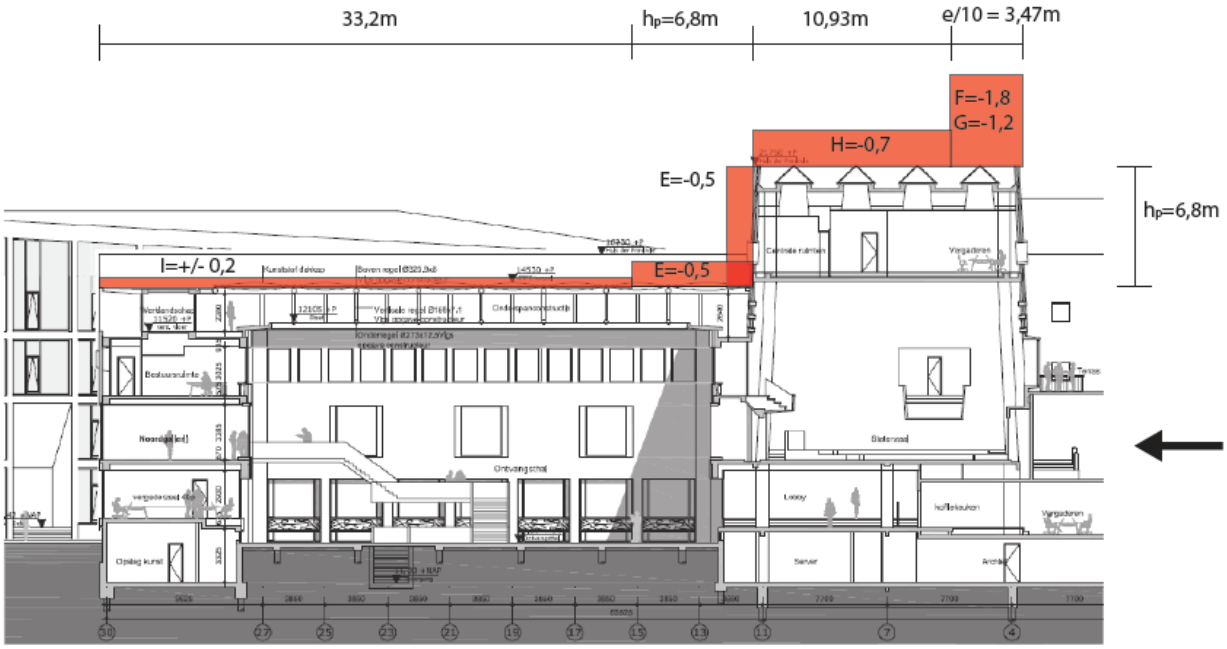

Figure 61 Wind case 3

Situation 2

In situation 2, wind comes from the longitudinal direction. Geometry parameters are as follows :

b = 56m

h = 16,23m

d = 56,6m

e = b or 2h = 32,5m

Due to symmetry line of the roof, there is no need to consider the wind from both left and right side. It is sufficient to consider a single case.

Wind case 4

In wind case 4, wind comes from the left and the whole roof is considered as flat.

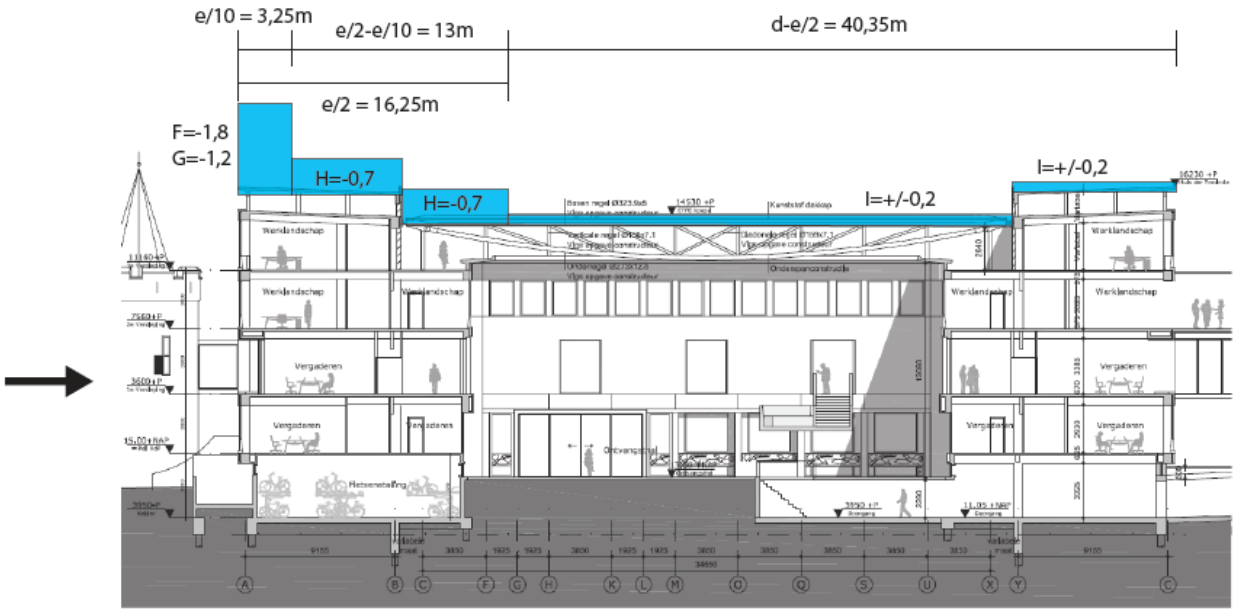

Figure 62 Wind case 4

Situation 3

The former two situations are applicable when the roof is surrounded by higher walls. In situation 3, a general roof is taken into consideration, assuming that the ETFE cushion covers the whole part of the roof area, which means that the wind zones are all within the ETFE area.

In this situation, wind comes from the longitudinal direction will cause the largest load. Due to symmetry line of the roof, there is no need to consider the wind from both left and right side. It is sufficient to consider a single case.

Geometry parameters are as follows :

b = 37,323m

h = 16,23m

d = 33,476m

e = b or 2h = 32,5m

Wind case 5

In wind case 5, wind comes from the left and the wind zones are all within the ETFE area. The most critical asymmetrical wind situation is assumed as if there are no flat roof areas next to the ETFE cushion, in this case zone F,G,H are in suction and zone I in pressure.

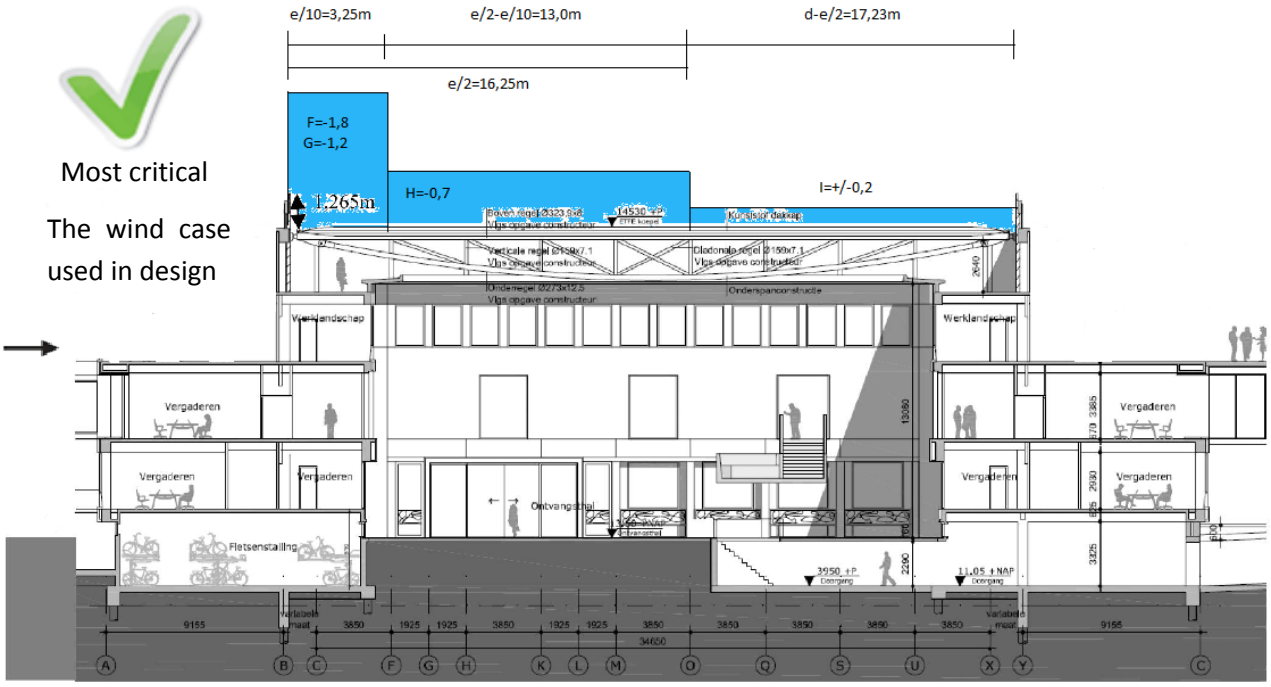

Figure 63 Wind case 5

Situation 4

In situation 4, assume that the whole ETFE cushion lies in the F zone. This is the most critical situation for symmetrical wind load where the largest wind suction load occurs. Geometry parameters are not required for calculation.

Wind case 6

In wind case 6 there is no need to consider the wind direction. The ETFE will take the largest possible wind suction load.

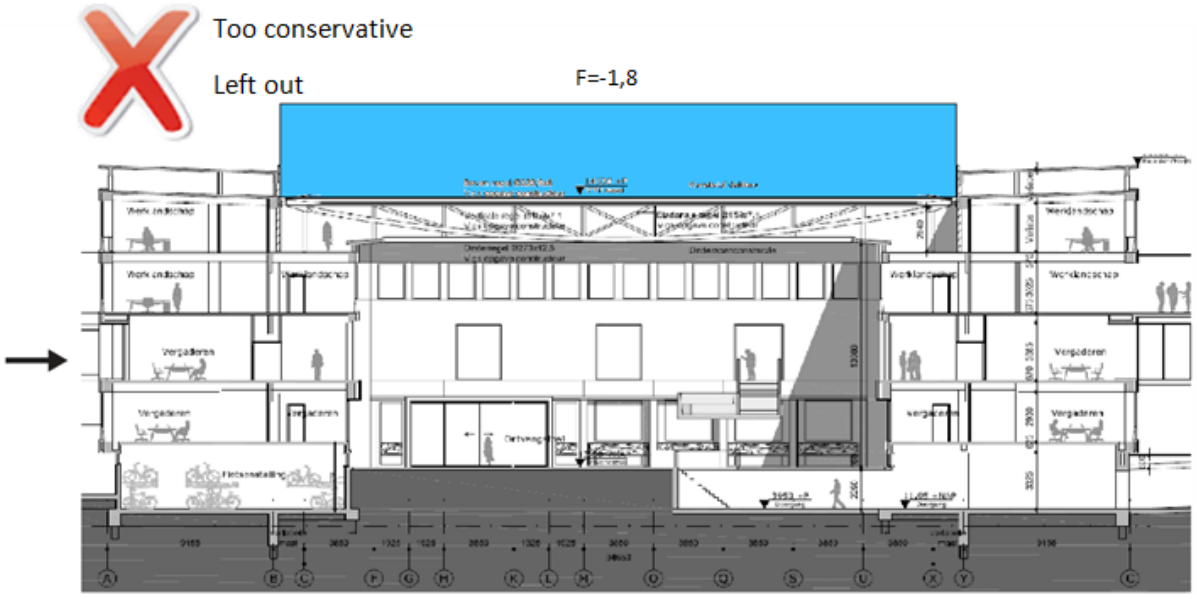

Figure 64 Wind case 6

However, the roof area is really big with an area of about 900 m^2, the assumed wind case is nearly impossible in real life. Thus the assumed wind case 6 is left out.

From the above investigation of wind load, wind case 5 is the most critical case and will be calculated in this research. The wind load is upward suction load.

Internal pressure

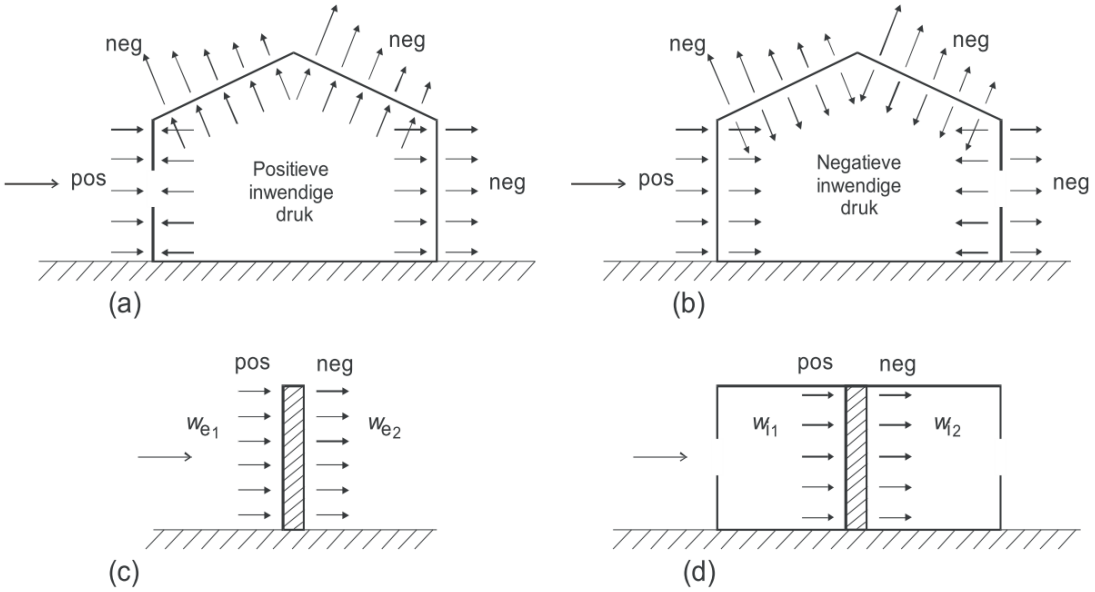

Figure 65 Pressure on surfaces

Inside the building internal suction is present due to the wind. The internal pressure coefficient is taken as c_{pi}=-0.3/+0.2, with a positive value means internal over pressure and negative value under pressure. In

zone I (see Table 8) the external wind coefficient c_{pe} has two values +/-0.2. Therefore wind case 5 with internal pressure has 4 combinations of force coefficient.

For the external wind coefficient c_{pe}, there are two values +/- 0.2 in zone I. In total for wind case 5 with internal pressure there are 4 combinations:

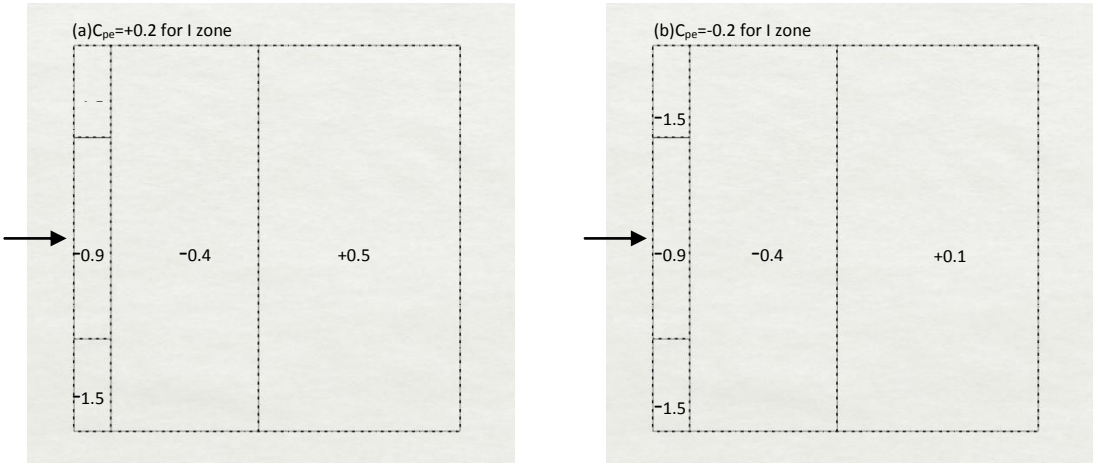

Figure 66 wind case 5 with internal under pressure (c_{pi}=-0.3)

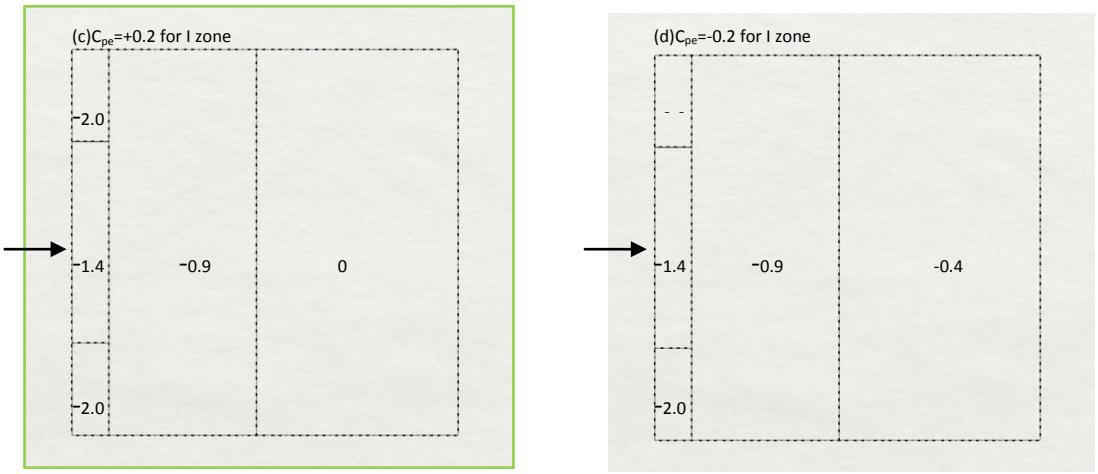

Figure 67 wind case 5 with internal over pressure (c_{pi}=+0.2)

In this design, snow load is the dominant downward load case that determines the minimum amount of pretension and vertical deflection. The upward wind suction load determines the cross section for top cables and for struts. Thus in the four combinations above, the one results in the largest resulting force is the most critical case. From the magnitude of the force coefficient, combination (c) and (d) are more critical than (a) and (b). Between (c) and (d), it is assumed that combination (c) will lead to larger resulting force in elements compared to combinations (d) due to asymmetry, which also proved to be true. Thus in this study, combination (c) for the wind coefficient c_f is chosen in calculation.

According to Eurocode, the wind pressure $w_e = q_{p(z)} \times c_f \times c_s c_d$

Wind load in the roof area is:

Table 9 Wind load

Wind zone	Wind pressure (kN/m^2)
F	-2,0
G	-1,4
H	-0,9
I	0

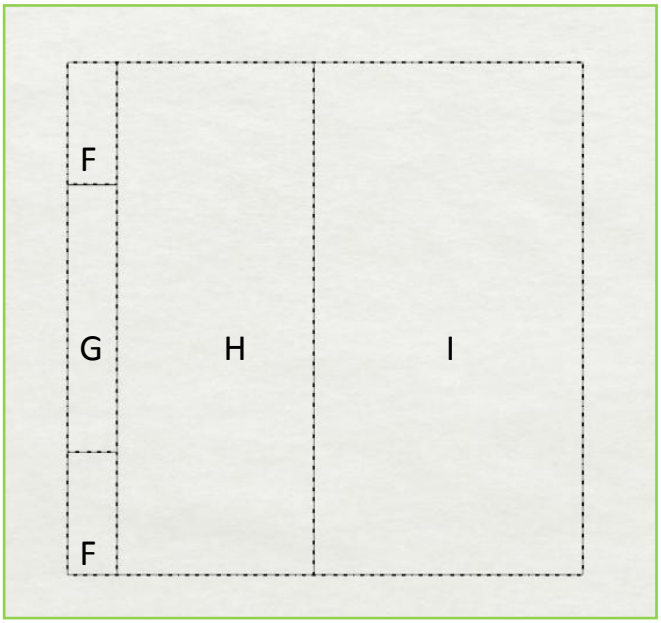

Figure 68 Wind zones in the roof area

Load Case 6: Rain load

The determination of the rain load depends on the height of the overflow and the shape of the roof. Water accumulation on the roof should be avoided. In this design, some minimum slope will be made on the ETFE beam grid by pulling the beams upward to a certain height. Then rain water will be guided to the gutters around the TFE beams. Therefore, rain load will not be taken into account.

Load Case 7 : Test load of 10kN

In the Netherlands, it is possible that a Christmas tree will be hang on the roof structure. Here a 10kN test load is taken into account to make sure the tensegrity structure has enough residual capability.

Load Case 8: Point load from maintenance

To clean the roof, access with climbers should be secured to the structure, and in case falling needs to be supported. This load is assumed to be a very large point load as 10kN due to acceleration from falling.

In the preliminary design phase, it has been found that this structure has high sensibility to asymmetrical loading. Applying point load at node with the largest downward displacement under snow load would lead to the most unfavourable situation. This load case will not be considered in the variable study, but be regarded in the final design to guarantee enough load-bearing capacity and usability. In the final design, the 10kN test load will be applied to check the SLS requirement, and both the test load and load from climber will be applied to check the ULS requirement to guarantee safety when people hang the Christmas tree with climber.

7.2 Load combinations

For every critical load case the load effects should be determined by combinations of the load cases which act at the same time. In this research project, LC represents the abbreviation of load combination.

Every structure has to comply with two possible limit states which are directly related to the reliability and usability of the structure. The ultimate limit state (ULS) is used to check structural safety. The serviceability limit state (SLS) is used to check the usability.

According to Eurocode, safety factors are used for the different load cases to represent the most unfavourable cases. Due to the measurability of pretension load, no safety factor is included for this load case.

Ultimate Limit State

Ultimate limit state concerns the safety of the structure. In Eurocode, ULS are divided into the following categories:

- EQU: Loss of equilibrium of the structure.
- STR: Internal failure or excessive deformation of the structure or structural member.
- GEO: Failure due to excessive deformation of the ground.
- FAT: Fatigue failure of the structure or structural members.

In this design, the situation of GEO and FAT are not that relevant to the roof structural performance thus not taken into consideration.

Table 10 Load safety factors for EQU. Reproduced from NEN-EN 1990:2002

Permanent actions		Leading variable action	Accompanying variable actions	
Unfavourable	Favourable		Main(if any)	Others
$\gamma_{Gj,sup}G_{ki,sup}$	$\gamma_{Gj,inf}G_{kj,inf}$	-	-	$\gamma_{Q,i}\,\psi_{0,i}Q_{k,i}$

Where the partial factors for the EQU situation are :

$\gamma_{Gj,sup}$ =1,1
$\gamma_{Gj,inf}$ =0,9
$\gamma_{Q,1}$ =1,5
$\gamma_{Q,I}$ =1,5

Table 11 Load safety factors for STR. Reproduced from NEN-EN 1990:2002

Permanent actions		Leading variable action	Accompanying variable actions	
Unfavourable	Favourable		Main(if any)	Others
$\gamma_{Gj,sup}G_{ki,sup}$	$\gamma_{Gj,inf}G_{kj,inf}$	-	-	$\gamma_{Q,i}\,\psi_{0,i}Q_{k,i}$
$\xi\gamma_{Gj,sup}G_{ki,sup}$	$\gamma_{Gj,inf}G_{kj,inf}$	$\gamma_{Q,1}Q_{k,1}$	-	$\gamma_{Q,i}\,\psi_{0,i}Q_{k,i}$

Where the partial factors for the STR situation are :

$\gamma_{Gj,sup}$ =1,35
$\gamma_{Gj,inf}$ =0,9
$\gamma_{Q,1}$ =1,5
$\gamma_{Q,I}$ =1,5
$\xi\gamma_{Gj,sup}$ =1,2

The load combination of actions for ULS:

$$\gamma_G \cdot G_k + \gamma_{Q,1} \cdot Q_{1,k} + \sum(\gamma_{Q,1}.\psi_{0,1} \cdot Q_{i,k}) \quad (7.3)$$

Where γ_G = partial factor for permanent loads

G_k = total permanent load

$\gamma_{Q,1}$ = partial factor for variable loads

$Q_{1,k}$ = characteristic value of the leading variable load

$\Psi_{0,1}$ = factor for combination of variable load I with the leading variable load, take 1,0

$Q_{i,k}$ = characteristic value of variable load i

The STR is leading and will be considered. EQU is left out of consideration. To clarify, the ULS is calculated with the following equations:

$$F_d=1,0P+1,35G_{k,j} \quad (7.4)$$

$$F_d=1,0P+1,2G_{k,j}+1,5Q_{k,1} \quad (7.5)$$

Where P = prestress.

Serviceability Limit State

Serviceability limit state concerns the functioning of the structure and the comfort of people.

The load combination of actions for SLS:

$$\gamma_m G_{k,j}+\gamma_m Q_{k,1} \quad (7.6)$$

Where γ_m is the partial factor for material characteristics and is equal to 1,0

Load Combinations

For calculations pretension, snow load, wind load and dead load from self weight and installations will be taken into account. No safety factor is used for pretension due to the measurability. The combination with snow load is leading for downward load. Wind load with favourable dead load will be calculated to evaluate the upward movement of the roof structure.

In the final design, seven load cases are considered, they are pretension, self weight, load from installations, snow load, wind load, 10kN test load, and point load from climber. The load combinations are described as follows:

LC1: Pretension+ Self weight+ Test load+ Climber

LC2: Pretension+ Self weight+ Snow load+ Test load+ Climber

LC3: Pretension+ Self weight(favourable)+ Wind load+ Test load+ Climber

Table 12 LC1: Pretension + Dead load

Load	ULS	SLS
Pretension	1,0	1,0
Dead load	1,35	1,0
Test load	1,0	1,0
Climber	1,5	0

Table 13 LC2: Pretension + Dead load+ Snow load

Load	ULS	SLS
Pretension	1,00	1,0
Dead load	1,20	1,0
Snow load	1,50	1,0
Test load	1,0	1,0
Climber	1,5	0

Table 14 LC3: Pretension+ Dead load+ Wind load

Load	ULS	SLS
Pretension	1,00	1,0
Dead load	0,90	1,0
Wind load	1,50	1,0
Test load	1,0	1,0
Climber	1,5	0

7.3 Structural requirements

The fundamental requirements for a structure are strength, stiffness and stability. Strength and stability check are under ULS, stiffness check is done according to SLS.

Resistance of the cross section

In any design the structure should be strong enough to resist every load and influence that may arise during construction and use. As a conservative approach, Von Mises stress is used to predict yielding of materials under any loading condition. The Von Mises stress (*Wikipedia, 2016*) can be written as:

$$\sigma_{vm} = \sqrt{\frac{(\sigma_{xx}-\sigma_{yy})^2+(\sigma_{yy}-\sigma_{zz})^2+(\sigma_{zz}-\sigma_{xx})^2+6(\tau_{xy}^2+\tau_{yz}^2+\tau_{xz}^2)}{2}} \quad (7.7)$$

σ_{xx}, σ_{yy}, σ_{zz} – normal stress

τ_{xy}, τ_{xy}, τ_{xy} – shear stress

The requirement is that:

$$\sigma_{vm} \leq f_y \quad (7.8)$$

The Von Mises stress equation take normal force, bending, and shear into consideration. It is worth mentioning that the maximum bending and maximum shear never occur at the same point. And from the static analysis results, at the weakest point bending is always the governing and shear force makes negligible contribution to the Von Mises stress. Which means in this roof structure, the maximum Von Mises stress is more or less the maximum axial stress. Therefore, another method for unity check for the ULS can be applied by making use of the following criterion:

$$\frac{N_{Ed}}{N_{Rd}} + \frac{M_{y,Ed}}{M_{y,Rd}} + \frac{M_{z,Ed}}{M_{z,Rd}} \leq 1 \quad (7.9) \qquad \text{or} \qquad \sigma = \frac{N}{A} + \frac{M_y}{W_y} + \frac{M_z}{W_z} \leq f_y \quad (7.10)$$

N_{Ed}, M_{Ed} – design values of the force

N_{Rd}, M_{Rd} – design values of the resistance of cross section

σ – combined stress in the cross section

f_y – yield stress of the material

Serviceability Limit State

The SLS deals with the usability requirements of a structure. Here vertical deflection will be checked with respect to deformation requirements in Eurocode.

Vertical deformation

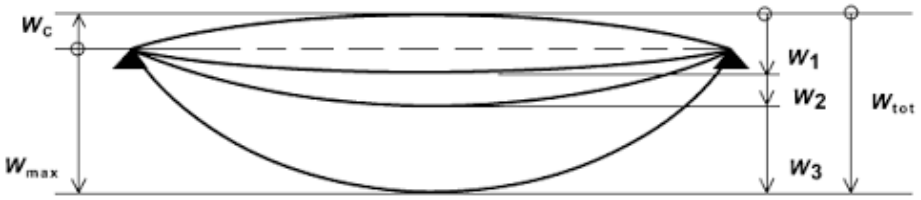

Figure 69 Definition of vertical displacements

- ω_c – Precamber in the unloaded structural member
- ω_1 – Initial part of the deflection under permanent loads
- ω_2 – Long-term part of the deflection under permanent loads
- ω_3 – Additional deformation due to variable loads
- ω_{tot} – Total deflection, the sum of $\omega_1 + \omega_2 + \omega_3$

The Eurocode describes that the maximum deformation for a roof structure is $0{,}004 l_{span}$ for a single bar. The objective is to achieve a structure that not only safe but also feels safe, thus heavy deformation fluctuations should be avoided when the roof is subjected to high variable loads. For a tensegrity roof there is no definitive deformation requirements. The constructive report [39] states it is permissible that the vertical deformation due to live load is between 1/200 and 1/150 of the roof span. This range is quite broad and it is very easy to meet this requirement. In the design phase, a more strict criterion to which the vertical deflection will be checked against is:

$$\delta < \frac{l_{span}}{200} \tag{7.11}$$

All displacements in the steel structure of the roof need to stay below 1/200 x 28602 = 143mm.

In the optimisation phase, there is no need to do SLS check since all the models have the vertical deflection due to live load within 1/200 and 1/150 of the roof span.

When water accumulates, large extra variable loads can act on the structural elements. The national annexes of the Eurocode NEN-EN 1990 NB A1.4.3 prescribe that a minimum slope of 1,6% together with the deformation requirement is sufficient to prevent water accumulation. The stiffness should be reduced with γ_M = 1,3 according to EN 1991-1-3 Note 7.2. This is equivalent to multiplying ω_{max} with 1,3.

Suppose the maximum deflection is at 7m from the edge, ω_{max} =143mm, at mid-span (17m) the inclination of the roof is:

(1,3 *143+7000*1,6%)/7000*100%=4,3%

Thus, the mid of the roof should be 17000*4,3%=731mm higher than the edge to avoid water accumulation.

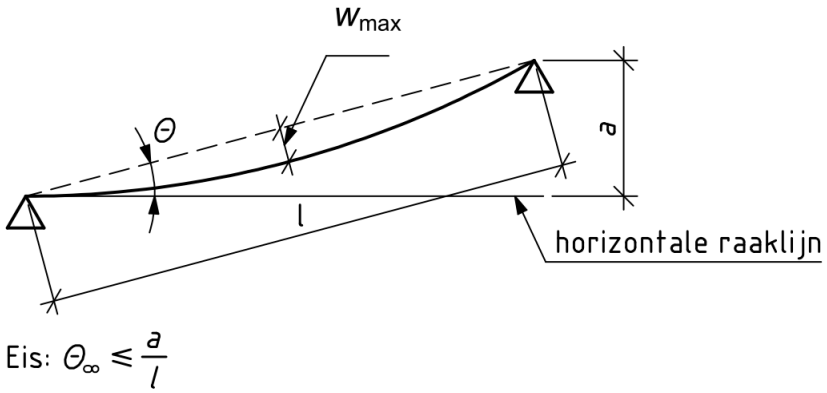

Figure 70 Required slope to prevent water accumulation.
Reproduced from NEN-EN 1990+A1+A1/C2:2011/NB:2011

Stability

Stability means the resistance of a structural member to buckling. The load at which buckling occurs depends on the stiffness of a component, not upon the strength of its material. Buckling refers to the loss of stability of a component. It is characterized by a sudden sideways failure of a structural member subjected to high compressive stress, where the compressive stress at the point of failure is less than the ultimate compressive stress that the material is capable of withstanding (*Wikipedia, 2016*).

General method for buckling check of structural elements can be applied with the criterion:

$$\frac{N_{Ed}}{\chi N_{Rk}/\gamma_{M1}} + \frac{M_{y,Ed}}{\chi_{LT} M_{y,Rk}/\gamma_{M1}} + \frac{M_{z,Ed}}{M_{z,Rk}/\gamma_{M1}} \leq 1 \qquad (7.12)$$

X, χ_{LT} – reduction factor for the relevant buckling mode

N_{Ed}, M_{Ed} – design values of the force

N_{Rk}, M_{Rk} – design values of the resistance of cross section

γ_{M1} – partial factor of elements for stability check, $\gamma_{M1} = 1{,}0$

In the finite element analysis, a finite element eigenvalue - eigenvector solution is used. The result is an eigenvalue, also called the buckling load factor (BLF). The BLF is the factor of safety against buckling or the ratio of the buckling loads to the applied loads.

Table 15 Interpretation of the Buckling load factor (*SOLIDWORKS Help, 2012*)

BLF Value	Buckling Status	Notes
BLF > 1	Buckling not predicted	The applied loads are less than the estimated critical loads. Buckling is not expected.
BLF = 1	Buckling predicted	The applied loads are exactly equal to the estimated critical loads. Buckling is expected.
0 < BLF < 1	Buckling predicted	The applied loads exceed the estimated critical loads. Buckling is expected.
-1 < BLF < 0	Buckling not predicted	Buckling is predicted if you reverse all loads.
BLF = -1	Buckling not predicted	Buckling is expected if you reverse the load directions
BLF < -1	Buckling not predicted	Buckling is not expected even if you reverse all loads.

Taking into account the imperfection, difference between model and real construction, and the sudden failure of buckling with no warning, a more strict standard with BLF>3 is applied as the boundary that buckling is not predicted.

8. Design process

There are many variables in this roof structure and all of them are interdependent. In order to find out the influences of different possible variables in this roof design, a model which satisfies both SLS and ULS check is designed and chosen as the standard model, based on which all the changes are made. To compare the performance of individual models to the standard model, a percentage (Rel.Std) is used to represent the performance relative to the standard model.

8.1 Variables and standard model

The variables are:

Table 16 Possible variables in the roof design

Order	Variable	Range
1st	Number of branches of the cable net	No. x-direction 6,7,8,9,10 No. y-direction 6,7,8,9,10
2nd	Position of intersection points	On ground(z=-13260) Close to infinity below support (z=-1000000)
3rd	Way of form finding	Self weight, Vertical point load, Radial pattern
4th	Height above support Height below support	1950mm<D_{top}<2350mm 2150mm<D_{bottom}<2550mm
5th	Pretension	120kN<P<200kN
6th	Sectional size of elements	Depends on locations and pretension

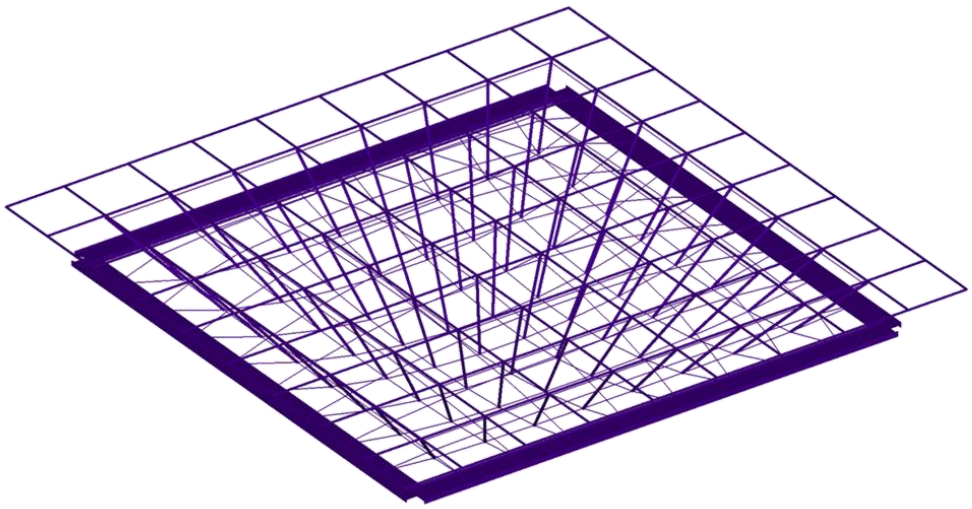

Figure 71 Standard model of the roof structure

Parameters of the standard model are listed in the tables below:

Table 17 Parameters of standard model

Variable	Choice
Number of branches of the cable net	No. x-direction 8 No. y-direction 8
Position of intersection points	Z=-13260
Way of form finding	Radial pattern
Height above support Height below support	D_{top}=2250mm D_{bottom}=-2350mm
Pretension	P_{top}=175kN P_{bottom}=160kN
Sectional size of elements	See Table 18

Table 18 Section size of the standard model

Name	Type	Material	Property	Size
ETFE beam	Beam	S355	CHS	114,3*3,2
Rods	Beam	S355	Circular Bar	d=55mm
Rec cable	Cable	PG40	Cable	A=237 mm^2
Cable net top	Cable	PG55	Cable	A=347 mm^2
Cable net bottom	Cable	PG75	Cable	A=467 mm^2
Hoop	Beam	S355	I beam	h=1300mm,b=300mm, t_{flange}=55mm,t_{web}=15mm
Strut	Beam	S355	CHS	152,4*12,5

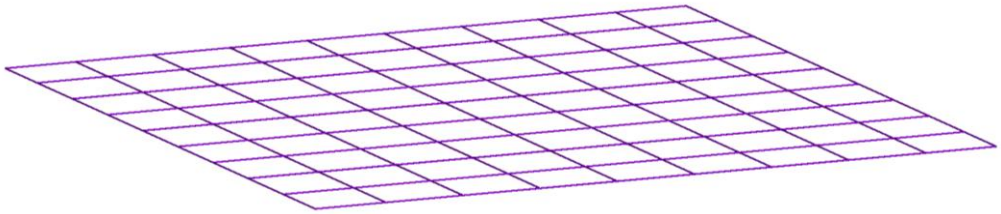

Figure 72 ETFE Beam

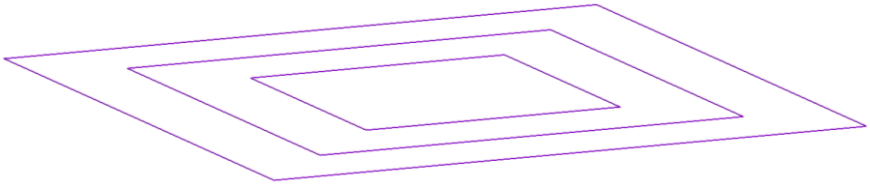

Figure 73 Rec Cable

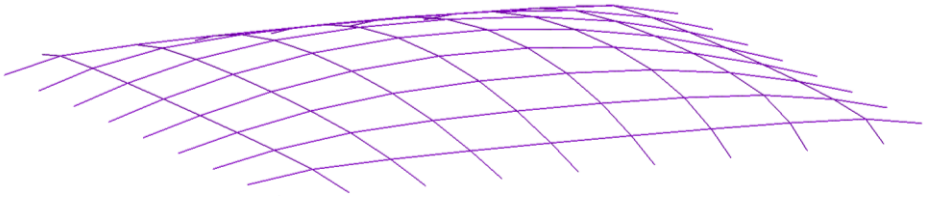

Figure 74 Cable net top

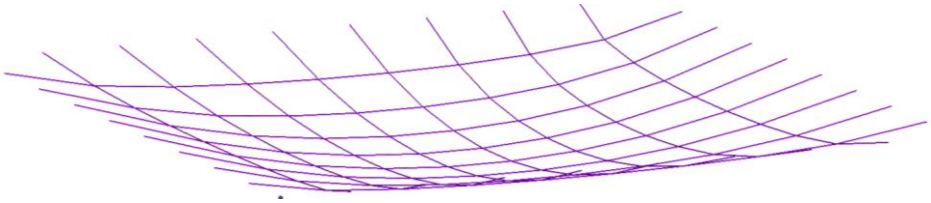

Figure 75 Cable net bottom

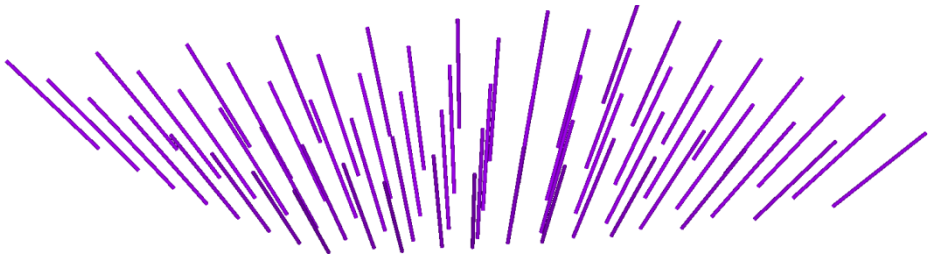

Figure 76 Strut

Figure 77 Hoop

Constraints of the standard model are depicted in Figure 78:

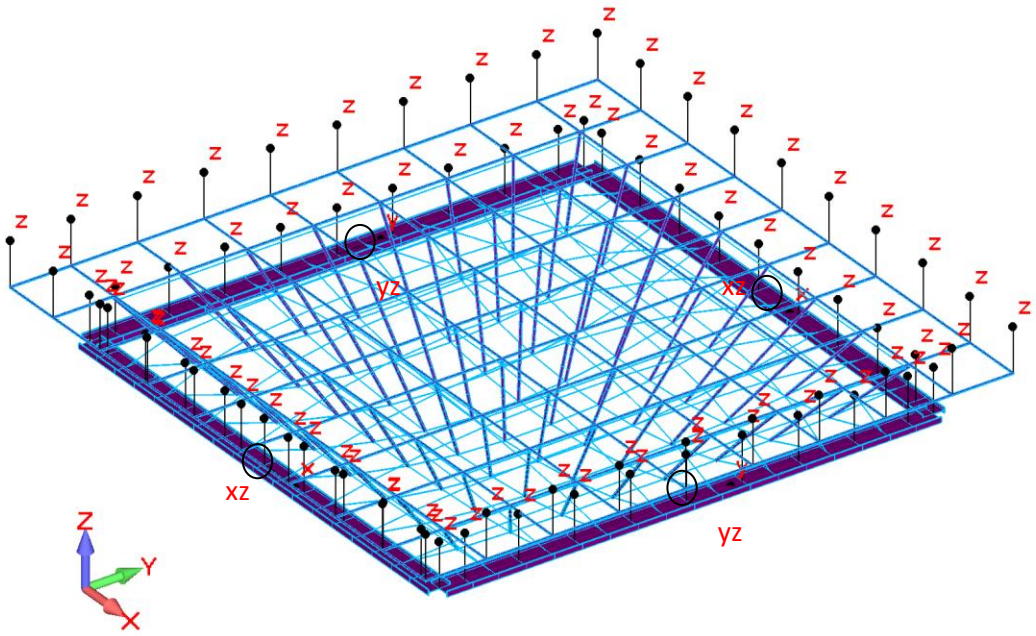

Figure 78 Constraints for the standard model

Loads on the structure are described in the figures below. Pretension is applied to bolt regions (see Appendix E) which is expressed by load (kN). Dead load from connections is applied on connection points as point load. The live loads from snow and wind are applied as line load on the ETFE beam elements (see Appendix F). Self weight is applied by defining the gravity acceleration.

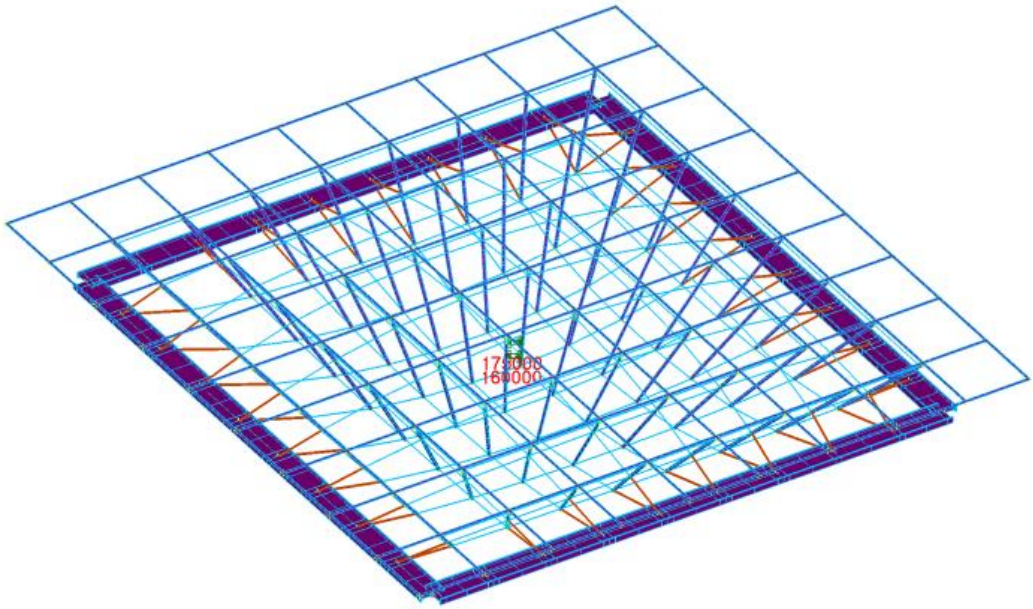

Figure 79 Pretension

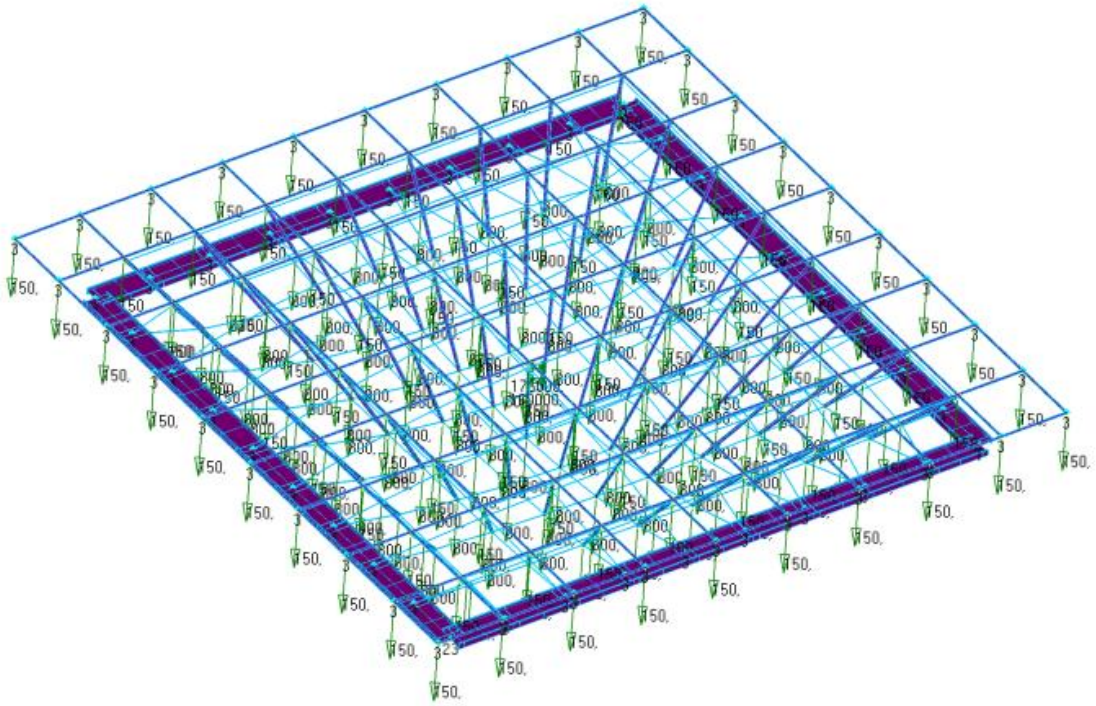

Figure 80 Dead load from connections

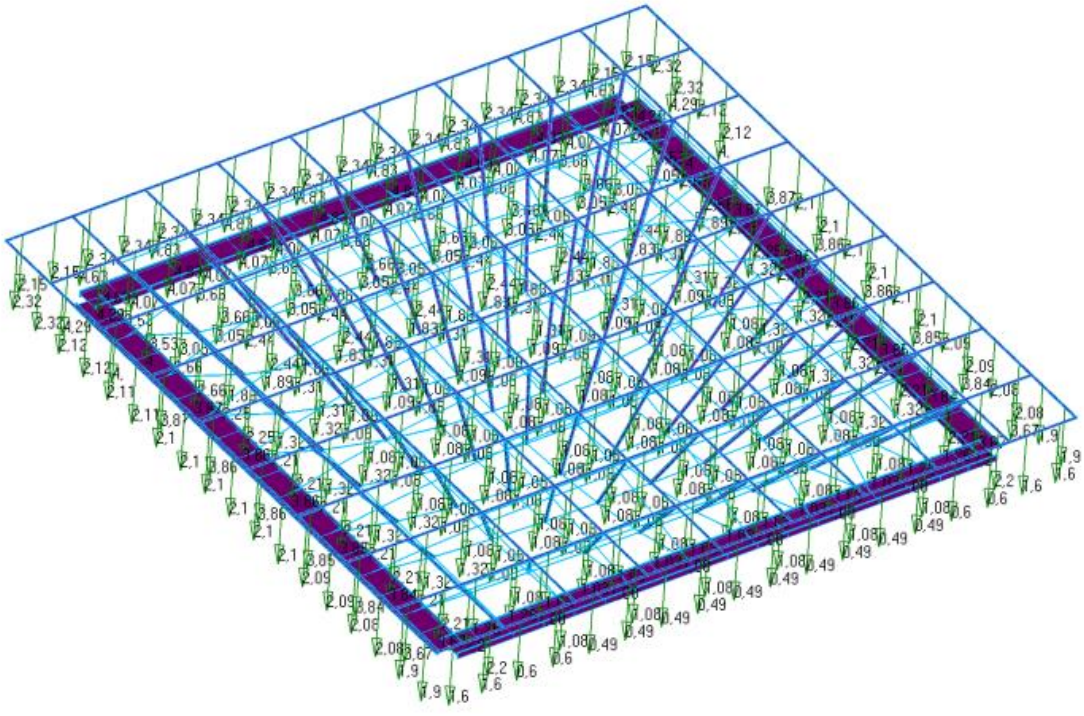

Figure 81 Snow load

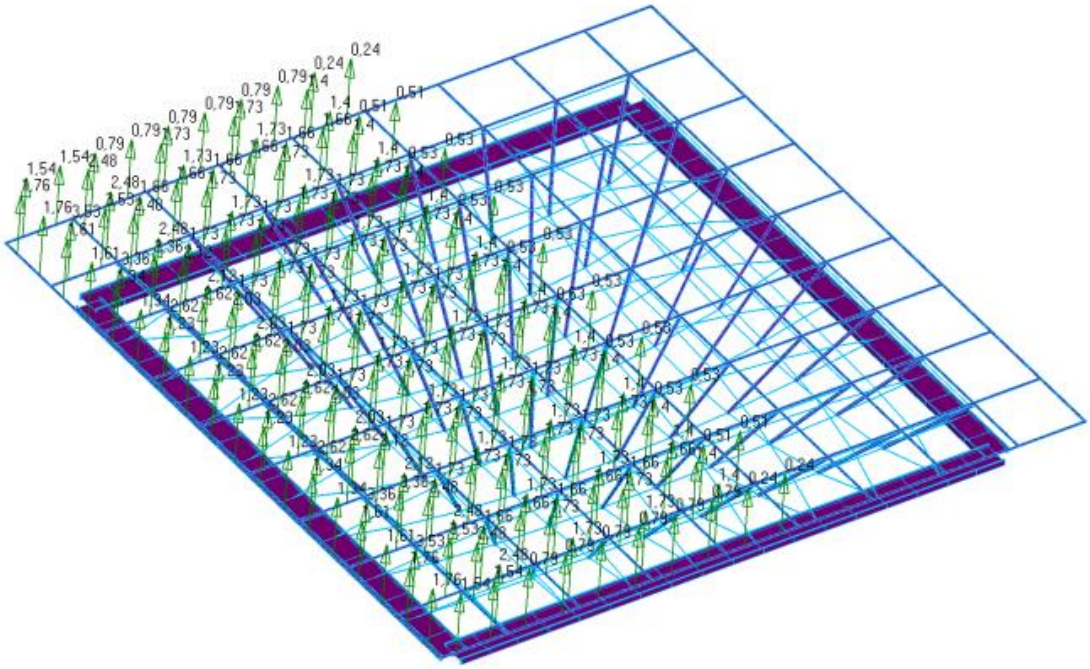

Figure 82 Wind load

8.2 Interdependence and design process

In this variable study, there are always three variables: the chosen variable (1st, 2nd, 3rd, 4th order), 5th order pretension, and 6th order cross section. Influences of changing a single variable will be found after this multi-variable study.

The pretensioned cable-strut model has an undetermined system which is loaded by variable loads. It is a very complex affair to design such a structure because every variable is dependent on the rest, also making changes to a single group of elements will bring changes to the other groups. The choice of the profile influences the roof structure as a whole. Deformations, resulting forces, required prestress, total mass, etc, will change in every element of the roof structure as one single variable changes.

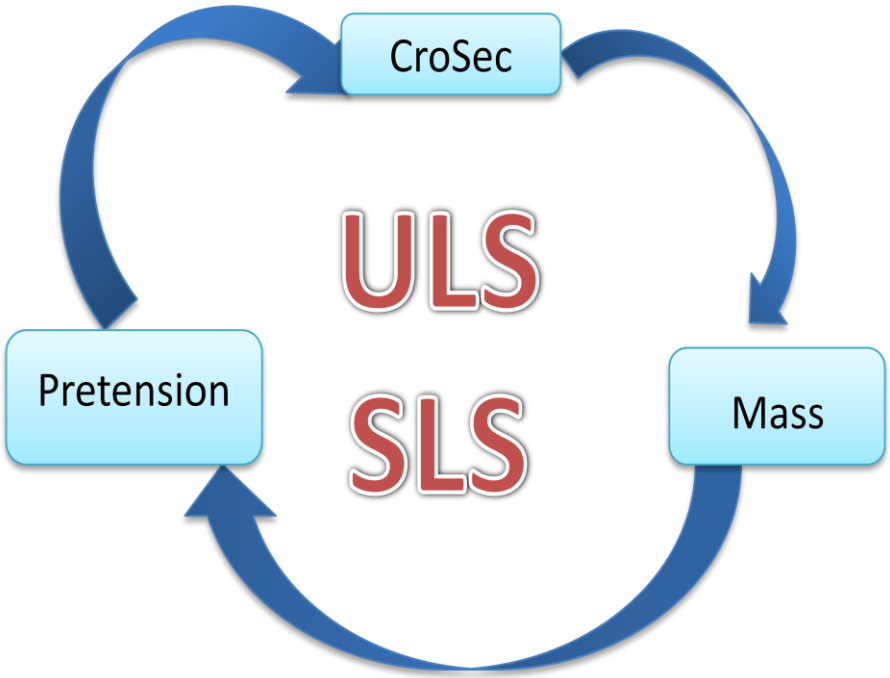

Figure 83 Interdependence of variables and results

The determination of the minimum pretension and right profile is an iterative process. To minimize influences on the results due to this interdependence, the determination of cross sections for elements is defined in sequence with regards to the load transfer path and mass percentage of elements in each group.

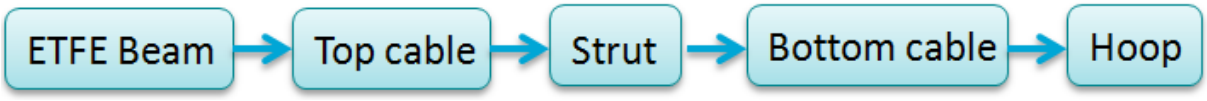

Figure 84 Load transfer path

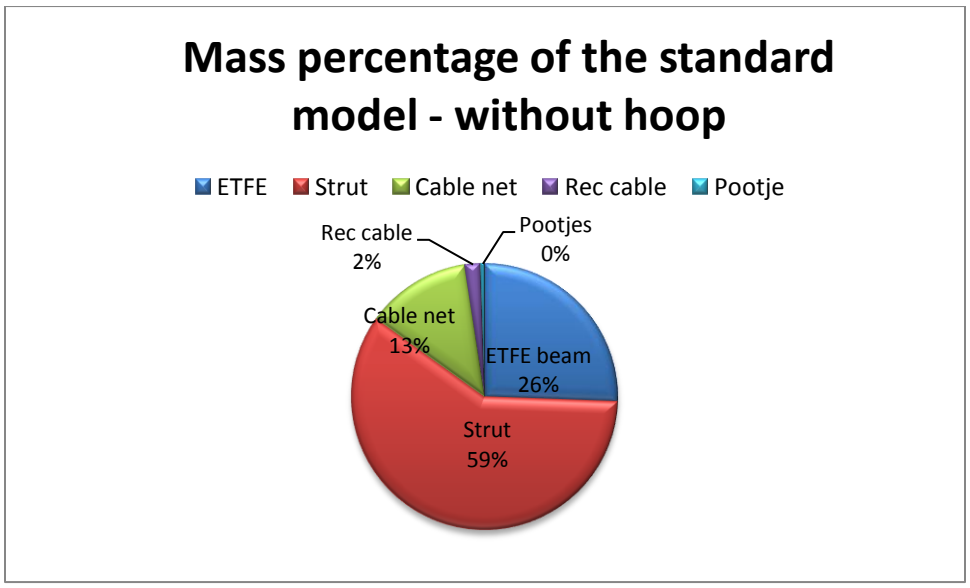

Figure 85 Mass percentage of elements in the standard model – without hoop

The interaction between elements in different groups is illustrated in the flow chart below.

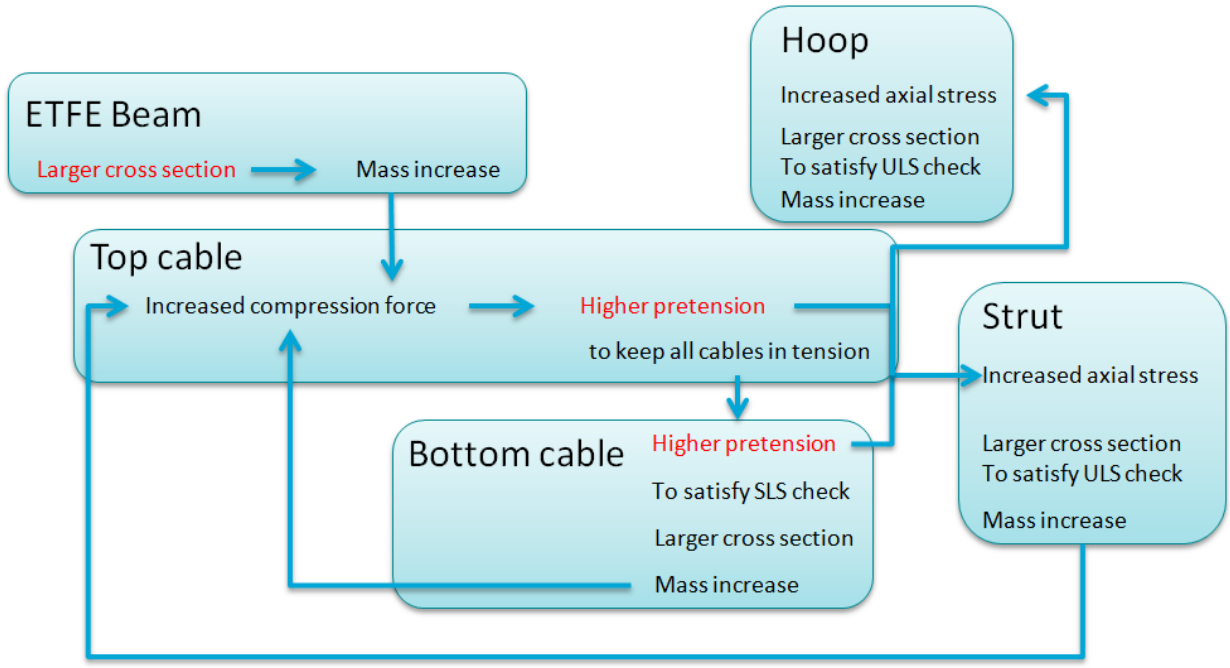

Figure 86 Interaction between elements in different groups

Assuming that the ETFE Beam elements need larger cross section, the increased mass of ETFE beam grid will bring larger compression force to the top cables due to self weight. Then higher pretension is required in the top cable net to make sure all the cables in tension. This increased pretension in top cable net has two main effects. First is that the pretension in the bottom cable net needs to be increased correspondingly to keep the structure to satisfy the SLS check requirement. Second is that the increased pretension will lead to a rise of axial stress in strut due to larger bending moments. Consequently

element with larger cross section size should be applied to strut, in return this mass increase will bring larger compression force to the top cable net. The interdependence forms a loop as depicted in the flow chart above. As for the hoop, the cross section is dependent on the total amount of axial force coming from the cables, which is determined by the amount of pretension and number of cables connected to the hoop.

To come to a design with enough strength, stiffness, and stability, four iterations are taken to determine the minimum required pretension and the right cross section size for elements in different groups. These iterations are:

- Iteration 1 – unity check for ETFE beam
- Iteration 2 – pretension check for cables and unity check for cable and strut system
- Iteration 3 – SLS check for the structure
- Iteration 4 – unity check for rods and rectangular cables

For each iteration, the minimum required pretension will be found to make sure all the cables in tension and to keep the structure under SLS check. At the same time, the cross section of elements will be modified by applying standard profiles, in such a way that the utilization of cross section is close to but smaller than 1,0. The choice of cross section for each model should provide a unity check value within 0,70-1,00 for the leading elements in different groups.

For the standard model, unity check results of elements in each group are listed in the table below:

Table 19 Results of unity check for the standard model - ULS check

Group	Profile	ULS LC2	ULS LC3
ETFE beam	CHS 114.3*3.2	0,94	0,68
Strut	CHS 152,4*12.5	0,41	0,91
Top cable	PG55 A=347 mm^2	0,44	0,75
Bottom cable	PG75 A=467 mm^2	0,78	0,44
Hoop	I beam h=1300mm,b=300mm,t_f=55mm,t_w=15mm	0,89	0,84
Rec cable	PG40 A=237mm^2	0,08	0,09
Rods	Circular bar d=55mm	0,88	0,94

Table 20 Results of unity check for the standard model - SLS check

Load combinations	Displacement upward (mm)	Displacement downward (mm)	UC
SLS LC1 1.0P+1.0G	0	-68	0,48
SLS LC2 1.0Snow+1.0P+1.0G	3	-139	0,97
SLS LC3 1.0Wind+1.0P+1.0G	27	-75	0,52

In this section, the design process of ETFE beam, Strut and Cable net are elaborated. Details about buckling check for hoop beam will be described in section 13.

1) ETFE beam

In the standard model, it has been found that the mass of ETFE beam accounts for about 26% of the structural mass (see Figure 85) apart from hoop beams. Changing the profile of ETFE Beam will have a big effect on its mass, which will bring a big difference to the compression force in the top cable net, thus also the required pretension and total mass change. Besides, the load transferred from the lower part of the structure to the ETFE beam grid is dependent on pretension which varies in a small range. Therefore, the cross section of ETFE beams is mainly determined by the live loads from snow and wind.

There are two steps towards the right choice of cross sections:

- Check for the original structure
  The first step is to check if the original profile has enough load-bearing capacity. In this design, unity check (UC) is taken as the resulting force/stress divided by the design value. UC<1 means the profile is strong enough and there is room for improvement. If UC>1, a stronger material or a larger cross section should be applied to guarantee safety of the structure.
- Choose diameter and thickness of the circular hollow section profile
  The second step is to determine diameter and thickness of the profile. The roof system has been divided into different groups. Elements subjected to the greatest loads is leading in the choice of the profile, all the structural elements in the same group are applied with the same profile.
  For the beam elements, axial stress is a result of beams under normal force and bending moment. Changing the diameter and thickness directly affects the resulting axial stress in two ways: first is that stiffness change of the system. Generally, stiffer elements share larger loads. Second is that modifying diameter and thickness directly changes the area and moment inertia of cross section thus makes a difference to the axial stress. The expression for the area A and moment inertia I of a circular hollow section are:

$$A = \pi(D^2 - d^2) \tag{8.1}$$

$$I = \frac{\pi}{64}(D^4 - d^4) \tag{8.2}$$

  Where D and d are the outer diameter and inner diameter of the tube respectively.
  For beam elements under large bending moments, it is more effective to choose a profile with a higher diameter/thickness ratio.
  Hand calculation for axial stress in beam elements follows expressions below:

$$\sigma_N = N/A \tag{8.3}$$

$$\sigma_{M_y} = M_y/W_y \tag{8.4}$$

$$\sigma_{M_z} = M_z/W_z \tag{8.5}$$

$$W_y = W_z = 2I/D \tag{8.6}$$

$$\sigma = \sigma_N + \sigma_{M_y} + \sigma_{M_z} \tag{8.7}$$

2) Strut

Design process for elements in Strut group is more or less the same as that for ETFE Beam since both use circular hollow section profile. However, the resulting forces in Strut are quite different from the resulting forces in ETFE Beam. First is that the maximum M_y and M_z does not occur in the same element, thus the maximum axial stress σ is not the simple addition of all the max value of σ_N ,σ_{My} , and σ_{Mz}. Second is that pretension is the governing factor which determines the resulting forces in strut.

To find out the reason why pretension has a big influence on the resulting forces (bending moment) in strut, here a simple model is made and only pretension is taken into account. In Figure 87, the red elements stand for strut. The strut elements are connected to cable net and rods. Number the three connection points and a simplified model of one strut is displayed in Figure 88, under the condition that pretension is the only existing load, as long as point 1, 2, and 3 are in the same line, no bending moment exists. Applying pretension to the cable system will result in displacement of the three connection points. This effect can be taken as applying a displacement δ at point 2, by doing so bending moment occurs. For the cable-strut system as a whole, changing the amount of pretension changes δ, thus bending moments vary.

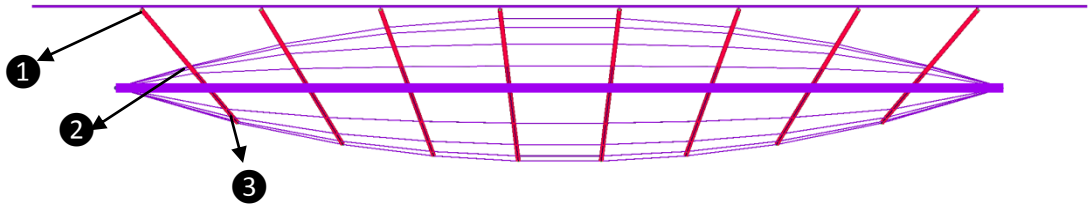

Figure 87 Pretensioned cable-strut system

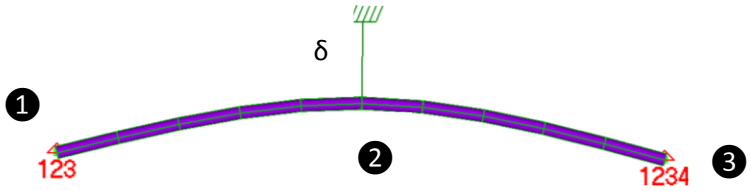

Figure 88 Simplified model of one strut

*123 means T_x, T_y, T_z, 456 means R_x, R_y, R_z

3) Cable system

Unlike beam or bar elements, cables resist load only through tension which is the most efficient way in material use. Besides, in the tensegrity structure efficiency is maximized with every particle of the structure contributing to the load-bearing capacity, resulting in a structure with high strength-to-mass ratio. This property gives cables an obvious advantage compared to other wide-span systems like truss or shell system.

For the cable system, the design has to meet certain requirements to reach a safe and stable structure. The requirements are summarized as follows:

- Strength – the maximum tensile force in elements should be smaller than the limit tension of the chosen profile, UC<1
- Stiffness and stability – pretension is required to ensure all the cables remain in tension under any load combination.
- Max deformation – the vertical displacement $\delta < \frac{l_{span}}{200} = 143mm$

This tensegrity system is formed by a continuous convex top cable layer, a continuous concave bottom cable layer, and a set of discontinuous compression struts in between the two layers of cables.

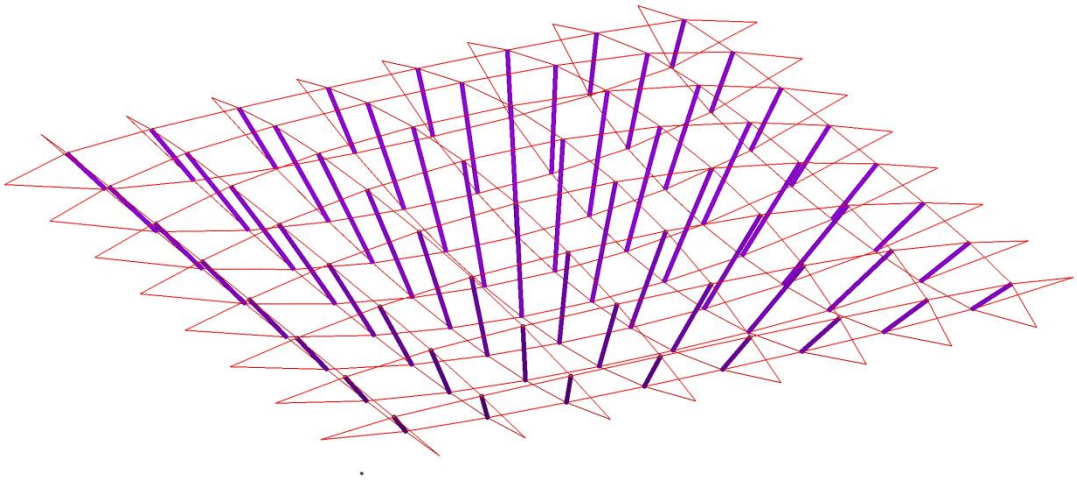

Figure 89 Cable-strut system

This tensegrity system works efficiently as a load-bearing system, which results in a light-weight structure. Pretension is applied to the cables to make sure that the applied compression forces are inferior to prestress thus all the cables stay in tension.

The fish-belly shape of the tensegrity is very suitable for carrying the on-site variable loads. The convex top cable net carries the downward force while the concave bottom cable net resist the upward force.

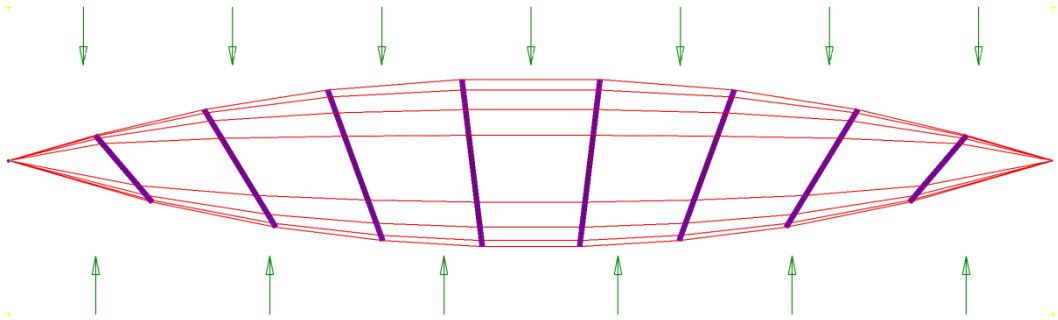

Figure 90 Cable-strut system front view

When a downward force (eg, snow load) is applied to the structure, the tensile force is increased in the bottom cable net but decreased in the top cable net. When the structure is subjected to an upward force (eg, wind), the tension in the top cable net increase but tension decrease in bottom cable net. The cable net as a whole can resist both upward and downward force. For different load combinations the required pretension varies, but the one set of pretension should be found which is applicable for the structure under all the load combinations.

To come to a good cable design, the variables that influence the stiffness of the structure are investigated and listed below:

- Depth of the cable net
- Pretension applied to cables
- Dimension of cables

Depth of the cable net

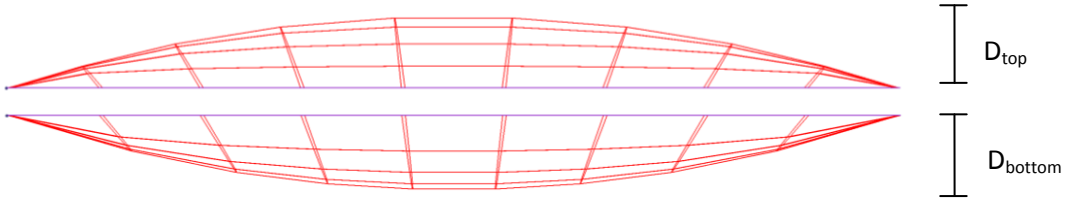

Figure 91 Depth of cable net

Stiffness of the cable net increases with an increase of the depth. In general, the required stiffness will be achieved if the maximum sag of the concave cable is 5% and for the convex cable a rise of 3% of the span assuming snow is the dominant load combination for the cable structure (*Buchholdt, H.A, 1999*).

The span of this roof structure is 28,6m, thus requirements for depth of the cable net are:

$$D_{bot} \geq l_{span} \times 5\% = 1{,}43m$$

$$D_{top} \geq l_{span} \times 3\% = 0{,}86m$$

In this study all the models satisfy the requirements for depth.

Amount of pretension

In the tensegrity structure, pretension is required to make sure all the cables stay in tension. As soon as tensile forces are eliminated, stiffness drops drastically and this cable becomes uncontrolled. However, stiffness and stability of tensegrity are not only related to prestress. If all the cables stay in tension, then geometry and the use of profiles determine the stiffness. Prestress increases the load-bearing capacity mainly by assuring that load path stays unchanged.

For the cable-strut system, if the top and bottom cable net are of different depth, the amount of pretension applied will also influence deformation of the structure. For the structure with $D_{bottom}>D_{top}$, increase pretension for top cable net only, the cable net will move downwardly. Correspondingly, increase pretension for the bottom cable net only will result in an upward movement. And increase pretension for both the top and bottom cable net with the same magnitude will also lead to an upward movement because of the asymmetry of the cable net.

In this research , the minimum amount of pretension is the pretension which is big enough to keep all the cables in tension at the same time guarantees that vertical displacement fulfills the SLS check. For each iteration step, the minimum amount of pretension is applied.

Dimension of cables

The larger the size of cables, the higher stiffness the structure will have. The required cross sectional area of the cables are chosen according to unity check to prevent yielding. In this design, standard profiles are chosen from the PG cable (see Appendix A). Properties of different cable profiles are listed in the table below:

Table 21 Properties of cable profiles

Cable Profile	Cross section(mm^2)	Limit tension(kN)	Breaking load(kN)
PG 40	237	222	367
PG 55	347	326	537
PG 75	467	438	722

9. Results of the standard model

This section gives the static analysis results of the standard model. All the variable studies are based on the standard model.

Standard model- unity check

Order of variable	Topological/Geometrical	Choice
1st	Number of branches	8X8
2nd	Position of intersection point	z=-13260
3rd	Height above support	2250mm
	Height below support	2350mm
4th	Way of form finding	radial pattern
5th	Pretension for top cable (kN)	175
	Pretension for bottom cable (kN)	160

Load combinations	Displacement (mm)<143	
	upward	downward
SLS LC1 1,0dead+1,0pre	0	-68
SLS LC2 1,0snow+1,0dead+1,0pre	3	-139
SLS LC3 1,0wind+1,0dead+1,0pre	27	-75

Type of connection	Number	Mass (kg)
ETFE beam connection	100	1500
cable and strut connection	128	10240
total		11740

6th	Cross section		ULS LC2 1,5snow+1,2dead+1,0pre			ULS LC3 1,5wind+0,9dead+1,0pre		
			Stress/Load (Max)		UC	Stress/Load (Max)		UC
group	Property	Mass (kg)	Quantity	Unit		Quantity	Unit	
ETFE beam	CHS114,3*3,2	5961	332	N/mm^2	94%	242	N/mm^2	68%
Strut	CHS152,4*12,5	13841	146	N/mm^2	41%	323	N/mm^2	91%
Hoop	h=1300mm,b=300mm, t_{flange}=55mm,t_{web}=15mm	45669	315	N/mm^2	89%	297	N/mm^2	84%
Rods	Circular bar d=55mm	119	311	N/mm^2	88%	332	N/mm^2	94%
Cable top	PG55 A=347mm^2	1259	143	kN	44%	245	kN	75%
Cable bottom	PG75 A=467mm^2	1706	343	kN	78%	191	kN	44%
Rectangular cable	PG40 A=237mm^2	427	17	kN	8%	21	kN	9%

Mass without hoop	23313	Kg
Mass with hoop	68982	kg
Total mass	80722	kg

minimum tensile force in cable	2333N

Standard model- resulting forces

Order of variable	Topological/Geometrical	Choice
1st	Number of branches	8X8
2nd	Position of intersection point	z=-13260
3rd	Height above support	2250mm
	Height below support	2350mm
4th	Way of form finding	radial pattern
5th	Pretension for top cable (kN)	175
	Pretension for bottom cable (kN)	160

Load combinations	Displacement (mm)<143	
	upward	downward
SLS LC1 1,0dead+1,0pre	0	-68
SLS LC2 1,0snow+1,0dead+1,0pre	3	-139
SLS LC3 1,0wind+1,0dead+1,0pre	27	-75

Type of connection	Number	Mass (kg)
ETFE beam connection	100	1500
cable and strut connection	128	10240
total		11740

6th	Cross section		ULS LC2 1,5snow+1,2dead+1,0pre			ULS LC3 1,5wind+0,9dead+1,0pre		
group	Property	Mass (kg)	N (kN)	M_y (kNm)	M_z (kNm)	N (kN)	M_y (kNm)	M_z (kNm)
ETFE beam	CHS114,3*3,2	5961	-	1,1	9,3	-	1,8	5,9
Strut	CHS152,4*12,5	13841	-	24,1	7,6	-	40,3	52,8
Hoop	h=1300mm,b=300mm, t_{flange}=55mm,t_{web}=15mm	45669	-	7123	47,7	-	6746	16,4
Rods	Circular bar d=55mm	119	-	3,8	3,7	-	3,8	4,9
Cable top	PG55 A=347mm^2	1259	143	0	0	245	0	0
Cable bottom	PG75 A=467mm^2	1706	343	0	0	191	0	0
Rectangular cable	PG40 A=237mm^2	427	17	0	0	21	0	0

Mass without hoop	23313	Kg
Mass with hoop	68982	kg
Total mass	80722	kg

minimum tensile force in cable	2333N

Static analysis results show that load combination ULS LC2 (1.5snow+1.2dead+1.0pre) determines the minimum amount of pretension, and correspondingly SLS LC2 (1.0snow+1.0dead+1.0pre) leads to the largest vertical deflection.

About the unity check, snow is the most critical load and will cause much larger loads compared to wind to elements in ETFE beam, hoop, and bottom cable group. However, wind load is dominant in the choice of cross section for elements in strut and top cable group. In both snow and wind case, no big difference of stress is witnessed in rods. And the rectangular cable will not fail in both cases due to the high redundancy. In this thesis, all the results are chosen from the most critical load combinations.

As for the resulting forces, beam elements take the loads by normal force and bending. For cables there is only tension.

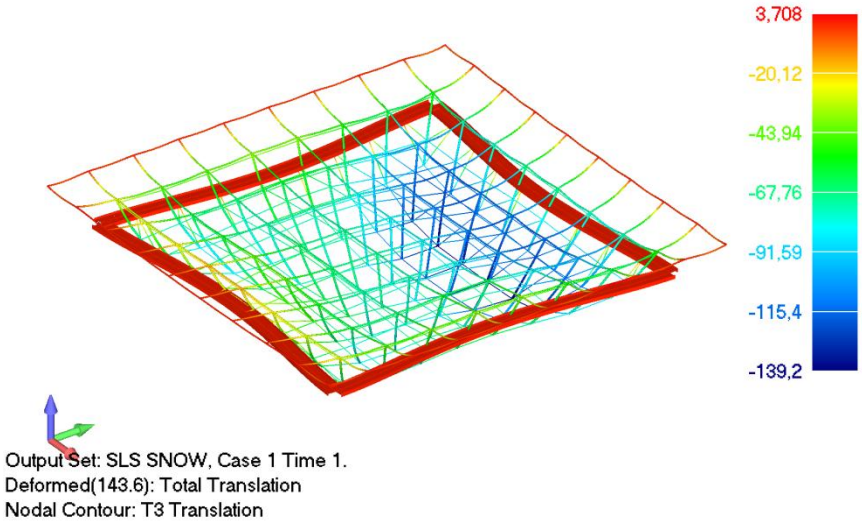

Figure 92 T3 translation for standard model under SLS LC2

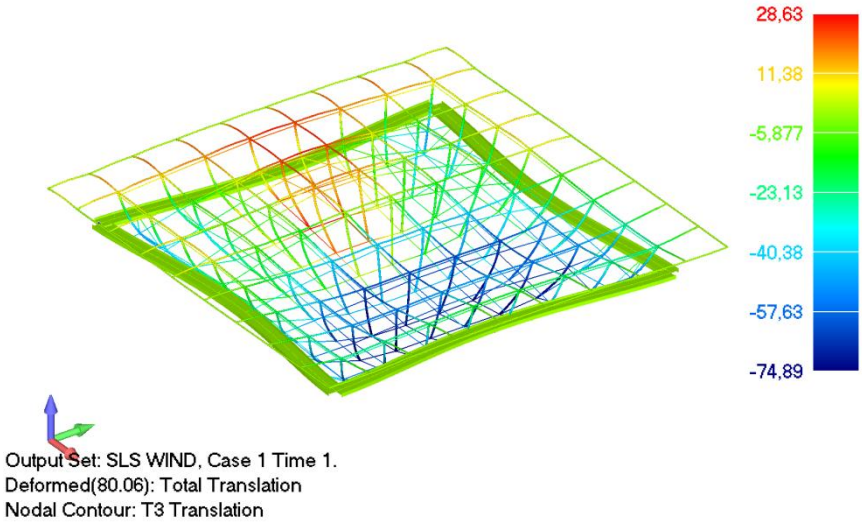

Figure 93 translation for standard model under SLS LC3

The maximum z-direction deflection is 139,2mm under SLS LC2, which satisfies the serviceability limit state check with $\delta < l_{span}/200 = 143$mm.

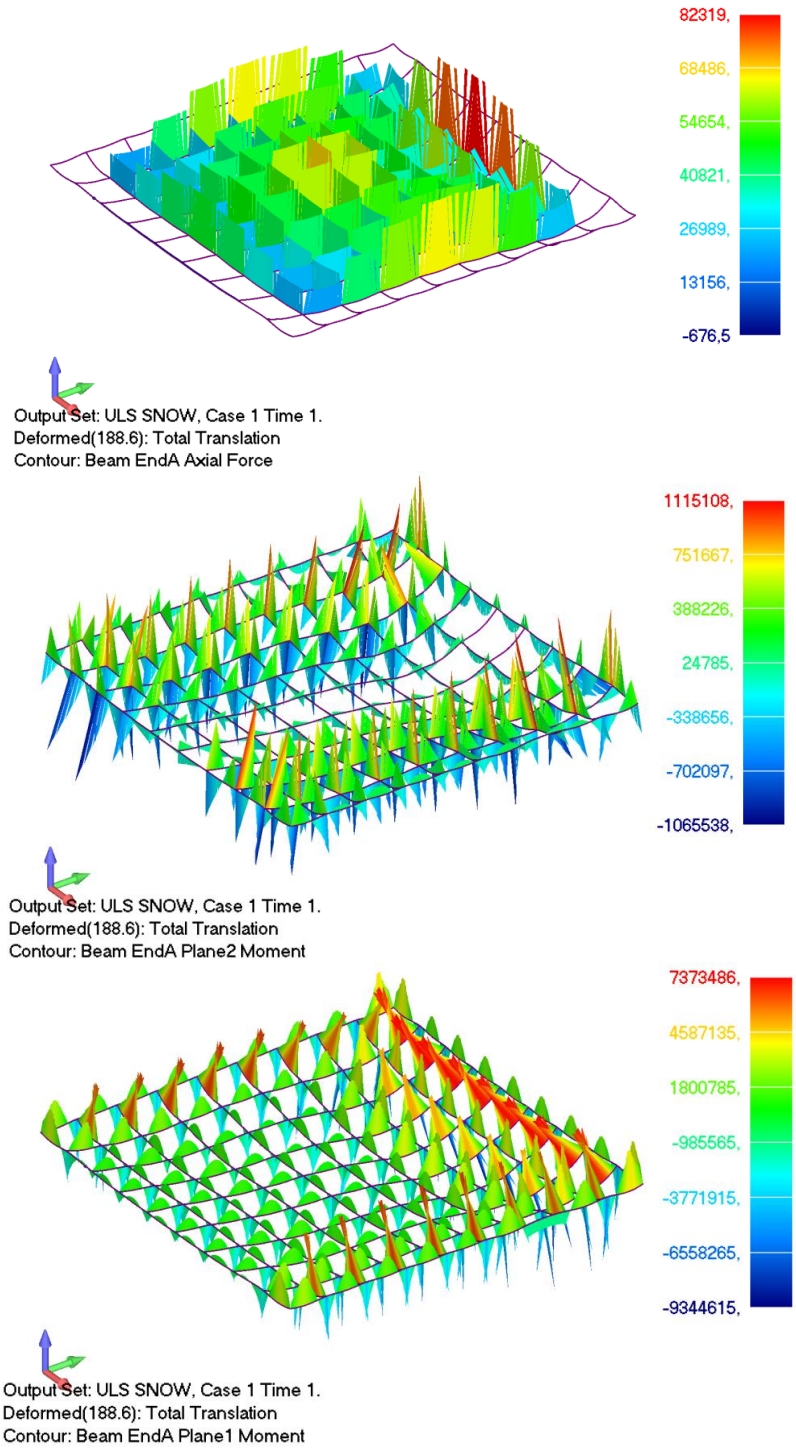

Figure 94 Resulting forces in ETFE beam under ULS LC2

*Plane1 means xz plane, Plane2 means xy plane.

Table 22 Maximum axial stress from each resulting force

Maximum Stress	σN=N/A	σMy=My/Wy	σMz=Mz/Wz
Quantity (N/mm^2)	73,7	37,0	309,6

*The maximum stress does not necessarily occur in the same element.

Bending is the governing forces that determine the axial stress in ETFE beam elements.

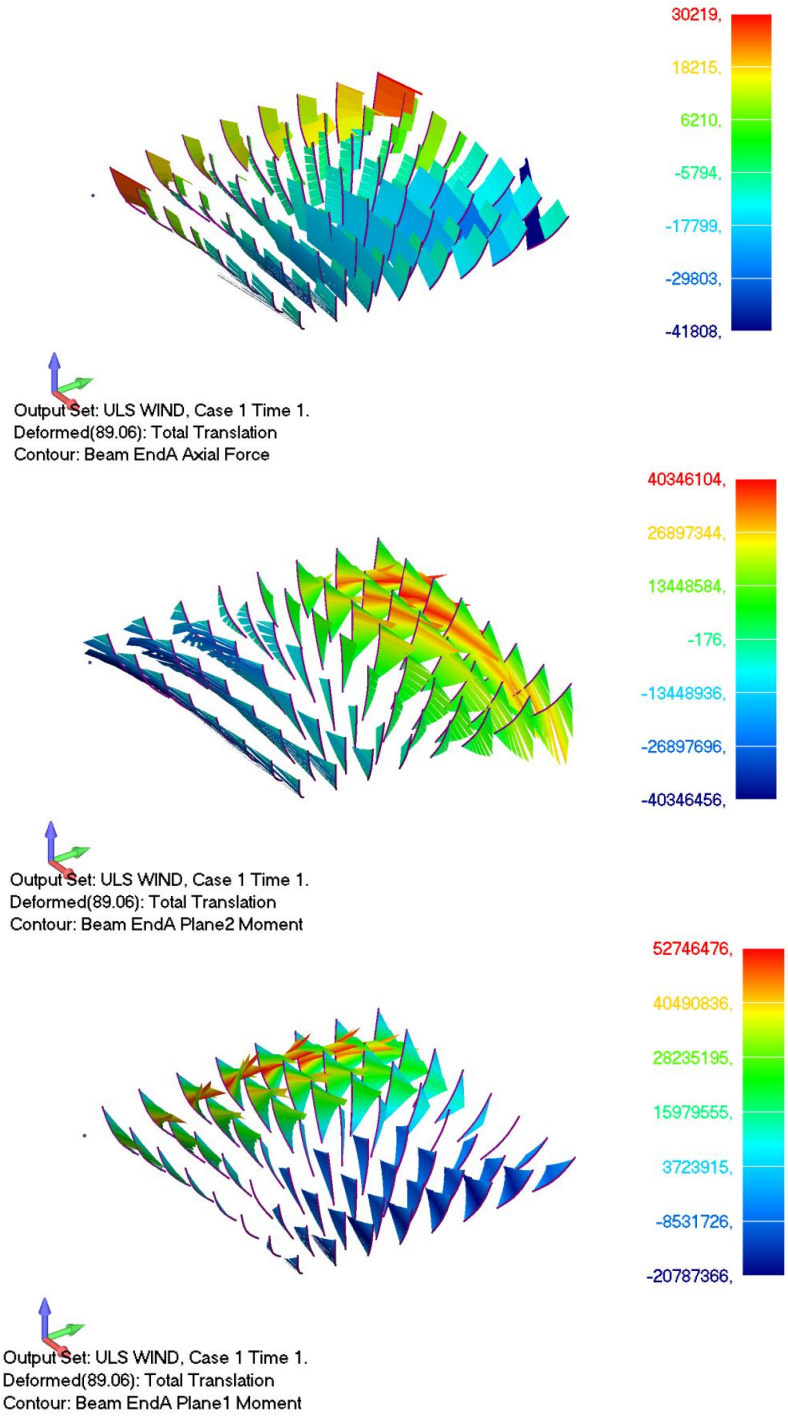

Figure 95 Resulting forces in strut under ULS LC3

*Plane1 means xz plane, Plane2 means xy plane.

Table 23 Maximum axial stress from each resulting force

Maximum Stress	σN=N/A	σMy=My/Wy	σMz=Mz/Wz
Quantity (N/mm^2)	7,6	226,9	296,6

*The maximum stress does not necessarily occur in the same element.

Bending is the governing forces that determine the axial stress in strut elements.

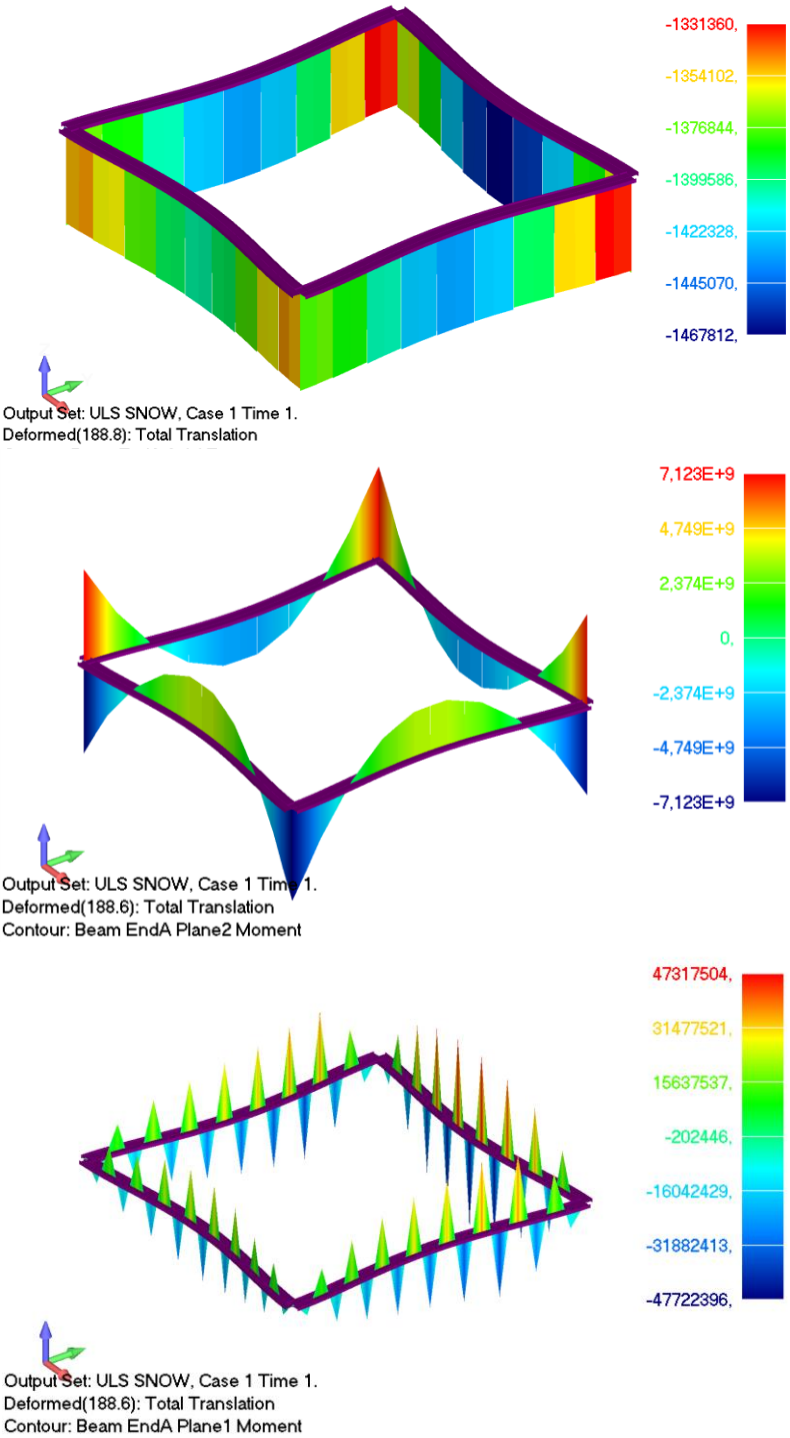

Figure 96 Resulting forces in hoop under ULS LC2

*Plane1 means xz plane, Plane2 means xy plane.

Table 24 Maximum axial stress from each resulting force

Maximum Stress	σN=N/A	σMy=My/Wy	σMz=Mz/Wz
Quantity (N/mm^2)	28,9	310,7	28,9

*The maximum stress does not necessarily occur in the same element.

Bending is the governing forces that determine the axial stress in hoop beam elements.

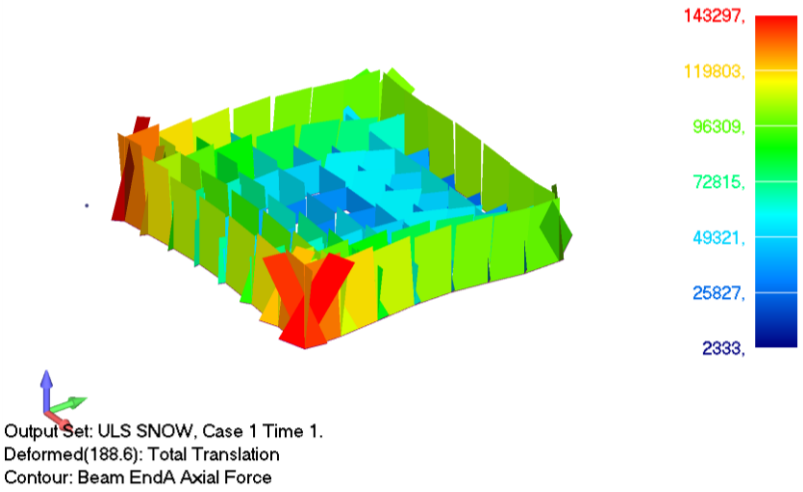

Figure 97 Resulting axial forces in top cable under ULS LC2 (minimum tension>0)

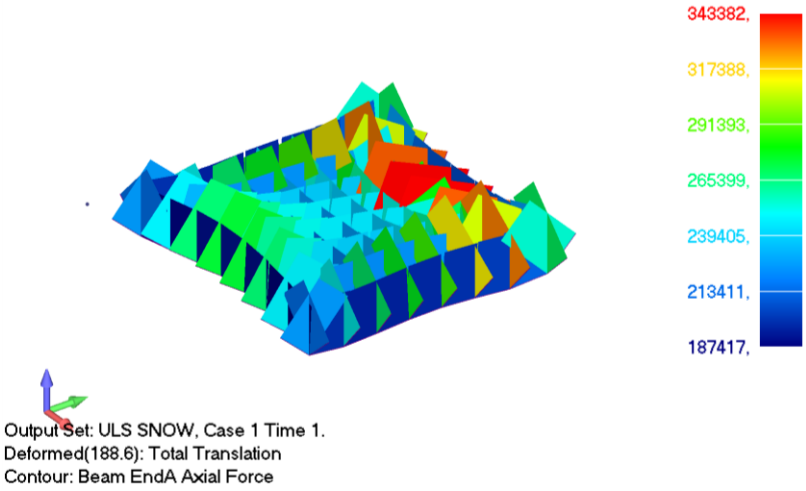

Figure 98 Resulting axial forces in bottom cable under ULS LC2 (maximum tension in bottom cable)

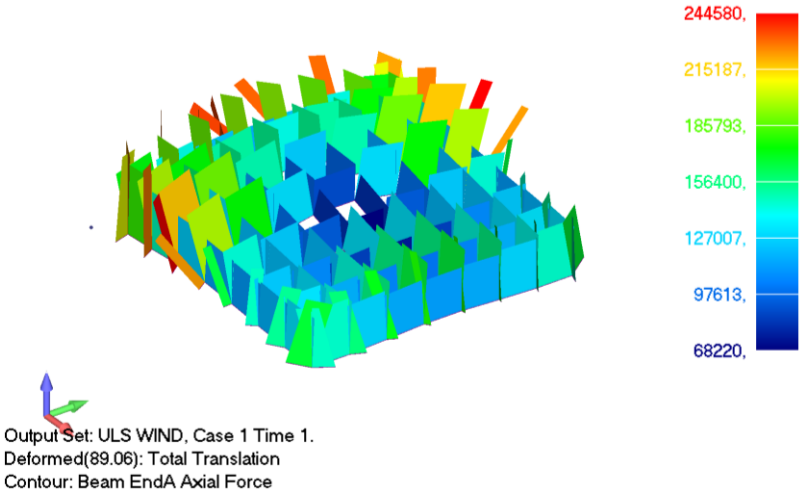

Figure 99 Resulting axial forces in top cable under ULS LC3 (maximum tension in top cable)

In the design of this roof structure, firstly the minimum required pretension is determined with some iteration steps. The minimum required pretension is the preloading in the top and bottom cable which make sure all the cables stay in tension under all the load combinations at the same time the structure satisfies the SLS check with vertical deformation $\delta < l_{span}/200 = 143$mm. Load combination ULS LC2 brings the largest downward snow load which determines the minimum required pretension for the top cable net and also the maximum axial forces in the bottom cable net. Upward wind suction load is the governing live load in ULS LC3, in this combination the maximum tensile forces in top cable net can be found. SLS LC2 gives the maximum vertical displacement of the structure under serviceability limit state which indicates the required pretension for bottom cable net.

The roof structure consists of cable and beam elements. Live loads firstly act on the upper ETFE beam grid, then transferred to the lower cable net though the strut. Under the downward snow load, the top cable net take the compression and results in additional tension in the bottom cable net. Conversely, under the upward wind load it is the opposite case with bottom cable net take compression and top cable net take tension. To guarantee enough stiffness of the cable-strut system, pretension is applied directly on the edge cables and transferred through cable-strut to the whole structure. Around the cable-strut system there is an I-shaped ring beam to take all the horizontal loads and to provide stability to the roof structure. In this design, all the beam elements react to external loads mainly by bending, both the cross section area and the section modulus decide the load-bearing capacity of a beam element. As for cables tension is the only resulting force thus the chosen material and cross section area determine the load-bearing capacity.

10. Results of variable study

10.1 Influence of changing number of branches

In this roof structure, changing the number of branches means to change the branches of cables, correspondingly the branches of ETFE beam grid, the number of struts and rods, the total length of rectangular cables, and the number of connections. This will make a radical difference on the stiffness, load path, required minimum pretension, and the total mass of the structure. Besides, adding or removing a branch in both x- and y-direction of the beam grid will result in a smaller or larger length of a single beam element, thus the resulting bending moments varies a lot in the ETFE beam grid.

In this variable study, the number of branches (1st order variable) is deliberately set to change, the required minimum pretension (5th order variable) and sectional size of elements (6th order variable) are adjusted consequently to get an efficient design. The range of 1st order variable is:

Table 25 Choice of No. branches

Group	1	2	3	4	5
No. branches	6x6	7x7	8x8	9x9	10x10
ETFE beam length (mm)	5400	4500	3850	3400	3000

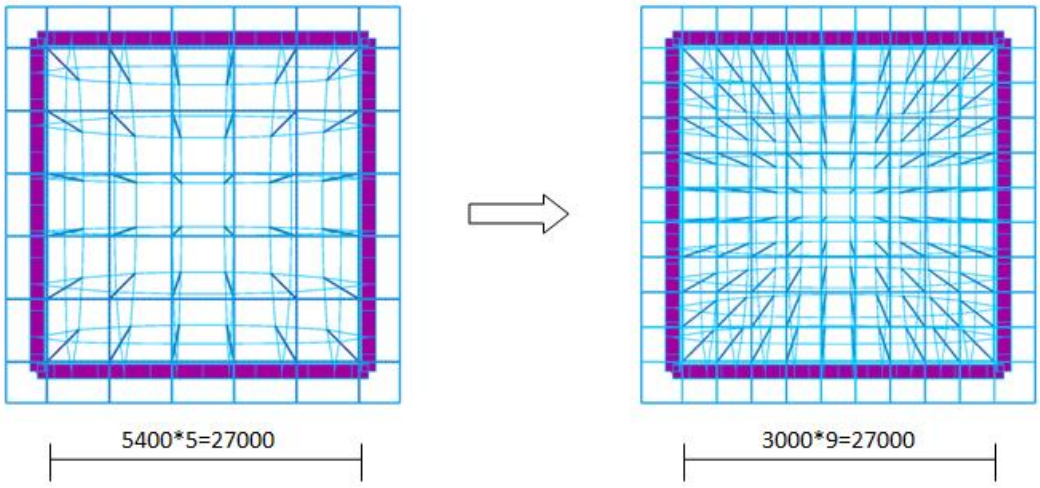

Figure 100 6x6 branch model to 10x10 branch model

As is found from the static analysis results (see Appendix G), the maximum downward displacement is witnessed under SLS LC2 (1,0snow+1,0dead+1,0pre) and the maximum upward displacement is witnessed under SLS LC3 (1,0wind+1,0dead+1,0pre). ULS LC2 and SLS LC2 reflect the minimum required pretension. The largest resulting forces in ETFE beam, hoop, and bottom cable group always occur under ULS LC2 (1,5snow+1,2dead+1,0pre). ULS LC3 (1,5wind+1,2dead+1,0pre) is the most critical load combination for elements in the strut and top cable group. In both snow and wind case, no big difference of stress is witnessed in rods. The rectangular cable will not fail in both cases due to the high redundancy.

In the variable study, results of elements in different groups are chosen from the corresponding critical load combinations.

Cross section

Below is the choice of cross sections for models with different numbers of branches. It is clear that larger cross sections are used for the hoop beams with an increase of the number of branches. The profile for rectangular cable remains unchanged. And with more branches, elements in the rest groups are applied with smaller cross sections.

Table 26 No. branches and cross sections

No. branches	6x6	7x7	8x8	9x9	10x10
ETFE beam	CHS139,7*5	CHS114,3*5	CHS114,3*3,2	CHS114,3*2,6	CHS101,6*2,6
Strut	CHS177,8*17,5	CHS152,4*14,2	CHS152,4*12,5	CHS152,4*10	CHS152,4*8
Hoop	t_{flange}=50mm, t_{web}=15mm	t_{flange}=50mm, t_{web}=15mm	t_{flange}=55mm, t_{web}=15mm	t_{flange}=60mm, t_{web}=15mm	t_{flange}=60mm, t_{web}=15mm
Rods	Circular bar d=65mm	Circular bar d=60mm	Circular bar d=55mm	Circular bar d=55mm	Circular bar d=50mm
Cable top	PG55 A=347 mm^2	PG55 A=347 mm^2	PG55 A=347 mm^2	PG40 A=237 mm^2	PG40 A=237 mm^2
Cable bottom	PG90 A=572 mm^2	PG75 A=467 mm^2	PG75 A=467 mm^2	PG55 A=347 mm^2	PG55 A=347 mm^2
Rectangular cable	PG40 A=237mm^2	PG40 A=237 mm^2	PG40 A=237 mm^2	PG40 A=237 mm^2	PG40 A=237 mm^2

*For hoop element in this design, the height and width of I-beam remains unchanged with h=1300mm,b=300mm.

Pretension

The line graph shows that the model with more branches needs smaller pretension in both top and bottom cables. In this design, the minimum pretension for top cable is determined as the amount of preloading to keep all the top cables in tension under ULS LC2, the pretension for bottom cable is adjusted according to the top pretension in order to limit the displacement under SLS LC2. In this study, the minimum tensile force in cable under ULS LC2 is controlled within 0kN and 10kN, and the downward displacement under SLS LC2 is controlled as close to 143mm as possible in order to get comparable and reliable results.

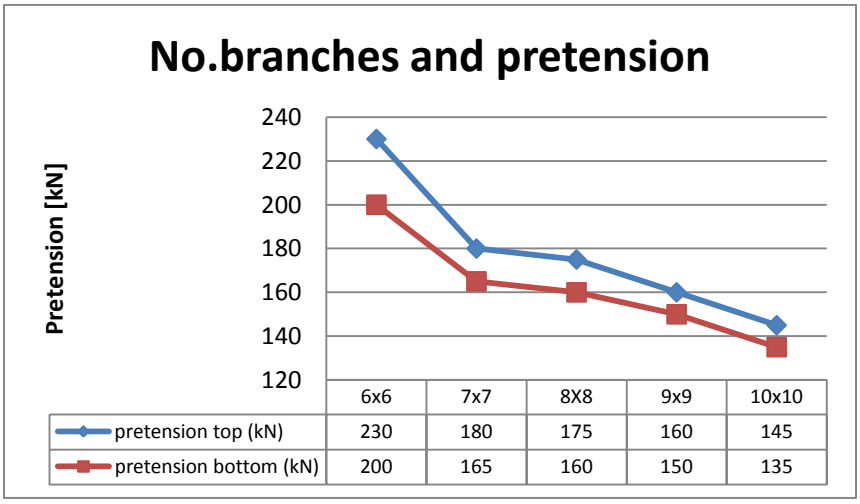

Figure 101 No. branches and Pretension

Table 27 Minimum tensile force in cable under ULS LC2

No. branches	6x6	7x7	8x8	9x9	10x10
minimum tensile force in cable (N)	1551	769	2333	3722	5323

From 6x6 model to 10x10 model, the cross sections of ETFE beam and strut elements keeps decreasing, leading to a reduced compression force due to self weight acting on the a single branch of cables. As a result smaller pretension is required for the top cables, correspondingly smaller pretension in bottom cables to adjust the displacement. From 6x6 model to 7x7 model, a slump of pretension is seen in both top and bottom cable, this corresponds to the big difference of cross section size in the ETFE beam and strut group.

Displacement

The bar graph below gives the maximum upward displacement under SLS LC2 and downward displacement under SLS LC3 of different models. All the results satisfy the SLS check requirement with $\delta < l_{span}/200 = 143$mm.

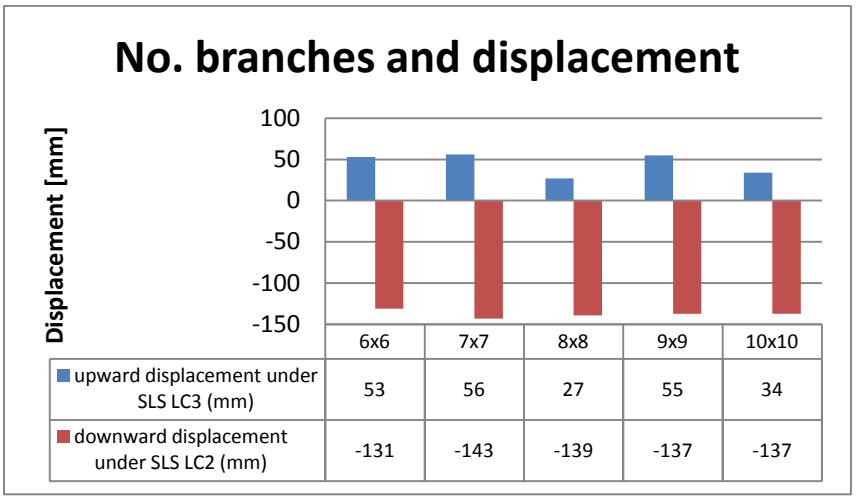

Figure 102 No. branches and displacement

Resulting forces

In the variable study, results of elements in different groups are plotted from the corresponding critical load combinations.

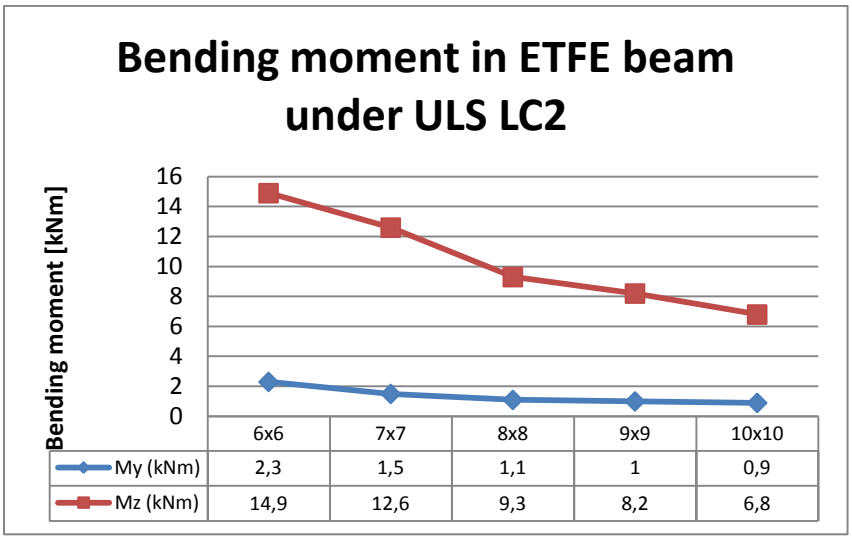

Figure 103 Bending moment in ETFE beam under ULS LC2

Axial stress in ETFE beam comes from live loads and the reaction forces from the lower system. The maximum stress in ETFE beams is witnessed under ULS LC2 where the largest line load acts on the beam elements. ETFE beams take external loads mainly by bending in z direction. With increased number of branches in the roof area, the line load on each beam is reduced. Also with more branches the span of each element is smaller. The decreased line load and the smaller element length explain the decrease of bending moment in ETFE beam with more branches.

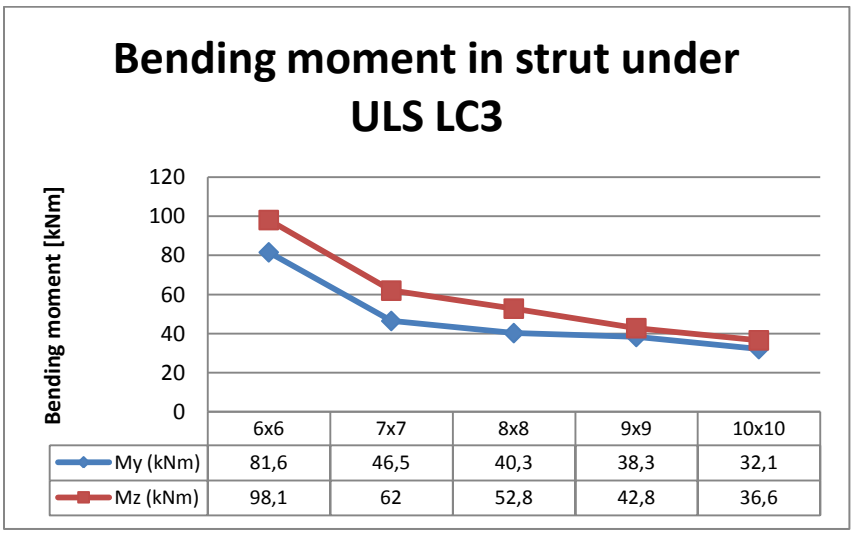

Figure 104 Bending moment in strut under ULS LC3

The resulting force in strut is determined by pretension, the load combination ULS LC3 with asymmetrical wind load brings the largest bending moment to the strut elements. The inclined struts take bending in both y and z direction. For models with more branches, the required pretension keeps going down thus smaller bending in struts. The abrupt drop from 6x6 model to 7x7 corresponds with the slump of pretension.

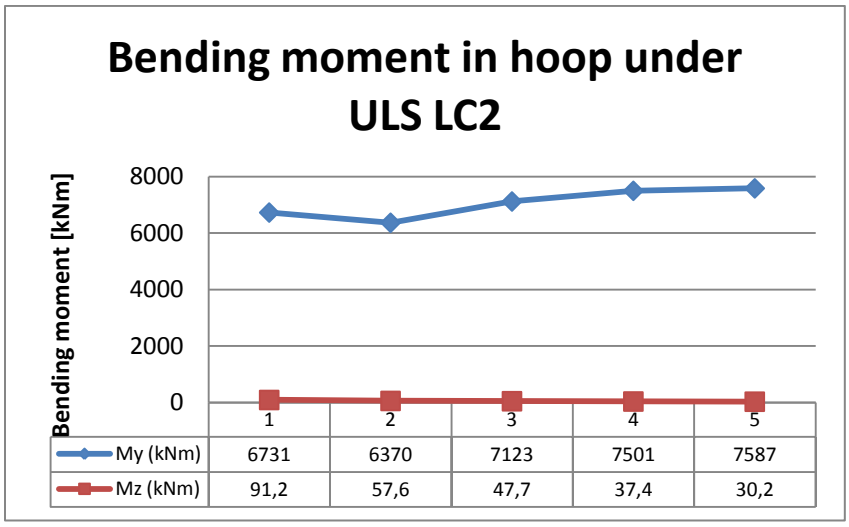

Figure 105 Bending moment in hoop under ULS LC2

Bending moment in hoop beam comes from the axial force in cables, in which pretension is the dominant load case. The maximum bending is witnessed under ULS LC2 because this load combination brings the largest total amount of forces. Only a small part of vertical load is taken by the supports on the outer ring of ETFE beam, most of the loads is transferred downwardly and withstand by the hoop system. The hoop is loaded mainly by in-plane bending, thus the strong axis of the I-beam should be put in the in-plane direction of hoop.

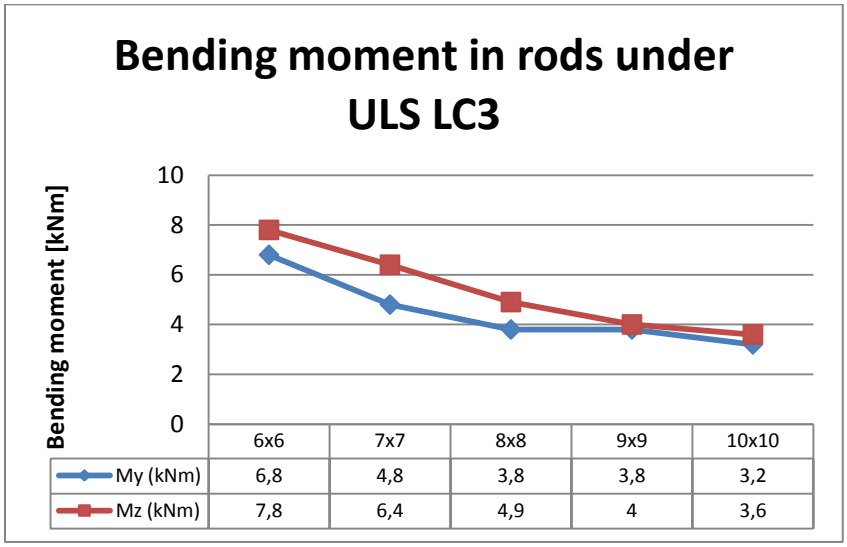

Figure 106 Bending moment in rods under ULS LC3

Bending moment in rods comes from live loads, the self-weight of ETFE beam grid, and the reacting force from struts which is determined by pretension. The resulting bending in rods keeps going down in model with more branches. This is because with more branches, both the live loads and self weight from ETFE beam grid decrease. Also smaller pretension leads to smaller reacting force from struts to rods. Therefore, bending in rods keeps going down in models with more branches.

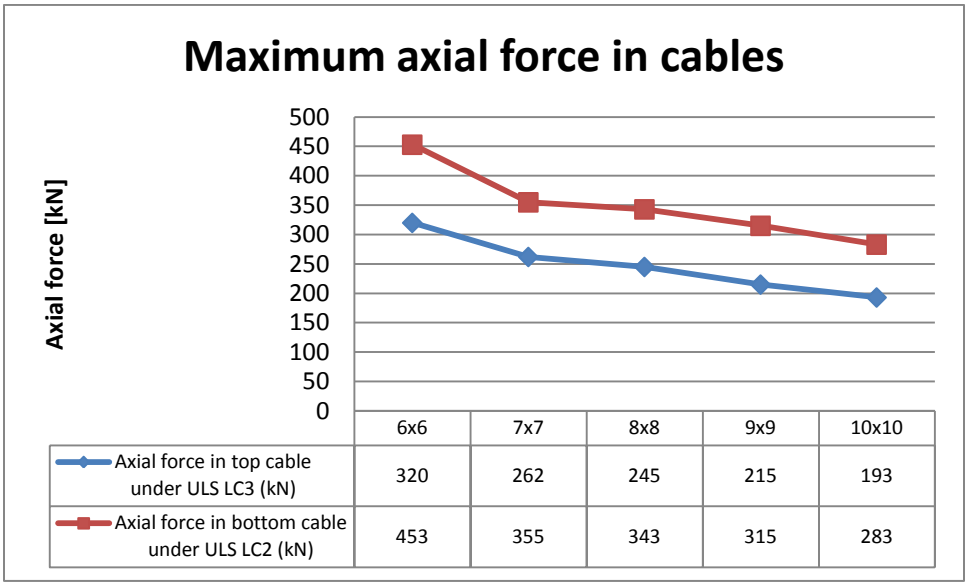

	6x6	7x7	8x8	9x9	10x10
Axial force in top cable under ULS LC3 (kN)	320	262	245	215	193
Axial force in bottom cable under ULS LC2 (kN)	453	355	343	315	283

Figure 107 Maximum axial force in cable net

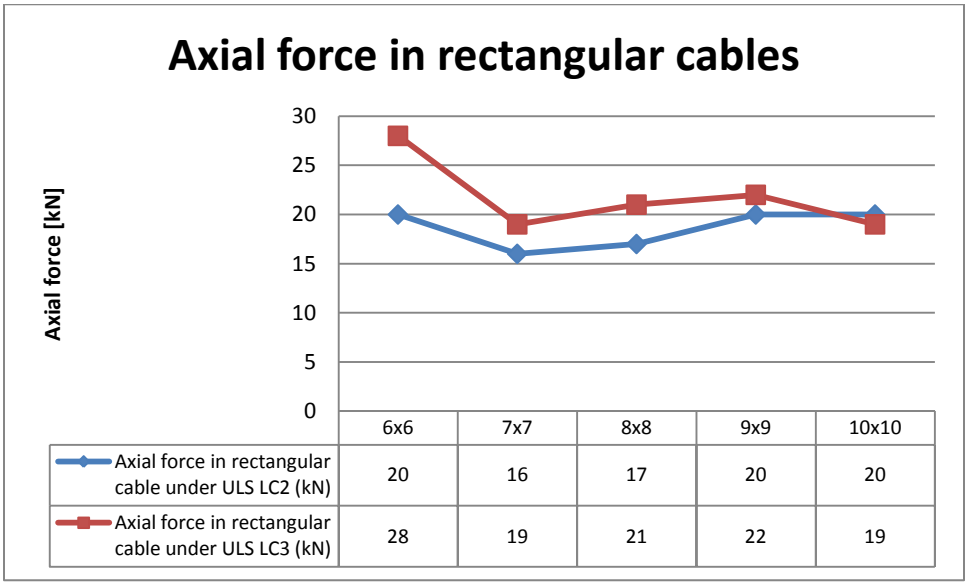

	6x6	7x7	8x8	9x9	10x10
Axial force in rectangular cable under ULS LC2 (kN)	20	16	17	20	20
Axial force in rectangular cable under ULS LC3 (kN)	28	19	21	22	19

Figure 108 Axial force in rectangular cable

For cables in this structure, with the same pretension for all the load combinations, the maximum axial force in top cable is witnessed under ULS LC3 due to upward wind suction. And the ULS LC2 with downward snow load causes the largest axial force in bottom cables.

Rectangular cable functions to hold the struts in the right position. Only a very small tensile force is witnessed.

Unity check

For beam element, the UC value is the maximum axial stress in element divided by the strength of material. For cable element, the UC value is the maximum axial force divided by the limit tension of the profile. As the result shows, apart from the rectangular cable, the leading element in each group gives a UC value within 0,70 to 1,00. Enough strength is guaranteed for all these models with high efficiency of material use.

Table 28 No. branches and UC value of elements in different groups

Group	6x6	7x7	8x8	9x9	10x10
ETFE beam	0,91	0,85	0,94	0,93	0,99
Strut	0,98	0,97	0,91	0,96	0,97
Hoop	0,90	0,85	0,89	0,87	0,88
Rods	0,89	0,87	0,94	0,81	0,92
Top cable	0,98	0,80	0,75	0,97	0,87
Bottom cable	0,84	0,81	0,78	0,97	0,87
Rectangular cable	0,13	0,09	0,09	0,10	0,09

Mass

In this roof structure, adding or removing a branch will lead to a change of the total length of element. By modifying the cross section to achieve a safe and efficient structure, no big change of mass is expected. Theoretically this could be true, but in the real case this is an ideal situation and cannot be witnessed in all the groups mainly because the area and moment inertia change of element is not linear, also the non-linear change of element length and the difference in pretension change also brings difficulty to reach such a case.

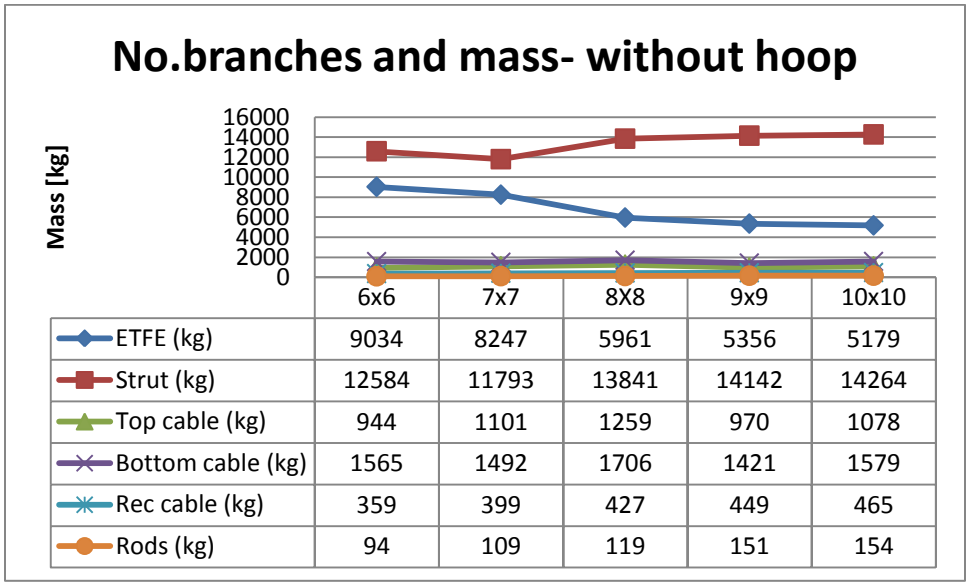

Figure 109 No. branches and mass of elements in different groups

The line graph above depicts that the 7x7 branch model has the strut elements with least total mass. The mass of strut first goes down from 6x6 to 7x7 model because of much less axial stresses in strut due to the slump of pretension thus much smaller cross sections can be applied. The mass reduction by using elements with smaller cross sections is even more than the mass increase by adding a branch of elements with the new cross section. From 7x7 to 8x8 model, there is a small increase of the strut mass. And for model with 8x8 to 10x10 branches, the mass of strut remains almost unchanged, which corresponds with the assumption that changing the number of branches does not necessarily brings a big change to the total mass by applying smaller cross sections.

The mass of ETFE beam simply goes down with more branches. This is because with increased number of branches in the roof area, the line load on each beam is reduced. Also with more branches the span of each element is smaller. The decreased line load and the smaller element length jointly reduce the resulting axial stress in ETFE beam. The mass reduction from cross section change is larger than the mass addition of an extra branch of elements with new cross sections.

For elements in top cable, bottom cable, rectangular cable, and rod group, small fluctuation of mass is witnessed. The cross section change of elements in these groups brings very limited difference to the total mass of the roof structure.

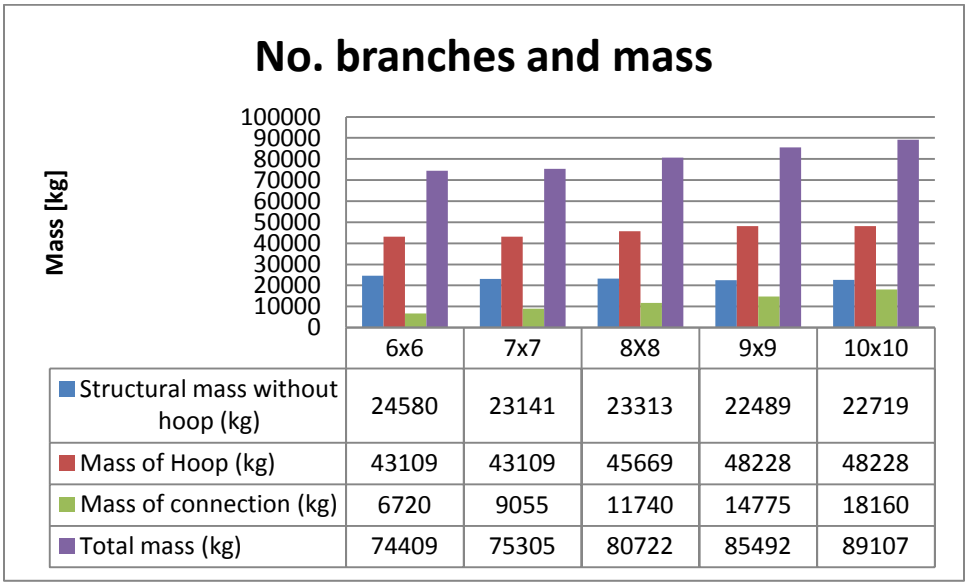

	6x6	7x7	8X8	9x9	10x10
Structural mass without hoop (kg)	24580	23141	23313	22489	22719
Mass of Hoop (kg)	43109	43109	45669	48228	48228
Mass of connection (kg)	6720	9055	11740	14775	18160
Total mass (kg)	74409	75305	80722	85492	89107

Figure 110 No. branches and mass-large mass

The bar graph above displays that for models with more branches, the structural mass without hoop tend to be smaller. This mass reduction mainly comes from the ETFE beam group. However, considering the mass of hoop and mass of connection, the total mass simply goes up.

Table 29 No. branches and total amount of pretension

No. branches	6x6	7x7	8x8	9x9	10x10
Total pretension (kN) each side	2580	2415	2680	2790	2700

The mass increase of hoop is witnessed from 7x7 to 9x9 branch model. This is because the total amount of pretension acting on each side of the hoop increases, larger cross section size is required to provide enough stiffness thus larger mass of hoop. From 6x6 to 7x7 and 9x9 to 10x10 model, the cross section of hoop does not change despite the change of total pretension. However, the utilization of elements is different.

The mass of ETFE beam connection and cable-strut connection is also calculated. Assuming the mass of a single connection remains unchanged, the more branches, the more connections thus higher mass of connection.

With increased number of branches, a higher total mass is witnessed.

The mass of elements in each group for models with different branches is listed in the table below.

Table 30 No. branches and Mass (kg) for elements in each group

Group	6x6	Rel.Std	7x7	Rel.Std	8x8	Rel.Std	9x9	Rel.Std	10x10	Rel.Std
ETFE	9034	152%	8247	138%	5961	-	5356	90%	5179	87%
Strut	12584	91%	11793	85%	13841	-	14142	102%	14264	103%
Top cable	944	75%	1101	87%	1259	-	970	77%	1078	86%
Bottom cable	1565	92%	1492	87%	1706	-	1421	83%	1579	93%
Rec cable	359	84%	399	93%	427	-	449	105%	465	109%
Rods	94	79%	109	92%	119	-	151	127%	154	129%
Hoop	43109	94%	43109	94%	45669	-	48228	106%	48228	106%
Total	67689	98%	66250	96%	68982	-	70717	103%	70947	103%

10.2 Results of changing converge point

A real project on site should fulfill not only the structural requirements, at the same time the structure should have good aesthetic functions. Often times, part of the structural performance sacrifices for aesthetics to achieve a balance between load-bearing capacity and structural appearance.

For this tensegrity roof, it has been defined that all the struts are inclined from the vertical plane in such a way that the extension line of all the struts converge at the same central point.

In this variable study, two models are investigated with different positions of central point:

Table 31 Position of intersection point

Group	Z (mm)	Position	Structure
1	-13260	on ground	Radial struts and cable net
2	-1000000	Close to infinity below support	Vertical struts and cable net

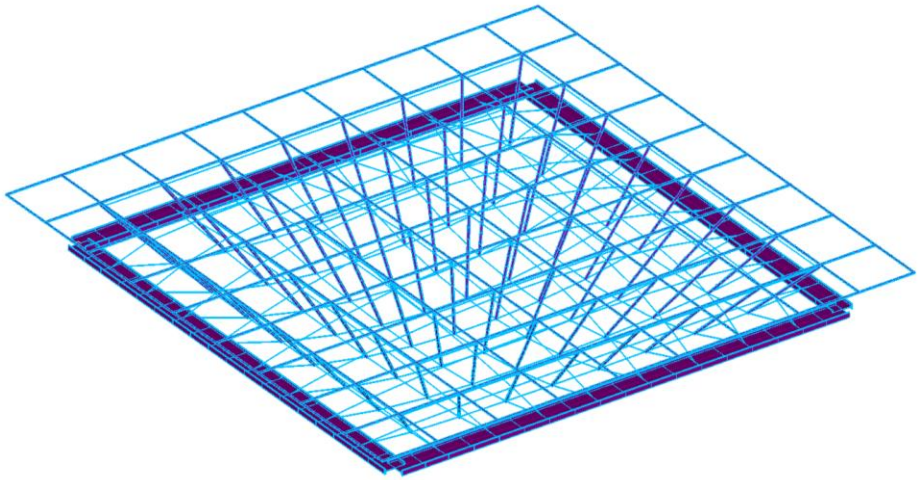

Figure 111 Model with radial struts

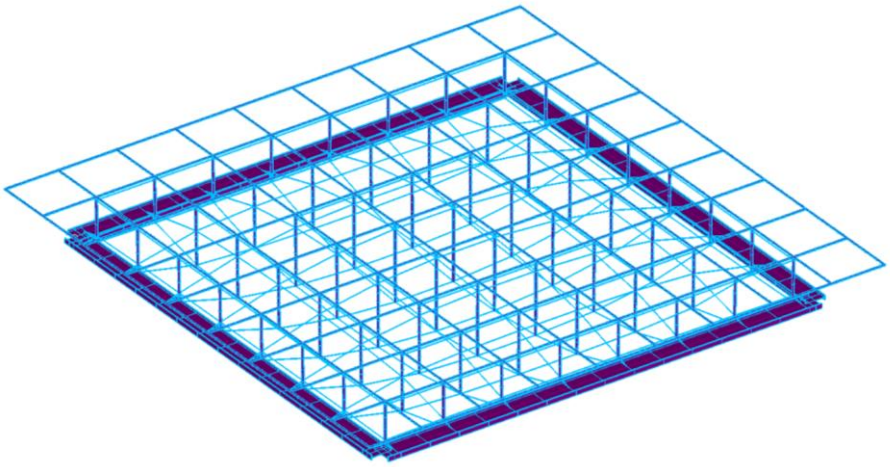

Figure 112 Model with vertical struts

Cross section

Compared with the standard model, the model with vertical struts requires larger cross section for elements in the upper part which includes ETFE beam and rods, and smaller cross section for elements in strut, hoop, and bottom cable.

The ETFE beam and rods require larger cross sections because smaller reacting force comes from struts, leading to larger bending moment in the beam elements. The reduced cross section for strut, hoop, and bottom cable is a result of the smaller pretension.

Assuming the two models under the same load combinations with the exact amount of pretension, the vertical struts will take less bending due to the smaller eccentricity. As a results, smaller cross section can be applied to struts thus a reduced minimum pretension is required. The reduced pretension leads to smaller axial force in cables, and smaller bending in struts and hoop. Therefore, smaller cross sections can be applied to elements in these groups.

Table 32 Cross section for model with radial and vertical struts

No. branches	Radial	Vertical
ETFE beam	CHS114,3*3,2	CHS114,3*5
Strut	CHS152,4*12,5	CHS152,4*6,3
Hoop	t_{flange}=55mm, t_{web}=15mm	t_{flange}=40mm, t_{web}=15mm
Rods	Circular bar d=55mm	Circular bar d=60mm
Cable top	PG55 A=347mm^2	PG55 A=347mm^2
Cable bottom	PG75 A=467mm^2	PG55 A=347mm^2
Rectangular cable	PG40 A=237mm^2	PG40 A=237mm^2

*For hoop element in this design, the height and width of I-beam remains unchanged with h=1300mm,b=300mm.

Pretension

The smaller pretension in model with vertical struts proves that the assumption is correct. The vertical struts shows better load transfer path which leads to smaller resulting forces compared to the radial struts under the same external loads. Thus the cross section size for vertical struts can be smaller than the radial ones, this difference results in a mass reduction in struts, which can also be seen as a reduction of compression force on the top cables. Therefore, smaller pretension is required to make sure all the cables in tension at the same time guarantee the SLS check.

Table 33 Converge point and minimum pretension

Force	Radial	Vertical
Pretension top (kN)	175	155
Pretension bottom (kN)	160	120

Table 34 Minimum tensile force in cable under ULS LC2

No. branches	Radial	Vertical
minimum tensile force in cable (N)	2333	348

Displacement

The table below gives the maximum upward displacement under SLS LC2 and downward displacement under SLS LC3 of different models. All the results satisfy the SLS check requirement with $\delta < l_{span}/200 = 143$mm.

Table 35 Converge point and displacement

Displacement	Radial	Vertical
Upward displacement under SLS LC3 (mm)	27	44
Downward displacement under SLS LC2 (mm)	-139	-127

Stress and Unity check

Table 36 Unity check for model with radial struts

Radial	ULS LC2 1,5snow+1,2dead+1,0pre			ULS LC3 1,5wind+0,9dead+1,0pre		
	Stress/Load	Unit	UC	Stress/Load	Unit	UC
ETFE beam	332	N/mm^2	0,94	242	N/mm^2	0,68
Strut	146	N/mm^2	0,41	323	N/mm^2	0,91
Hoop	315	N/mm^2	0,89	297	N/mm^2	0,84
Rods	311	N/mm^2	0,88	332	N/mm^2	0,94
Cable top	143	kN	0,44	245	kN	0,75
Cable bottom	343	kN	0,78	192	kN	0,44
Rectangular cable	17	kN	0,08	21	kN	0,09

Table 37 Unity check for model with vertical struts

Vertical	ULS LC2 1,5snow+1,2dead+1,0pre			ULS LC3 1,5wind+0,9dead+1,0pre		
	Stress/Load	Unit	UC	Stress/Load	Unit	UC
ETFE beam	329	N/mm^2	0,93	210	N/mm^2	0,59
Strut	266	N/mm^2	0,75	266	N/mm^2	0,75
Hoop	253	N/mm^2	0,71	260	N/mm^2	0,73
Rods	177	N/mm^2	0,50	266	N/mm^2	0,75
Cable top	133	kN	0,41	237	kN	0,73
Cable bottom	279	kN	0,86	163	kN	0,50
Rectangular cable	9	kN	0,04	16	kN	0,07

Apart from rectangular cable group, the leading elements in each group give a UC value within 0,70 to 1,00 under the most critical load combinations.

Mass

The table below shows considerable mass change in strut, the vertical strut weighs only 37% as the radial struts. A 26% mass reduction is also seen in bottom cable in the model with vertical struts. And the hoop with smaller cross section is of 17% less mass. All the mass reduction is a result of the smaller required minimum pretension. For ETFE beam, the larger cross section in model with vertical struts brings about 54% higher mass. For the vertical strut model, a 19% mass increase is also seen in the rods. All the mass increase is due to smaller reacting force transferred from the vertical struts to the ETFE beam grid. Considering all the mass change in different groups, the model with vertical struts has less total mass, which is about 80% of the mass of the standard model.

Table 38 Converge point and Mass (kg)

Group	Radial	Vertical	Rel.Std
ETFE beam	5961	9163	154%
Strut	13841	5141	37%
Rods	119	142	119%
Cable top	1259	1257	100%
Cable bottom	1706	1258	74%
Rectangular cable	427	430	101%
Mass without hoop	23313	17391	75%
Hoop	45669	37990	83%
Total structural mass	68982	55381	80%

In general, the model with radial struts does not lead to the most efficient design but of different aesthetics. Structurally, the model with vertical struts has better load transfer paths which allow the application of much smaller cross sections for strut elements, this leads to smaller required pretension and thus a further reduction of element mass in strut, bottom cable, and hoop. In practical sense, the structure with vertical struts is also easier to assemble compared to the one with radial struts. In conclusion, the model with vertical struts has better structural performance than the standard model.

10.3 Results of changing way of form-finding

In the 3rd order variable study, different ways of form finding are applied to a flat grid in order to get different shapes of the cables net and compare their structural performances. Force density method is used for tensile structures based on the concept 'form follow force'. The process starts with defining internal and external forces and all further structural constraints. Then use the FEM to search for the equilibrium of all external and internal forces which results in a form under this load case. Based on the standard model, three ways of form-finding are applied and the resulting shapes are as below:

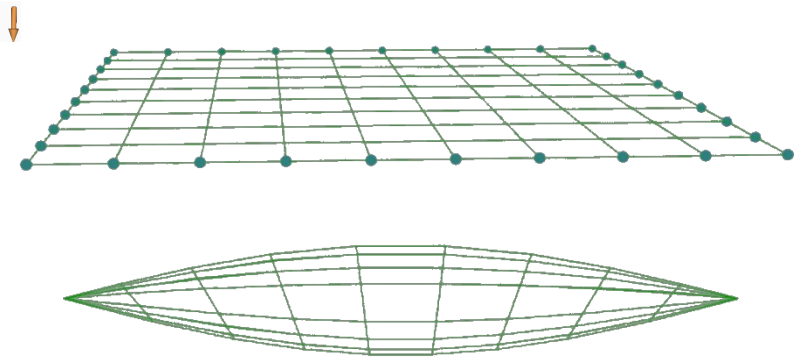

Figure 113 Self-weight and resulting shape
*The blue dots stands for the constraints for Tz translation.

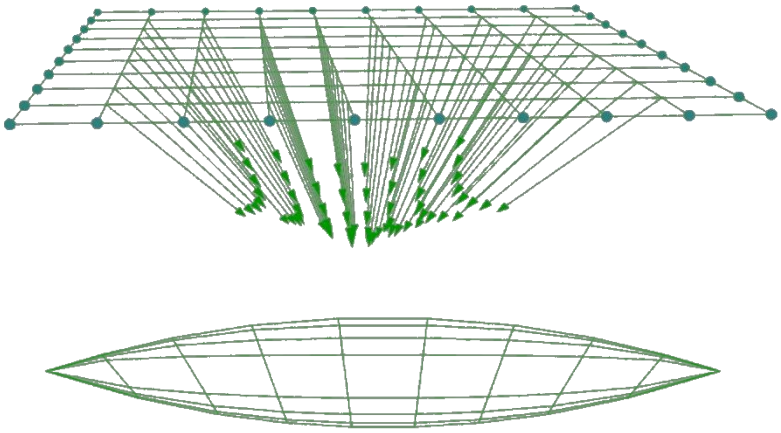

Figure 114 Radial loads and resulting shape

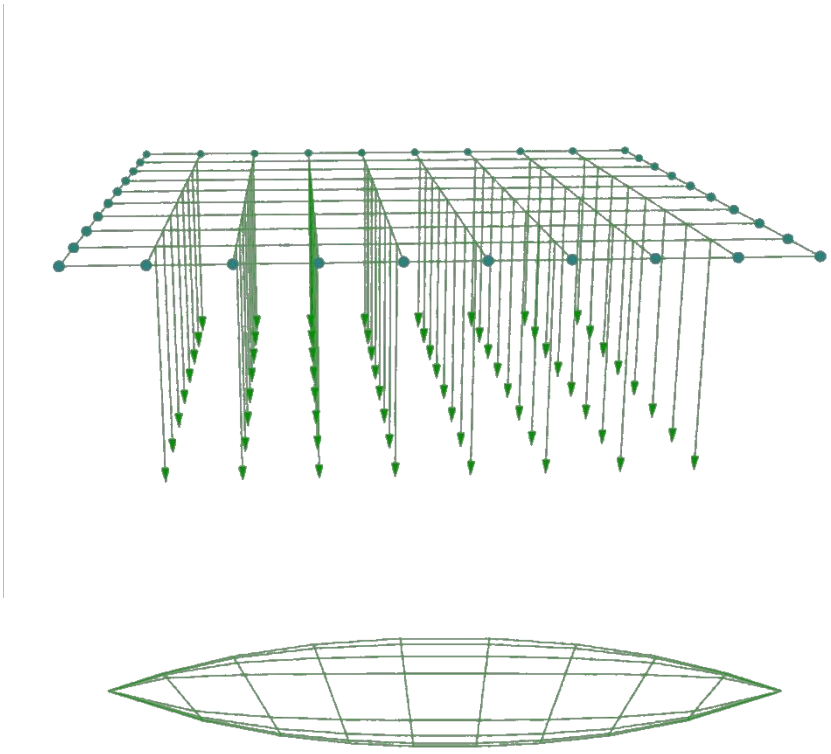

Figure 115 Vertical loads and resulting shape

Cross section

Compared to the standard model, the model with form from vertical loads needs larger cross sections for ETFE beams. And a bigger cross section for hoop beam is applied for model with form from gravity. For elements in the rest groups, the cross sections remain the same as the standard model.

Table 39 Form-finding and cross sections

Group	Gravity	Radial loads	Vertical loads
ETFE beam	CHS114,3*3,2	CHS114,3*3,2	CHS114,3*4
Strut	CHS152,4*12,5	CHS152,4*12,5	CHS152,4*12,5
Hoop	t_{flange}=60mm,t_{web}=15mm	t_{flange}=55mm,t_{web}=15mm	t_{flange}=55mm,t_{web}=15mm
Rods	Circular bar d=55mm	Circular bar d=55mm	Circular bar d=55mm
Cable top	PG55 A=347mm^2	PG55 A=347mm^2	PG55 A=347mm^2
Cable bottom	PG75 A=467mm^2	PG75 A=467mm^2	PG75 A=467mm^2
Rectangular cable	PG40 A=237mm^2	PG40 A=237mm^2	PG40 A=237mm^2

Pretension

The line graph below shows that the model with form from gravity requires the largest amount of pretension for both top and bottom cable net. Consequently, the largest bending moment occurs in hoop beams for the model with form from gravity thus a larger cross section is required.

For the rest two models, compared to the standard model, the one with form from vertical loads needs smaller pretension for top cable net and larger pretension for bottom cable net, but these two models have the same total amount of pretension. This means that the top cable net from vertical loads can take larger compression compared to the standard one, so that smaller pretension is required for the top cables. Conversely, the bottom cable net from vertical loads is less stiff than the standard one which leads to higher required minimum pretension in spite of smaller pretension in top cables. However, the pretension difference is very small.

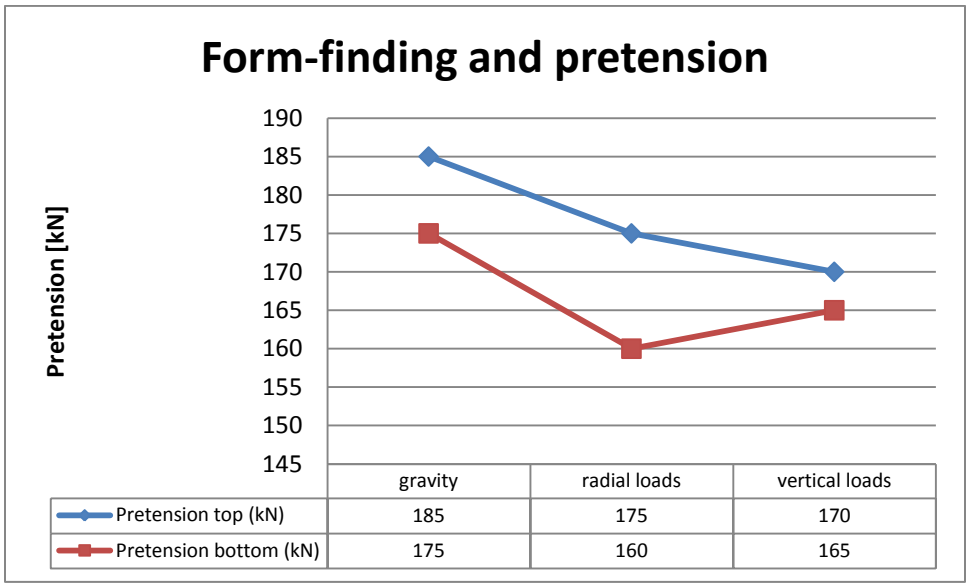

Figure 116 Form-finding and pretension

For all the models the minimum tension in cables under ULS LC2 is controlled larger than 0kN to make sure all cables in tension and guarantee the stiffness of the cable net, but smaller than 10kN to get comparable results.

Table 40 Minimum tensile force in cable under ULS LC2

Group	Gravity	Radial loads	Vertical loads
minimum tensile force in cable (N)	3813	2333	2192

Displacement

The maximum upward and downward displacement can be found under ULS LC3 and ULS LC2 respectively. Both fulfills the SLS check with $\delta < l_{span}/200 = 143mm$.

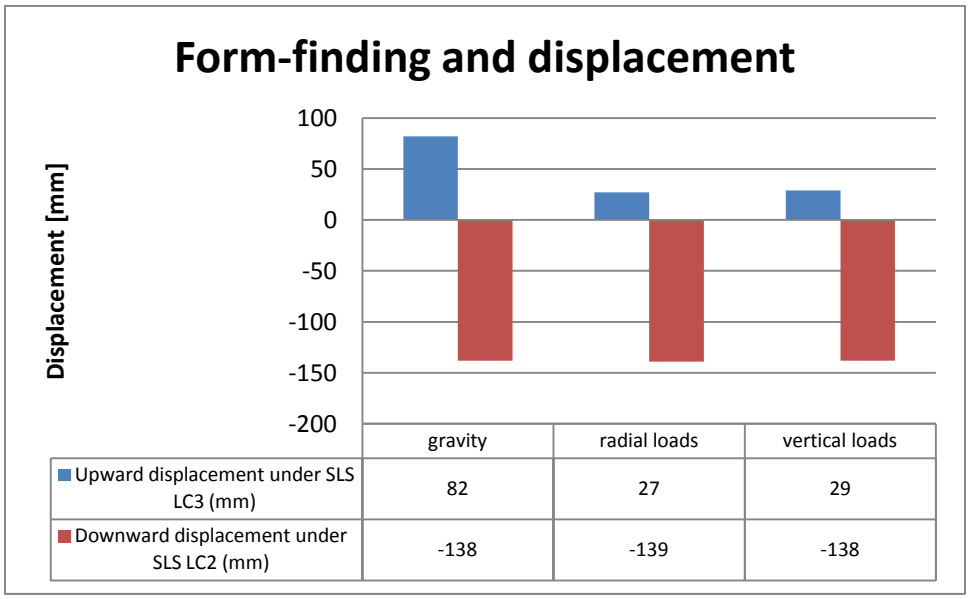

Figure 117 Form-finding and displacement

Conspicuous upward displacement under SLS LC3 is witnessed for model with form from gravity. It proves that the form from gravity is not good at withstanding upward loads. Model with form from radial loads and vertical loads have almost the same displacement with similar pretension.

Resulting forces

For all the three models from different ways of form-finding, ULS LC2 is the most critical load case for elements in ETFE beam, hoop, bottom cable group, and ULS LC3 is the most critical load case for elements in strut, rods, top cable and rectangular cable group.

Unity check

As is shown in the table below, apart from the rectangular cable, the leading element in each group gives a UC value within 0,70 to 1,00. Enough strength is guaranteed for all these models with high efficiency of material use.

Table 41 Form-finding and unity check

Group	Gravity	Radial loads	Vertical loads
ETFE beam	0,96	0,94	0,85
Strut	0,81	0,91	0,92
Hoop	0,97	0,89	0,87
Rods	1,00	0,94	0,97
Cable top	0,83	0,75	0,72
Cable bottom	0,84	0,78	0,78
Rectangular cable	0,12	0,09	0,09

Mass

Table below gives the mass of elements in each group. For the three models, different ways of form-finding may change the position of each connection node on the cable net, resulting in a small difference in the length of struts. This difference is also reflected in the mass change of strut. The model from gravity has smaller mass of strut compared to the standard model, and the model from vertical loads has larger mass of strut.

The cross section change also leads to a change of the element mass. Model with form from vertical loads has the larger cross section for ETFE beam and model with form from gravity has larger cross section for hoop beam.

In summary, the standard model, which has the shape of cable net from radial loads, has the smallest total mass.

Table 42 Form-finding and Mass (kg) of elements in each group

Group	Gravity	Rel.Std	Radial loads	Rel.Std	Vertical loads	Rel.Std
ETFE beam	5961	100%	5961	-	7398	124%
Strut	13176	95%	13841	-	14194	103%
Hoop	48228	106%	45669	-	45669	100%
Rods	119	100%	119	-	119	100%
Cable top	1256	100%	1259	-	1262	100%
Cable bottom	1701	100%	1706	-	1710	100%
Rectangular cable	427	100%	427	-	427	100%
Mass without hoop	22640	97%	23313	-	25110	108%
Mass with hoop	70868	103%	68982	-	70779	103%

10.4 Influences of changing depth of cable net

In this structure, a lens-shaped (or fish-belly shaped) cable-strut system is used. Assuming there is no influence on the cable net from hoop, there are two factors that determine the stiffness of cable net:

- Depth of the cable net;
- Material and section size of elements.

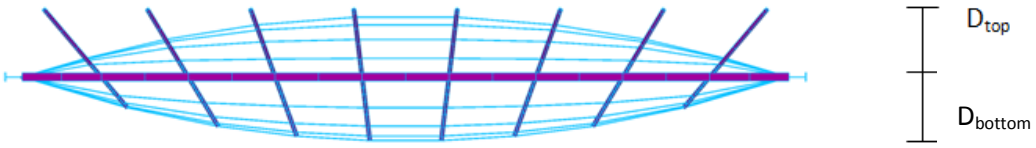

Figure 118 Cable net with radial struts

In this section, D_{top} stands for the depth of cable net above the supports in hoop plane, D_{bottom} for the depth below the supports in hoop plane. The changes of D_{top} and D_{bottom} are made separately to get a clear insight into their influences. The range of variables are listed in the table below:

Table 43 Depth of cable net

Group	1	2	3	4	5	6	7	8	9	10
D_{top} (mm)	2250					1950	2050	2150	2250	2350
D_{bottom} (mm)	2150	2250	2350	2450	2550	2350				

In this section, changes are made based on the standard model with inclined struts. For each group, the only variable is the depth of top or bottom cable net, the rest geometric parameters are exactly the same as the standard model.

1) D_{top}=2250mm, change D_{bottom}

Cross section

In this variable study, the change of D_{bottom} brings very little influence on the resulting forces in elements. All the choices of cross sections are the same as the standard model.

Table 44 Cross section for model from group 1-5

Group	Cross section
ETFE beam	CHS114,3*3,2
Strut	CHS152,4*12,5
Hoop	h=1300mm,b=300mm, t_{flange}=55mm,t_{web}=15mm
Rods	Circular bar d=55mm
Cable top	PG55 A=347mm^2
Cable bottom	PG75 A=467 mm^2
Rectangular cable	PG40 A=237 mm^2

Pretension

The line graph shows that increasing D_{bottom} leads to a model with smaller minimum required pretension for both top and bottom cable net. It is also witnessed that with an increase of D_{bottom}, the difference of pretension between top and bottom cable net becomes larger with less pretension in the bottom cable net.

These results first indicate that the model with larger D_{bottom} has higher stiffness, thus a smaller pretension is required for the top cable net to keep all the cables under tension, which also leads to smaller pretension in bottom cable net to control the downward displacement. Second, the asymmetric shape of the cable net makes a difference to the minimum required pretension in bottom cable net. Assuming the external loads remain unchanged, increasing D_{bottom} will reduce the downward displacement, thus smaller pretension can be applied to the bottom cable net.

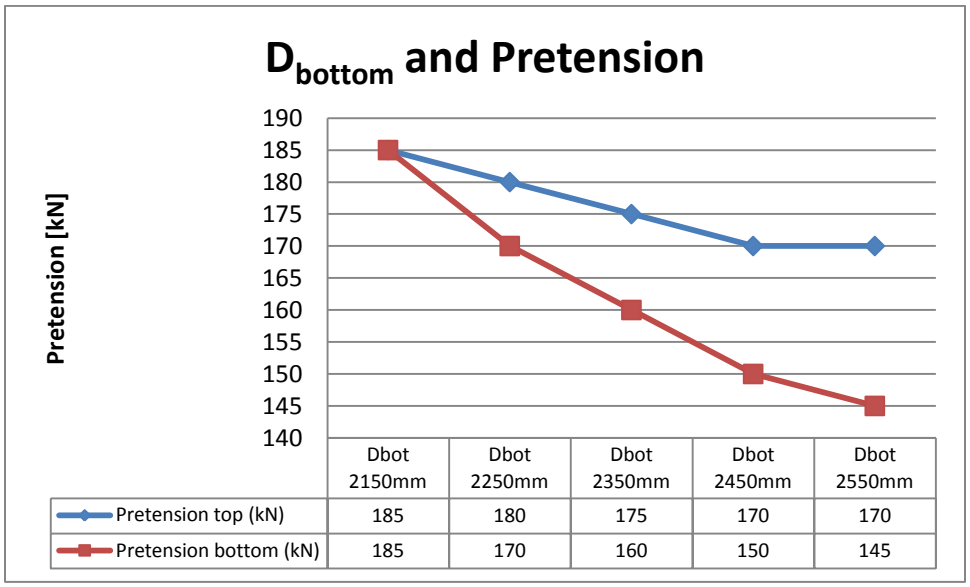

*D_{top}=2250mm

Figure 119 D_{bottom} and pretension

In this study, the minimum tensile force in cables under ULS LC2 is controlled within 0kN to 10kN. And the downward displacement under SLS LC2 is controlled as close to 143mm as possible in order to get comparable and reliable results.

Table 45 D_{bottom} and minimum tension in cables under ULS LC2

D_{bottom} (mm)	2150	2250	2350	2450	2550
minimum tension in cables (N)	5655	3949	2333	622	4218

Displacement

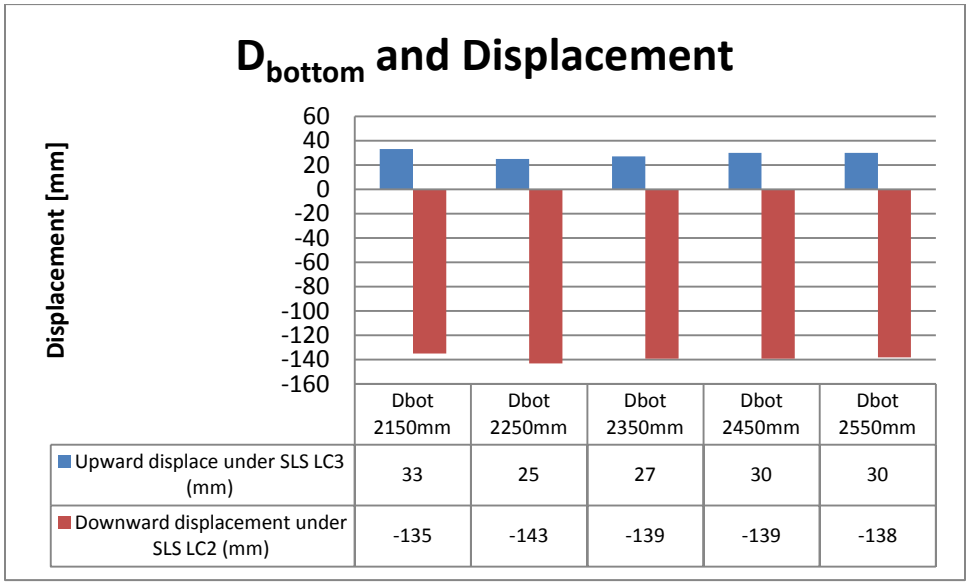

Figure 120 D_{bottom} and displacement

Resulting forces and Unity check

In the variable study, ULS LC2 is the most critical load combination for elements in ETFE beam, hoop, and bottom cable group. ULS LC3 is the most critical load combination for elements in strut, rods, top cable, and rectangular cable group. Results of elements in different groups are taken from the corresponding critical load combinations.

Table 46 D_{bottom} and unity check for beam elements

D_{bottom} (mm)	2150		2250		2350		2450		2550	
Group	Stress (N/mm^2)	UC	Stress (N/mm^2)	UC	Stress (N/mm^2)	UC	Stress (N/mm^2)	UC	Stress (N/mm^2)	UC
ETFE beam	331	0,93	331	0,93	332	0,94	333	0,94	334	0,94
Strut	325	0,92	327	0,92	323	0,91	320	0,90	321	0,90
Hoop	343	0,97	327	0,92	315	0,89	302	0,85	299	0,84
Rods	349	0,98	339	0,95	332	0,94	324	0,91	320	0,90

Table 47 D_{bottom} and unity check for cables

D_{bottom} (mm)	2150		2250		2350		2450		2550	
Group	Force (kN)	UC	Force (kN)	UC	Force (kN)	UC	Force (kN)	UC	Force (kN)	UC
Cable top	257	0,79	251	0,77	245	0,75	238	0,73	237	0,73
Cable bottom	370	0,84	355	0,81	343	0,78	332	0,76	325	0,74
Rectangular cable	23	0,10	22	0,10	21	0,09	21	0,09	21	0,09

Mass

Changing D_{bottom} only brings very limited change to the total length of elements in bottom cable and strut group. This difference is so small that can be neglected.

Table 48 D_{bottom} and Mass (kg)

D_{bottom} (mm)	2150	2250	2350	2450	2550
ETFE beam	5961	5961	5961	5961	5961
Strut	13359	13599	13841	14086	14334
Hoop	45669	45669	45669	45669	45669
Rods	119	119	119	119	119
Cable top	1259	1259	1259	1259	1259
Cable bottom	1702	1704	1706	1708	1711
Rectangular cable	427	427	427	427	427
Mass without Hoop	22827	23069	23313	23560	23811
Mass with Hoop	68496	68738	68982	69229	69480

2) D_{bottom}=2350mm, change D_{top}

Cross section

Similar to the change of D_{bottom}, changing D_{top} also brings very little influence on the resulting forces in elements. For models with D_{top} from 1950mm to 2250mm, the cross section remains the same as that of the standard model. For model with D_{top}=2350mm, a bigger cross section for rods is applied.

Table 49 D_{top} and cross section

D_{top} (mm)	1950~2250	2350
ETFE beam	CHS114,3*3,2	CHS114,3*3,2
Strut	CHS152,4*12,5	CHS152,4*12,5
Hoop	h=1300mm,b=300mm, t_{flange}=55mm,t_{web}=15mm	h=1300mm,b=300mm, t_{flange}=55mm,t_{web}=15mm
Rods	Circular bar d=55mm	Circular bar d=60mm
Cable top	PG55 A=347mm^2	PG55 A=347mm^2
Cable bottom	PG75 A=467 mm^2	PG75 A=467 mm^2
Rectangular cable	PG40 A=237 mm^2	PG40 A=237 mm^2

Pretension

The pretension in top cable net first drops in model with D_{top} from 1950mm to 2150mm and then remains unchanged. However, a continuous increase of pretension in bottom cable net is seen with an increase of D_{top}.

These results first says that the model is stiffer with higher D_{top} so that a smaller pretension is required to keep all the cables under tension. Second, the asymmetric shape of the cable net makes a difference to the minimum required pretension in bottom cable net. Assuming the external loads remain unchanged, increasing D_{top} will lead to larger downward displacement, thus higher pretension is required in bottom cable net to limit the downward displacement.

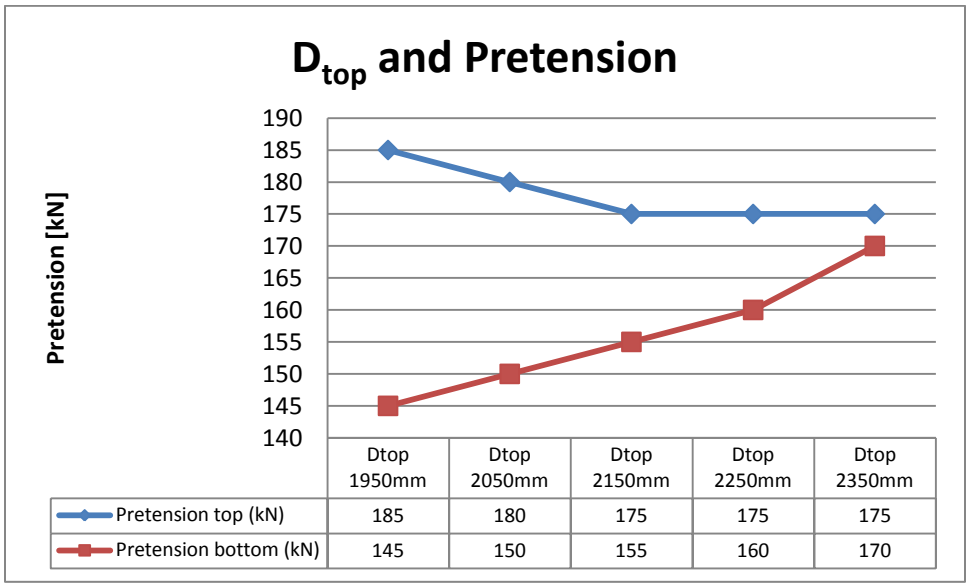

Figure 121 D_{top} and pretension

Table 50 D_{top} and minimum tension in cables under ULS LC2

D_{top} (mm)	1950	2050	2150	2250	2350
minimum tension in cables (N)	4012	5366	1245	2333	3414

Displacement

In this study, the minimum tensile force in cables under ULS LC2 is controlled within 0kN to 10kN. And the downward displacement under SLS LC2 is controlled as close to 143mm as possible in order to get comparable and reliable results.

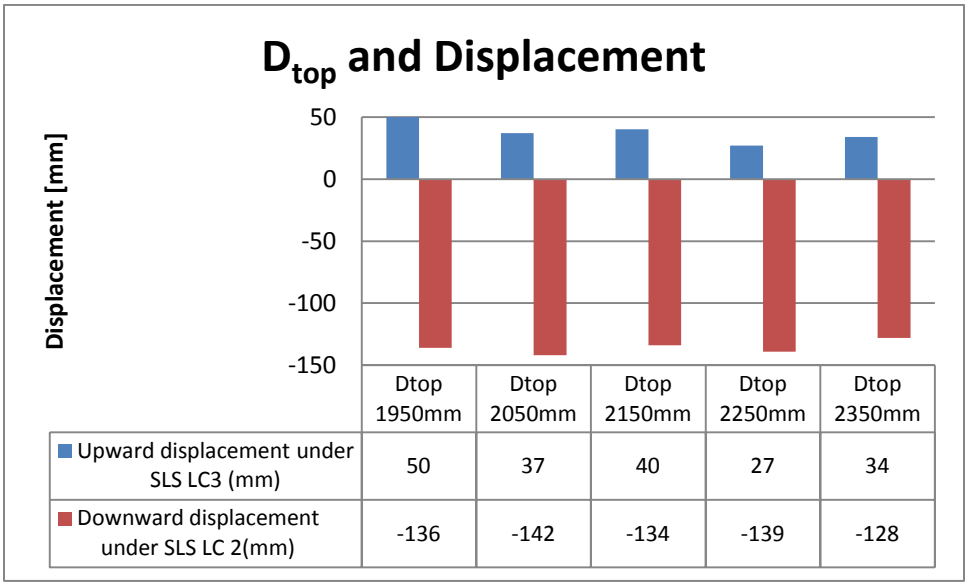

Figure 122 D_{top} and displacement

Resulting forces

In the variable study, ULS LC2 is the most critical load combination for elements in ETFE beam, hoop, and bottom cable group. ULS LC3 is the most critical load combination for elements in strut, top cable, and rectangular cable group. For elements in all the mentioned groups, the resulting force remains almost unchanged in models with different D_{top}, this is because the changes are very small in both the geometry and the pretension. As for elements in the group of rods, the most critical load combination changes as D_{top} changes.

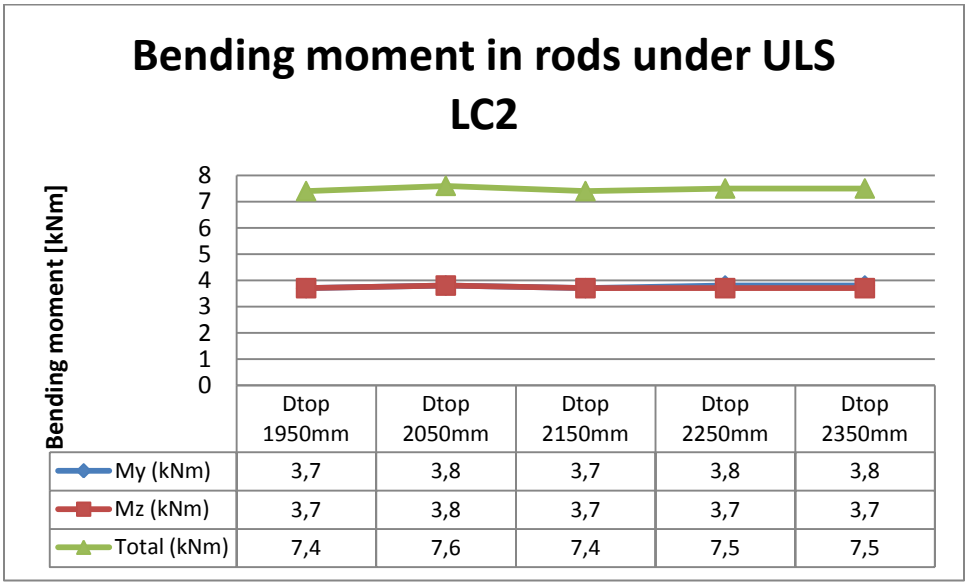

Figure 123 Bending moment in rods under ULS LC2

Snow is the governing load case in ULS LC2, the downward force from the upper part of rods is not affected by D_{top}, the change of reacting force from struts is very limited due to the small variation of pretension.

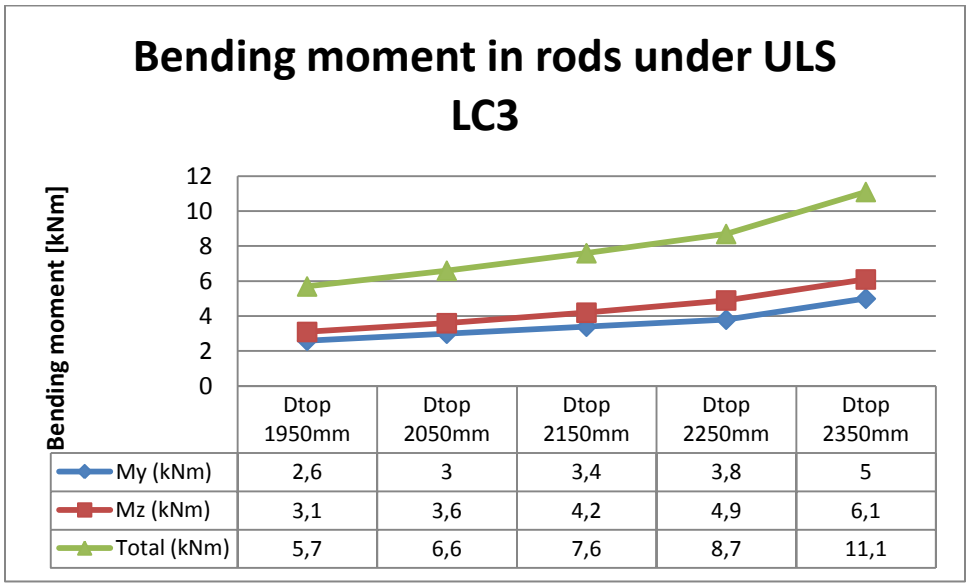

	Dtop 1950mm	Dtop 2050mm	Dtop 2150mm	Dtop 2250mm	Dtop 2350mm
My (kNm)	2,6	3	3,4	3,8	5
Mz (kNm)	3,1	3,6	4,2	4,9	6,1
Total (kNm)	5,7	6,6	7,6	8,7	11,1

Figure 124 Bending moment in rods under ULS LC3

As for the upward wind suction load which is governing in ULS LC3, it works together with pretension and makes a big difference to the resulting forces in rods. From the line graphs above, bending in rods under ULS LC3 keeps going up with higher D_{top}. For model with D_{top} higher than 2150mm, the total bending in rods under ULS LC3 is larger than that under ULS LC2, the most critical load combination switched. This explains why a bigger cross section is applied for rods in the model with the highest D_{top}.

Unity check

For models with different D_{top}, due to the same cross section and small difference in resulting forces, UC for elements in different groups are almost the same.

Table 51 D_{top} and UC value of elements in different groups

D_{top} (mm)	1950	2050	2150	2250	2350
ETFE beam	0,94	0,94	0,94	0,94	0,94
Strut	0,93	0,93	0,93	0,91	0,89
Hoop	0,88	0,89	0,89	0,88	0,9
Rods	0,87	0,88	0,88	0,87	0,91
Cable top	0,77	0,77	0,77	0,75	0,75
Cable bottom	0,78	0,78	0,78	0,78	0,79
Rectangular cable	0,08	0,09	0,09	0,09	0,11

Mass

Geometrically, changing D_{top} only brings very limited change to the total length of elements in top cable group. The mass change due to larger cross sections for rods in D_{top}=2350mm is negligible compared to the total mass. In summary, changing D_{top} brings almost no change to mass of this structure.

Table 52 D_{top} and Mass (kg) of elements in each group

D_{top} (mm)	1950	2050	2150	2250	2350
ETFE beam	5961	5961	5961	5961	5961
Strut	13841	13841	13841	13841	13841
Hoop	45669	45669	45669	45669	45669
Rods	119	119	119	119	142
Cable top	1256	1257	1258	1259	1261
Cable bottom	1706	1706	1706	1706	1706
Rectangular cable	427	427	427	427	427
Mass without hoop	23310	23311	23312	23313	23338
Mass with hoop	68979	68980	68981	68982	69007

11. Discussion for variable study

For a tensegrity structure there are numerous possible variables. In this variable study, firstly the load combinations and boundary conditions have been defined. Within the boundary conditions the possible variables in this roof design have been chosen and classified into 6 orders. The initial assumption is that the higher the order, the more radical change it makes if modified. Then a model which satisfies both SLS and ULS check has been designed with the minimum amount of pretension and proper cross sections for elements in each group. This model was chosen as the standard model, based on which all the changes were made in the later variable study. From the static analysis of the standard model, it has been found that ULS LC2 determines the minimum amount of pretension, and SLS LC2 leads to the largest vertical deflection. As for the resulting forces, cables are all loaded in tension, and bending is the governing forces that determine the axial stress in all the beam elements.

In this variable study, there are always three variables modified: the chosen variable (1^{st}, 2^{nd}, 3^{rd}, 4^{th} order), 5^{th} order variable (pretension), and 6^{th} order variable (cross section). It is a very complex affair to design such a structure because of the interdependence. Here the interdependence means that every variable is dependent on the rest, also making changes to a single group of elements will bring changes to elements in the other groups.

In this roof design, it can be summarized that deliberate change of the chosen variable makes a difference to the structure mainly by changing the required minimum pretension since the 5^{th} order variable is not only a variable affecting the whole structure but also a result which is affected by other variables. Under the condition that higher pretension is required to keep all the top cables in tension, a corresponding increase of pretension is expected in bottom cables to limit the downward displacement. The higher pretension may leads to larger bending moments in struts and higher tensile forces in cables. Therefore, larger cross sections are required to guarantee enough strength, and this resulting mass addition again brings larger compression to the top cables. The above steps can form a loop which brings complexity in the design of such a roof structure. As for the hoop system around the cable net, the axial stress mainly comes from bending, which is determined by pretension and the number of branches.

For each order of the variable study, the minimum tensile force in cables under ULS LC2 is controlled within 0kN and 10kN, and the downward displacement under SLS LC2 is controlled as close to 143mm as possible in order to get comparable and reliable results. Then the cross sections, minimum required pretension, vertical displacement, resulting forces, utilization, and mass of elements in each group are looked into. Influences of changing a single variable are summarized as follows:

- 1^{st} order number of branches

  In this roof design, adding or removing a branch of elements will bring radical change to the structure. In the first order variable study, it is clear that the model with more branches has a larger total length of elements in all the groups except hoop. However, this does not necessarily brings an addition of the mass of elements in each group considering the cross section changes. For elements in all the groups but hoop, the applied cross sections tend to be smaller in a model with more branches. But the hoop tends to require a larger cross section in model with more branches.

This variation starts with the ETFE beam grid. In this roof area, increasing the number of branches will lead to a decrease of the line load on each ETFE beam. Besides, with more branches the span of each element is smaller. The decreased line load and smaller element length collectively results in smaller bending moment in ETFE beam with more branches. Then a smaller cross section can be used , leading to a reduced compression force due to reduced self weight acting on the single branch cables. As a result, smaller pretension is required to guarantee all cables in tension and to control the downward displacement. Different cross sections are applied to elements in different groups to guarantee enough strength and high efficiency of material use.

A continuous decrease in mass of ETFE beam is seen in model with more branches. However, considering the total structural mass with hoop and the mass of connection, the total mass simply goes up with more branches.

- 2nd order position of converge point

In the 2nd order variable study, two models are investigated with different positions of central point. In one model the central point is on the ground which gives the model radial struts as the standard model, for the other model the central point is close to infinity below supports which leads to a model with vertical struts.

Radial struts or vertical struts directly affects the load transfer path in struts. It is noticeable that the model with vertical struts has better load transfer paths with smaller eccentricity. As a result, smaller pretension can be applied to the vertical struts, leading to the reduced cross sections for struts and hoop beams.

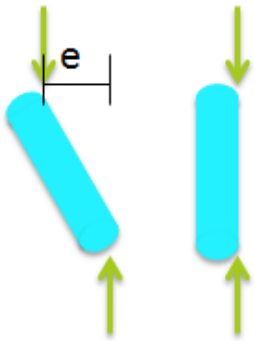

Figure 125 Struts with different eccentricities

In summary, the model with radial struts does not lead to the most efficient design but of different aesthetics. Structurally, the model with vertical struts has better load transfer path thus smaller pretension can be applied. Consequently smaller bending occurs which allows the application of smaller cross sections for strut and hoop beams. The mass reduction from smaller strut and hoop in model with vertical struts gives a structure with less structural mass, which is about 80% of the standard model (see Table 38).

- 3rd order way of form-finding

In the 3rd order variable study, self-weight, radial loads, and vertical loads are applied to a flat grid respectively. Different ways of form-finding lead to cable-strut systems with different positions of connection nodes, small difference is witnessed in the length of struts.

The model with form from gravity requires the largest amount of pretension. However, this does not necessarily lead to the largest axial stress in struts because of the reduction of strut length. Actually, smaller axial stress is found in strut. But a larger cross section is required for hoop due to large pretension.

As for the model with form from vertical loads, it has the same total amount of pretension as the standard model. A difference worth mentioning is that larger bending occurs in the ETFE beams in model with form from vertical loads thus a larger cross section is applied. This is because changing the way of form-finding also makes a difference to the resulting force from struts to the ETFE beam grid.

Considering the mass of the structure, the standard model which has the shape of cable net from radial loads is the optimal.

- 4th order depth of cable net

In the design of cable net, it is the depth of cable net, material and section size of elements that determines the stiffness. From the results, no change occurs in the choice of cross sections for different models except the model with D_{top}=2350mm. The difference of element length in different models is also very limited. Therefore, changing the depth of cable net brings almost no difference in the total mass.

The stiffness change is reflected in the minimum required pretension. It has been found that increasing the depth of cable net may lead to a stiffer structure which requires smaller pretension in top cables to keep them all in tension. Also smaller pretension in bottom cable net is seen in models with higher D_{bottom}. But larger pretension is required in bottom cable net in models with higher D_{top}. This difference comes from the asymmetric shape of the cable net.

By doing the multi-variable study, influences of changing a single variable have been found. Buckling check for the hoop is required to guarantee enough stiffness. And further optimisation can be performed to find model with better structural behavior under defined load cases.

Chapter 5
Detailed design

12. Optimisation check with Karamba

This section aims to answer the question raised in the beginning: If it is possible to make a loop and do optimisation, which means to build a model that allows the program to find the minimum required pretension and proper cross sections with high efficiency of material use automatically. Results from Karamba are compared with that from Femap to come to the conclusion.

12.1 Introduction

In the parametric model, firstly geometry, material, property and loads are defined according to the standard model in Femap. Galapagos and Karamba are used to form a loop for optimisation. Considering the complex loading acting on this structure and the interaction both between elements and between variables, optimisation is divided into two steps: optimize pretension and optimize cross sections. Details are described in the figure below:

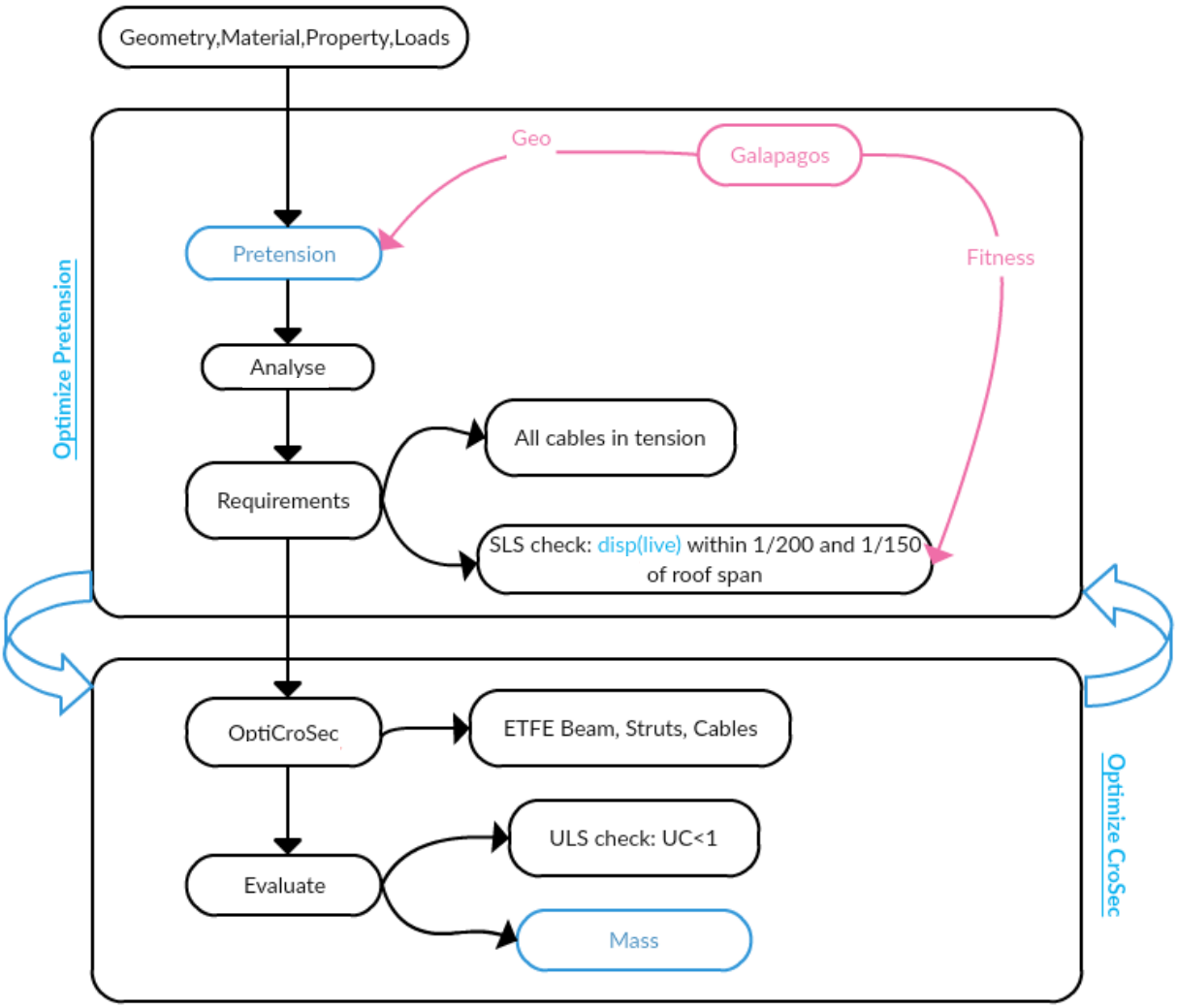

Figure 126 General idea about Optimisation with Karamba

There are two components in the Grasshopper environment that is necessary in forming the loop to optimise the structure automatically. They are Galapagos Evolutionary Solver and OptiCroSec (Optimise Cross Section).

Galapagos

Galapagos is a program that provides a generic platform for the application of Evolutionary Algorithms (*David Rutten, 2010*). With Galapagos, the proper amount of pretension is found under the condition that all the top cables in tension and the downward displacement fulfills the SLS check.

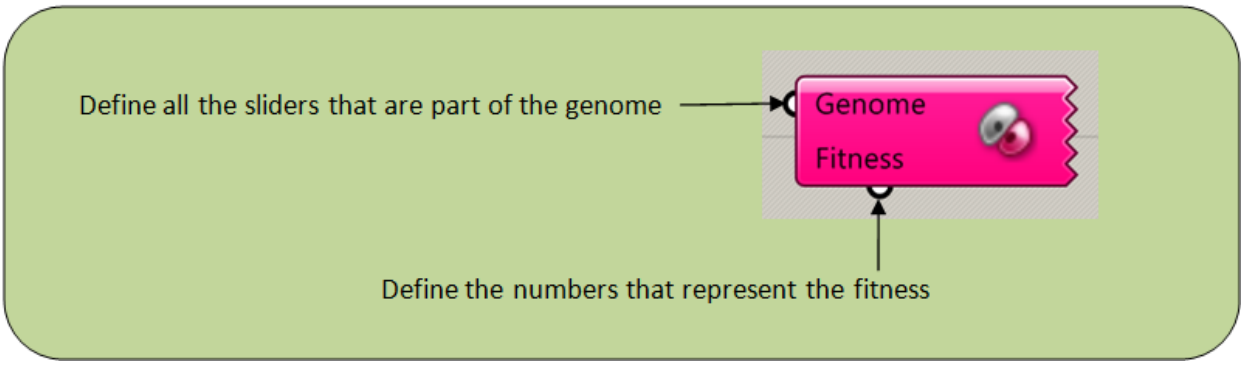

Figure 127 Component - Galapagos

OptiCroSec

OptiCroSec is a component from the plug-in Karamba. It selects optimum cross section for beams and shells in the model according to EC3 (EN 1993-1-1) for steel structures. With this component, the proper cross sections for elements in different groups can be found.

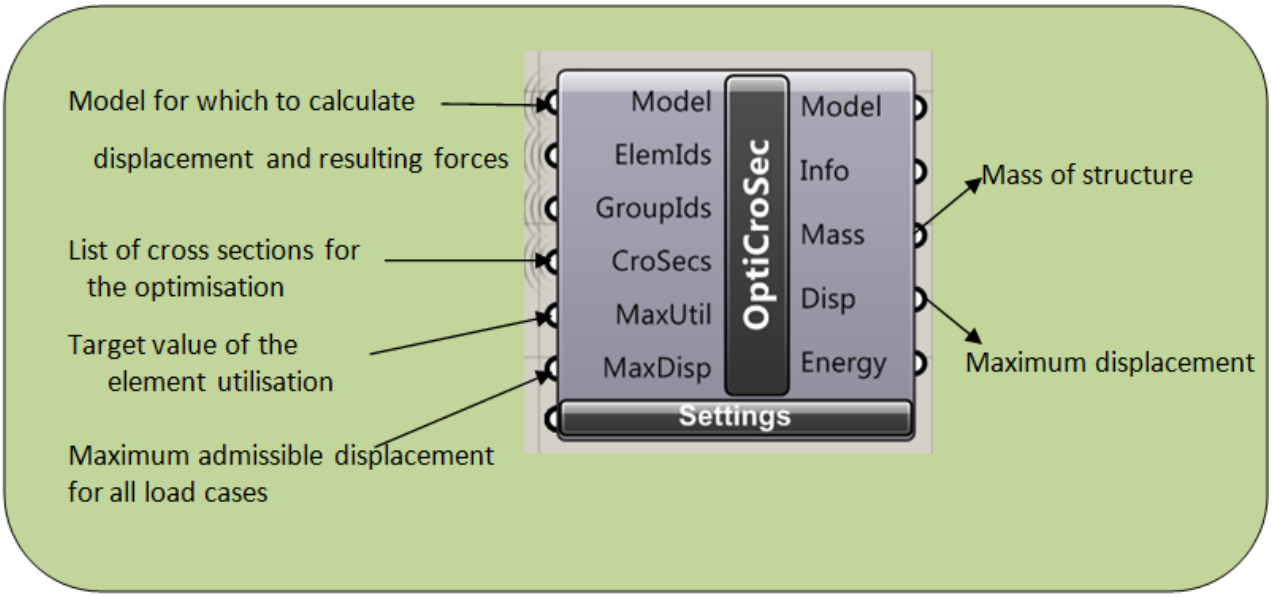

Figure 128 Component - OptiCroSec

Interfaces about Galapagos are as follows:

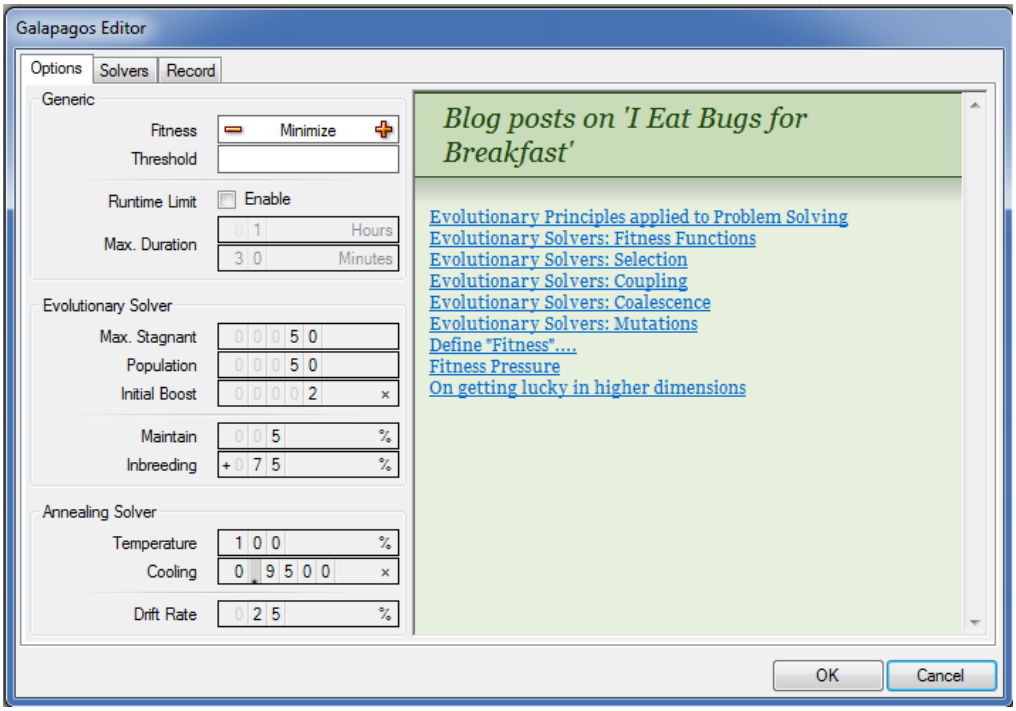

Figure 129 Galapagos solver settings

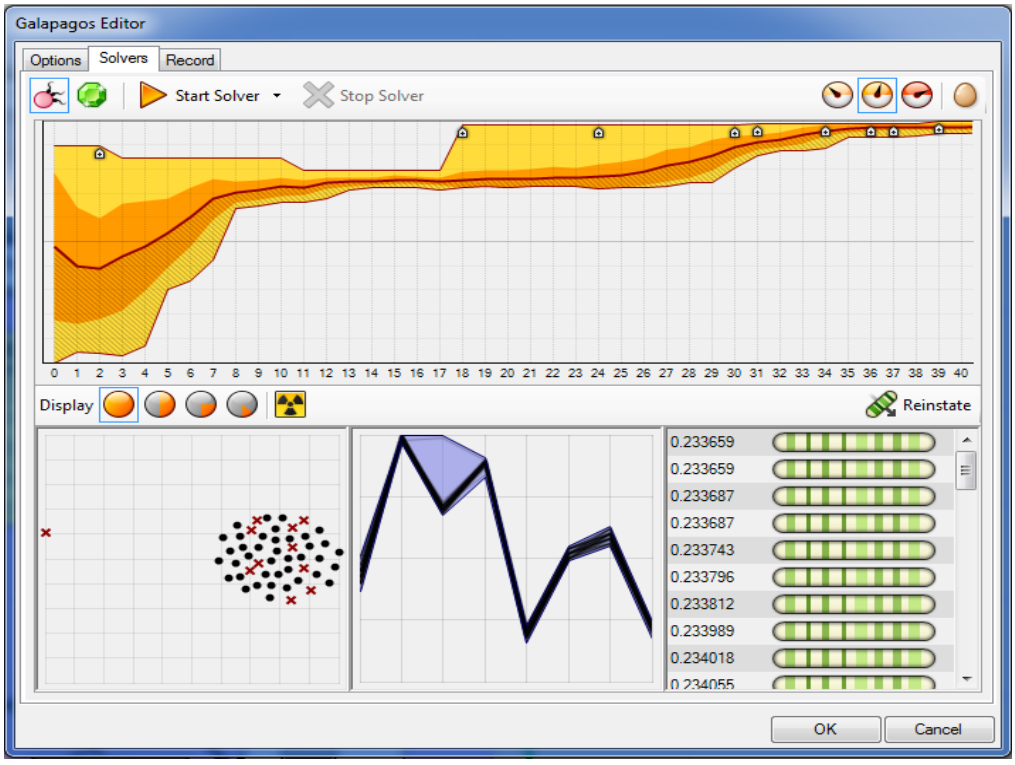

Figure 130 Galapagos run

12.2 A different way for applying pretension and live loads in Karamba

For both models in Femap and in Karamba, they have the same geometry, material, property, and boundary conditions. The only difference is the way for applying pretension and live loads. In Femap, pretension is applied to all the edge cables with defined preloading. In Karamba, pretension is applied to the whole cable network with defined prestrain. This difference results from the reasons stated below:

1) In karamba, there are two ways for adding pretension to the cables: prestrain or temperature loading. In both cases preloading is applied by elongation of elements. But in Femap, pretension can be added by directly defining the amount of bolt preloading in regions.
2) In Karamba, there is pretension loss in cables due to inward displacement of hoop beams. In Femap, the defined preloading is the exact amount of internal force from pretension.

In Karamba, the variable loads are transformed into point loads on the connection points in ETFE beam grid, while in Femap the variable loads are transformed into line loads on the beam elements.

In this design, since the variable loads are more or less symmetrical at lease in one direction, the pretension are applied symmetrically to both the top and bottom cable net. Cables with the same numbering are applied the same pretension.

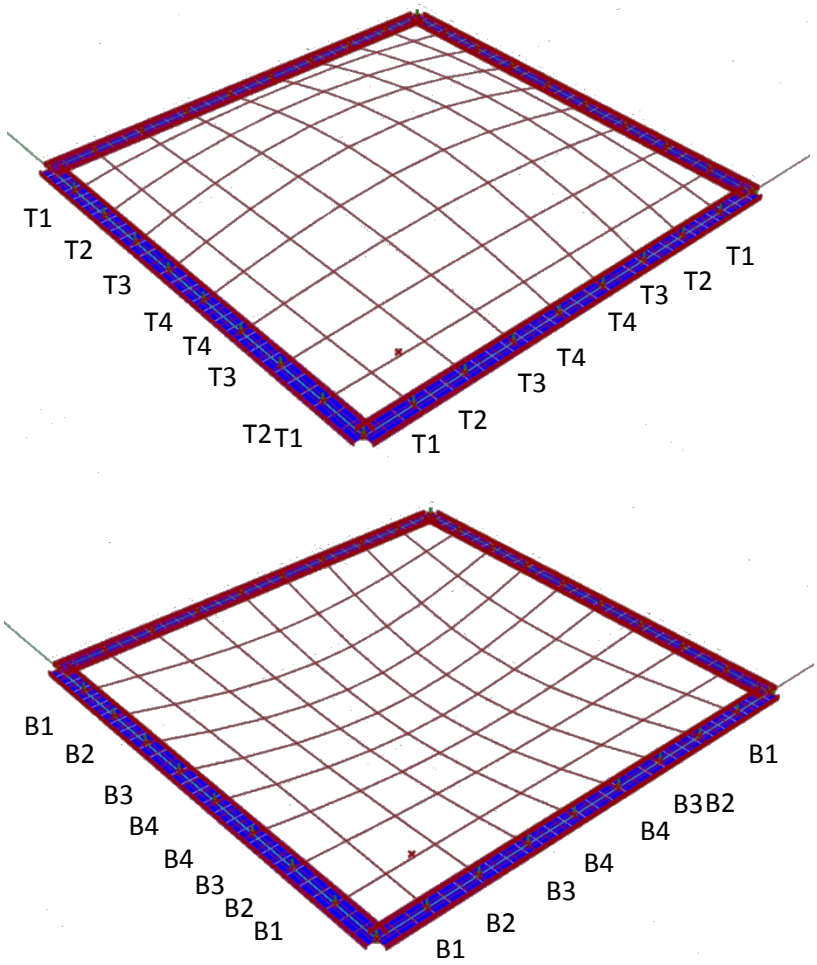

Figure 131 Numbering of cables for pretension

12.3 Optimize pretension

Ideas about optimizing pretension are illustrated in the figure below. With Galapagos, different sets of pretension are found by using the evolutionary solver. There is always a better solution but the best solution. The elongation ε takes into account the pretension loss due to hoop displacement.

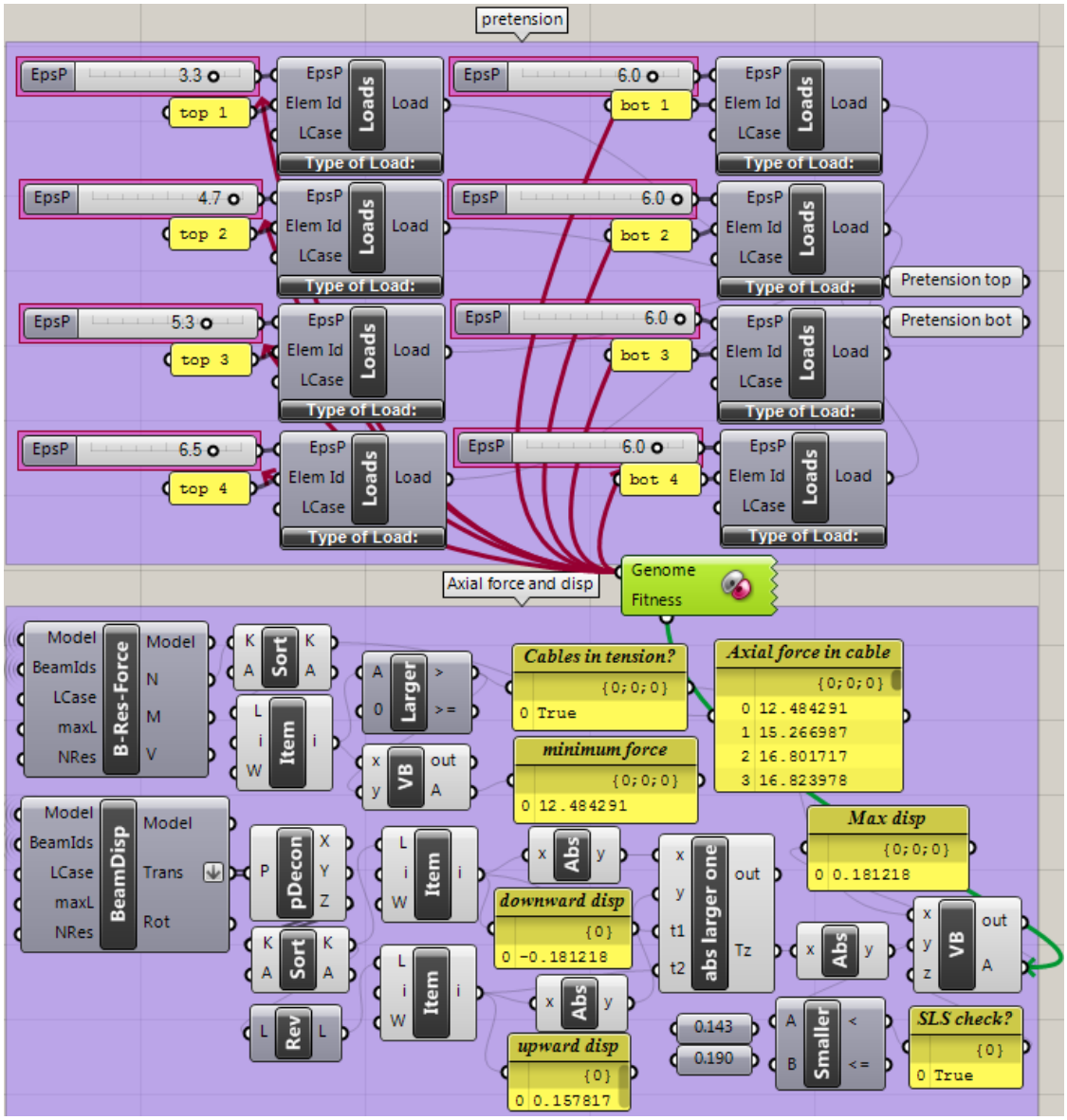

Figure 132 Optimisation for pretension

One possible set of pretension is listed in the table:

Table 53 One possible set of pretension

Cable	Top1	Top2	Top3	Top4	Bot1	Bot2	Bot3	Bot4
Prestrain (mm/m)	3,3	4,7	5.3	6,5	6	6	6	6

*Here Bot stands for Bottom

12.4 Optimize cross sections

In Karamba, the component OptiCroSec works to find a better solution by choosing the optimum cross sections from a cross section range selector. Since the final model has already been defined in Femap with specific cross sections for different groups of elements, the range of cross sections will be narrowed to 20 and all are chosen from standard profiles for higher possibility of reuse and recycling. In this research with Karamba, firstly all the cross sections are defined the same as that of the final model in Femap, then the struts, and cables are optimized in sequence.

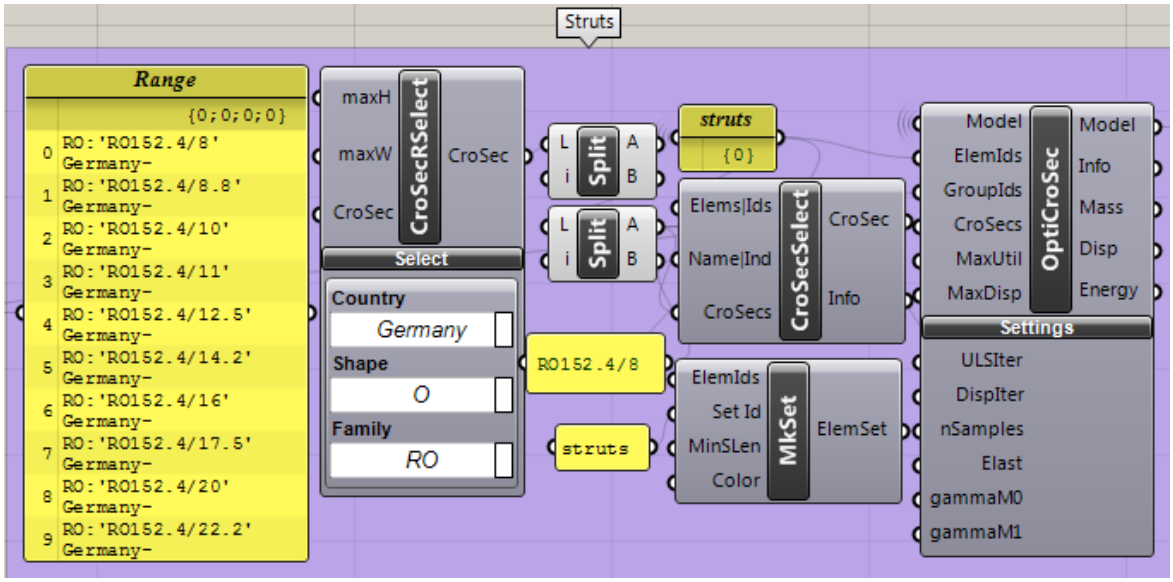

Figure 133 Optimize Struts

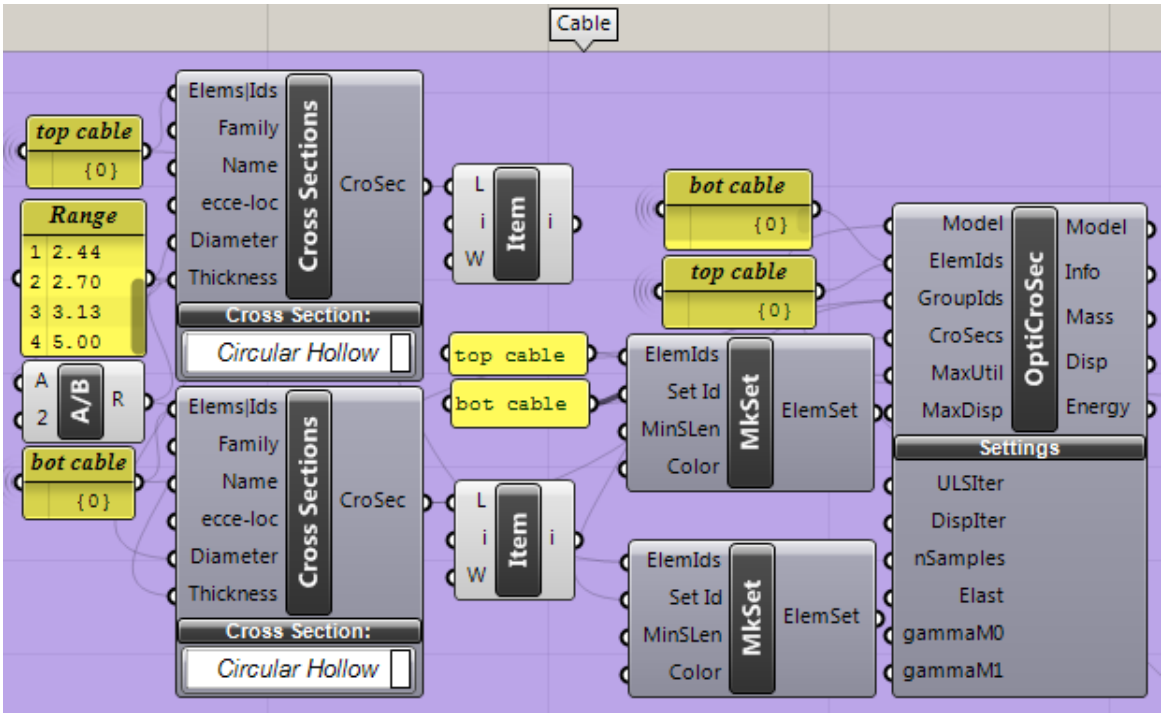

Figure 134 Optimize Cables

12.5 Discussions and limitations

In Section 12, the way of doing optimisation automatically with Galapagos and Karamba is interpreted in detail and the results are compared with those from Femap.

Table 54 Results in Femap and Karamba

Group	Femap	Karamba
Strut	RO152,4/12,5	Ro152,4/12,5
Top Cable	PG55 A=347mm^2	PG55 A=347 mm^2
Bottom Cable	PG75 A=467 mm^2	PG75 A=467 mm^2

Table 54 displays that Karamba and Femap give the same cross section for elements in cable groups after optimisation regardless of the different ways for applying pretension and variable loads. As for the strut elements, different cross sections are applied to different elements according to the results from Karamba, but most of the elements use the same cross section as that in Femap.

The study in this section proves that with Galapagos and Karamba, it is possible to form a loop and use the program to choose the proper set of pretension and the right cross sections for elements.

However, in the optimisation model the live loads are transformed into point loads on the connection points of the ETFE beam grid, bending moment is not considered in ETFE beams. Therefore the ETFE beam elements are not optimised. Additionally, the cross section for hoop beam elements is too big which cannot be found from the range of standard profile thus not included in this optimisation procedure.

Due to time issues, optimisation with Galapagos and Karamba is proved to be possible but not explored in depth. Further study can be conducted to build a model which is capable of finding the proper pretension and cross sections for all the elements by defining all the boundary conditions.

13. Buckling check for hoop

In this roof structure, a hoop with I-shaped cross section is applied around the cable-strut system to provide stability to the whole structure and to transfer forces to the building. The hoop system should have enough strength to withstand the large compression and bending due to the tensile force from cables, at the same time enough stiffness is required to prevent buckling. The hoop is loaded mainly by in-plane bending, thus the strong axis of the I-beam should be put in the in-plane direction of hoop. It is noticeable that the inward deformation of the compression hoop will also lead to sag of the pretensioned cables.

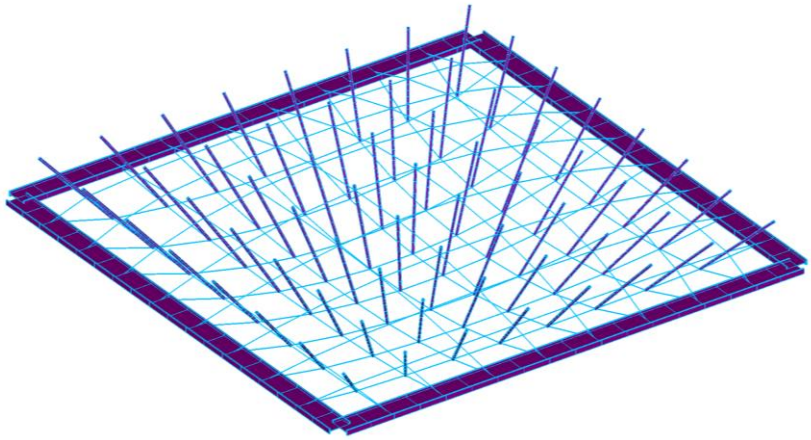

Figure 135 Cable -strut system with compression hoop

In this section, buckling check for hoop beams is performed based on the standard model. Related parameters of the I-profile are listed in the table below:

Table 55 Parameters of the hoop beam profile

Profile	h (mm)	b (mm)	t_{flange} (mm)	t_{web} (mm)	A (mm^2)	I_{yy} (mm^4)	I_{zz} (mm^4)
I-profile	1300	300	55	15	50850	$1{,}49x10^{10}$	$2{,}48x10^{8}$

13.1 Buckling

Buckling is the phenomenon when a member or part of a member displaces laterally or out of its plane due to compressive forces or stresses. Structural members without intermediate restraint or with only flexible intermediate restraint along their length can buckle when subject to either compression, bending, or a combination of both.

Buckling modes

For individual members there are four possible buckling modes under different external loads:

- Flexural buckling
  For structural members with a small out-of-straight imperfection, the compression force will result in transverse displacement and flexural stresses. For the I-section member, in this case it may buckle around its weak axis.
- Torsional and flexural-torsional buckling
  This buckling mode can occur at a load lower than that for flexural buckling when twist exists in the compression member. This mode is only relevant to angle and channel bracing members.
- Lateral-torsional buckling
  Lateral-torsional buckling is a frequent consideration for the design of I-section members without intermediate restraint. When a simply supported I-beam is loaded in flexure along its major axis, the top flange is in compression and will tend to buckle laterally, the cross section will also twist in torsion, resulting in a failure mode known as lateral-torsional buckling.
- Local buckling
  In addition to the buckling of the member as a whole, slender flanges can buckle locally under compression and slender webs can buckle under compression or shear.

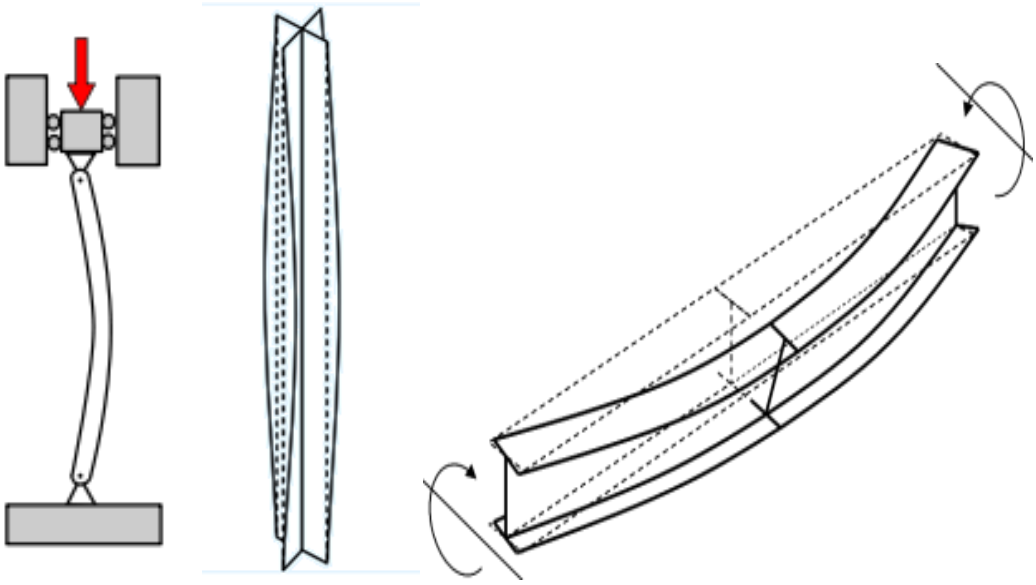

Figure 136 Flexural buckling, Torsional buckling, and lateral-torsional buckling

For flexural buckling, the elastic critical buckling force N_{cr} is often referred to as Euler load:

$$N_{cr} = \frac{\pi^2 EI}{(kL)^2} \qquad (13.1)$$

E – modulus of elasticity

I – moment inertia about the weak axis

L – length of the beam between two points with restraints

k – reduction factor, k=1 for both ends pinned, k=0,5 for both ends fixed and k=0,7 for one end pinned, one end fixed. The expression *kL* is often referred to as the buckling length

For lateral-torsional buckling, a similar approach can be adopted by determining the elastic critical buckling moment:

$$M_{cr} = \frac{\pi^2 E I_Z}{(kL)^2}\sqrt{\frac{I_w}{I_z} + \frac{(kL)^2 G I_T}{\pi^2 E I_z}} \qquad (13.2)$$

G – shear modulus of elasticity

I_z – moment inertia about the weak axis

I_T – torsional constant

I_w – warping constant

Solution by FEM

In this roof structure, the complex loading acting on this hoop and the interaction between components make it difficult to determine the boundary conditions for the most critical components. Hand calculation is not that applicable in this situation, only finite element analysis is used for buckling check.

In the finite element analysis, a finite element eigenvalue-eigenvector solution is used. The result is an eigenvalue, also called the buckling load factor (BLF). The BLF is the factor of safety against buckling or the ratio of the buckling loads to the applied loads.

Table 56 Interpretation of the Buckling load factor (***SOLIDWORKS Help, 2012***)

BLF Value	Buckling Status	Notes
BLF > 1	Buckling not predicted	The applied loads are less than the estimated critical loads. Buckling is not expected.
BLF = 1	Buckling predicted	The applied loads are exactly equal to the estimated critical loads. Buckling is expected.
0 < BLF < 1	Buckling predicted	The applied loads exceed the estimated critical loads. Buckling is expected.
-1 < BLF < 0	Buckling not predicted	Buckling is predicted if you reverse all loads.
BLF = -1	Buckling not predicted	Buckling is expected if you reverse the load directions
BLF < -1	Buckling not predicted	Buckling is not expected even if you reverse all loads.

Taking into account the imperfection, difference between model and real construction, and the sudden failure of buckling with no warning, a more strict standard with BLF>3 is applied as the boundary that buckling is not predicted.

First order analysis will determine the elastic critical buckling loads by considering a particular loading situation and evaluating the eigenvalues for the stiffness matrix. Material non-linearity and geometric deformation are not taken into account. Each eigenvalue has a corresponding eigenvector that defines the particular buckling mode associated with that value and thus it is only the lowest values that are of relevance.

13.2 Design process

In order to do buckling check, new models with only the beam elements for compression hoop are made. As is shown in figures below, for each connection point of the edge cables, the sum of horizontal component forces will be the load set applied to the new model with only hoop beam elements.

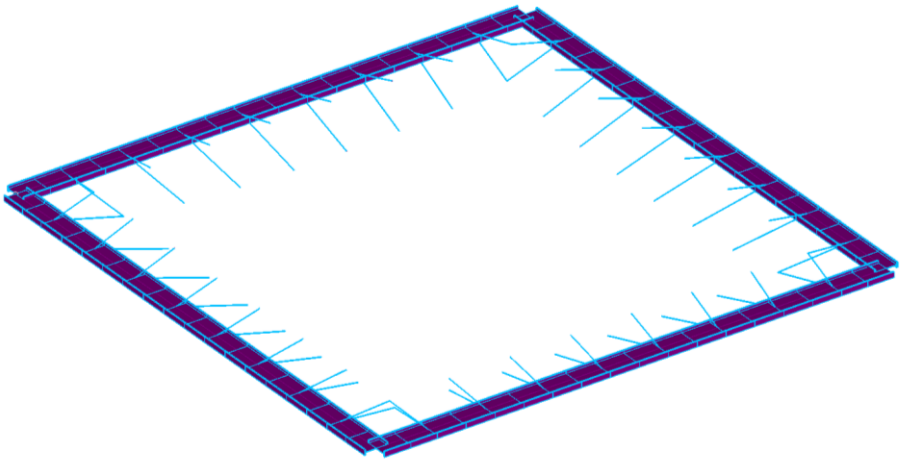

Figure 137 Hoop with edge cables

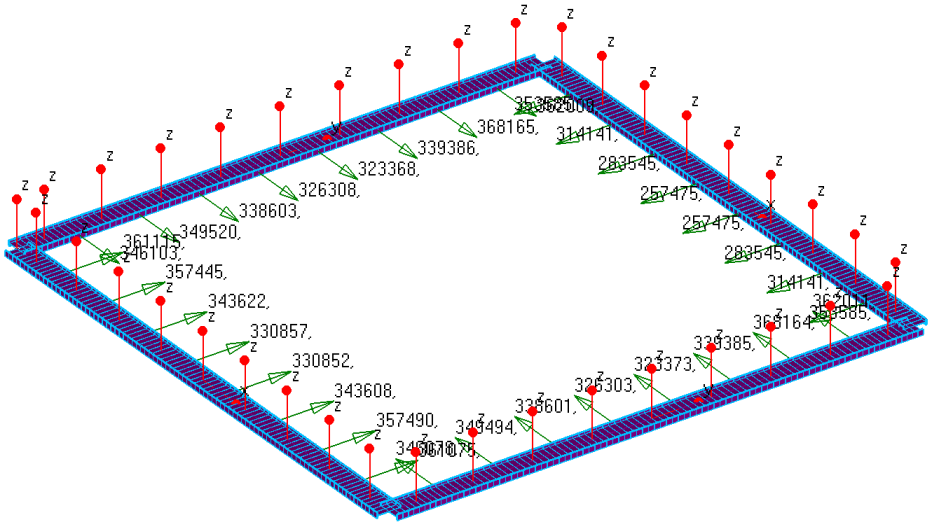

Figure 138 Hoop with equivalent horizontal load

For buckling analysis, ULS LC2 is used because this load combination requires the largest pretension and results in the largest axial forces in edge cables.

Line model

The line model displays that the lowest eigenvalue is 2,28, which means when the external load is multiplied by this value, out-of-plane flexural buckling occurs at the corner as displayed below.

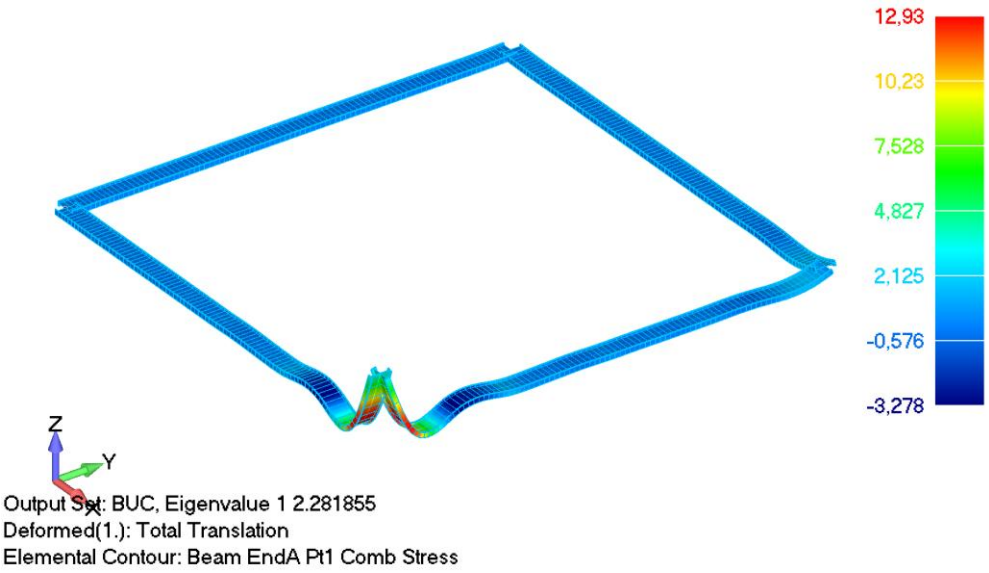

Figure 139 Buckling analysis for line model – BLF=2,28

It is also witnessed that in-plane buckling occurs when BLF is raised to 55,10, it means that under the defined boundary condition the hoop is really good for resisting in-plane buckling.

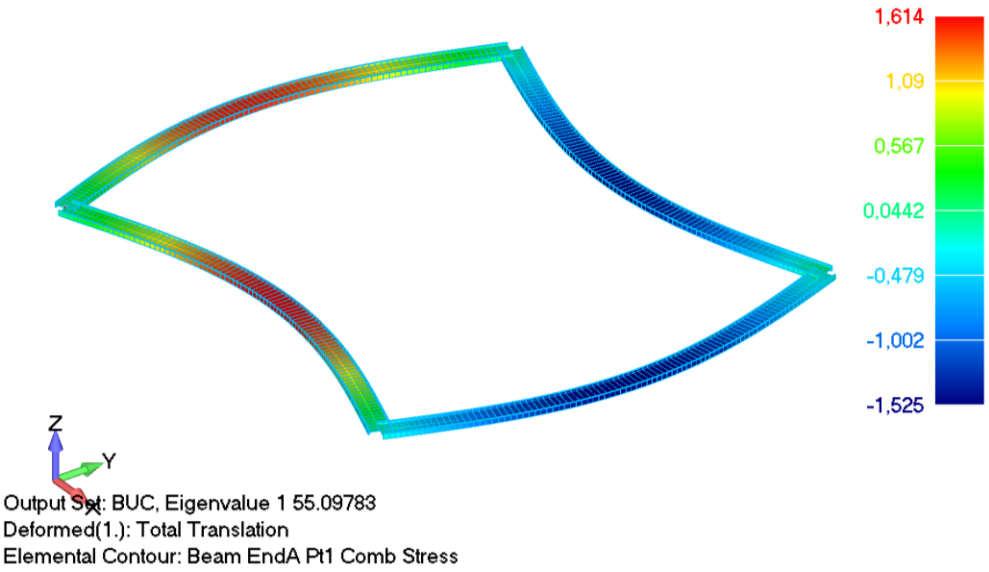

Figure 140 Buckling analysis for line mode – BLF=50,10

However, for each line there is only one dimension, which means torsional buckling is not considered in the line model. While torsional buckling can occur in a lower load than flexural buckling. Thus, the result from line model is not reliable. Further analysis needs to be conducted with plate model.

Plate model

Half of the hoop is modeled because both the geometry and loads are symmetrical. Some general information for the plate model is listed in the table below:

Table 57 General information for plate model

Group	Element type	Material	Property
Web	Plate	S355	t_{web}=15mm
Flange	Plate	S355	t_{flange}=50mm

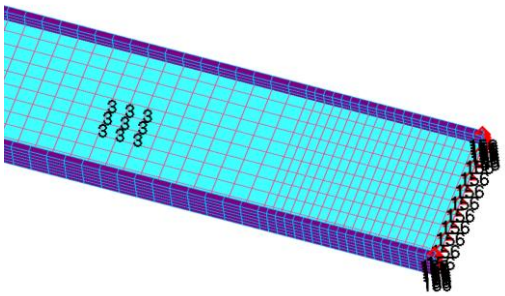

Figure 141 Constraint equations and nodal constraints

For plate model, external loads are the same as those of line model (see Figure 138).

As for constraints, the position and DOF are also unchanged. The difference is that the constraints are no longer applied on one single node because dimension of constraints should be 1-D less than elements to avoid singularity problem. Instead, constraint equations are applied to a group of nodes of which the sum of their y- or z-direction translation equals to 0. Additionally, DOF 1,5,6 are restrained for all the nodes on axis of symmetry.

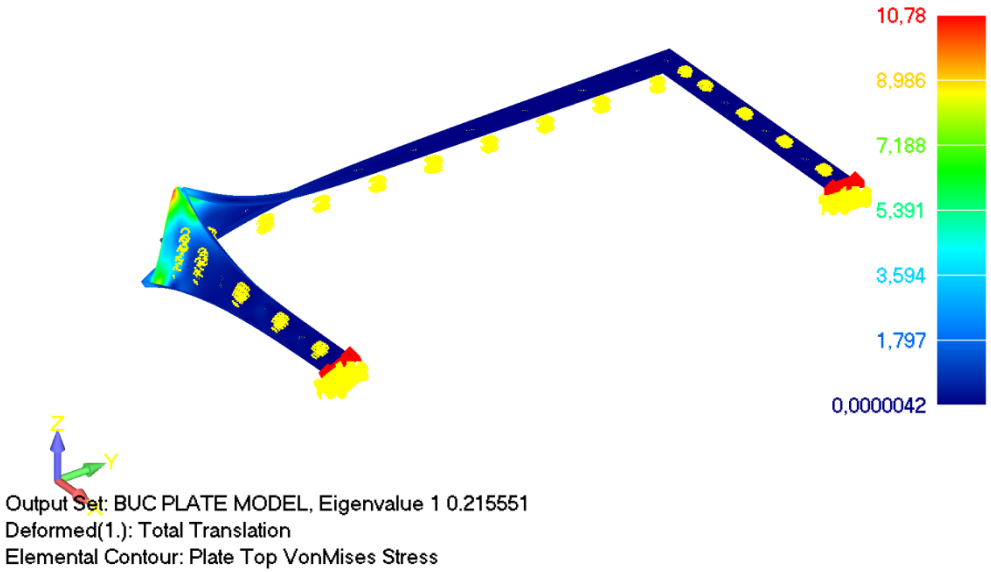

Figure 142 Buckling analysis for the plate model - BLF=0,22

By modeling the hoop with plate elements, the BLF drops drastically. Result shows that lateral-torsional buckling occurs at the corner with the eigenvalue at 0,22. The hoop needs to be stiffened in z direction, which is the weak axis of the I-profile. This can be easily done by adding stiffeners to the I-section.

Plate model with stiffeners

In this model, stiffeners are applied to both top and bottom sides of the web at three positions: the hoop corners, the support locations, and the positions for cable and hoop connection. Besides, two constraint equations are applied on the same stiffener to increase the resistance to torsional buckling. Property of the stiffeners is the same as that of the flange plate (t=55mm).

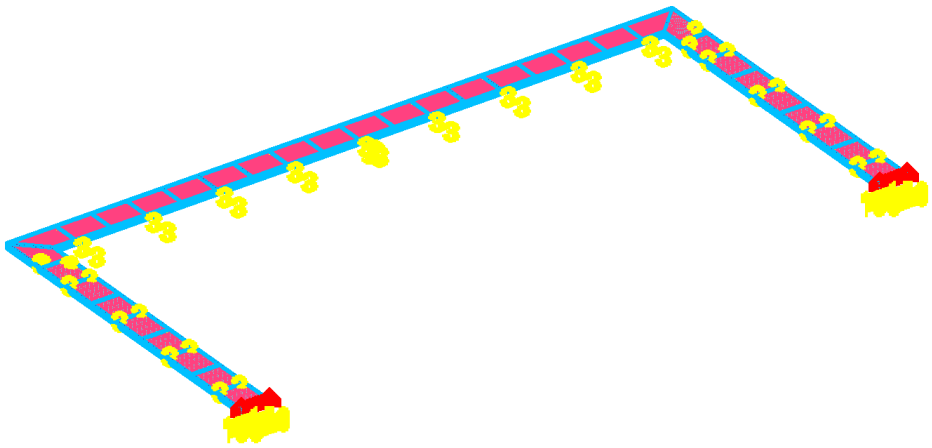

Figure 143 Half of the hoop with stiffeners

FEM result below shows that adding stiffeners to web plates is very effective in raising the buckling resistance with an eigenvalue raised from 0,22 to 1,55. Local buckling is associated with this eigenvalue. Other measures have to be taken to make this hoop stiffer.

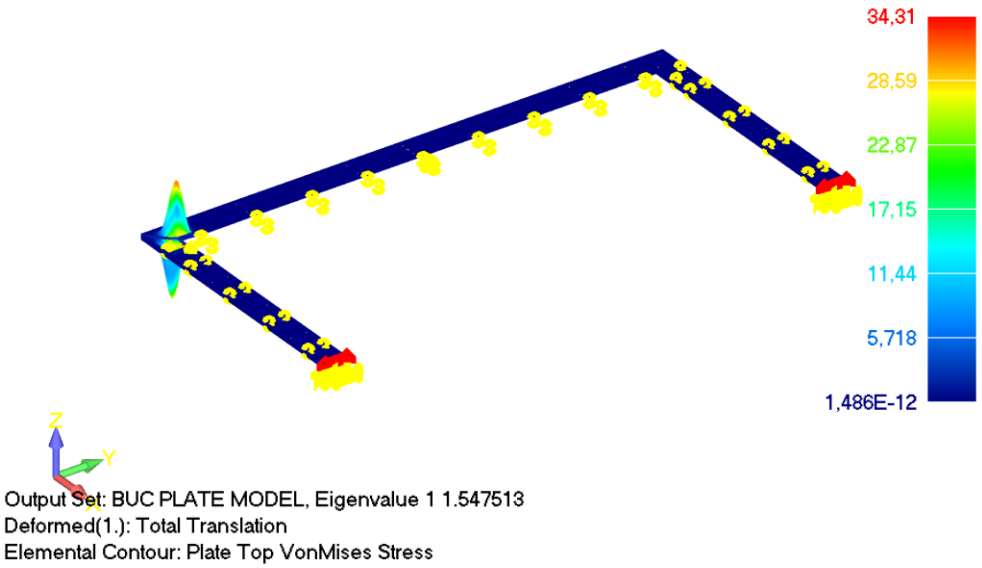

Figure 144 Buckling analysis for the plate model with stiffeners - BLF=1,55

Increase plate thickness

To further improve the buckling resistance, measures needs to be taken with regards to the local buckling on the web. In this design, the thickness of corner web plates is doubled (t=30mm).

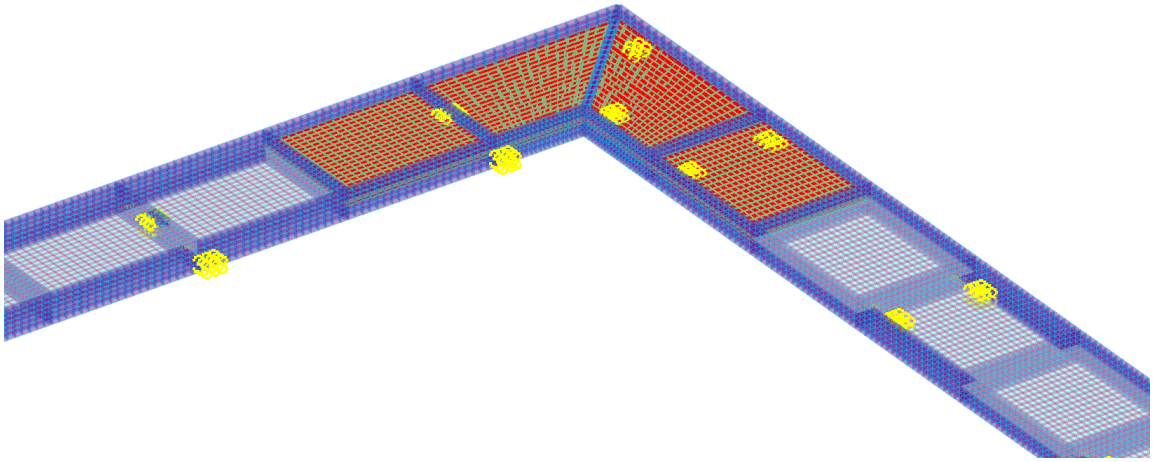

Figure 145 Corner web plates with double thickness

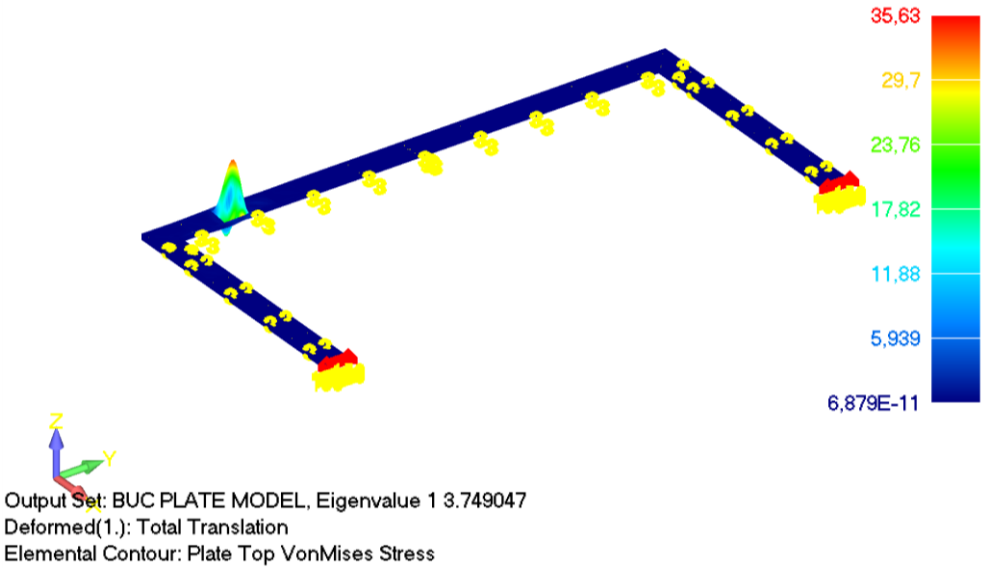

Figure 146 Plate model with stiffeners and double corner web thickness - BLF=3,75

By increasing the thickness of corner web plates, the buckling resistance got further improved with an eigenvalue raised from 1,55 to 3,75. The hoop should have enough stiffness thus enough buckling resistance under the defined load combinations.

13.3 Results and discussion

In the buckling design, different models are made to find a hoop system with enough buckling resistance to the defined load combinations. Results are listed in the table below:

Table 58 Buckling check results for hoop beams

Model type	Stiffener	Increased web thickness	BLF	Buckling mode	Mass (kg)
Line model	No	No	2,28	Flexural buckling	45669
Plate model	No	No	0,22	Lateral-torsional buckling	23238*2=46476
Plate model	Yes	No	1,55	Local buckling	29039*2=58078
Plate model	Yes	Double thickness for corner web	3,75	Local buckling	30910*2=61820

All these models have the same geometry, and the property of elements are the same except the model with different corner web.

For the line model and plate model without stiffener, the difference in the corner connection results in the mass difference.

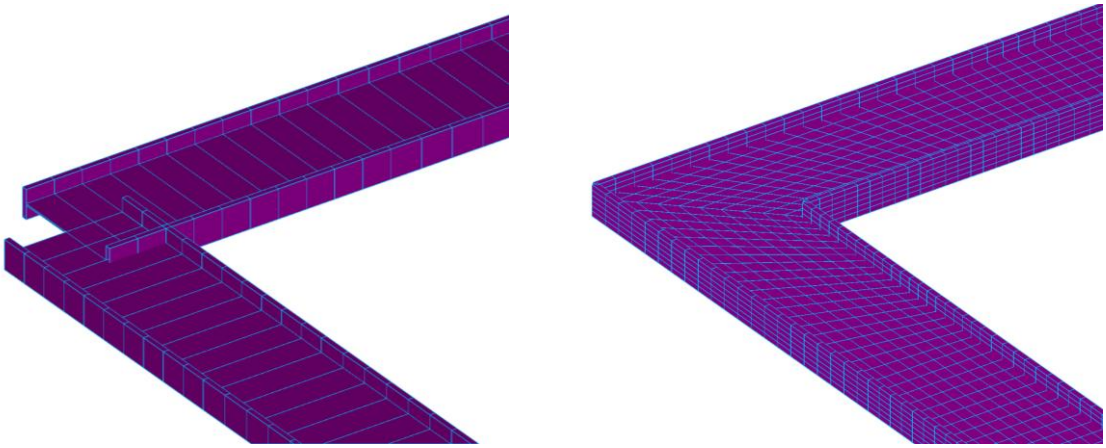

Figure 147 Corner connection of hoop beams- left: line model, right: plate model

Line model gives a result which is much higher than the plate model. The BLF results from line models are not reliable because it ignores the torsional buckling which tends to take place in prior to flexural buckling.

The plate model has very small buckling resistance, lateral-torsional buckling is witnessed at BLF=0,22. However, adding stiffeners perpendicular to the web plate can effectively increase this factor to 1,55 when local buckling takes place, but at the same time this brings large mass addition at about 25%.

To further improve the buckling resistance, measures to resist local buckling are taken. By choosing the corner web plates with double thickness, the BLF climbed to 3,75 which means this hoop should have enough stiffness. But a 33% mass increase of the hoop is seen compared to that of the standard model.

14. Static analysis of this roof structure

Based on the standard model, a final design for this roof structure is determined by taking into account all the possible load cases as described in Section 7. In the final design, the 10kN test load is applied to check the SLS requirement, and both the test load and load from the climber are considered to check the ULS requirement to guarantee safety when people hang the Christmas tree with the climber. These additional point loads are applied at the node with the largest downward displacement which leads to the most unfavourable situation. Load combinations are:

LC1: Pretension+ Self weight+ Test load+ Climber

LC2: Pretension+ Self weight+ Snow load+ Test load+ Climber

LC3: Pretension+ Self weight (favourable)+ Wind load+ Test load+ Climber

Table 59 Pretension + Dead load

Load	ULS	SLS
Pretension	1,0	1,0
Dead load	1,35	1,0
Test load	1,0	1,0
Climber	1,5	0

Table 60 Pretension + Dead load+ Snow load

Load	ULS	SLS
Pretension	1,00	1,0
Dead load	1,20	1,0
Snow load	1,50	1,0
Test load	1,0	1,0
Climber	1,5	0

Table 61 Pretension+ Dead load+ Wind load

Load	ULS	SLS
Pretension	1,00	1,0
Dead load	0,90	1,0
Wind load	1,50	1,0
Test load	1,0	1,0
Climber	1,5	0

In this section, firstly the static analysis results of the final design is given. Then based on the final design three different cases that may lead to failure of this roof structure are considered.

14.1 Results of the final design

Due to the different load combinations, the required minimum pretension changes for cables, resulting in a change of the cross sections, displacement, resulting forces, and total mass. Results are listed in tables below:

Cross section

Larger cross sections are applied to ETFE beam, rods, and hoop. For ETFE beam and rods, larger cross sections are required because of smaller reacting forces from struts due to the downward point loads. The cross section for hoop beam is increased in response to the increased pretension.

Table 62 Cross sections for elements in different groups

Group	Standard model	Final design
ETFE beam	CHS114,3*3,2	CHS114,3*4
Strut	CHS152,4*12,5	CHS152,4*12,5
Hoop	t_{flange}=55mm,t_{web}=15mm	t_{flange}=60mm,t_{web}=15mm
Rods	Circular bar d=55mm	Circular bar d=60mm
Cable top	PG55 A=347mm^2	PG55 A=347mm^2
Cable bottom	PG75 A=467mm^2	PG75 A=467mm^2
Rectangular cable	PG40 A=237mm^2	PG40 A=237mm^2

*The height and width of I-beam remains unchanged with h=1300mm, b=300mm

Pretension

Pretension for both top cable bottom cable net are higher than those in the standard model.

Table 63 Pretension in cables

Force	Standard model	Final design
Pretension top (kN)	175	180
Pretension bottom (kN)	160	180
Minimum tension in cable (N)	2333	3081

Displacement

Both upward and downward displacement in different load combinations satisfy the SLS check.

Table 64 Displacement

Load combinations	Displacement (mm)<143	
	upward	downward
SLS LC1 1,0dead+1,0pre	31	-54
SLS LC2 1,0snow+1,0dead+1,0pre	22	-134
SLS LC3 1,0wind+1,0dead+1,0pre	74	-57

Unity check

Apart from the rectangular cable, the leading element in each group gives a UC value within 0,7 to 1,00. Enough strength is guaranteed with high efficiency of material use.

Table 65 Axial stress and unity check

group	ULS LC2 1,5snow+1,2dead+1,0pre			ULS LC3 1,5wind+0,9dead+1,0pre		
	Quantity	Unit	UC	Quantity	Unit	UC
ETFE beam	322	N/mm^2	0,91	203	N/mm^2	0,57
Strut	181	N/mm^2	0,51	309	N/mm^2	0,87
Hoop	340	N/mm^2	0,96	326	N/mm^2	0,92
Rods	235	N/mm^2	0,66	292	N/mm^2	0,82
Cable top	147	kN	0,45	249	kN	0,76
Cable bottom	365	kN	0,83	222	kN	0,51
Rectangular cable	19	kN	0,09	21	kN	0,09

Buckling check

In the final design, stiffeners are applied to the I-profile, also the thickness for corner web is doubled (see Section 13). Under the new load combinations, the buckling analysis gives the lowest BLF=3,69. This hoop system has enough buckling resistance under the defined load combinations.

Table 66 Property of hoop beams

Profile	h (mm)	b (mm)	t_{flange} (mm)	t_{web} (mm)	Mass (kg)
I-profile	1300	300	60	15	65570

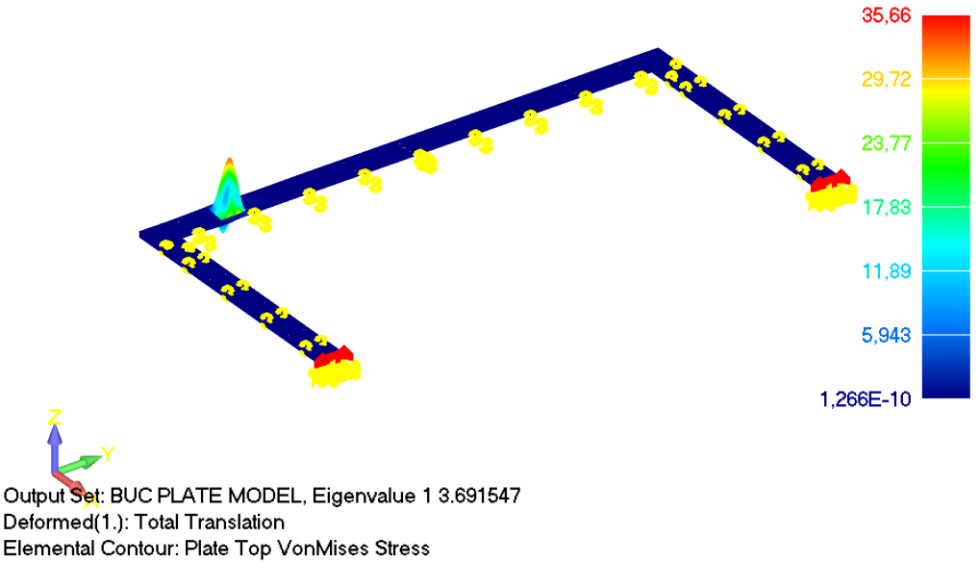

Figure 148 Buckling analysis for hoop beam - BLF=3,69

Mass

The table below show that the total structural mass is about 90 tonnes. The hoop take the biggest share of the total structural mass, accounting for 72,6%. The following are strut and ETFE beam with 15,3% and 8,2% respectively. Due to a large strength to mass ratio, the cables are quite light-weight, all the cables in this design accounts for only 3,3% of the total structural mass.

Table 67 Mass and percentage of elements in different groups

Group	Mass (kg)	Percentage (%)
ETFE beam	7398	8,2%
Strut	13841	15,3%
Hoop	65570	72,6%
Rods	142	0,2%
Cable top	1259	1,4%
Cable bottom	1706	1,9%
Rectangular cable	427	0,5%
Total structural mass	90343	100,0%

A pie graph below gives a clear description about the mass percentage of elements in each group without hoop. Strut weighs the most at about 56% of the structural mass without hoop, the ETFE beam takes up 30%, the rest 14% of mass is taken by the cables.

Figure 149 Mass percentage with hoop

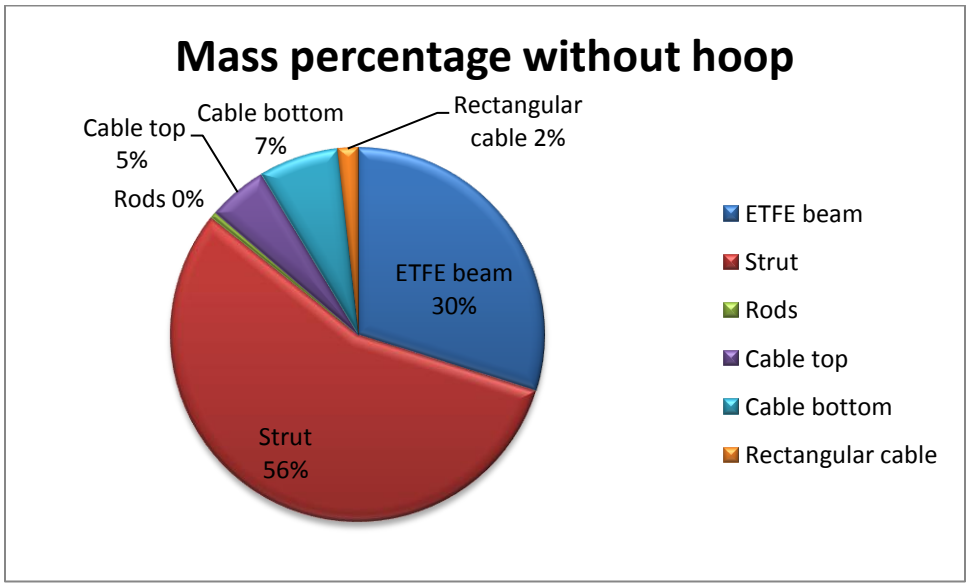

Figure 150 Mass percentage without hoop

14.2 Case 1: One cable break due to accidental loads

Based on the final design, the first case in which one single cable is broken due to accidental loads is modelled. One cable in the bottom cable net is chosen to be cut off, this is simulated by changing the elastic modulus of a single cable to E = 1 N/mm^2. However, pretension still exists in this branch of cables. Therefore, this model simulates the moment when a cable is cut off. Results are depicted with diagrams.

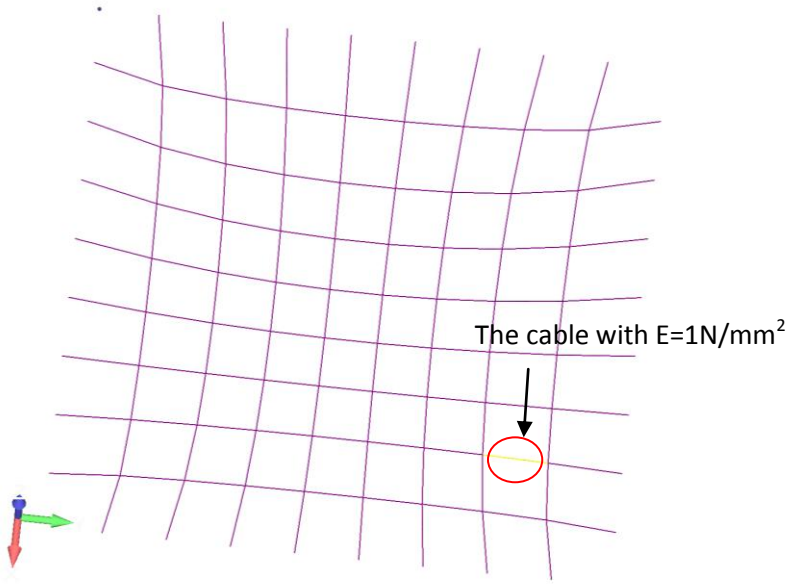

Figure 151 Position of the cable with E=1 N/mm^2 in bottom cable net

SLS check

The diagrams for SLS check under different load combinations show that large displacement both upward and downward occur when a cable is broken. The structure doe not satisfy the SLS check.

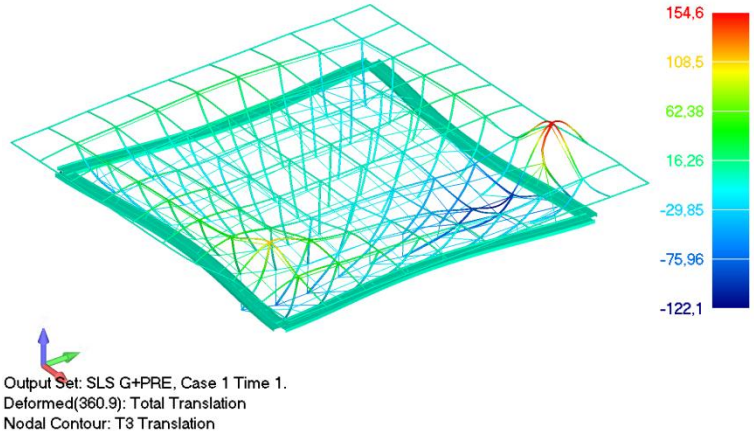

Figure 152 T3 translation under SLS LC1

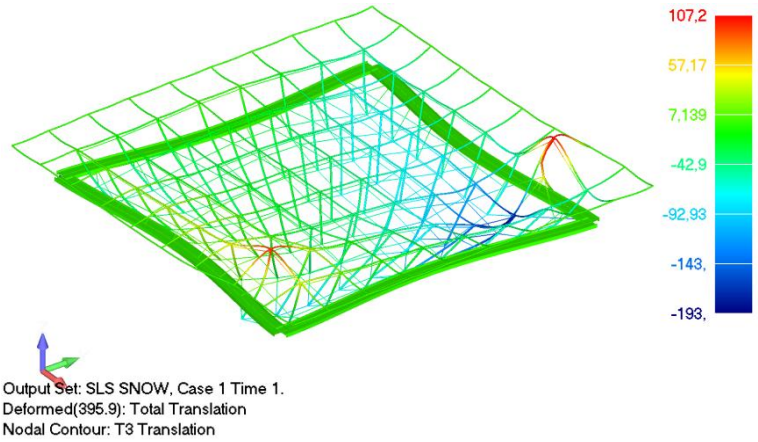

Figure 153 T3 translation under SLS LC2

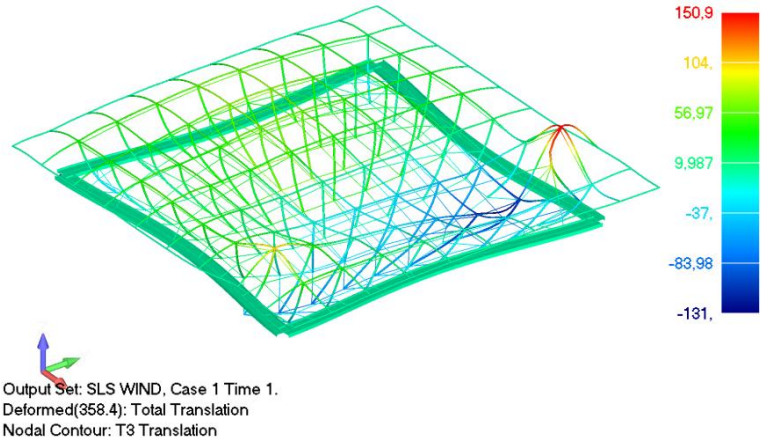

Figure 154 T3 translation under SLS LC3

Axial force

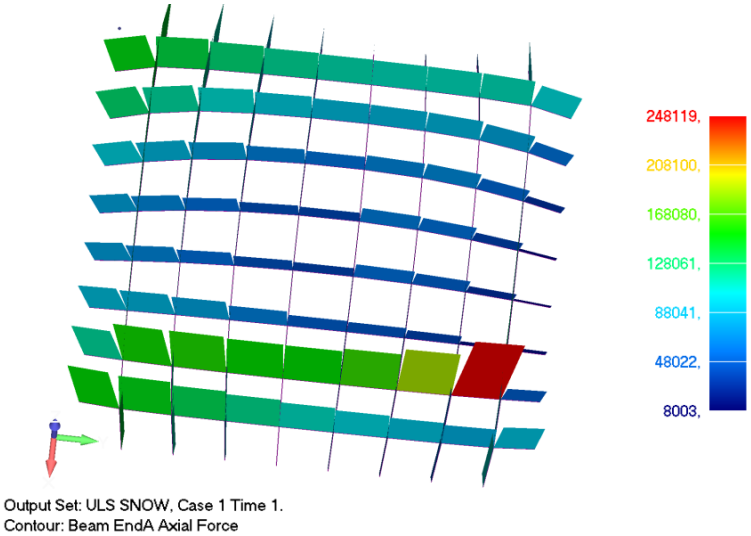

Figure 155 Resulting axial forces in the top cable net under ULS LC2

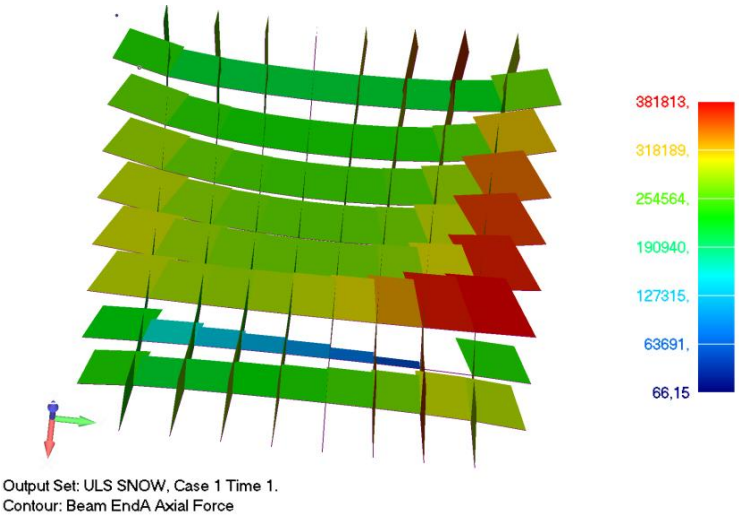

Figure 156 Resulting axial forces in the bottom cable net under ULS LC2

From the diagrams, the broken cable takes no tension. Consequently, large tension occurs in the corresponding top cable due to the uncontrolled movement of the struts.

Unity check

Since the occurrence of this case that a single cable is cut off is really low, for the resulting stress/load and unity check, results are taken from the load combinations for SLS check. The ETFE beam, strut, and top cable are at a risk of failure. No enough strength is guaranteed due to the change of load path thus the very large resulting stresses in elements.

Table 68 Unity check for the model with one cable broken

group	SLS LC2 1,0snow+1,0dead+1,0pre			SLS LC3 1,0wind+1,0dead+1,0pre		
	Stress/Load	Unit	UC	Stress/Load	Unit	UC
ETFE beam	962	N/mm^2	271%	841	N/mm^2	237%
Strut	1245	N/mm^2	351%	1063	N/mm^2	299%
Hoop	333	N/mm^2	94%	325	N/mm^2	92%
Rods	327	N/mm^2	92%	315	N/mm^2	89%
Cable top	280	kN	86%	334	kN	102%
Cable bottom	330	kN	75%	267	kN	61%
Rectangular cable	53	kN	24%	52	kN	23%

Conclusion

By modelling this roof structure with one broken cable unable to transfer tensile forces, results show that the structure becomes uncontrolled and large displacement occurs. Additionally, the different load path leads to extremely high resulting stresses in elements which are far beyond the tensile strength of material. In summary, in this case the structure has to be adjusted to a higher safety level.

14.3 Case 2: Pretension loss- No tensile force in one branch of cable

In this case, the branch of cables with the smallest tensile forces under ULS LC2 is given no pretension to simulate the situation when compression is superior to tension in the specific branch of cables due to pretension loss. Results are depicted with diagrams.

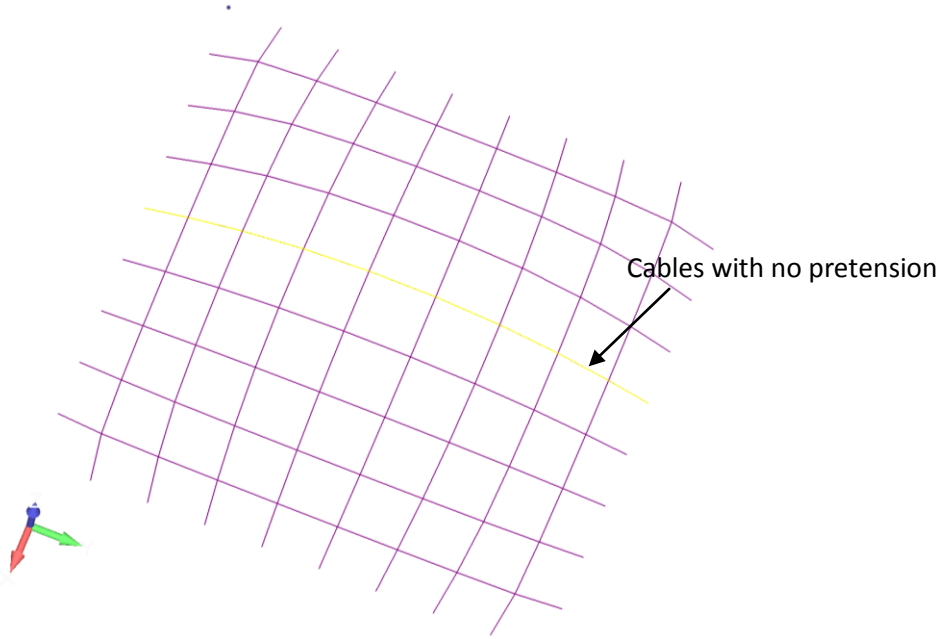

Figure 157 Cables with no pretension

SLS check

The diagrams for SLS check under different load combinations show that large upward displacement occurs when tension is eliminated in one branch of cables. The structure doe not satisfy the SLS check.

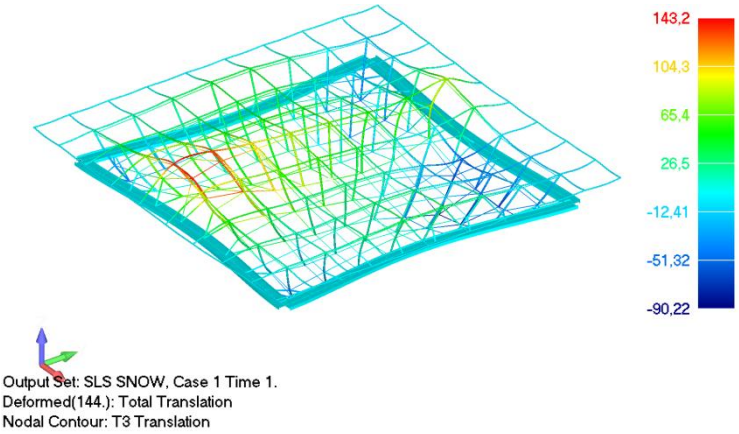

Figure 158 T3 translation under SLS LC2

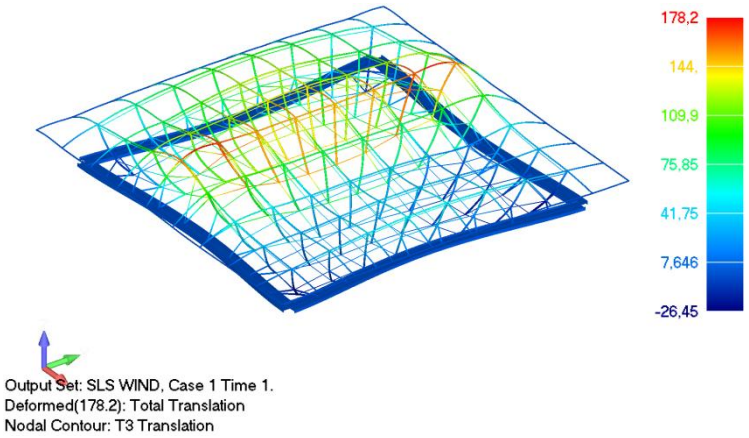

Figure 159 T3 translation under SLS LC3

Unity check

From the table for unity check, ETFE beam and strut may yield under ULS LC2. Elements in the rest groups have enough strength under the defined load combinations despite that no pretension in one branch of cables.

Table 69 Unity check for the model with no tension in one branch of cables

group	ULS LC2 1,5snow+1,2dead+1,0pre			ULS LC3 1,5wind+0,9dead+1,0pre		
	Stress/Load (Max)		UC	Stress/Load (Max)		UC
	Quantity	Unit		Quantity	Unit	
ETFE beam	441	N/mm^2	124%	224	N/mm^2	63%
Strut	433	N/mm^2	122%	268	N/mm^2	75%
Hoop	324	N/mm^2	91%	312	N/mm^2	88%
Rods	236	N/mm^2	66%	343	N/mm^2	97%
Cable top	148	kN	45%	251	kN	77%
Cable bottom	362	kN	83%	221	kN	50%
Rectangular cable	20	kN	9%	21	kN	9%

Conclusion

By modelling this roof structure with no pretension in one branch of cables (this branch of cables have the smallest tensile forces under ULS LC2), results show that the resulting upward deformation under SLS LC3 goes beyond the requirement for SLS check.

Additionally, the resulting axial stresses in ETFE beam and strut are about 24% higher than the yield stress. This indicates that permanent deformation may occur in ETFE beam and strut elements. However, the maximum stress (max 441 N/mm^2) is lower than the tensile strength (470-630 N/mm^2), therefore break of element is not expected.

Buckling of the hoop is not expected as smaller forces are acting on hoop.

In summary, collapse of the structure is not expected.

14.4 Case 3: Over-preloading

In case 3, pretension is increased by 20% for both top and bottom cable net to simulate the situation when over-pretension is applied to cables to compensate for the possible pretension loss. The rest load cases are the same as the final model. Results are listed in the tables below:

Displacement

With pretension increased by 20% for both top and bottom cable net, the displacement of the structure under all the load combinations satisfy the SLS check.

Table 70 T3 translation

Load combinations	Displacement (mm)<143	
	upward	downward
SLS LC1 1,0dead+1,2pre	35	-50
SLS LC2 1,0snow+1,0dead+1,2pre	26	-126
SLS LC3 1,0wind+1,0dead+1,2pre	73	-52

Pretension

In this case, pretension goes far beyond the compression forces on the cable net. The minimum tensile force in cable is about 42kN.

Table 71 Pretension and minimum tension

Force	Standard model
Pretension top (kN)	216
Pretension bottom (kN)	216
Minimum tension in cable (N)	42231

Unity check

The maximum axial stresses in hoop beam is about 14% higher than the material strength under ULS LC2, therefore yielding is expected in hoop beam. However, elements in the rest groups all have enough strength with high efficiency of material use.

Table 72 Unity check for the model with over pretension

group	ULS LC2 1,5snow+1,2dead+1,2pre			ULS LC3 1,5wind+0,9dead+1,2pre		
	Stress/Load (Max)		UC	Stress/Load (Max)		UC
	Quantity	Unit		Quantity	Unit	
ETFE beam	336	N/mm^2	95%	225	N/mm^2	63%
Strut	168	N/mm^2	47%	340	N/mm^2	96%
Hoop	404	N/mm^2	114%	391	N/mm^2	110%
Rods	251	N/mm^2	71%	324	N/mm^2	91%
Cable top	185	kN	57%	282	kN	87%
Cable bottom	397	kN	91%	255	kN	58%
Rectangular cable	20	kN	9%	25	kN	11%

Buckling check

The new load combination (ULS LC2) with increased pretension is applied to the hoop beam model and static analysis results give the first BLF to be 3,10. This means the hoop system is stiff enough to resist buckling under the defined load combinations.

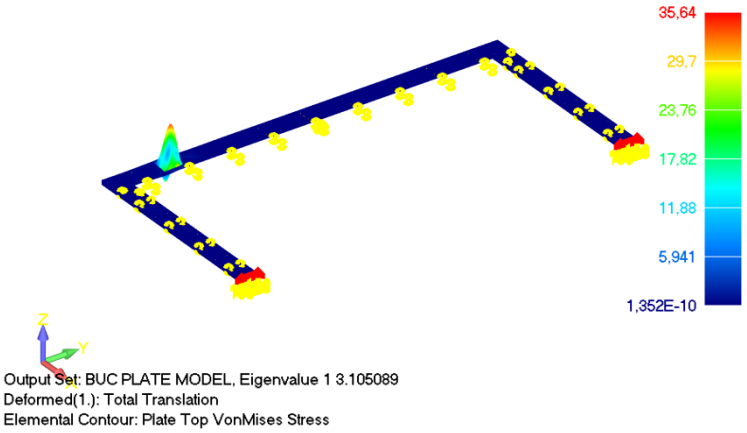

Figure 160 Buckling analysis for hoop beam with 1,2pretension – BLF=3,10

Conclusion

By modeling this roof structure with 20% increased pretension, static analysis results show that the structure still has good serviceability with the displacement $\delta < l_{span}/200 = 143mm$. Unity check shows that the hoop beam may yield due to the large pretension. However, the maximum stress is lower than the tensile strength (470-630 N/mm^2), no failure is expected. Buckling is not expected in hoop with BLF=3,10. In summary, a certain amount of over-pretension can be applied to this roof structure to compensate for the possible pretension loss.

15. Connection and Detailing

For the design of a steel structure, all the elements will be prefabricated in the factory and then assembled on site. The choice of connection is very important in the design process, which can be influenced by a lot of factors like prefabrication, assembly, finance, aesthetic, and limit of transportation. The chosen connection should be able to fulfill the requirement of function, limit of transportation, and have a certain level of aesthetics. In this section, Seven different connections designed for this cable-strut system are illustrated with some sketch-ups. These connections are:

1) Choice of end fitting
2) Cable and hoop connection
3) Rods and strut connection
4) Cable and strut connection
5) ETFE beam connection
6) Hoop beam connection
7) Supports

15.1 Choice of end fitting

End fittings are used to provide easier load transfer path to the supporting structure. The end fittings must be strong enough to withstand the load from cables without significant yielding. The choice of end fittings is dependent on the type of cables.

In this design, cables and end fittings are chosen from the producer PFEIFER.

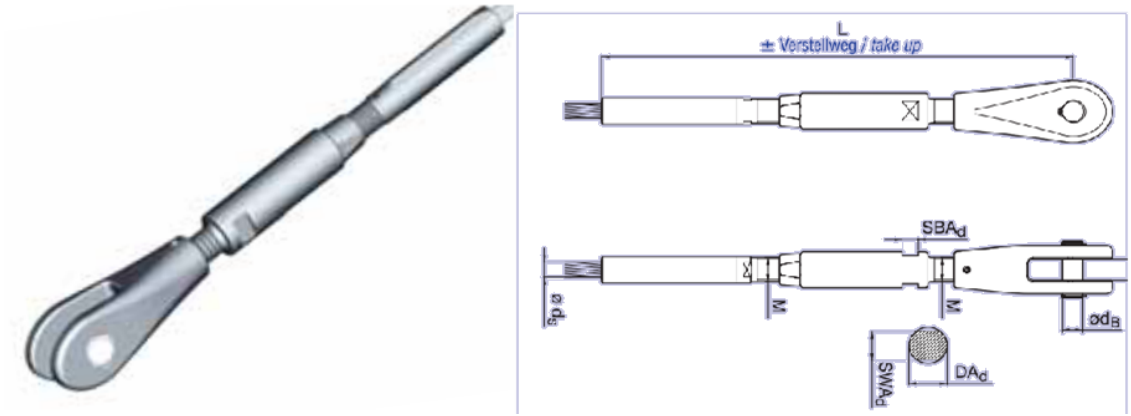

Figure 161 Fork Connector with Adapter and Threaded Fitting

This fitting comes with an adaptor with thread to provide the possibility to adjust the length and tensile force of cables after preloading.

15.2 Cable and hoop connection

Loads in cables need to be transferred to the compression hoop beams. The stiffeners are designed not only to increase the buckling resistance, but to provided connection point for cable and hoop. In this design, both top and bottom cable fittings will be connected to the same position of the stiffener.

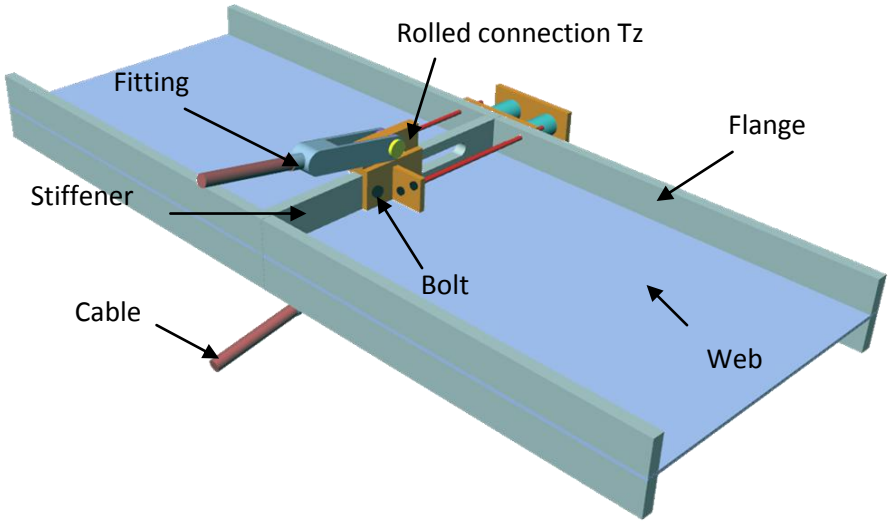

Figure 162 Cable and Hoop connection

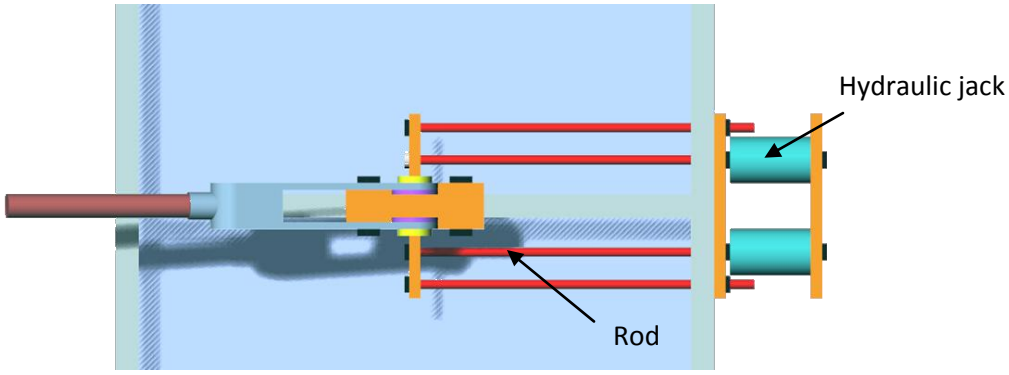

Figure 163 Cable and Hoop connection – top view

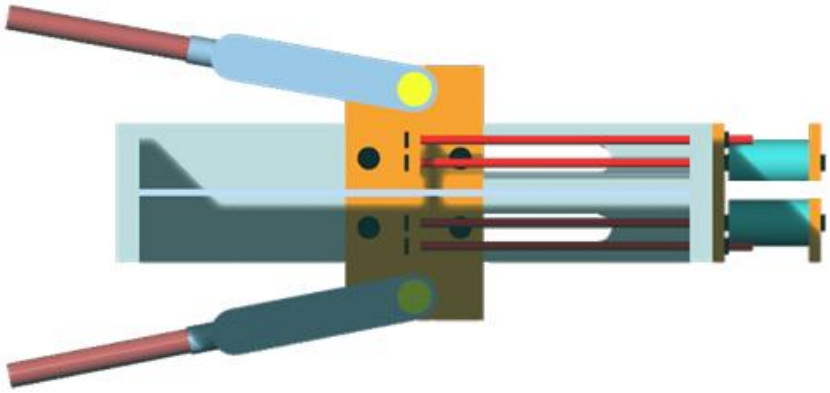

Figure 164 Cable and Hoop connection – front view

Force equilibrium of this hoop and cable connection is depicted as the following sketches. Despite that the loads do not converge at the same point, the bending moment due to eccentricity can be counteracted.

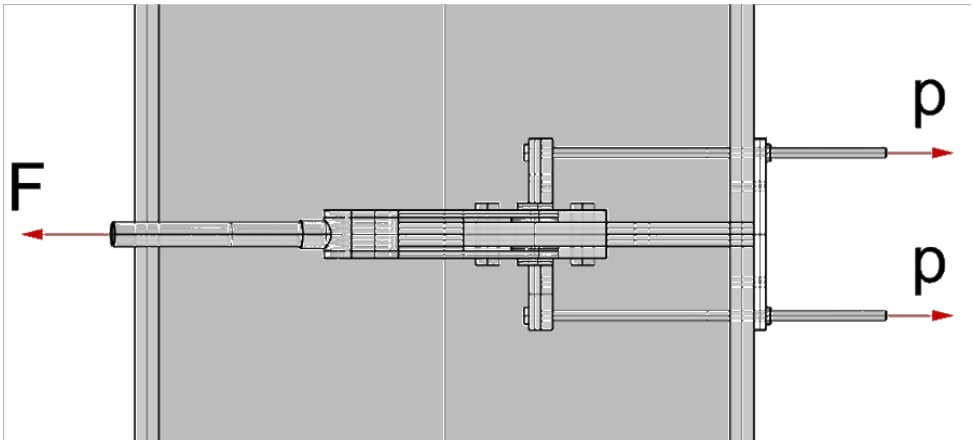

Figure 165 Equilibrium for Hoop and Cable connection – top view

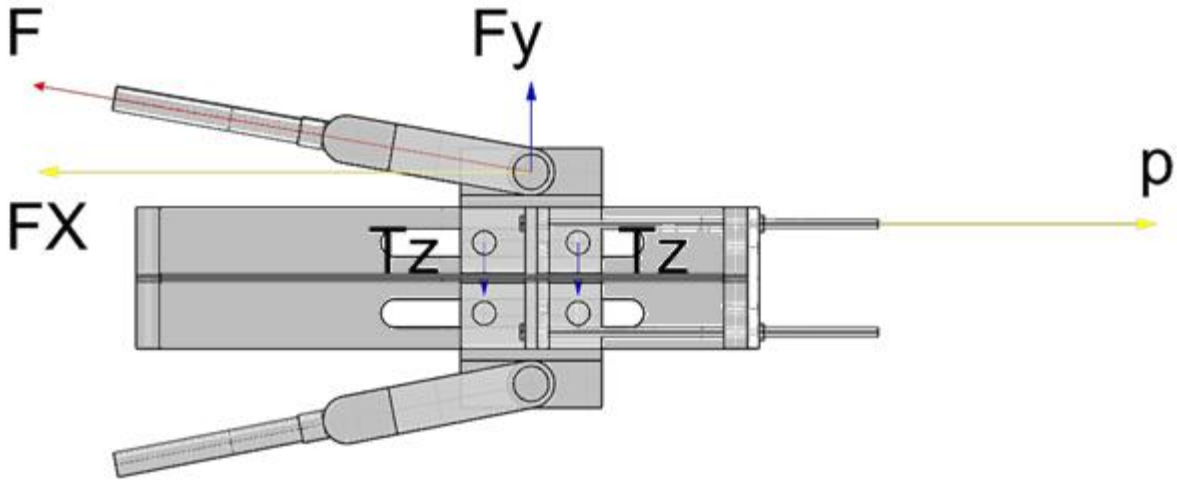

Figure 166 Equilibrium for Hoop and Cable connection - front view , top part

15.3 Rods and strut connection

Rods and struts are connected with bolts, which allows rotation to adjust the angle of struts. Rectangular cables are connected to struts to guarantee that the elements stay in the right position. The design sketch is as follows:

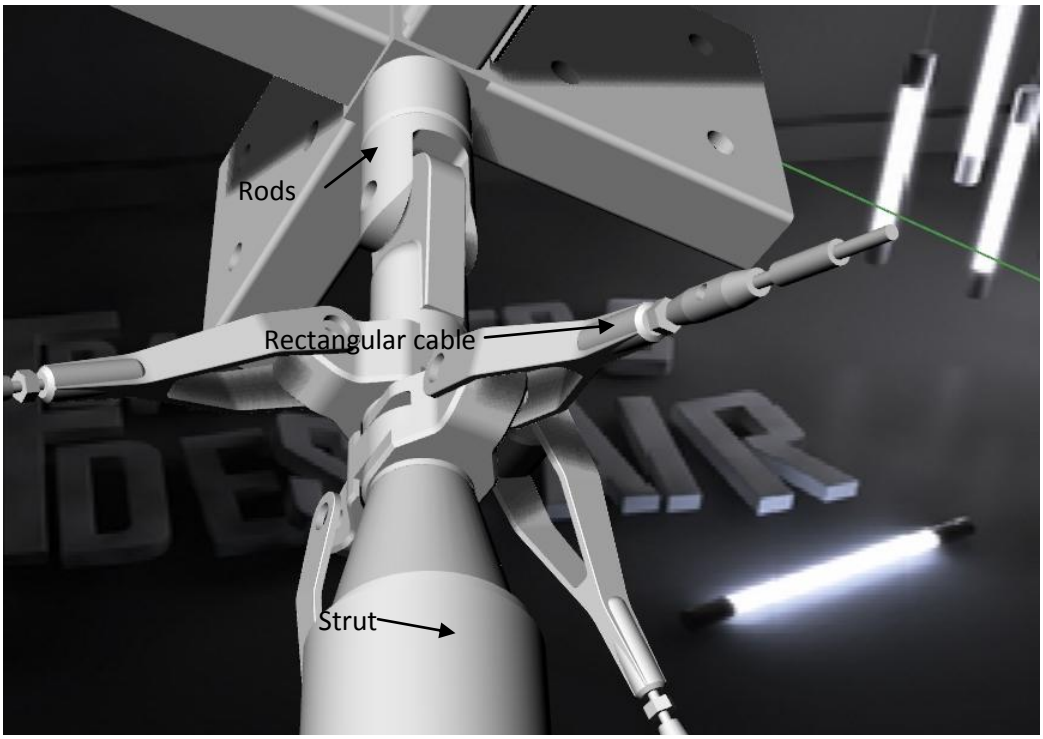

Figure 167 Rods, strut, and rectangular cable connection (***Peter Fotiadis, 2016***)

15.4 Cable and strut connection

In this roof system, design the way for cable and strut connection is of great importance. This connection functions in three ways:

1) To guarantee that the cables and struts stay in the right position.
2) To transfer axial force between cables and struts
3) To transfer bending moments between strut elements.

This requires the connection to be strong enough to withstand external loads and to restrict sliding between cable and strut. Strength of the connection is not tested in this thesis work, but the concept for an efficient design is derived (see Appendix I).

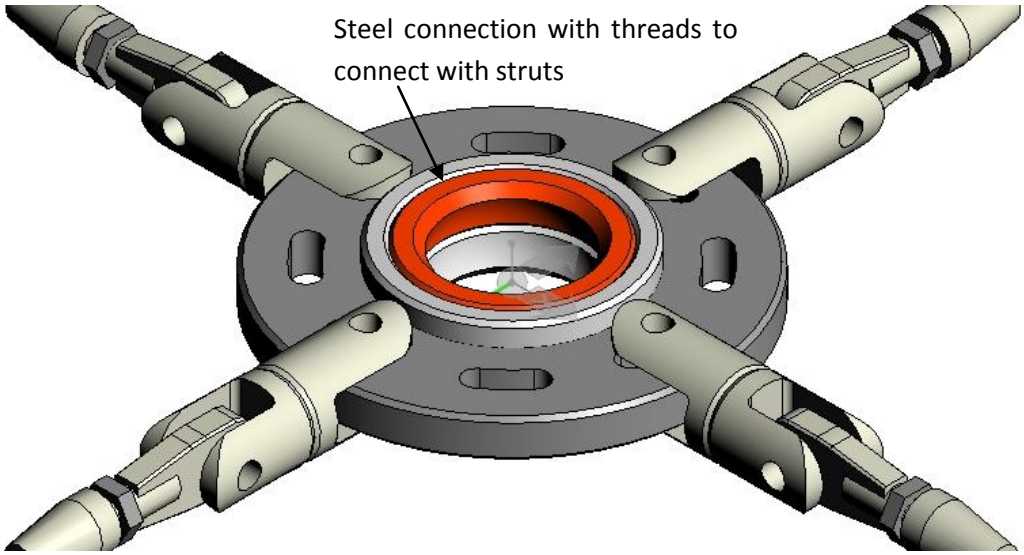

Figure 168 Connector for cable and strut connection (***Peter Fotiadis, 2016***)

As is shown in the design sketch, cable segments are used and bolted to a special base in between two strut elements. The struts and the base can be connected with threads since there is no torque in strut elements. With the end fittings the angle of cables are adjustable thus this connector can be applied to all the cable and strut connections.

15.5 ETFE beam connection

The ETFE beam grid covers the opening area of 34 m x 34 m. In the design process, it is necessary to take into account the transport limit of prefabricated elements. Vehicles with rigid vehicle length less than 18,65 m, width less than 2,9 m, gross weight less than 44 tonnes, with no axle weight over 11,5 tonnes, and overall height less than 4,95 m can travel anywhere at any time, except where the route includes an underbridge with weight restriction or an over-bridge with height restriction (*Davison, Buick., 2003*).

According to the requirement for transportation, the ETFE beam grid is designed into 20 components. As is displayed in the figure below, component 2 to 9 are the same as piece 1 which is marked as yellow. The element piece numbered 10 is different. By dividing the ETFE beam grid in such a way, the maximum size of the grid component is 14mx3,9m, which is possible for transportation.

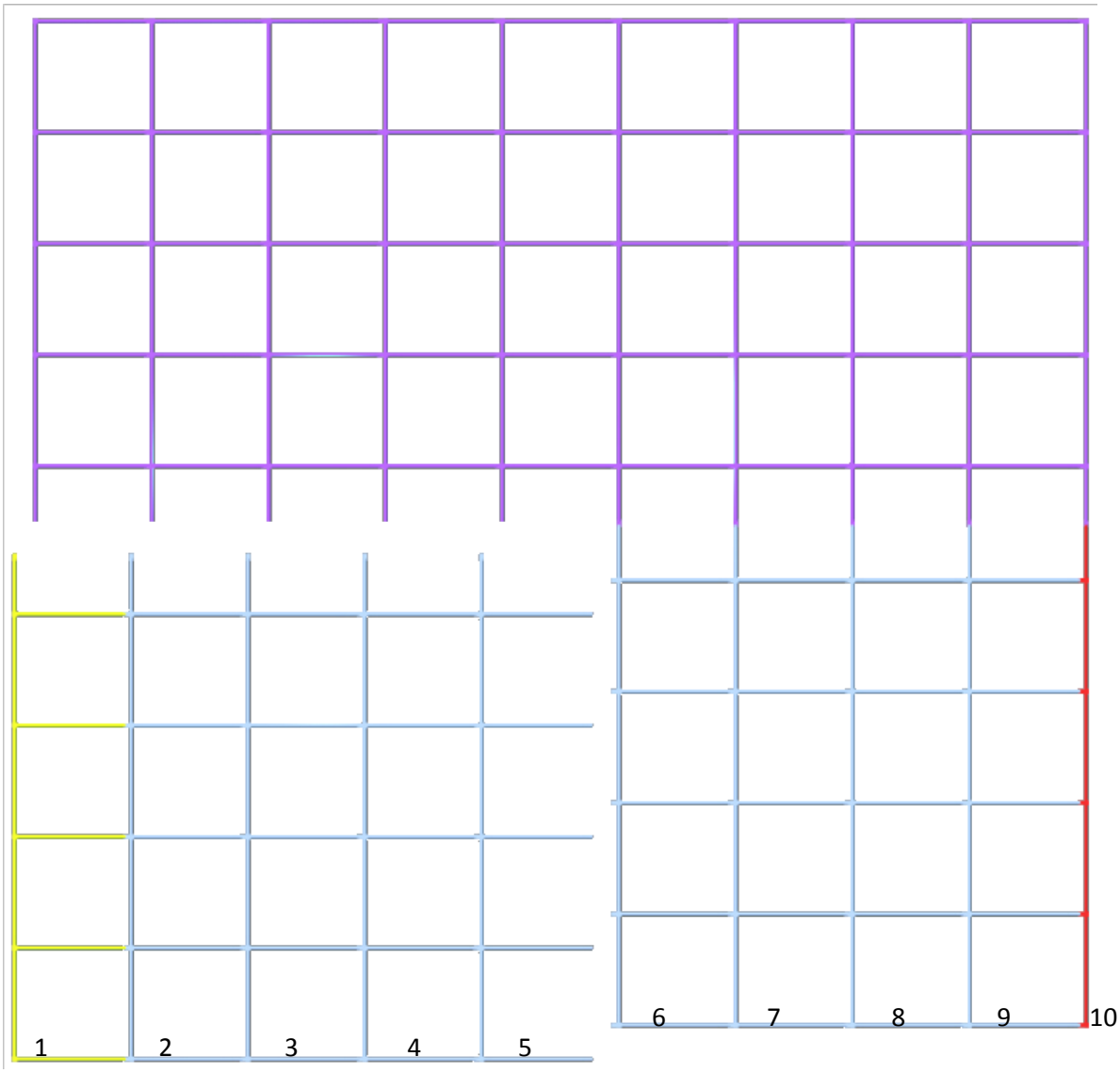

Figure 169 ETFE beam grid

For each grid component, the single CHS elements with smaller diameter are welded to a steel box. All the grid components will be assembled on site by bolt connections.

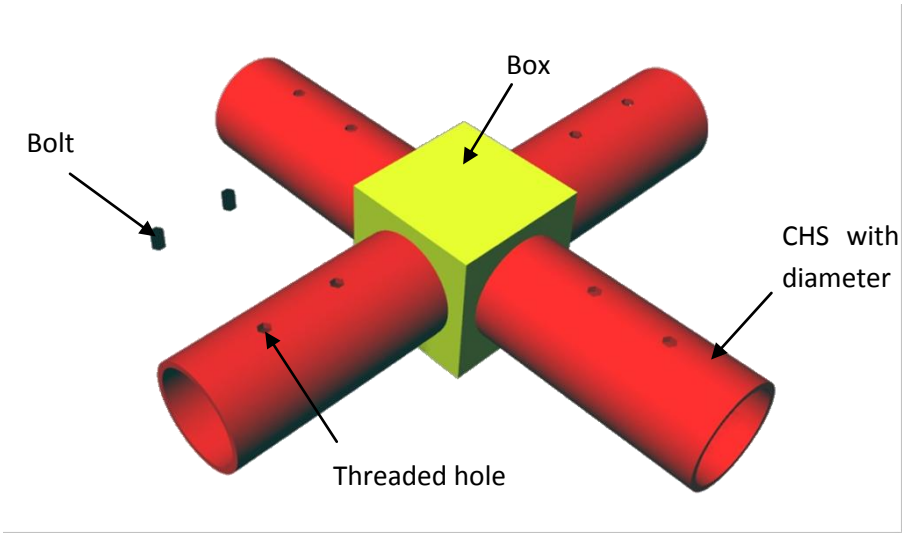

Figure 170 ETFE beam grid connection - Detail 1

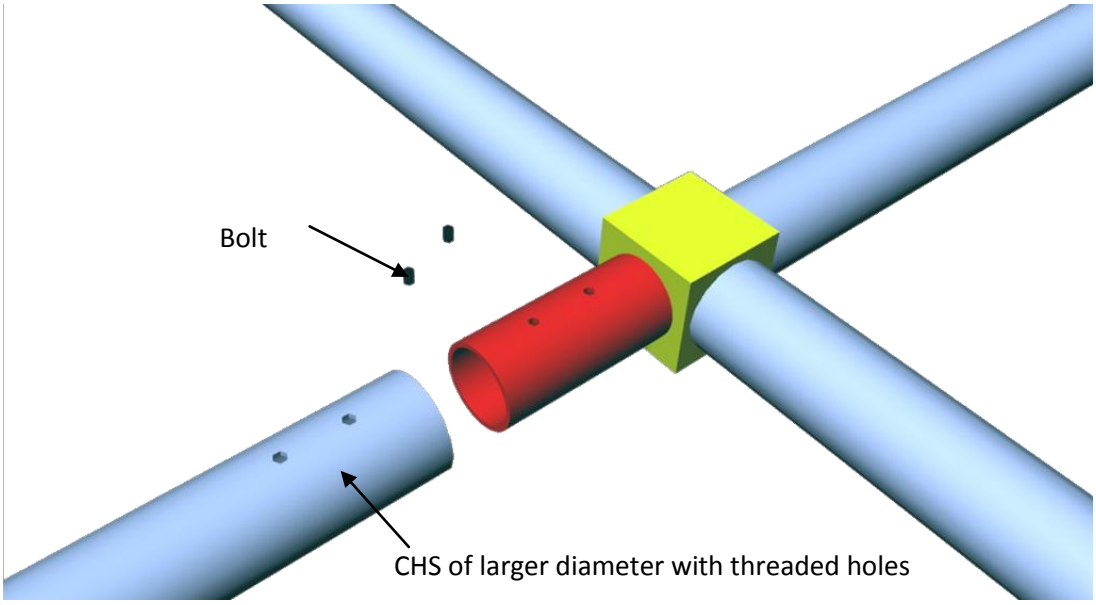

Figure 171 ETFE beam grid connection - Detail 2

As is shown in the figures above, two sizes of circular hollow sections are applied. The smaller CHS (red part) go through the larger one (lavender) with the outer surface of the small one touches the inner surface of the large one. Two bolts are applied to the threaded holes on both the top and bottom sides of the CHS. By tightening the bolts, translation and rotation between these two CHS elements are restricted.

15.6 Hoop beam connection

The hoop is subjected to very large bending moment, normal force only accounts for approximately 8% of the axial stress. Special attention should be paid to the locations for hoop beam connections. In the design of the hoop beam connection, the point with zero bending moment is found first and then chosen as the location for beam connection. From the FEM result, in the hoop beam system over 90% of the bending moment comes from pretension in cable system. Thus for this roof design, the bending moment diagram for the hoop system should be almost the same for all the load combinations. In the figure below, the shrinked diagram (where the gap means the position for cables) clearly shows the favourable locations for hoop beam connection, where the bending is zero.

However, considering the transport limit, the hoop beam system is divided into three components. Component 1 and component 2 have the same total length at about 6,5 m, also the same weight at 3,75 tonnes. Component 3 is 9,5m long, weighs 5,5 tonnes.

All these beam components will be assembled on site by bolt connections.

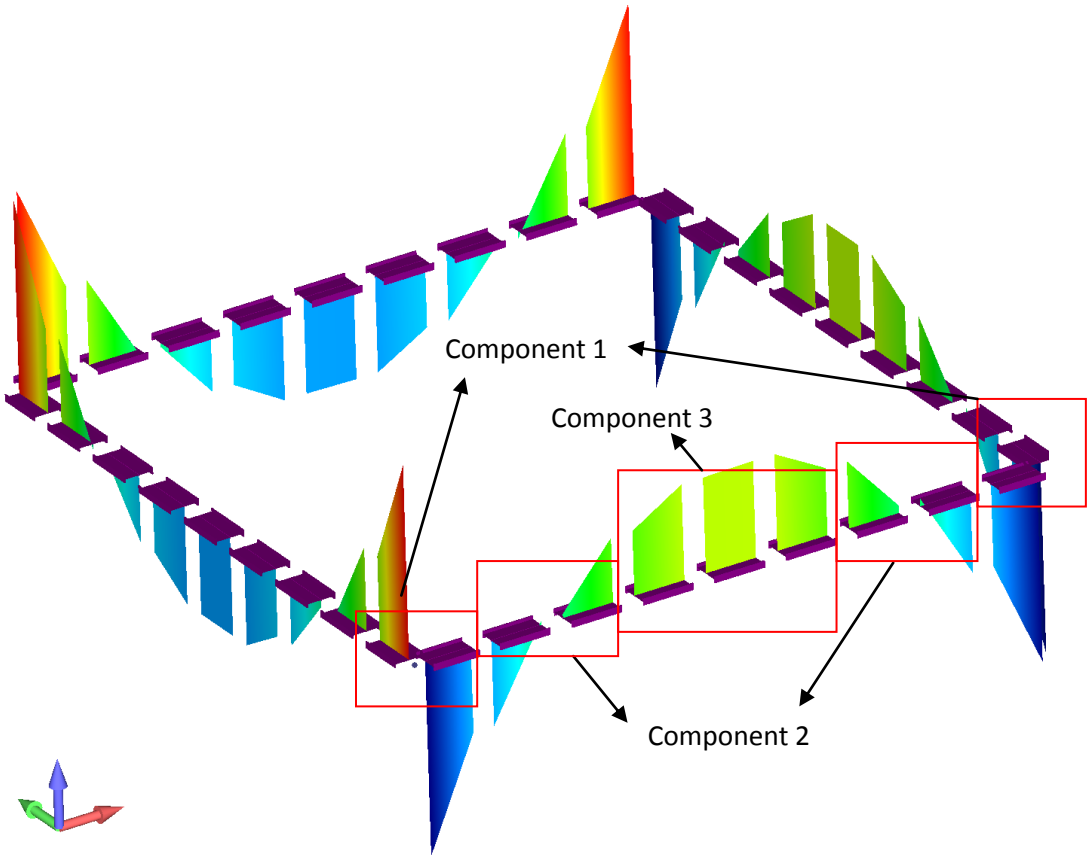

Figure 172 Bending moment diagram in Hoop beam (shrink mode)

From the bending moment diagram, the applied connections should be capable of bearing a certain amount of bending. Additional steel plates are used.

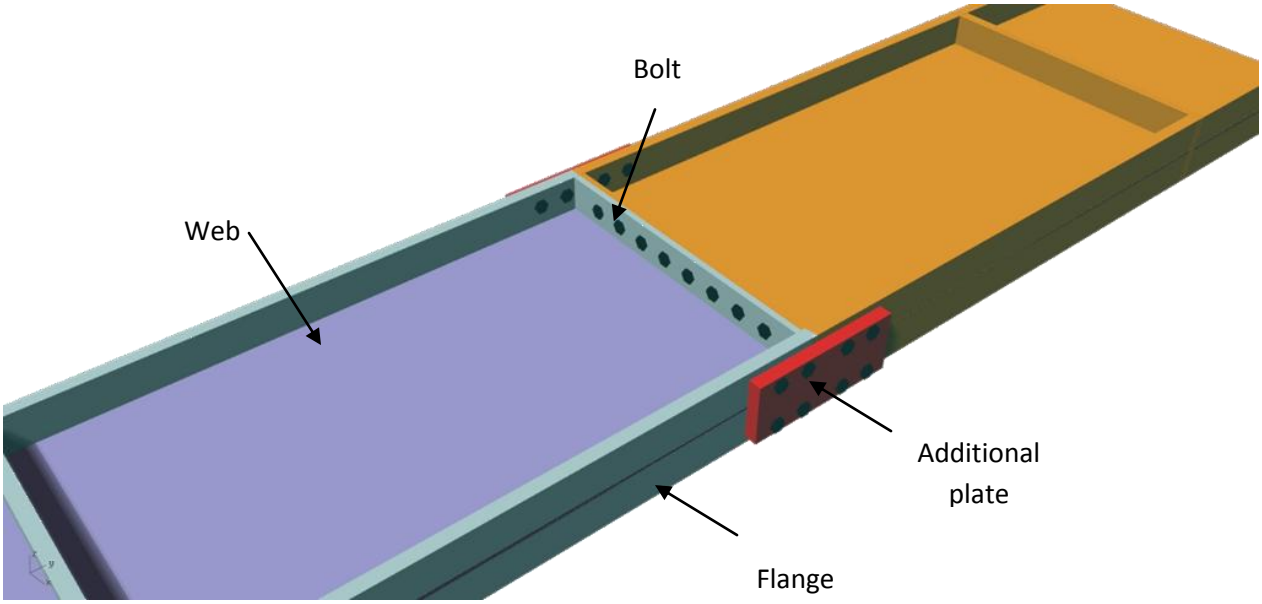

Figure 173 Hoop beam connection

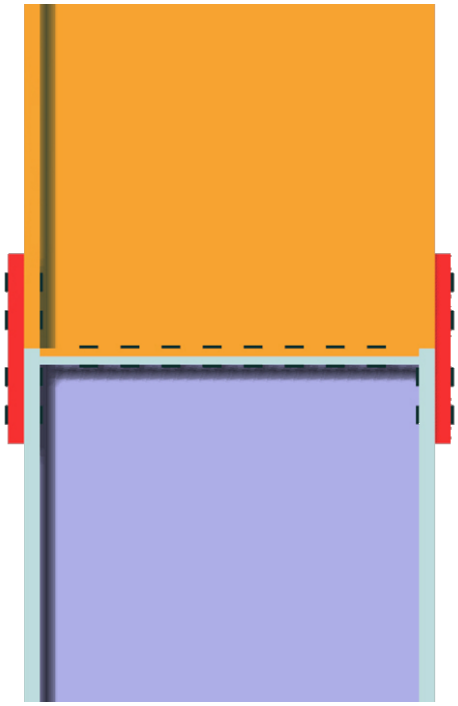

Figure 174 Hoop beam connection - top view

Hoop beams on the corner are welded together in the factory, no more connection method is required on site.

15.7 Supports of hoop system

The choice of type of supports influences the structural behaviour of the roof structure. In this design, the hoop system will be supported at the stiffeners in between two cable branches.

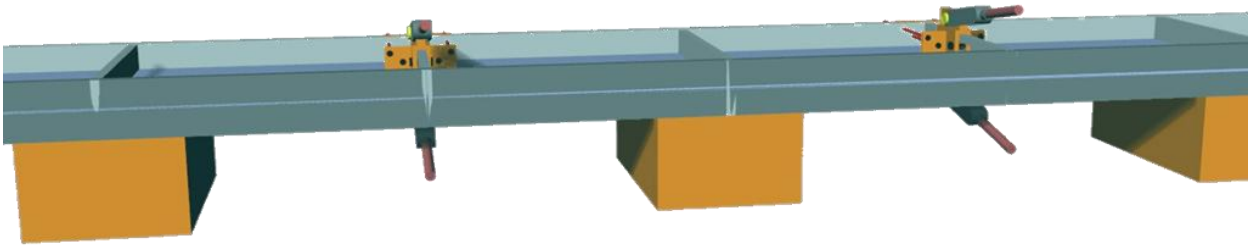

Figure 175 Support for Hoop

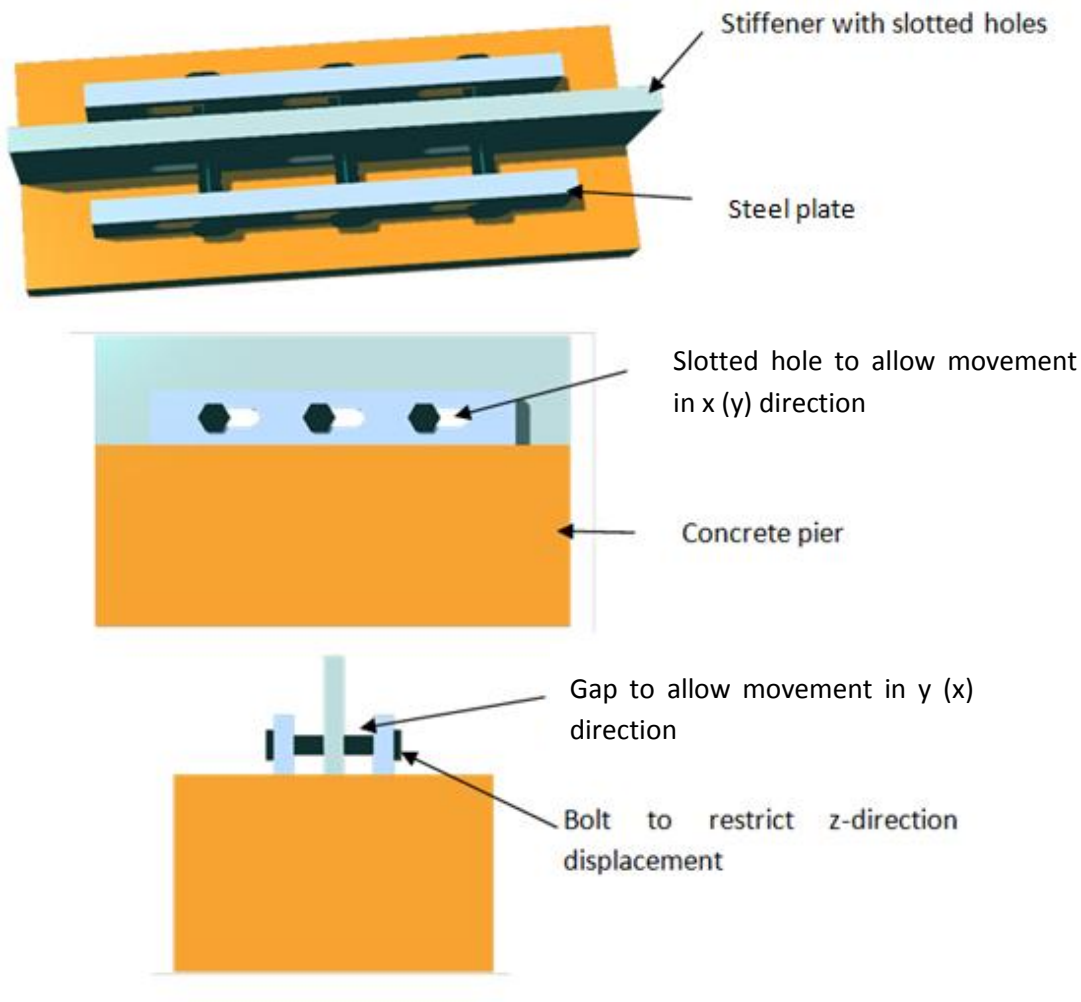

Figure 176 Detail for T_z Hoop support

By eliminating the gap and replace the rectangular steel plate with steel angle plate, the support can restrict the translation in both z- and the local x-direction.

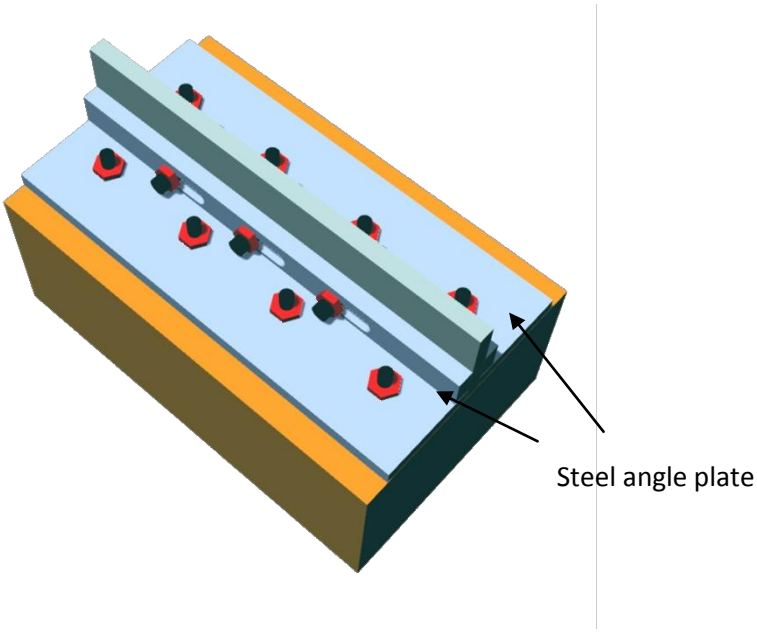

Figure 177 Detail for hoop translation support in xz/yz direction

Force equilibrium of this support is depicted as the following sketch. All the normal forces and bending moments are negated by reaction forces from the angle plate.

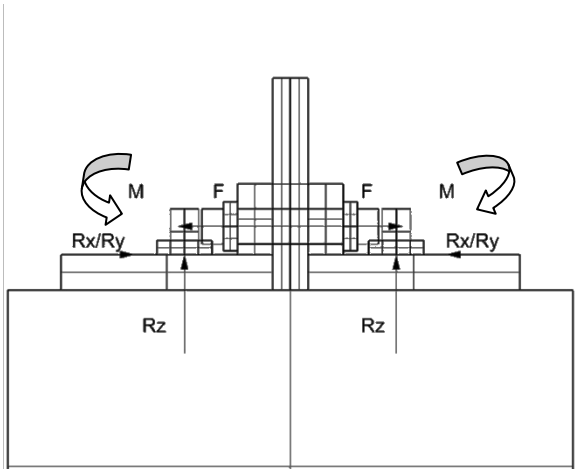

Figure 178 Equilibrium for T_z and local x-direction support for hoop

16. LCA of steel

Life-cycle assessment (LCA), also known as life-cycle analysis, eco-balance, and cradle-to-grave analysis, is a technique to assess environmental impacts associated with all the stages of a product's life from cradle to grave (i.e., from raw material extraction through materials processing, manufacture, distribution, use, repair and maintenance, and disposal or recycling) (*US Environmental Protection Agency, 2010*).

LCA involves the collection and evaluation of quantitative data on the inputs and outputs of material, energy and waste flows associated with a product over its entire life cycle so that its whole-life environmental impacts can be determined.

In this study, the scope of LCA is defined within two subsets:

- Reuse and recycling of steel;
- Embodied carbon of steel over its entire life.

16.1 What is recycling and reuse

The construction industry in the UK accounts for the use of 295 million tonnes of virgin material per year, displaces 22 million tonnes of industrial 'by-product' by industrial ecology each year and produces approximately 150 million tonnes of construction and demolition waste annually. Of this, 46 million tonnes is recycled for use as building products, in road construction, or land reclamation thereby reducing the amount of material that is landfilled and reducing the need for virgin materials in new construction (*The Concrete Center, 2016*). Therefore there is significant space for improving the efficiency of material use in the construction industry.

Major improvements in materials resource efficiency are possible without increasing cost by:

- Reducing the quantity of materials being sent to landfill during the construction process by 'designing out waste' and effective site waste management
- Reusing, recycling and recovering waste material as appropriate as possible
- Utilizing materials and products with a high recycling and reuse potential.

The UK Waste Hierarchy (*Defra, 2016*) ranks waste management options according to what is best for the environment. It gives top priority to preventing the production of waste in the first place. After waste is produced, it gives priority to preparing it for reuse and recycling, followed by recovery and last of all disposal. Reusing and recycling construction products avoids or reduces waste and saves primary resources. By using materials that have a greater potential for reuse and recycling, it is more likely that the value of these products at their end-of-life stage will be realized in future applications.

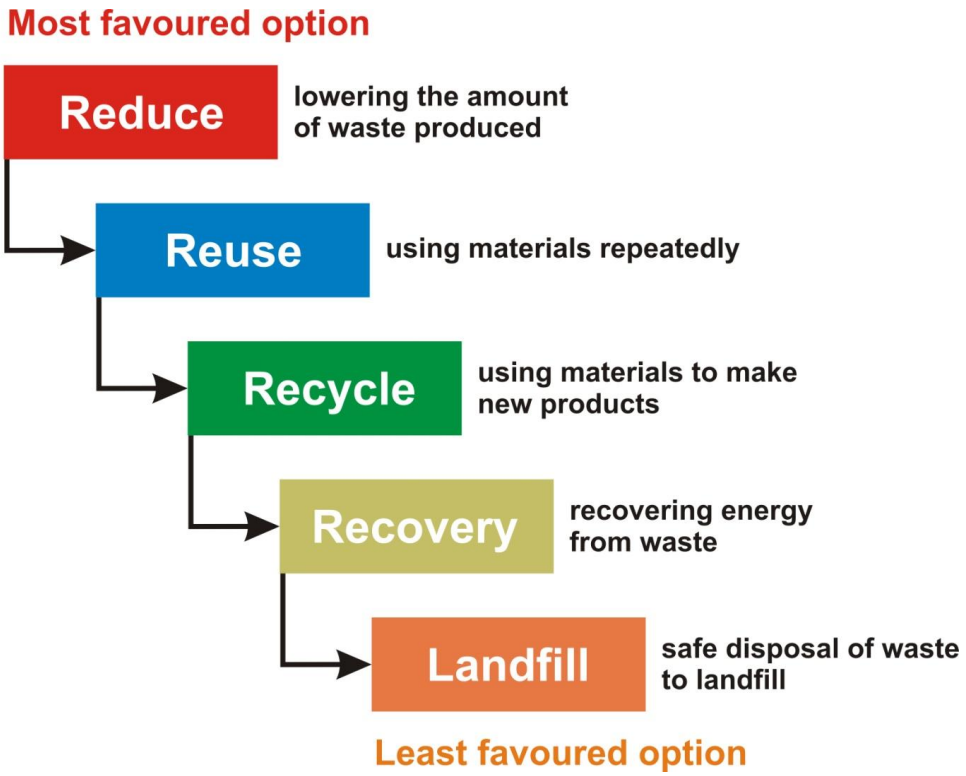

Figure 179 UK waste hierarchy (*Torridge, 2016*)

Recycling

Recycling is the process of converting waste materials into reusable objects (*Wikipedia, 2016*). A more sustainable development can be achieved by reducing waste and by saving primary resources. Also, recycling saves energy and reduces the potential greenhouse gas emissions because it requires less energy to produce a new product from the recycled materials than from the primary resources.

Recyclable means these materials are able to be made into functionally equivalent products. Different materials have different recycle rate due to their distinct properties which influence the environmental benefit and the amount able to be recycled. Steel is 100% recyclable and is highly recycled. In the UK, the overall average recycle rate of steel from buildings has been estimated to be 96% (*M. Sansom, 2014*). In terms of heavy structural steel, 100% of demolition arisings are either reused or recycled. However, for practical purposes a 99% recycling/reuse rate is generally assumed in order to account for small losses of material during the lifecycle of the product. Other products are mostly “down-cycled” into new products of less quality and reduced functionality because the recycled products usually have lower material properties.

For recycling to be sustainable in the long term, it is important that the recycling process is financially viable. This is frequently the biggest hurdle to recycling, particularly for products and materials that are down-cycled into lower grade, low value applications.

Reuse

To reuse is to use an item again after it has been used. By taking useful products and exchanging them without reprocessing, reuse helps to save resources, energy, and reduce the potential GHG (greenhouse gas) emissions. It has greater environmental advantage than recycling since there is no environmental impacts associated with reprocessing.

As with recycling, reuse rate varies among different construction products and systems. Steel construction products are highly demountable thus steel can be reused at both the product and the building level. One standard process for reuse of steel in the building industry can be: inspect the deconstructed sections to verify their dimensions, test strength and section properties of the deconstructed material, remove coatings by sand blasting, re-fabricate and cut the product to the required length.

There is significant scope for increasing reuse rate of steel in building and construction industry. This lies not only on the material but also on the design. Steps (*SteelConstruction, 2016*) that the designer can take to maximize the possibility for reusing structural steel include:

- Use bolted connections in preference to welded joints
- Use standard connection details including bolt sizes and the spacing of holes
- Try to avoid coatings or coverings that prevent visual assessment of the condition of the steel
- Minimize the use of fixings to avoid welding, drilling holes, or fixing with Hilti nails
- Use bar-coding or e-tagging to give easy identification of properties of the products
- Use long-span beams to allow larger flexibility of reuse
- Ensure easy and permanent access to connections

Current situation

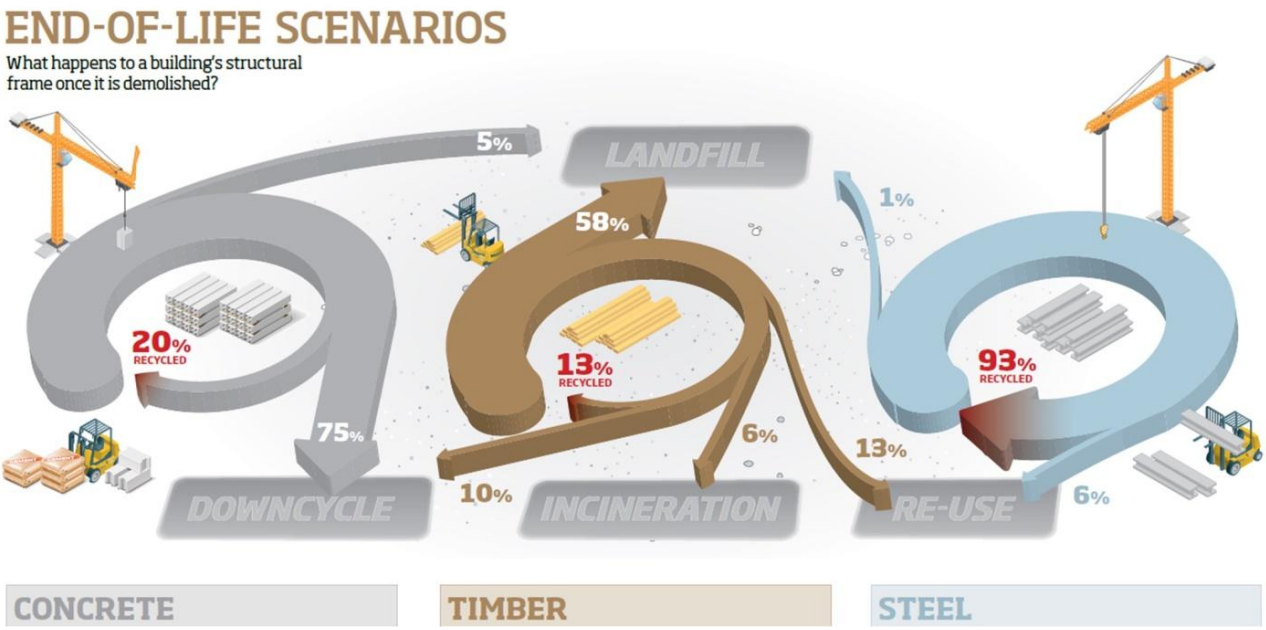

Figure 180 End-of-life scenarios (***Urbaneco, 2016***)

Figure 180 is the end-of-life scenarios for three most commonly used construction materials. It illustrates that steel is highly recycled (93%) , which is much higher than concrete(20%) and timber (13%).

Table 73 Summary of reuse and recycling rate from 2012 Eurofer survey (*M. Sansom, 2014*)

Product	% Reused	% Recycled	% Lost
Heavy structural sections/tubes	7	93	0
Rebar (in concrete superstructure)	0	98	2
Rebar (in concrete sub-structure or foundations)	2	95	3
Steel piles (sheet and bearing)	15	71	14
Light structural steel (e.g. galvanized purlin, supports, etc.)	5	93	2
Profile steel cladding (roof/facade)	10	89	1
Internal light steel (e.g. plaster profiles, door frames)	0	94	6
Other (e.g. stainless steel)	3	96	1
Average (across all products)	5	91	4

The results from table 73 show that recycling and reuse rates for steel from building demolition are very high. The combined reuse and recycling rate is 96%, with 91% recycled and 5% reused. This is of great significance to increase resource efficiency, save energy and reduce GHG emission, and form a sustainable development circle. It also shows that there is significant scope for increasing reuse of steel in the building and construction industry.

16.2 Embodied carbon of steel

In the building life cycle embodied carbon (*SteelConstruction, 2016*) is the carbon dioxide equivalent (CO_2e) or greenhouse gas (GHG) emissions associated with the non-operational phase of the project. This includes emissions caused by extraction, manufacture, transportation, assembly, maintenance, replacement, deconstruction, disposal and end of life aspects of the materials and systems that make up a building. The whole life carbon of the building is both the embodied carbon and the carbon associated with operation (heating, cooling, powering, providing water etc).

Table 74 Carbon and energy impacts of steel construction products in the UK (*TataSteel, 2016*)

Steel products	Plate	Sections	Tubes	Hot Dip Galvanized	Purlins and Side Rails
CO_2 (t/t)	0,919	0,76	0,857	1,35	1,10
Energy (GJ /t)	17,37	13,12	15,42	21,63	19,38

16.3 LCA of this roof design

Considering the environmental impacts associated with the lifecycle of this roof structure, mainly two points are considered in the design of this roof structure:

- Reduced the amount of material to be used

  This is achieved by applying the proper cross sections with the leading elements in each group have the utilisation between 0,70 and 1,00 so that both enough strength and high efficiency of material used are guaranteed

- Increase the reuse and recycling rate after demolition

  The steel structure is 100% recyclable. Some measures are taken to increase the reuse rate. First the cross sections are chosen from the standard profiles. Moreover, bolted connections are applied in preference to welded joints. And the single elements are designed as long as possible to allow flexibility of reuse.

For the final design of this roof structure, an approximation of the embodied carbon and energy of elements in each group are listed in the table below:

Table 75 Embodied carbon and energy of the final design

Group	Mass (kg)	Carbon (t)	Energy (GJ)
ETFE beam	7398	5,6	97
Strut	13841	10,5	182
Hoop	65570	60,3	1139
Rods	142	0,1	2
Cable top	1259	1,0	17
Cable bottom	1706	1,3	22
Rectangular cable	427	0,3	6
Total	**90343**	**79,1**	**1464**

Chapter 6

Construction

Construction here means building construction, which is the process of assembling the cable-strut system on site. In this chapter, details about how to apply the right amount of pretension are described. Then the assemble sequence of this cable-strut system is illustrated with some sketch-ups. Lastly the maintenance of this roof system is describe briefly.

17. Pretension

The cable system is symmetrical in both x and y directions, with two layers of prestressed cables placed every 3178 mm. In total there are 32 branches of cables which can be divided into 8 groups according to their length. The required pretension is 180 kN for all the cables. This section shows how the cables are tensioned.

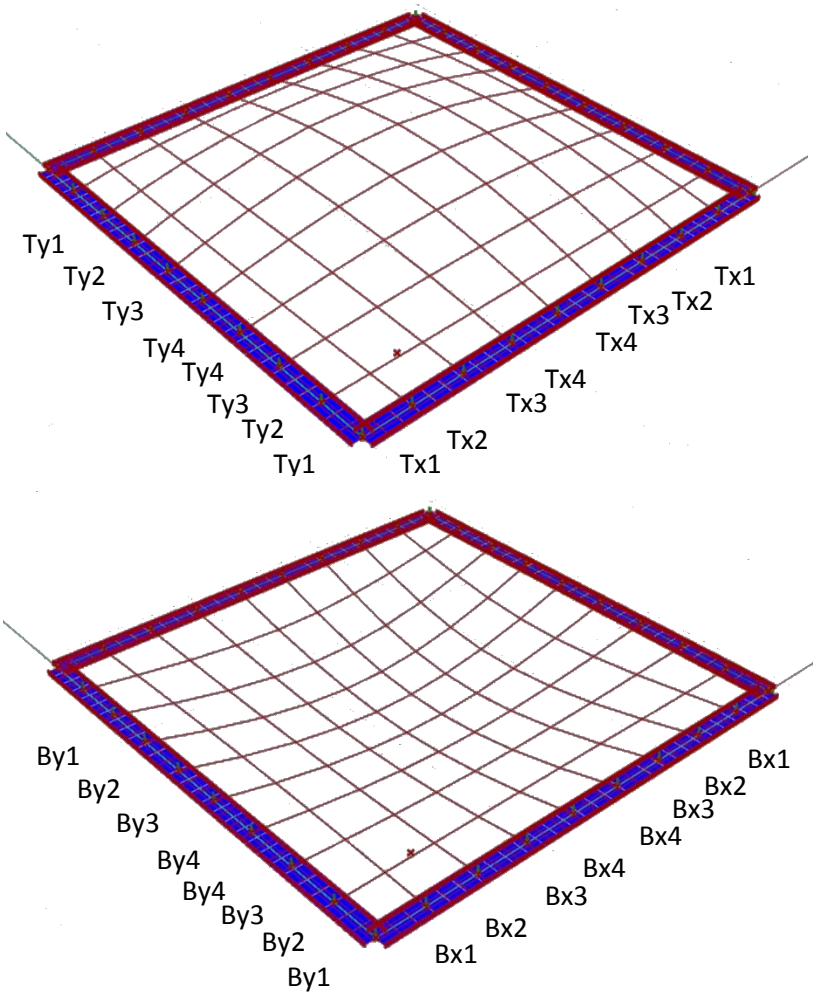

Figure 181 Numbering of cables

*T means top, B means bottom. X,Y means x, y directions

Pretension loss in the cable network may occur as a result of:

- Inward displacement and creep of compression hoop
- Temperature change in cables
- Relaxation of cables due to creep
- Tolerance of elements

This pretension loss may lead to reduction of stiffness and stability of the whole system and thus larger deflection and degraded security. To compensate for the possible loss of pretension in cables, the actual length should be shorter than that defined in the geometric model.

17.1 Material

The cables used are spiral strand cable from PFEIFER (See Appendix A). Two sizes are used, they are PG55 with nominal diameter 24,4 mm for top cable and PG75 with nominal diameter 28,3 mm for bottom cable. Details can also be found in table below:

Table 76 Parameters of cable material

Group	Size	Breaking Load (kN)	Tension Limit (kN)	Surface area (mm^2)	Weight (kg/m)	Nominal Diameter (mm)	E-Modulus (kN/mm^2)
Top Cable	PG 55	537	326	347	2,7	24,4	160 ± 10
Bottom Cable	PG 75	722	438	467	3,7	28,3	160 ± 10

*In this research, elastic modulus is taken as 160 kN/mm^2

Figure 182 Cables in the factory (*Peter van de Rotten, 2013*)

The breaking load is 1,65 times of the tension limit load, which means the cables have a linear behaviour up to 60% of the minimum tensile strength.

17.2 Length of cables

In real construction, pretension is applied to cables by elongation of the cable elements. And the amount of prestress is very sensitive to the cable length. So it is of great importance to define the cable length in a proper range before construction to guarantee sufficient pretension in cables after assembly. It is certain that the product length should be shorter as defined in the parametric model. There are many factors that lead to pretension loss which means this part should be compensated. The tolerance and end fixing of element should also be taken into account. Only when the influences of all the factors are combined can the final length of the elements be found.

1) Pretension Loss from hoop displacement

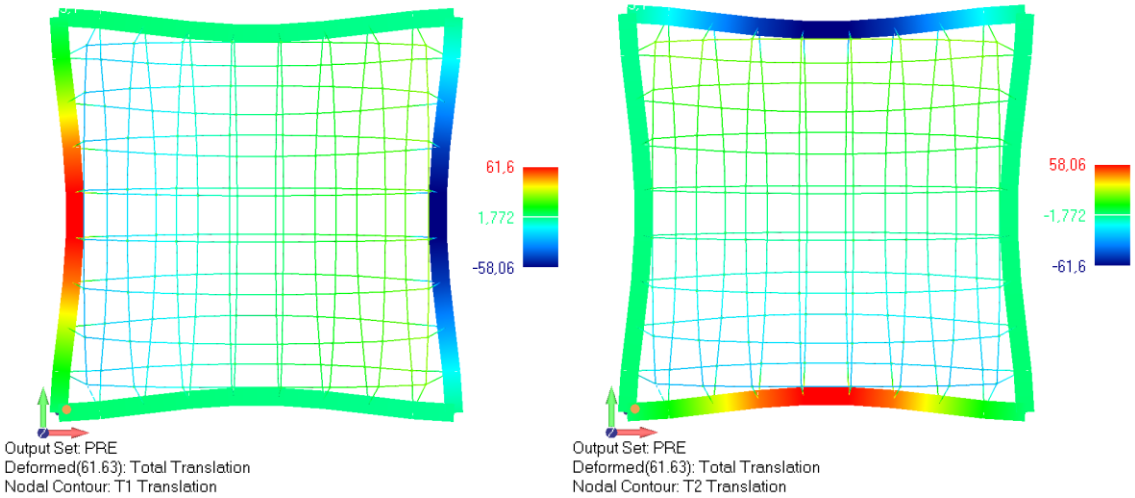

Figure 183 Hoop displacement under pretension only

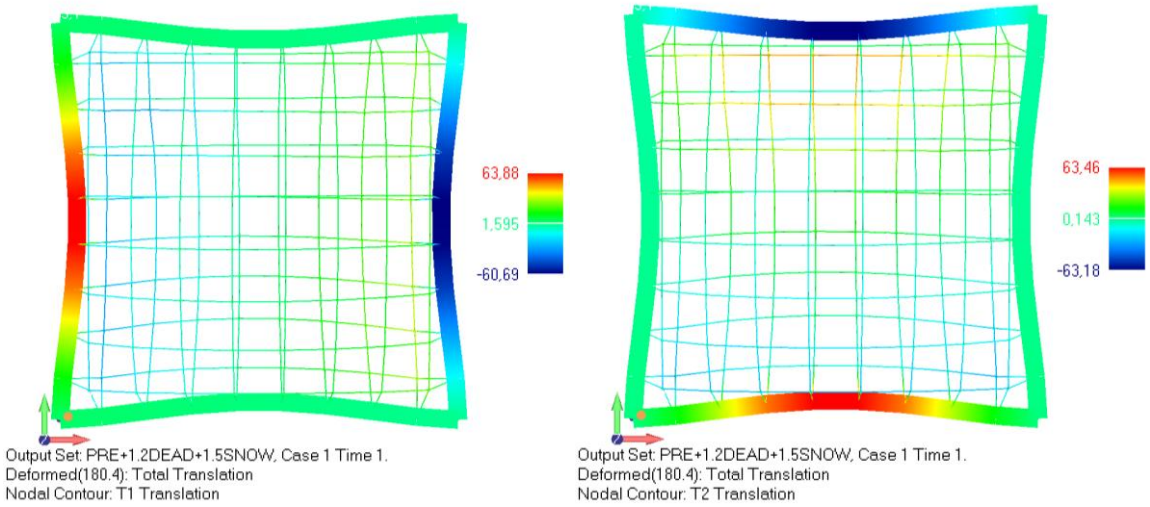

Figure 184 Hoop displacement under LC2: 1,0Pre+1,2Self Weight+1,5Snow

For the cable-strut system, there is a I-beam compression hoop around to provide stability to the whole system and transfer loads to constraints. This hoop deforms inwardly to take loads from cables, which will result in sag of cables and thus pretension loss. The inward displacement mainly comes from the preloading. Figure 184 shows that the maximum inward displacement of Hoop is around 65mm. This displacement varies for every constraint point, resulting in different length of each cable.

2) Pretension Loss from Thermal Expansion

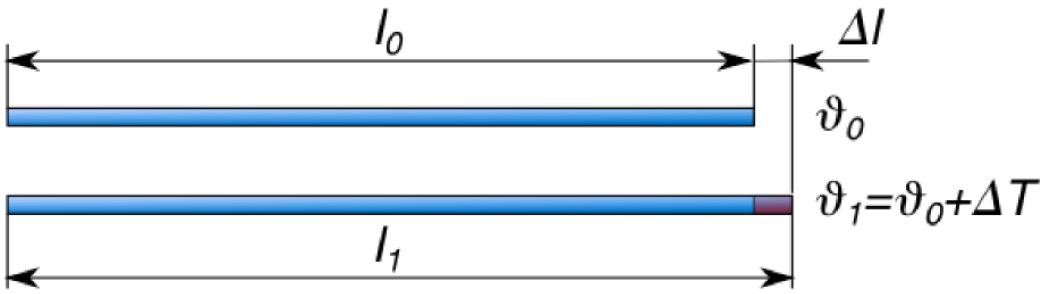

Figure 185 Element length change due to thermal expansion

The cables are manufactured in factory at a normal room temperature. On the construction site, the temperature may be different from the production temperature, then thermal expansion or shrinkage occurs. To a first approximation, the change in length measurements of an object due to thermal expansion is related to temperature change by a linear expansion coefficient α , it is the fractional change in length per degree of temperature change. Relationship between thermal elongation ΔL and thermal coefficient α can be expressed as:

$$\varepsilon = \alpha \Delta T \tag{17.1}$$

$$\Delta L = \varepsilon L \tag{17.2}$$

Where ε is the thermal strain, ΔT is the temperature difference, L is the length of cable.

The cables used on site is produced by Pfeifer with a thermal coefficient of $10*10^{-6}$ K^{-1}, by calculation:

$$\Delta L = \alpha \Delta T L = 0{,}29 mm/K$$

The temperature may vary during the installation. When temperature increases, cables are longer on the construction site, the applied pretension should be larger. Conversely, when temperature decreases, cables are shorter thus less pretension is required. Here mainly the pretension loss due to thermal expansion is taken into account, assuming the maximum temperature difference to be ΔT = 60 K, the corresponding elongation of cables:

$$\Delta L = 0{,}29 \times 60 = 17 mm$$

3) Cable Tolerance

$$\Delta L = \pm (\sqrt{L\,[m]} + 5\ mm)$$

Figure 186 Tolerance of cable

The cable tolerance is determined according to Pfeifer :

$$\Delta L = \pm(\sqrt{(L[m])} + 5mm) = \pm 10mm$$

4) Cable Creep

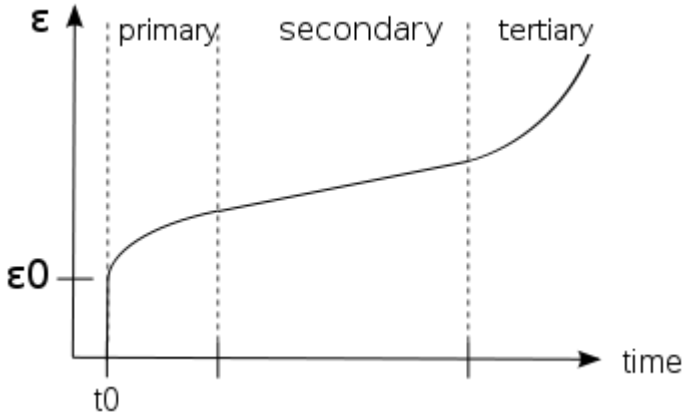

Figure 187 Creep - Strain as a function of time

Creep is the tendency of a solid material to deform permanently under the influence of high levels of stress. The cable creep according to Pfeifer is 0,35‰, the elongation due to creep is:

$$\Delta L = 0{,}35‰ \times 28602 = 10mm$$

According to a former project, the Markthal, realized by Octatube, the relaxation of pretensioned cables occurs within 5 days since installation. After five days, the creep is too small to be calculated.

5) Elongation by prestress

For the final design the minimum requirement pretension is 180 kN for each cable. The corresponding elongation is:

$$\text{Top cable } \Delta L_{top} = \frac{FL}{EA} = \frac{150\times28602}{160\times347} = 77mm$$

$$\text{Bottom cable } \Delta L_{bot} = \frac{FL}{EA} = \frac{150\times28602}{160\times467} = 57mm$$

6) End Fitting

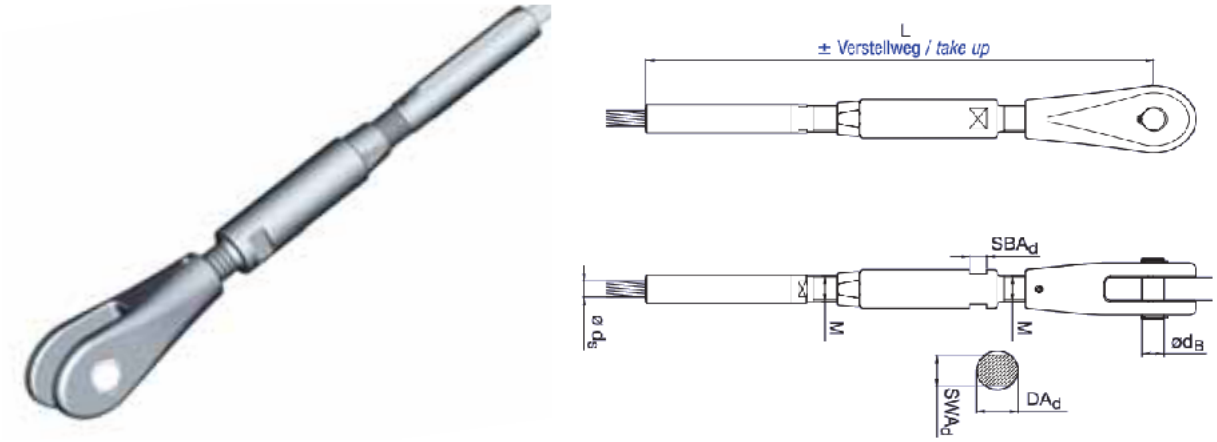

Figure 188 Fork Connector with Adapter and Threaded Fitting

The cable ends are fork connector with adapter and threaded fitting. This fitting can adjust the length of cables with extended thread ends to compensate for the pretension loss due to the factors mentioned above. The parameters of this fitting with adaptor can be found in the table below:

Table 77 Parameters for end fittings

Group	Size	L (mm)	Lg (mm)	ds (mm)
Top cable	PG55	678	144	28,3
Bottom cable	PG75	782	168	31,3

*L means total length of the fitting, Lg means the length of thread

7) Conclusion

Due to the various factors that may influence the cable length and lead to relaxation and pretension loss of cables, the cables will be supplied at a shorter length than that in the parametric model. By calculation, the maximum reduced length are 117*2=234mm and 107*2=214mm for a single branch of top and bottom cables respectively. The length of each cable element can easily be adjusted by adapters. Besides, in this design the special connection for cable and hoop can provide adjustability to the cable length to compensate for pretension loss.

17.3 Pretensioning

In this project, hydraulic jacks will be used to apply pretension. There are four steps for applying pretension:

- Installing hydraulic jacks
- Prentensioning of cables
- Tightening the bolts and fixing the cables
- Demounting hydraulic jacks

The procedure for applying pretension to a single cable is illustrated in the following figures.

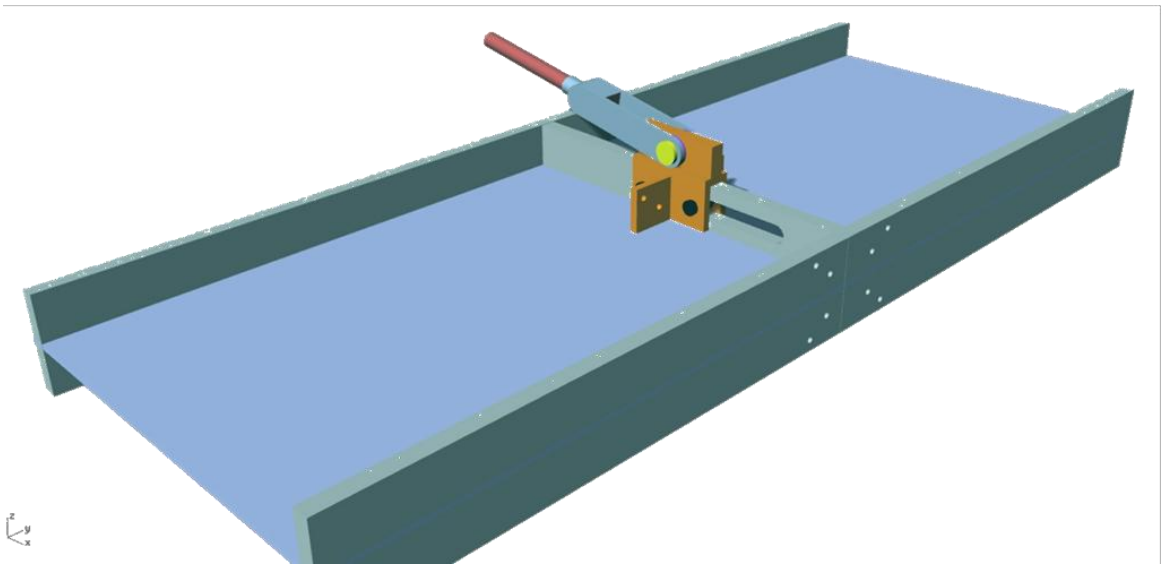

Figure 189 Before Pretensioning

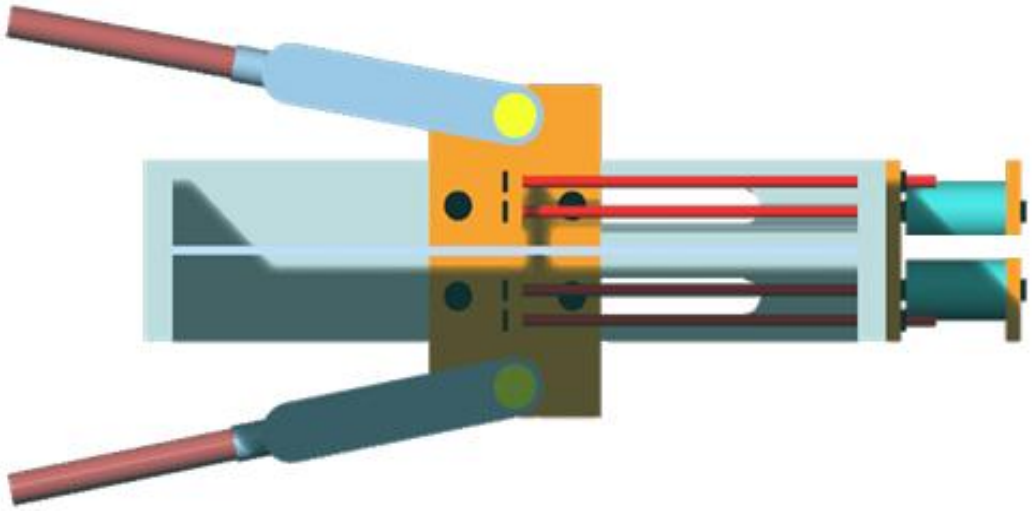

Figure 190 Install hydraulic jack

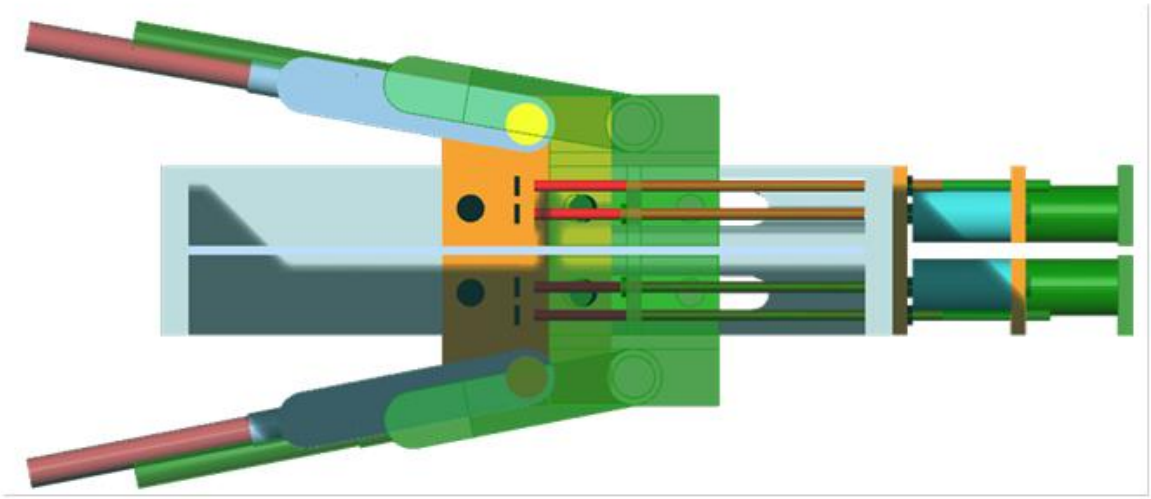

Figure 191 Apply pretension

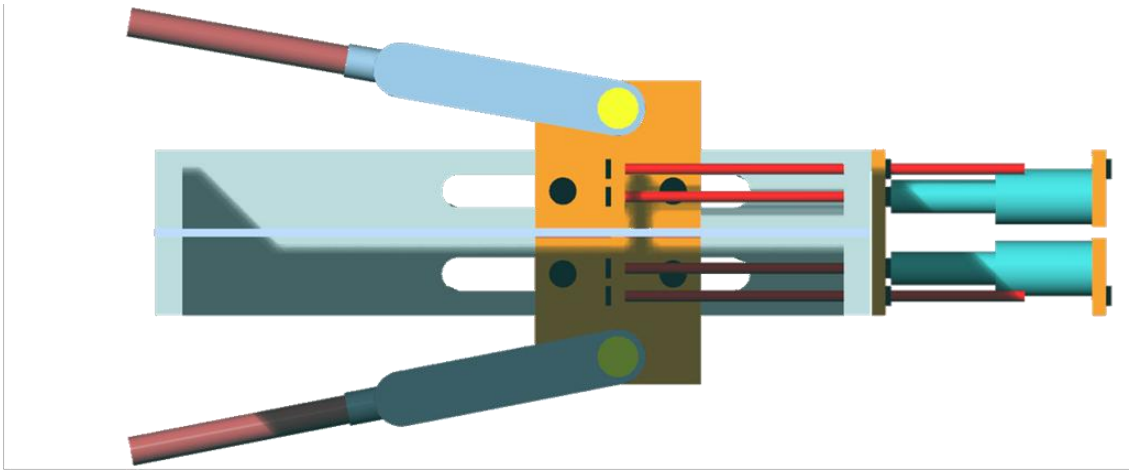

Figure 192 After pretensioning – with hydraulic jack

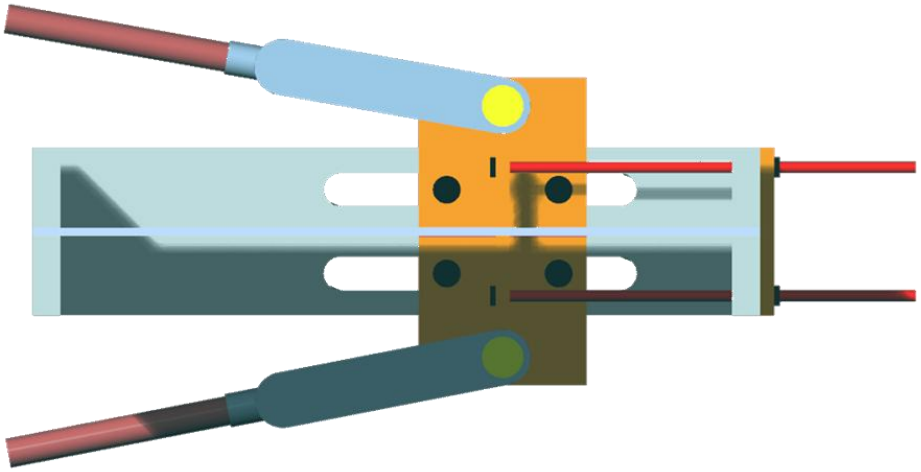

Figure 193 After pretensioning – demount hydraulic jack

More details about pretension are:

- For the cable network, it is suggested that the hydraulic jacks should be installed at both ends of the cables, and pretension at both ends should be applied at the same time. This could effectively reduce the asymmetrical movement of the compression struts due to pretension.
- In this structure, the same amount of preloading is applied to all the cables, thus there is only one set of pretension which can be applied at the same time for all the cables.
- In the construction, firstly all the cables will be pretensioned to 100%. This preloading will be kept for five days to allow the creep of cables under loading. After five days, raise the pretension to a certain amount and fix the cables. This over-preloading should be determined according to the on-site environment to compensate for the possible loss of pretension.

Figure 194 Hydraulic jack with pressure guage (***Peter van de Rotten, 2013***)

18. Assembly and Maintenance

18.1 Assembly sequence

The assembly (*Octatube, 2015*) is envisioned to be performed by using mobile cranes and scaffolds to support both the unfinished structure as well as the workmen.

A scaffold will be erected in the middle of the building site. The scaffold will have a work platform under the lowest members of the roof. To the sides it will extend as close as possible to the concrete walls. The scaffold should be strong enough to support the steel structure as long as not all members of the structure are in place.

Before hoisting the members into their final location, the strut elements are connected with connector in between, also the ETFE beam grid and compression hoop components are fitted, and will be assembled at their final location in the roof.

The final assembly will start with the hoop beams. The hoop beam components are hoisted by the crane and supported on the right location. Components of hoop beam are connected on site with bolts.

After the assembly of hoop beam the struts will be put into place. Because both the assembly of struts and ETFE beam grid need the help of crane for hoisting the elements, the struts must be assembled in prior to the ETFE beam grid. All the struts are hold by the scaffold. No tensioned cables are fitted in the struts at this stage.

After all the struts are placed at the right position, cables will be assembled. Also the cable end fittings will be connected to the hoop beam.

In the next step, hydraulic jacks will be installed at both ends of the cables and pretension will be applied to all the cables at the same time. The pretension process should last about one week, including the time for the creep of cables. After pretension, the cables will be fixed and hydraulic jacks will be demounted. After pretensioning of the cables, the struts can be fully supported by the cables thus the forces on the scaffold are removed up to a great extent.

With all the steps above, the cable-strut system has been assembled on site. Then the ETFE Beam grid should be put on above the struts.

After all the members are adjusted carefully, the ETFE cushion and other installations will be fitted.

This cable-strut roof system contains 7 groups of elements, all these groups of elements should be assembled in a proper way to guarantee safety and provide easy installation.

Step1 – Assembly of the scaffolding with open platform

Since the roof system is 16m higher than the ground, it is necessary to install the scaffold with an open platform to provide working space for construction.

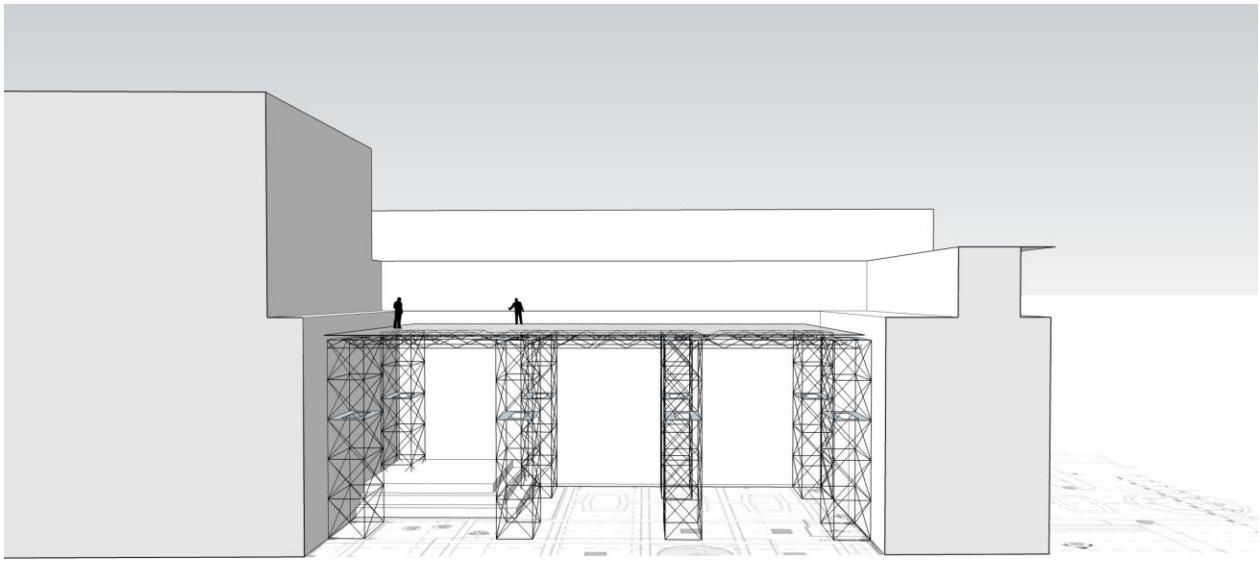

Figure 195 Scaffolding with open platform

Step2 – Installation of the compression hoop

Compression hoop accounts for over 70% of the total mass of this roof structure. It is fundamental for transferring loads to constraints and providing stability to the whole system. The hoop beam elements are assembled with crane.

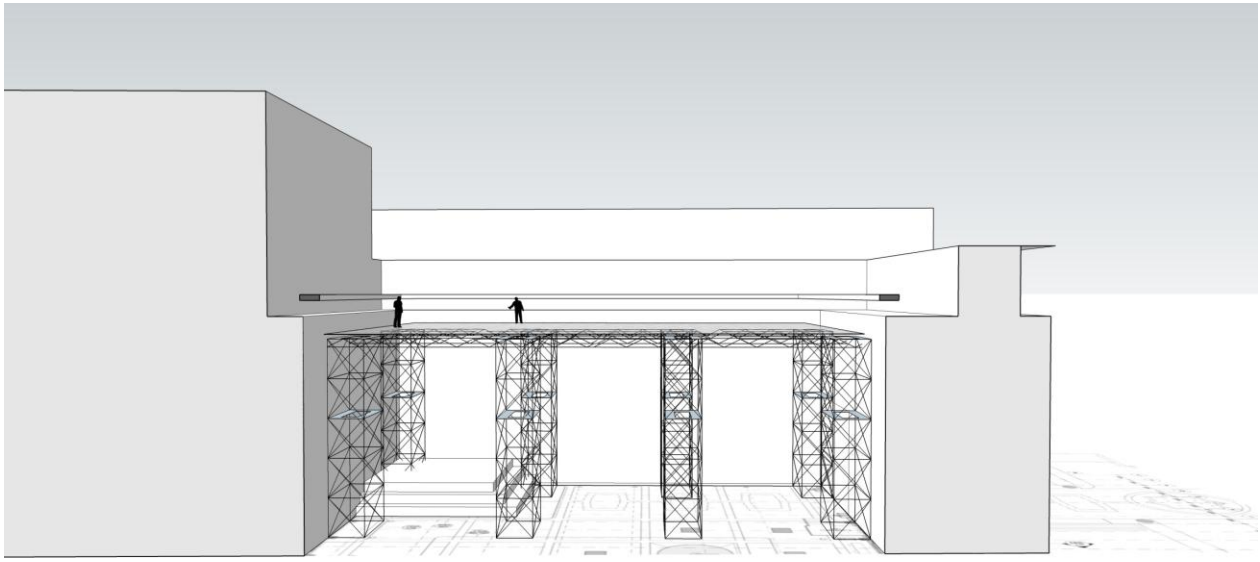

Figure 196 Install compression hoop

Step3 – Assembly of an extra floor level of scaffolding to locate compression struts

In the assembly sequence it is worth mentioning that the installation of struts should be prior to installation of ETFE Beam because elements in both groups are of large mass which requires crane for hoisting and placing them at the right position. This can only be achieved by assembling the structure from lower level to higher level.

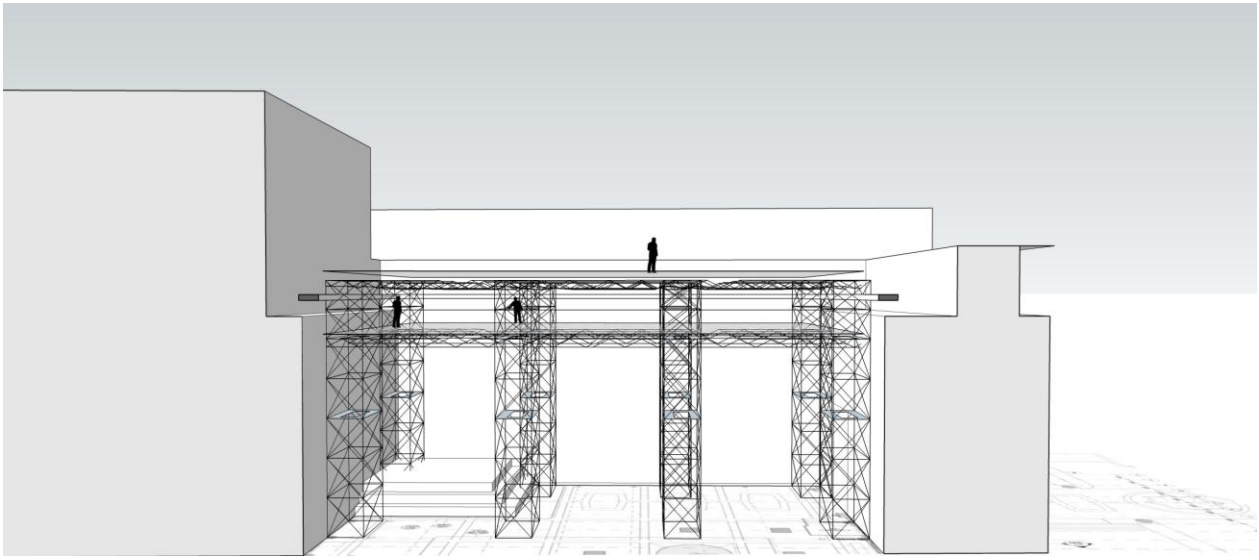

Figure 197 Scaffolding for locating struts

Step4 – Placing the struts with crane

Struts are hoisted and placed at the right location with a crane from outside the building. It is also very important to guarantee that the same branch of struts are in the same plane.

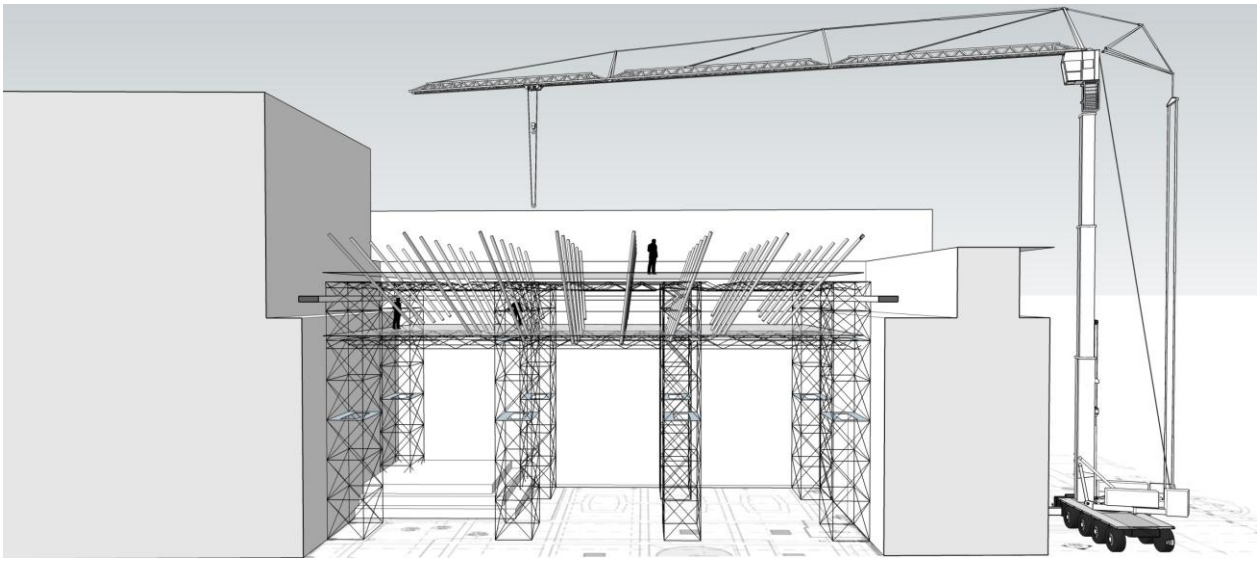

Figure 198 Placing the struts with crane

Step5 – Installation and pretensioning of cables

In this step, cables are installed to the right position. Then pretension is applied to both end of the cables at the same time.

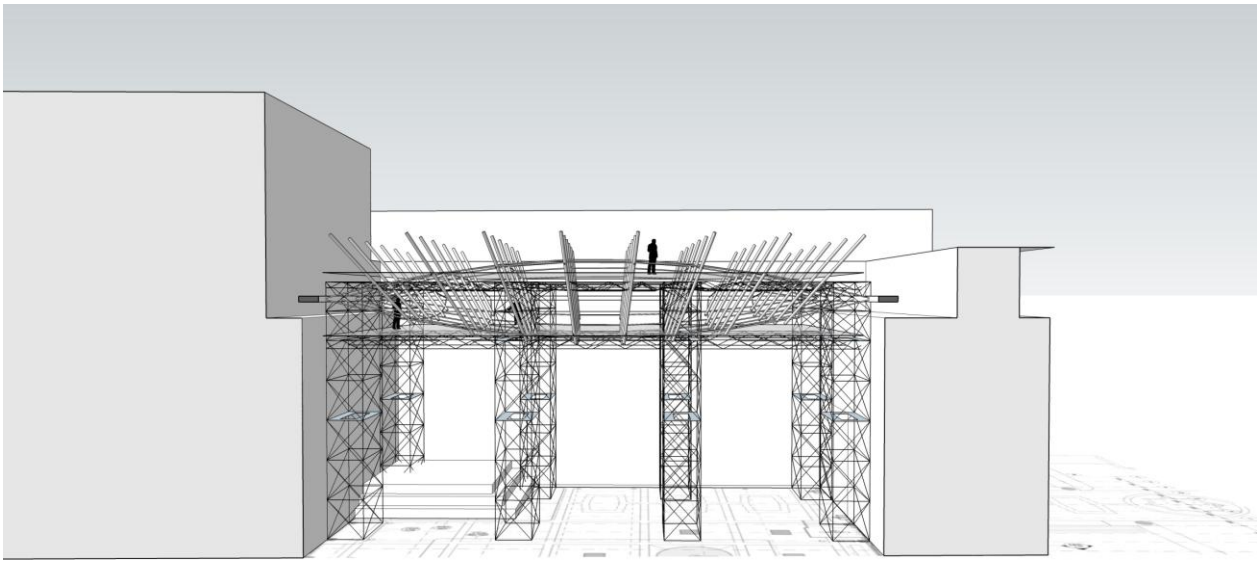

Figure 199 Installation of cables

Step6 – Installation of gutters for rainwater

Gutters are installed against the building walls to provide drainage of the rainwater from the ETFE cushion.

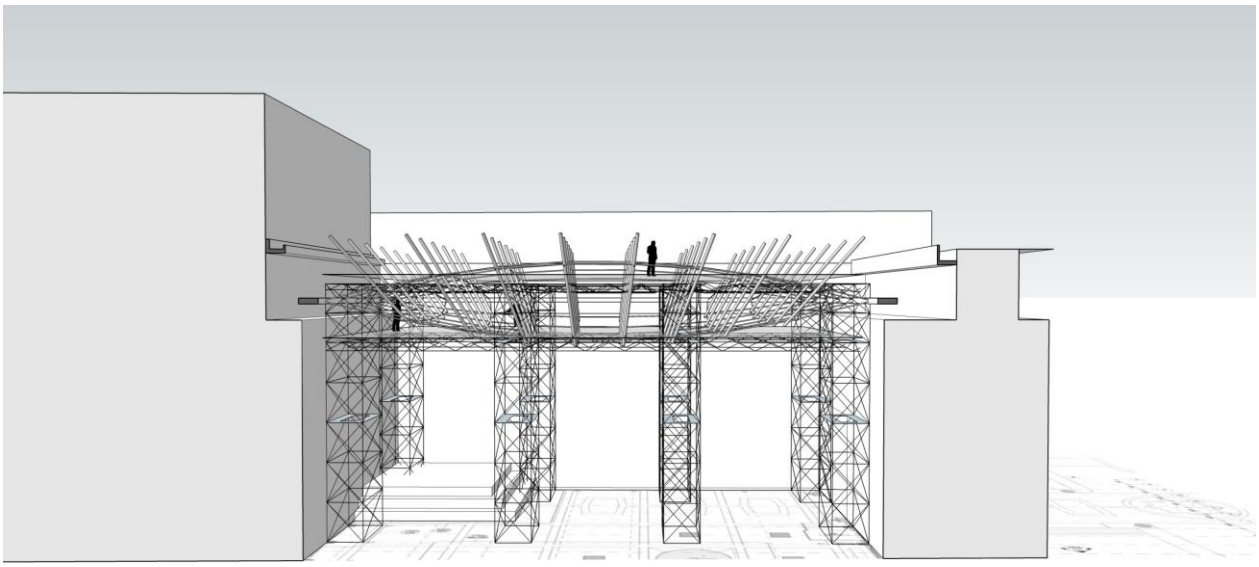

Figure 200 Installation of gutters

Step7 – Installation of beam grid and ETFE cushion

The Beam grid will be installed with the crane, and the attach the ETFE cushion on above. Also the final waterproofing and ventilation ducts are installed.

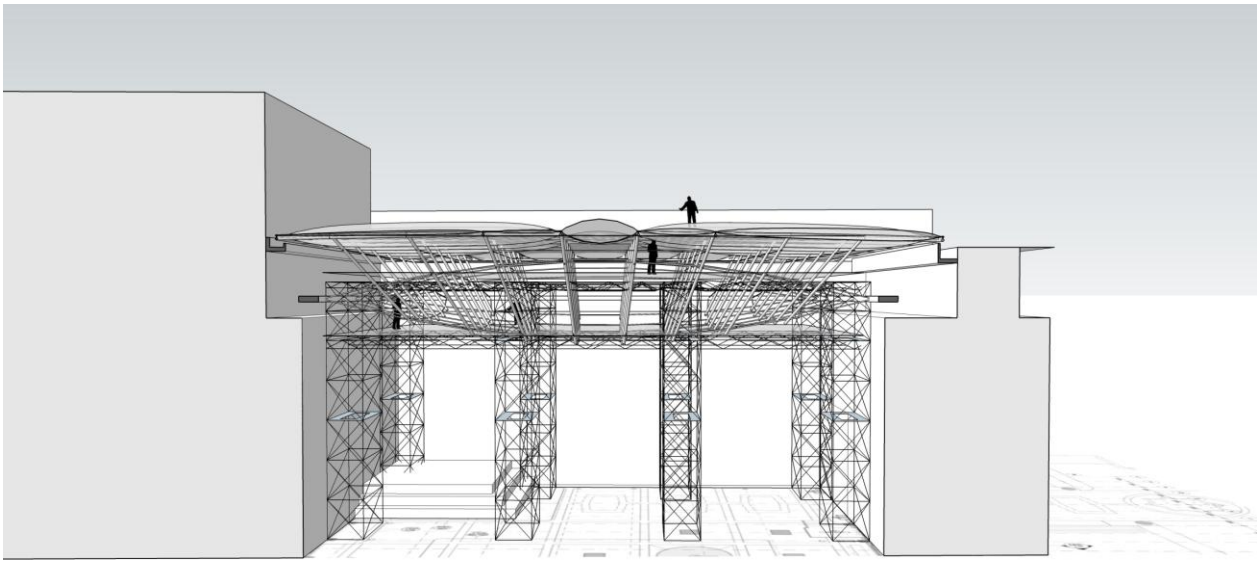

Figure 201 installation of beam grid and ETFE cushion

Step8 – Demounting of scaffolding

The last step is to demount the scaffolding.

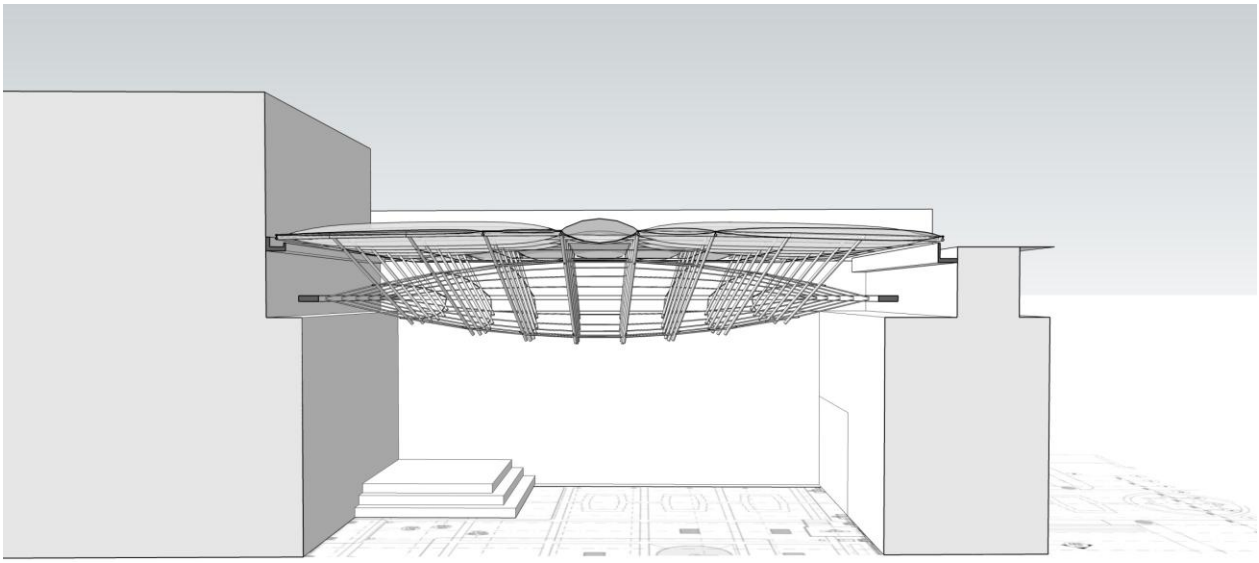

Figure 202 Demounting of scaffolding

18.2 Maintenance

For this cable-strut roof system with ETFE cushion on above, it should be easy for maintenance . For this roof structure, annually inspection is required to make sure all the cables stay in tension. Some details for maintenance are:

- Cleaning of this roof structure is mainly from inside because the ETFE cushion is basically self-cleaning.
- The ETFE roof and gutters are walkable thus provide access to the roof outside the building.
- The pretension in cables must be checked annually.
- The profiles, pipes, air blowers and accessories must be inspected annually.
- Snow accumulation is allowed on the roof. But still access to the roof is provided thus also the possibility for snow removal manually.

Chapter 7

Conclusions

And

Recommendations

19. Discussion

The aim of this research project has been to make a pretensioned cable-strut roof system for the opening of Het Gelders Huis in Arnhem, the Netherlands. The research question that has been posed was:

> *How to design a high efficiency light-weight cable-strut roof structure which shows good performance both under large asymmetrical snow load and upward wind suction load?*

To answer the research question, firstly literature study has been performed to gain insight and knowledge in the use of tensegrity for roof structures. Then a plug-in and some design components based on the Grasshopper environment have been developed to realize a parametric model. With the parametric model, a number of designs and analysis have been performed based on a standard model, and the influences of changing variables that exist in this roof design have been investigated.

To answer the question if it is possible to use software to find the minimum pretension and proper cross sections with high efficiency of material use, another parametric model with Galapagos and Karamba based on the Grasshopper environment has been made, and results similar to those from Femap have been found. Also three failure modes have been simulated to evaluate the redundancy. Apart from the structural analysis of different finite element models, supports and connections have been designed in detail with the concept to increase the reuse rate of materials after demolition of this structure. Also the assembly sequence of this roof and the process for applying pretension to cables have been investigated. In the end, a final design has been given which satisfies SLS and ULS check both under downward snow load and upward wind suction at the same time with high efficiency of material use, and most of the steel materials are reusable after demolition of this structure.

Tensegrity

The determining quality for the performances of this cable-strut roof is the presence of stiffness in the structure. Stiffness (*Wikipedia, 2016*) is the extent to which a structure or an element resists deformation in response to an applied force. Thus the aim of this research can be interpreted as to design a roof structure with large stiffness while still having a low structural mass. From the variable study, there are three key factors that determine the global stiffness of this cable-strut system:

- Geometry of the structure (1^{st} to 4^{th} order variable)
- The applied pretension (5^{th} order variable)
- Section size of elements (6^{th} order variable)

For a tensegrity structure there are numerous possible variables. The interdependence between variables and also between elements makes it quite difficult to analyse the influence of changing a single parameter. Therefore the variable study is a multi-variable study. In this study, firstly a standard model (see Section 9) is determined, based on which all the changes are made. To compare the performance of individual models to the standard model, a percentage (Rel.Std) is used to represent the performance relative to the standard model. And the design process is defined into four iterations with regards to the load transfer path and mass percentage of elements in each group to offset the interdependence.

Hoop beams

The hoop system accounts for over 70% of the total mass in the final design. It functions to stabilize the roof structure by taking loads from cables and transferring them to supports. The hoop is loaded in compression and bending. Compression forces make up only a small part of the unity check (around 8%) for the hoop, the rest are from bending moments caused mainly by pretension. There is a clear relation between the mass and pretension for the compression hoop. The higher pretension requires hoop beam with larger cross section thus a larger mass.

As the hoop beam is loaded both in compression and in bending, torsional buckling may occur when the load reaches the critical value. This roof design has been made with the buckling design taken into consideration. Stiffeners (see Section 13) have been applied on the hoop beams and the thickness for the corner web plates has been doubled which effectively improved the buckling resistance with an eigenvalue raised from 0,22 to 3,75 for the standard model.

Connection

Generally, all nodes in tensegrities are supposed to be hinged. Fixed connections can give false impression of stability. In real construction, it is very hard to make fixed connection. Differences between hinges and fixed connections depend on stiffness proportions between elements.

In the modelling of the roof structure only beam elements have been used. However, beam elements are allowed to accommodate both axial forces and bending moments, but for cables only tensile forces. To model the structure with beam elements in a proper way, pin releases have been applied at all the nodes in the cable net. Introducing pin releases can eliminate the options for transferring moments from struts to cables.

As for the real construction, it is envisioned that all the structural elements will be prefabricated in the factory and assembled on site. The large system like the ETFE beam grid and compression hoop are divided into identical pieces with regards to transport limit. Bolt connections will be used in preference to welding by considering the environmental influences.

Non-linearity

The nonlinear character of tensegrity results in a structure distributing loads to the most stable elements. When a tensegrity is under loading, initial displacement occurs and individual elements rearrange, leading to the change of strength and stiffness. Normally stronger and stiffer elements take more loads.

Limitations

The limitations in the design of this roof structure are listed as follows:

- For the overall design fatigue and dynamic loading have not been taken into account due to the emphasis of this research project on designing a high efficient roof structure under snow and wind load.

- The assumption of live loads (See Appendix F) on the ETFE beams is not accurate which leads to smaller bending despite the same total amount of forces.

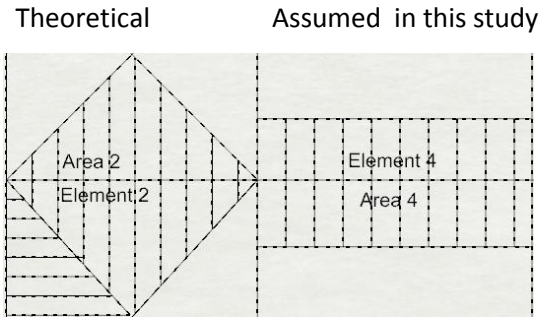

Figure 203 Assumption of live loads

- In the variable study, the maximum displacement under SLS LC2 has controlled smaller but as close to l_{span}/200=143mm as possible, the minimum tension in cables under ULS LC2 has been controlled between 0 and 10 kN, and the utilisation of the leading elements in each group is between 0,70 and 1,00. All the three criteria are adjustable within a range, which means to some extent the results from variable study are subjective.

Table 78 Results of two qualified models

Criterion	Model 1	Model 2
Displacement (mm)<143	139	127
Minimum tension in cable (kN)	1	8
UC	0,75	0,95

As shown from the table above are the results of two qualified models in the variable study, both satisfy the SLS and ULS check but they have different pretension and cross sections. It is up to the designer to choose which one be included in the results of the variable study.
Moreover, due to the limitation of the standard profile, there is not always the theoretically optimal cross section available.

- The mass and resulting dead load of connections have been assumed to be unchanged in spite of different cross sections which leads to a bit inaccuracy in the resulting forces and the mass of connections. However, this difference is not big compared to the total amount of loads in different load combinations.
- In the optimisation with Karamba and Galapagos, the defined live loads from snow and wind have been transformed into point loads and applied on the connection points of the ETFE beam grid. Therefore, the cross sections for the ETFE beam elements have not been optimised.

20. Conclusions

This roof design is a combination of tensegrity and beam system which shows the advantage of both structures. After the variable study and detailed design, the following conclusions can be drawn from the studies:

Analysis of the standard model

From the static analysis results of the standard model, it can be concluded that:

- ULS LC2 (1,5snow+1,2dead+1,0pre) determines the minimum required pretension, and SLS LC2 (1,0snow+1,0dead+1,0pre) leads to the largest vertical displacement (see Figure 92, 93).
- Beam elements in this roof structure react to external loads mainly by bending.

Variable study

From the variable study, it can be concluded that:

- Increasing the number of branches (1st order variable) does not necessarily lead to larger mass in a certain group of elements considering the application of smaller cross sections.
  In the 1st order variable study, increasing the number of branches will lead to a big difference to the resulting forces in ETFE beams. The decreased line load and smaller element length collectively results in smaller bending moments in ETFE beam grid with more branches. Therefore, smaller cross sections can be applied to the ETFE beam elements.
  However, considering the mass of connections, the total mass simply goes up with more branches.
- The model with vertical struts (2nd order variable) has better load transfer path with smaller eccentricity (see Figure 125) thus smaller bending occurs which allows the application of smaller pretension, also the applied cross sections for strut and hoop beams are smaller. The mass reduction from smaller strut and hoop in model with vertical struts gives a structure with less structural mass, which is about 80% of the standard model.
- By comparing the mass of structure with shape of cable net from self-weight, radial loads, and vertical loads, it can be concluded that the model with shape of cable net from radial loads has the smallest structural mass thus the best performances under the defined load combinations.
- Changing the depth of cable net (4th order variable) brings almost no difference to the total mass. However, increasing the depth of cable net leads to a stiffer structure.
- From the 1st order to the 4th order variable, the higher the order, the more radical influences it brings to the structure by changing the variable.
- Displacement of the roof structure can be controlled by pretension in the top and bottom cable net due to the asymmetry of the cable net.
- Deliberate change of one chosen variable brings difference to the whole structure by affecting the minimum required pretension. The displacement, resulting forces, cross sections, and resulting mass all change in response to pretension change.

Optimisation with Karamba

From optimisation with Karamba, it can be concluded that:

- The similar cross sections for elements in strut and cable groups in Grasshopper proves it is possible to use programs like Galapagos and Karamba to find the minimum required pretension and proper cross sections with high efficiency of material use.

Fail mode of the final design

By simulating the three possible failure cases, conclusions are:

- If one single cable element is broken, the structure has to be adjusted to a higher safety level.
- If one single branch of cable is not longer in tension due to pretension loss, vertical displacement of this roof structure will go beyond the SLS requirement and elements in ETFE beam and strut may yield due to the increased resulting stresses. However, collapse is not expected because all the elements have enough tensile strength.
- There is residual load-bearing capacity in the cable net and a certain amount of over-pretension is allowed. A 20% over-pretension has been applied to both top and bottom cable net, results shows only the resulting stresses in hoop elements go beyond the yield stress, elements in the rest groups fulfill the unity check and SLS check.

Connections and lifecycle assessment

With careful design of the connections by taking into account the environmental impacts, it can be concluded that:

- By applying bolted connections in preference to welded connections, and using beam elements as long as possible with the transport limit taken into account, the steel elements are highly reusable after demolition of this structure.

21. Recommendations

For this design work, the final model was reached after optimisation of pretension and cross section with all the possible load cases taken into consideration. However, potential improvements can be made to find a structure with higher efficiency. In this section recommendations are given for future study.

Asymmetric structure

The cable-strut roof structure is made symmetrical both in geometry and in the sectional choice of elements. This makes the design and analysis comprehensive. The structure is able to withstand loads in every direction and display good performances. However, for the specific situation for the opening in Het Gelders Huis, the snow accumulation provides a very high unbalanced load. A special design for carrying the snow load can be achieved by making the cable net asymmetric. It is recommended that the side for snow accumulation should be made steeper. This shape of structure can be achieved by applying the snow load as the load case for form finding.

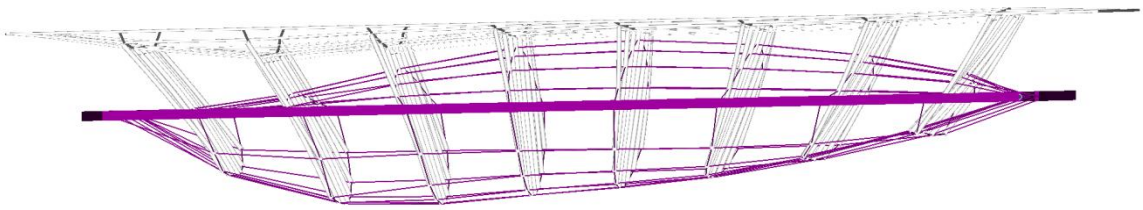

Figure 204 Asymmetric model

Vertical struts

From the 2nd order variable study, it has been concluded that the model with vertical struts has better structural performances than the model with radial struts due to different load path. In practical sense, the structure with vertical struts is also easier to assemble compared to the one with radial struts.

Therefore, with an intention to save the structural material and for easier construction, it is recommended to design a roof structure with vertical struts.

Loads

For the overall design a time-dependent effect like fatigue and dynamic loading are not studied. It is recommended that this effect be considered to determine the resilience of the structure in the long time.

Pretension in the cables can also be further optimised by applying different preloading to different cables. This can effectively reduce the amount of pretension and potentially the section size of elements and total mass. However, applying different pretension to cables would bring more difficulties for construction. Investigation is recommended to determine whether it is financially beneficial to do this.

Profile

For the design, only S355 and PG cables have been used. To find a structure with higher efficiency, different kinds of steel grade can be applied. By using a steel type with higher yield strength, less material is needed with regards to load-bearing capacity. However, it is recommended that special attention be paid to the stiffness and the final cost.

Additionally, in the design, the same cross section has been chosen for elements in the same group. A better solution can be found when each element is given its own sectional choice. As for the hoop beam, it can be designed per segment but careful consideration should be paid to the buckling resistance.

Structural requirement

In Eurocode, there is no definitive deformation requirements for a tensegrity. In this research project, the requirement for SLS check is chosen as:

$$\delta < \frac{l_{span}}{200}$$

Actually considering the properties of tensegrity like tension-stabilization and geometric nonlinear, a more general criterion can be applied. It is recommended to find the boundary of the vertical displacement for such structures. If the allowable maximum deflections for the tensegrity are known, this structural requirement could be updated and a structure can be made with less pretension thus possibly less material.

Connection

Precision and adjustment are of great importance to cope with the tolerance and any unexpected difference between modeling and reality. For the future research, it is recommended to develop some connections with higher adjustability that avoid mistakes for assembly on site.

References

[1] Het Gelders Huis, accessed 18 May 2016, http://www.visserensmitbouw.nl/nl/projecten/detail/huis-der-provincie-arnhem, 2016.

[2] De Boeck, J., et al. Tensegrity Bridges: Concept Design of Pedestrian Bridges Using Tensegrity As Load Carrying System, 2013. Web.

[3] Motro, René. Tensegrity : Structural Systems for the Future.London: Kogage, 2003. Print.

[4] Wang, Bin Bing. Free-Standing Tension Structures : From Tensegrity Systems to Cable-Strut Systems.London: Spon, 2004. Print.

[5] R. E. Skelton, R. Adhikari, J. P. Pinaud, Waileung Chan and J. W. Helton, "An introduction to the mechanics of tensegrity structures," Decision and Control, 2001, Proceedings of the 40th IEEE Conference on, Orlando, FL, 2001, pp. 4254-4259 vol.5.

[6] Mick Eekhout, Prinsenhof, accessed 17 May 2016, http://www.octatube.nl/projecten/30/prinsenhof/, 1997.

[7] J. van Stigt, Droogbak, accessed 17 May 2016, http://www.octatube.nl/projecten/86/droogbak/, 1999.

[8] Kevin Roche, Bancopolis, accessed 17 May 2016, http://www.octatube.nl/projecten/25/bancopolis/, 2005.

[9] Alfonso Millanes, Glass Cube, accessed 17 May 2016, http://www.octatube.nl/en/projects/12/glazen-kubus/, 2009.

[10] Beetz, J., Telgen, M.V. van, Snijder, H.H. & Habraken, A.P.H.W. Parametric design and calculation of circular and elliptical tensegrity domes, 2012.Web.

[11] image courtesy of Simmons @2015 Microsoft Corporation.

[12] Gómez-Jáuregui, V. Tensegrity Structures and their Application to Architecture. Servicio de Publicaciones Universidad de Cantabria,2010.

[13] Eleanor Hartley, Kenneth Snelson; Art and Ideas, 2013. Web.

[14] Korkmaz et al, Determining Control Strategies for Damage Tolerance of an Active Tensegrity Structure, Engineering Structures, 2011.

[15] Kenneth Snelson, Needle Tower 1968. On view @ Hirschhorn Sculpture Garden.

[16] Geiger, D.H. The design and construction of two cable domes for the Korea Olympics. Shells, Membranes and Space Frame. In: Proceedings of IASS Symposium, 1986.

[17] Geiger, D.H., Seoul Olympic Gymnastics Hall and Fencing Hall, http://www.tensinet.com/database/viewProject/4013.html, 1986.

[18] Jord den Hollander, Pylons Bridge, accessed 17 May 2016, http://www.octatube.nl/projecten/59/mastenbrug/, 2000,

[19] Yildirim Hurmuzlu, Osita D.I. Nwokah. Mechanical Systems Design Handbook: Modeling, Measurement, and Control. CRC Press LLC, 2002. Print.

[20] i.o.v. TEAM, HET GELDERS HUIS – ARNHEM, accessed 18 May 2016, SID STUDIO, http://www.sidstudio.nl/projecten-pages/p0063-het-gelders-huis.html, 2015.

[21] Dennis R. Holloway, “Bicentennial Solar Pavilion for the Arts”,accessed 17 May 2015, http://www.dennisrhollowayarchitect.com/SolarPavilionPaper.html, 1975.

[22] Yue Liu, Bernd Zwingmann and Mike Schlaich, Spoked wheel cable roof with CFRP Continuous Band Winding System, accessed 18 May 2016,

[23] Geiger Associates, AN 8-SEGMENT CABLE DOME STRUCTURE, accessed 18 May 2016, http://www.columbia.edu/cu/gsapp/BT/DOMES/SEOUL/sol-34.jpg, 1988.

[24] Angelo Simone, CIE 4190 An Introduction to the Analysis of Slender Structures ,2011,

[25] Przemieniecki, J. S. Theory of Matrix Structural Analysis. New York: McGraw-Hill, 1967. Print.

[26] Timoshenko, Stephen. History of Strength of Materials : With a Brief Account of the History of Theory of Elasticity and Theory of Structures. New York: McGraw-Hill, 1953. Print.

[27] Boom, I., R, F.S.K, S, & J. Tensile-compression ring: A study for football stadia roof structures, 2012. Web.

Wikipedia, Sagrada Família, accessed 21 June 2016, https://en.wikipedia.org/wiki/Sagrada_Fam%C3%ADlia, Wikipedia®, last modified on 14 June 2016.

[28] Sophie’s mazes, Sagrada Familia scale models, accessed 18 May 2016, http://sophie-g.net/photo/build/barcelona/sagrada17.htm, 2007.

[29] Wikipedia, Structural engineering, accessed 23 May 2016, https://en.wikipedia.org/wiki/Structural_engineering#cite_note-IStructE-2, Wikipedia®, last modified on 15 April 2016.

[30] Piscitelli, G., et al. Form Finding of Arches in Tensile Structures, 2015. Web.

[31] Schek, H.-J. "The Force Density Method for Form Finding and Computation of General Networks." Computer Methods in Applied Mechanics and Engineering3.1 (1974): 115-134. Print.

[32] Computational Desin Software, accessed 23 May 2016, https://www.bentley.com/en/products/product-line/modeling-and-visualization-software/generativecomponents, BENTLEY SYSTEMS, 2016.

[33] Coenders, J.L., L.A.G, and J.N.J.A. NetworkedDesign: Next Generation Infrastructure for Computational Design.VSSD, 2011, Print.

[34] Wikipedia, Parametric design, accessed 18 May 2016, https://en.wikipedia.org/wiki/Parametric_design, Wikipedia®, last modified on 1 May 2016.

[35] Michael van Telgen, FEM model genereren, Octatube, 2015.

[36] Slobbe, G., et al. Optimisation of Reinforced Concrete Structures, 2015. Web.

[37] P. W. Christensen and A. Klarbring, An Introduction to Structural Optimization, Springer, 2009.

[38] P. Papalambros and D. Wilde, Principles of Optimal Design - Modeling and Computation, Cambridge University Press, 2000.

[39] Koos Fritzsche, FemGrassVBA, Octatube,2015.

[40] Chris H. Luebkeman, Support and Connection Type, accessed 14 June 2016 http://web.mit.edu/4.441/1_lectures/1_lecture13/1_lecture13.html.

[41] S.D. Guest , The Stiffness of Tensegrity Structures, Department of Engineering, University of Cambridge, 2010, Web.

[42] i.o.v. TEAM V,UITGANGSPUNTEN CONSTRUCTIEVE UITWERKING ETFE-DAKCONSTRUCTIE-REV C, SID studio,25 FEBRUARI 2015.

[43] Wikipedia, Buckling, accessed 21 June 2016, https://en.wikipedia.org/wiki/Von_Mises_yield_criterion, Wikipedia®, last modified on 8 May 2016. Web.

[44] Wikipedia, Buckling, accessed 21 June 2016, https://en.wikipedia.org/wiki/Buckling, Wikipedia®, last modified on 17 May 2016. Web.

[45] Buckling load factor, accessed 18 May 2016, http://help.solidworks.com/2012/English/SolidWorks/cworks/Buckling_Load_Factor.htm, © 1995-2016 Dassault Systèmes.

[46] Buchholdt, H. A. An Introduction to Cable Roof Structures. 2nd ed. London: Thomas Telford, 1999. Print.

[47] David Rutten, Evolutionary Principles applied to Problem Solving, accessed 15 June 2016, http://www.grasshopper3d.com/profiles/blogs/evolutionary-principles.

[48] image courtesy of Peter Fotiadis, 2016.

[49] Davison, Buick., Graham W. Owens, and Steel Construction Institute (Great Britain). Steel Designers' Manual. 6th ed. Oxford, UK: Blackwell Science, 2003. Print.

[50] Defining Life Cycle Assessment (LCA). US Environmental Protection Agency. 17 October 2010, Web.

[51] End of life recycling, accessed 18 May 2016, http://www.concretecentre.com/Performance-Sustainability-(1)/Material-Effieciency/End-of-life-recycling.aspx, The Concrete Center, 2016. Web.

[52] The UK Waster Hierarchy accessed 18 May 2016, www.defra.gov.uk, © Crown copyright, 2016. Web.

[53] The Waste Hierarchy, accessed 5 July 2016, http://www.torridge.gov.uk/article/12059/Residents, Copyright © 2016 Torridge District Council

[54] Wikipedia, Recycling, accessed 22 May 2016, https://en.wikipedia.org/wiki/Recycling, Wikipedia®, last modified on 22 May 2016.

[55] M. Sansom and N. Avery, Reuse and recycling rates of UK steel demolition arisings. Sanson. Proceedings of the Institution of Civil Engineers Engineering Sustainability 167, June 2014, Issue ES3.

[56] Design for Reuse, accessed 22 May 2016, http://www.steelconstruction.info/Recycling_and_reuse#Recycling, 2016. Web.

[57] End-of-life scenarios, accessed 22 May 2016, http://www.urbaneco.ch/concept/recycling-and-reuse/. 2015. Web.

[58] What is embodied carbon, accessed 22 May 2016, http://www.steelconstruction.info/Life_cycle_assessment_and_embodied_carbon#What_is_embodied_carbon.3F, 2016. Web.

[59] Embodied carbon of steel, accessed 12 March 2016, https://www.tatasteelconstruction.com/en_GB/sustainability/Embodied-carbon/Embodied-carbon, © Copyright Tata Steel Europe, 2016. Web.

[60] Ir.P.A van de Rotten, Markthal Rotterdam, Octatube,2013.

[61] Het Geldershuis, Arnhem – Presentatie, Octatube, 2015.10,29.

[62] Wikipedia, Stiffness, accessed 21 June 2016, https://en.wikipedia.org/wiki/Stiffness, Wikipedia®,last modified on 13 June 2016.

Building codes

Eurocode 0 EN 1990: Basis of structural design (Including the NA)

Eurocode 1 EN 1991: Actions on structures (Including the NA)

Eurocode 3 EN 1993: Design of steel structures

Design Systems overview

[1] Grasshopper, http://www.grashopper3d.com, Grasshopper (McNeel, 2008) is a parametric and associative design system developed as a plugin for Rhinoceros developed by David Rutten of McNeel. Originally, it was called ExplicitHistory.

[2] Femap, https://www.plm.automation.siemens.com/en_us/products/femap/, Femap is an engineering analysis program sold by Siemens PLM Software that is used to build finite element models of complex engineering problems and view solution results.

[3] Rhinoceros, http://www.rhino3d.com, Rhinoceros or Rhino3D is an advanced NURBS modelling system by Robert McNeel and Associates which supports extension by plug-ins through its extensive API.

[4] AutoCAD, http://www.autodesk.com/autocad, CAD system developed by Autodesk Inc. Originally, AutoCAD aimed at 2D drafting, but recently has moved towards 3D modelling.

[5] Visual Studio, https://www.visualstudio.com/, Microsoft Visual Studio is an integrated development environment from Microsoft. It is used to develop computer programs for Microsoft Windows, as well as web sites, web applications and web services.

[6] Visual Basic, https://msdn.microsoft.com/en-us/library/2x7h1hfk.aspx, Visual Basic is a third-generation event-driven programming language and integrated development environment (IDE) from Microsoft for its COM programming model first released in 1991 and declared legacy in 2008.

[7] Karamba 3d, http://www.karamba3d.com/, Karamba is a parametric structural engineering tool which provides accurate analysis of spatial trusses, frames and shells. Karamba is fully embedded in the parametric design environment of Grasshopper, a plug-in for the 3d modeling tool Rhinoceros.

[8] Galapagos, http://www.grasshopper3d.com/group/galapagos, Galapagos is a program that provides generic platform for the application of Evolutionary Algorithms.

Appendix A: Pfeifer cables

Spiralseil DIN EN 12385 – GALFAN
Spiral Strand DIN EN 12385 – GALFAN

Zulassungsnummer
Approval-Number
Z-14.7-413

PG

1 x 19  1 x 37  1 x 61 

Technische Daten	*Technical Data*
Material: unlegierter Qualitätsstahl	*Material:* *unalloyed quality steel*
Elastizitätsmodul: 160 ± 10 kN/mm²	*Modulus of Elasticity:* *160 ± 10 kN/mm²*
Toleranz d_S: + 3%	*Tolerance d_S:* *+ 3%*
Korrosionsschutz: GALFAN verzinkt ohne Innenverfüllung	*Corrosion Protection:* *GALFAN coated without inner filling*

Größe *size*	Charakt. Bruchkraft *charact. breaking load* $Z_{B,k}$ DIN 18800* kN	Grenzzugkraft *limit tension* $Z_{R,d}$ DIN 18800 kN	Metall. Querschnitt *metallic cross section* ca./*approx.* mm²	Gewicht *weight* ca./*approx.* kg/m	Konstruktion *construction*	Seil-Nenndurchmesser *nomin. strand dia.* d_S mm
PG 5	59	36	39	0,3	1 x 19	8,1
PG 10	93	56	60	0,5	1 x 19	10,1
PG 15	134	81	87	0,7	1 x 19	12,2
PG 20	181	109	117	0,9	1 x 37	14,1
PG 25	260	158	168	1,3	1 x 37	17,0
PG 40	367	222	237	1,9	1 x 37	20,1
PG 55	537	326	347	2,7	1 x 37	24,4
PG 75	722	438	467	3,7	1 x 37	28,3
PG 90	884	536	572	4,5	1 x 61	31,3
PG 125	1189	721	769	6,1	1 x 61	36,3

*nach EC 3 = $F_{u,k}$ und nach ASCE 19-96 = S_d
Konstruktionsänderungen vorbehalten
Größere Abmessungen und Zwischengrößen auf Anfrage

**according EC 3 = $F_{u,k}$ and according ASCE 19-96 = S_d*
Subject to technical modification
Bigger dimensions and intermediate dimensions upon request

Gabelkopf mit Adapter und Gewindefitting
Fork Connector with Adapter and Threaded Fitting

Zulassungsnummer
Approval-Number
Z-14.4-433

Technische Daten		***Technical Data***	
Gabelkopf	siehe Datenblatt 860	*Forked end*	*see data sheet 860*
Adapter	siehe Datenblatt 860	*Adapter*	*see data sheet 860*
Gewindefitting	siehe Datenblatt 988 PG	*Swaged fitting*	*see data sheet 988 PG*

Anwendungsgebiet / ***Field of Application***

Aussteifungen:
Windverbände Dach, Wände, Stützen — *Bracings for roofs, walls, girders*

Abspannungen:
Dachelemente, Pylone — *Stays for roof elements, pylons*

Unterspannungen:
Stahl-, Holzbinder, Raumfachwerke — *In-line tensioning for steel-, wooden truss and steel structures, space frames*

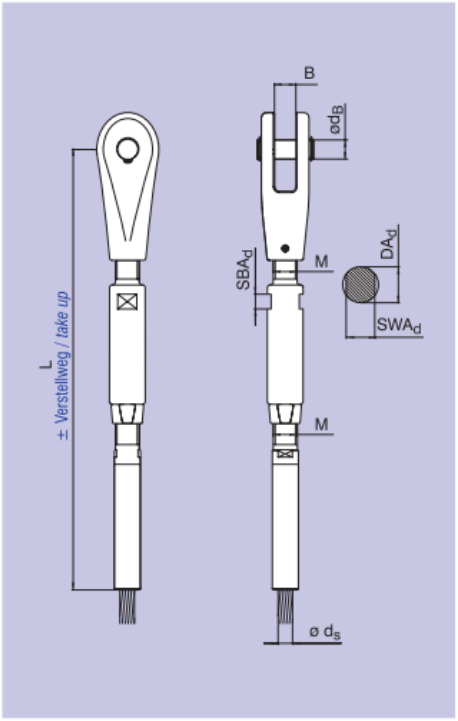

Typ *Type*	Größe *size* $M_{(LH/RH)}$	Grenzzugkraft *limit tension* $Z_{R,d}$ DIN 18800 kN	D_{Ad} mm	SW_{Ad} mm	SB_{Ad} mm	L mm	Verstellweg *take up* ± mm	B mm	d_B mm	d_S mm
860-988	16	56	24	19	10	300	23	15	14	10,1
860-988	20	81	30	24	12	368	29	18	16	12,2
860-988	24	109	37	30	14	440	35	23	22	14,1
860-988	27	158	41	32	16	500	40	23	24	17,0
860-988	30	222	45	36	18	562	43	28	28	20,1
860-988	36	326	54	46	22	678	52	28	32	24,4
860-988	42	438	63	50	25	782	61	33	36	28,3
860-988	48	536	72	60	29	877	68	38	40	31,3
860-988	56	721	84	70	34	1024	82	43	50	36,3

Konstruktionsänderungen vorbehalten
Maßangaben ohne Korrosionsschutz!

Subject to technical modification
Dimensions without corrosion protection!

Appendix B: Structural Mechanics of slender structures

A number of structural analysis methodologies for tensegrity can be found in the referenced literature. Hereby, the tensegrity structure will be simplified with the knowledge of Slender Structures.

1. Bar element under normal force – cable and strut system

Derivation of equations for normal force and distributed load

Generally, tensegrity is a combination of compression struts and tension cables. These cables or struts have only one single degree of freedom in the longitudinal direction which can be considered as bar elements. The governing normal force guarantees its high-efficiency of material use. In this section three equations will be derived for a bar element undergoing axial deformation:

1) Kinematic Assumptions

A straight bar under the action of a distributed load q acting along its axis. Assuming that at the position x the cross section with area A will displace u(x), and the displacement of cross section at (x+dx) will be u(x+dx)=u+du.

Figure1 A bar under axial distributed load

This deformation is measured by the axial strain:

$$\varepsilon = \frac{u(x+dx)-u(x)}{dx} = \frac{(u+du)-u}{dx} = \frac{du}{dx} \tag{1.1}$$

$$\varepsilon = \frac{du}{dx} \tag{1.2}$$

Where u is the deformation, ε is the axial strain.

2) Constitutive Relations

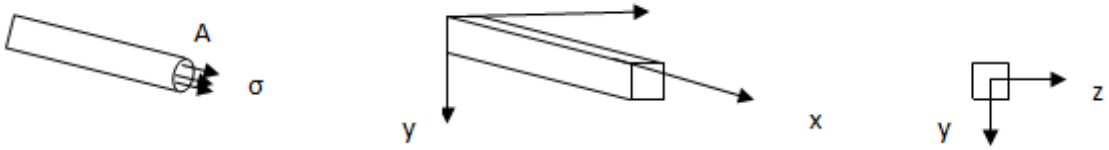

Figure 2 Elastic body under axial stress

In an elastic body, the stresses and deformations can be measured by Hooke's Law:

$$\sigma = E\varepsilon \tag{1.3}$$

Where σ is the axial stress, E is the elastic modulus.

Resultant forces can be derived by integration of the stress over the cross section area:

$$N = \int_A \sigma dA = \int_A E\frac{du}{dx}dA = E\frac{du}{dx}\int_A dA \tag{1.4}$$

$$N = EA\frac{du}{dx} \tag{1.5}$$

3) Equilibrium Equations

From the equilibrium in horizontal direction:

$$N - qdx - N - dN = 0 \tag{1.6}$$

$$\frac{dN}{dx} = -q \tag{1.7}$$

By combining the above three equations, we can get equations for normal force and distributed load:

$$N(x) = EA\frac{du}{dx} \tag{1.8}$$

$$q(x) = -EA\frac{d^2u}{dx^2} \tag{1.9}$$

Matrix displacement method

The matrix displacement method is a numerical procedure to determine displacement and stress fields of a structural system under the action of applied loads. It can be considered as a form of the finite element method.

This part will elaborate the theory of the matrix displacement method. Assume that the deformation is much smaller than the length of structure u<<L.

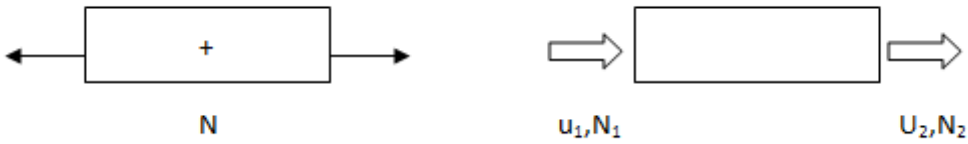

Figure 3 A bar under axial force

$$a = \begin{bmatrix} u_1 \\ u_2 \end{bmatrix} \tag{1.10}$$

$$f = \begin{bmatrix} N_1 \\ N_2 \end{bmatrix} \tag{1.11}$$

The relation between force and displacement in a bar element under axial force can be described as:

$$ka = f \tag{1.12}$$

With:

$$k = \begin{bmatrix} k_{11} & k_{12} \\ k_{21} & k_{22} \end{bmatrix} \tag{1.13}$$

The differential equation is integrated to obtain the deformation:

$$u(x) = \frac{N}{EA}x + C_1 \tag{1.14}$$

Where C_1 is a certain integration constant.

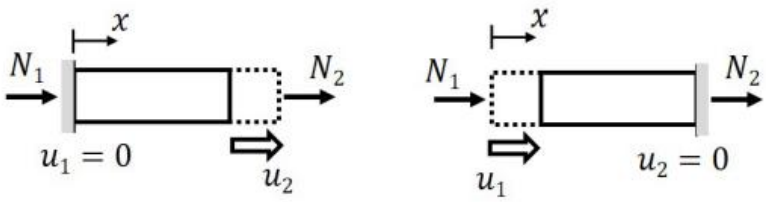

Figure 4 Boundary conditions

Applying the boundary conditions, we can get:

$$k_{11} = \frac{EA}{L} \tag{1.15}$$

$$k_{21} = -\frac{EA}{L} \tag{1.16}$$

The remaining terms of the stiffness matrix can be derived by symmetry, we obtain $k_{11}=k_{22}$, $k_{12}=k_{21}$, We can obtain the matrix equation for a 1D bar element:

$$\begin{bmatrix} N_1 \\ N_2 \end{bmatrix} = \frac{EA}{L}\begin{bmatrix} 1 & -1 \\ -1 & 1 \end{bmatrix}\begin{bmatrix} u_1 \\ u_2 \end{bmatrix} \tag{1.17}$$

To assemble the 3D tensegrity, this bar element should be transformed from a local coordinate system to a global coordinate system.

Analysing the bar element locally, and then transform and combine matrix to find the equation for the entire system is the characteristic of the matrix displacement method.

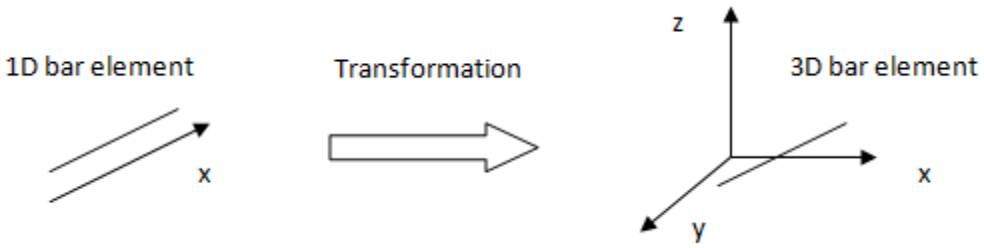

Figure 5 From local to global

To transform a bar from local coordinate system to a 3D global system, the "rotation matrix" is applied.

$$R = \begin{bmatrix} \cos\alpha & \sin\alpha & 0 \\ -\sin\alpha & \cos\alpha & 0 \\ 0 & 0 & 1 \end{bmatrix}\begin{bmatrix} \cos\beta & 0 & \sin\beta \\ 0 & 1 & 0 \\ -\sin\beta & 0 & \cos\beta \end{bmatrix}\begin{bmatrix} 1 & 0 & 0 \\ 0 & \cos\gamma & \sin\gamma \\ 0 & -\sin\gamma & \cos\gamma \end{bmatrix} \tag{1.18}$$

Where α, β, and γ are the applied rotations in x-y plane, x-z plane, and y-z plane respectively.

Then we can obtain the transformation matrix:

$$T = \begin{bmatrix} R & 0 \\ 0 & R \end{bmatrix} \tag{1.19}$$

Hence, $a' = Ta, f' = Tf, and\ k'a' = f'$, they can be written as $T^{\mathrm{T}}k'Ta = f = ka$.

We can get the global stiffness matrix:

$$K_{global} = T^{\mathrm{T}}K_{local}T \tag{1.20}$$

$$K_{global} = \frac{EA}{L}\begin{bmatrix} cos^2(\alpha) & \cos\beta\cos\alpha & \cos\gamma\cos\alpha & -cos^2(\alpha) & -\cos\beta\cos\alpha & -\cos\gamma\cos\alpha \\ \cos\alpha\cos\beta & cos^2(\beta) & \cos\gamma\cos\beta & -\cos\alpha\cos\beta & -cos^2(\beta) & -\cos\gamma\cos\beta \\ \cos\alpha\cos\gamma & \cos\beta\cos\gamma & cos^2(\gamma) & -\cos\alpha\cos\gamma & -\cos\beta\cos\gamma & -cos^2(\gamma) \\ -cos^2(\alpha) & -\cos\beta\cos\alpha & -\cos\gamma\cos\alpha & cos^2(\alpha) & \cos\beta\cos\alpha & \cos\gamma\cos\alpha \\ -\cos\alpha\cos\beta & -cos^2(\beta) & -\cos\gamma\cos\beta & \cos\alpha\cos\beta & cos^2(\beta) & \cos\gamma\cos\beta \\ -\cos\alpha\cos\gamma & -\cos\beta\cos\gamma & -cos^2(\gamma) & \cos\alpha\cos\gamma & \cos\beta\cos\gamma & cos^2(\gamma) \end{bmatrix} \tag{1.21}$$

It can be concluded that the key factors that influence the stiffness are:

- Extensional rigidity (EA) – Material use and section size
- Shape of the structure
- Length of element

The increase of the extensional rigidity has a positive effect on the increase of the global stiffness. The increase of the element length, however, has a negative effect on the structure.

In this case, the global stiffness matrix has 3 degrees of freedom for each node in the model. Next step is to solve the system by applying the boundary conditions and forces to the equation. After inverting the system, we can obtain the deformation of each node by equation $K^{-1}f = u$. Then the strain $\varepsilon = \frac{du}{dx}$ is easily found. With Hooke's law $N = \sigma A = EA\varepsilon$, we can find the normal forces.

2. Beam element under bending – hoop system

The hoop system consists of a square beam system transferring bending moments and shear forces from the tensegrity cable net system to the surrounding walls and floors to keep the structure stable. For the investigation of the hoop structure, physical non-linear and geometrical non-linear performances are not considered.

Euler-Bernoulli beam Bending

According to the Euler-Bernoulli beam theory, bending M occurs with a resultant shearing force V. However, here we take the assupmtion that shear stiffness $GA_s \to \infty$, thus the rotation of the axis of the beam is infinitesimal and shear strain is approximately zero. The beam is linear with symmetrical cross section.

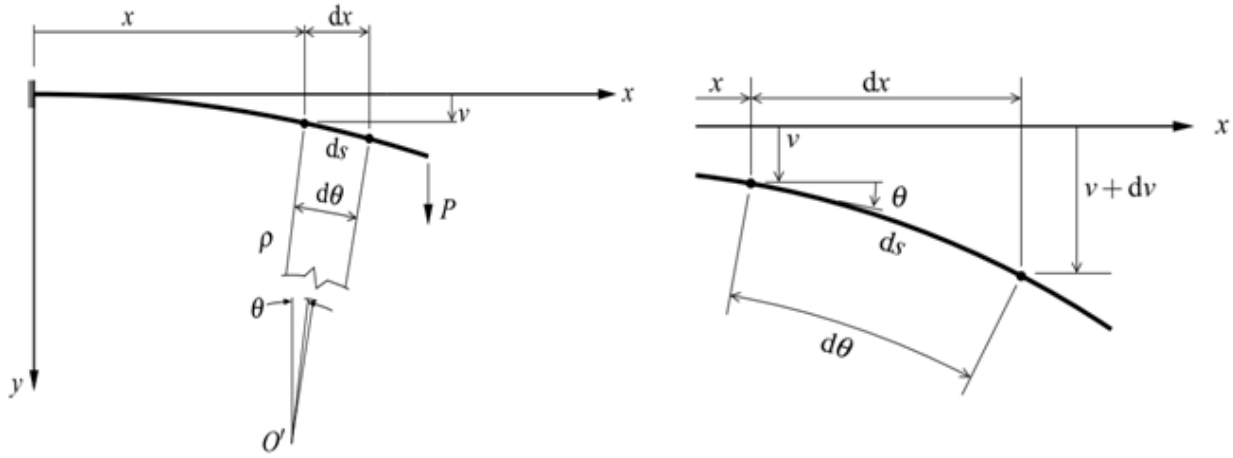

Figure 6 Cantilever beam under shear force

From basic geometric considerations, we can get:

$$ds = \rho d\theta \tag{2.1}$$

$$\kappa = \frac{1}{\rho} = \frac{d\theta}{ds} \tag{2.2}$$

With κ the curvature and ρ the radius of curvature.

By assumption that the rotation of the axis of the beam is infinitesimal, we get $\tan\theta \approx \theta$ and $\cos\theta \approx 1$.

$$dv = dx \tan\theta \approx \theta dx \tag{2.3}$$

$$dx = ds \cos\theta \approx ds \tag{2.4}$$

Taking the first derivative of θ and using the expressin of curvature we obtain **the relationship between deflection and curvature**:

$$\kappa = \frac{1}{\rho} = \frac{d^2v}{dx^2} = \theta' \tag{2.5}$$

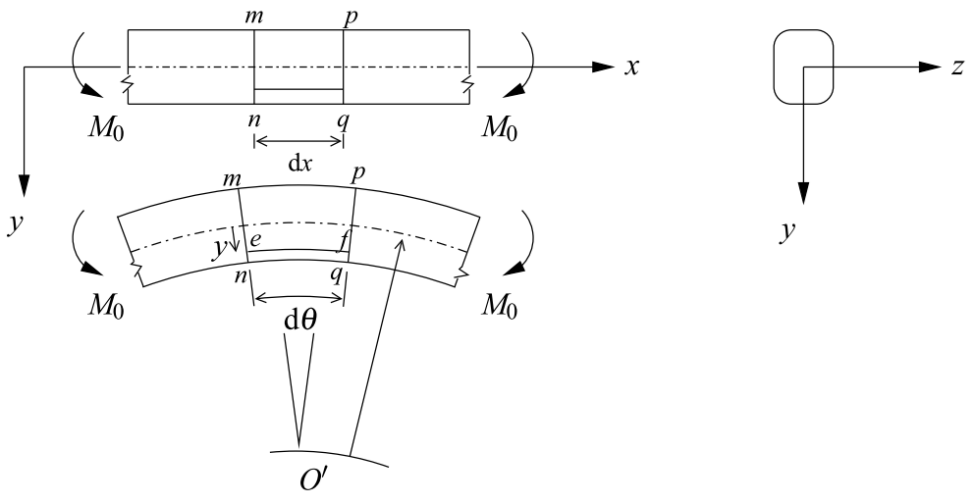

Figure 7 Beam under pure bending

In Figure 7, a portion of beam is loaded in pure bending by two couples M_0 . Due to deformation, the upper part above neutral plane is in tension and the lower part in compression. According to the defintion of neutral plane, the length of fibers on the neutral plane remains unchanged as dx.

Take a fiber with a vertical distance y to the neutral axis, assume the length to be ds.

$$dx = \rho d\theta \tag{2.6}$$

$$ds = (\rho - y)d\theta \tag{2.7}$$

Hence, the strain in the portion after bending can be calculated:

$$\varepsilon = \frac{ds-dx}{dx} = -y\frac{d\theta}{dx} \tag{2.8}$$

We can obtain **the relationship between the curvature and longitudinal strain**:

$$\varepsilon = -\kappa y = -\frac{d^2v}{dx^2}y \tag{2.9}$$

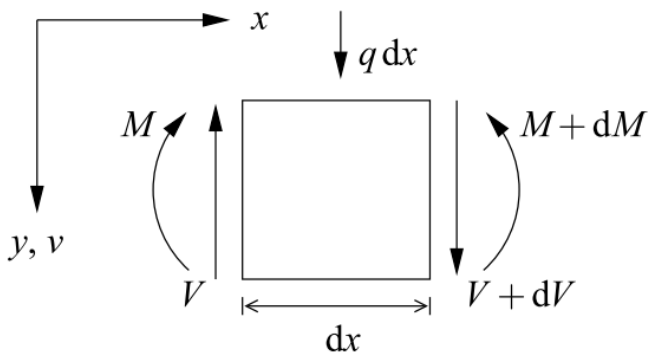

Figure 8 Element with length dx of a beam

Take an infinitesimal element dx of a beam under bending with a distributed load q as is shown in Figure 7, By equilibrium ,we can get **the relationship between load, shear force and bending moment**:

$$\frac{dV}{dx} = -q \tag{2.10}$$

$$\frac{dM}{dx} = V \tag{2.11}$$

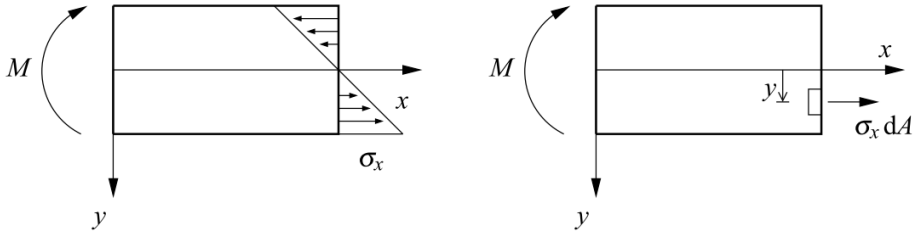

Figure 9 Cross section of a beam under bending

Then select a part of the beam under bending, we firstly draw the corresponding stress distribution at one side of the cross section. The equilibrium can be obtained by integration of the moments over the corss section area:

$$M = \int dM = \int \sigma_x \, ydA = \int E\varepsilon ydA - E\kappa \int y^2 dA \tag{2.12}$$

We can obtain **the relationship between internal bending moment and curvature**:

$$M = -EI\kappa = -EI\frac{d^2v}{dx^2} \tag{2.13}$$

By combining equations above,

$$V = -EI\frac{d^3v}{dx^3} \tag{2.14}$$

$$q = EI\frac{d^4v}{dx^4} \tag{2.15}$$

By integration of equation, we can get the equations for V, M ,θ, and v expressed by q:

$$-V = EIv''' = qx + C_1 \tag{2.16}$$

$$-M = EIv'' = \frac{1}{2}qx^2 + C_1x + C_2 \tag{2.17}$$

$$EI\theta = EIv' = \frac{1}{6}qx^3 + \frac{1}{2}C_1x^2 + C_2x + C_3 \tag{2.18}$$

$$EIv = \frac{1}{24}qx^4 + \frac{1}{6}C_1x^3 + \frac{1}{2}C_{2x^2+}C_3x + C_4 \tag{2.19}$$

It can be concluded that the key factors that influence the performances under bending are:

- Bending stiffness (EI) – Material and cross section
- External loads on the beam

The increase of the bending stiffness has a positive effect on the decrease of the resulting deflection.

In this case, the next step is to solve the system by applying the boundary conditions and external forces to the equation.

Deflection due to Shear forces

According to the Euller-Bernoulli beam theory, bending M occurs with a resultant shearing force V. In the investigation we take an ideal shear beam with bending stiffness $EI \to \infty$ as an example, assuming a constant shear stress over a cross section at the same time no flexural deformation is taken into account.

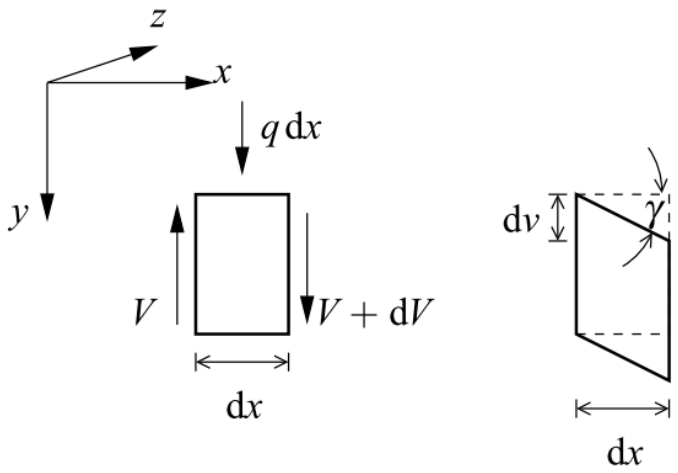

Figure 10 Cross section of a beam under shear

As is shown in the Figure 10, the shear distortion can be expressed by deflection with regard to kinematic relationship:

$$\gamma = \frac{dv}{dx} \tag{2.20}$$

Assuming a linear elastic material, the consitutive relationship can be derived from Hooker's law:

$$\tau = G\gamma \tag{2.21}$$

Considering the general expression of stress, the shear stress can be formulated as:

$$\tau = \frac{V}{A_s} \tag{2.22}$$

Where A_s is the effective area under shear. We can express the shear deformation as:

$$\gamma = \frac{V}{GA_s} \tag{2.23}$$

From the equilibrium in y direction:

$$q = -\frac{dV}{dx} \tag{2.24}$$

$$q(x) = -GA_s\frac{d^2v}{dx^2} \tag{2.25}$$

By integration of equation, we can get the equations for V and v expressed by q:

$$-V = -GA_s\frac{dv}{dx} = qx + C_1 \tag{2.26}$$

$$-GA_s v = \frac{1}{2}qx^2 + C_1x + C_2 \tag{2.27}$$

It can be concluded that the key factors that influence the performances under shear are:

- Shear stiffness (GA_s) – Material and effective shear area
- External loads on the beam

The increase of the shear stiffness has a positive effect on the decrease of the resulting deflection.

In this case, the next step is to solve the system by applying the boundary conditions and external forces to the equation. We can easily find the deflection and shear forces.

Deformation ratio of shear to bending

While designing a beam, we normally go ahead drawing the bending moment diagram to find the maximum bending moment value rather than trying to find the maximum shear stress value. Most of the time shear stress is ignored with the reasons below:

- The value of the maximum shear stress is negligible compared to the maximum bending stress value in most cases of beam design. Similarly, the deformation due to shear is negligible compared to that due to bending.
- The maximum bending stress occurs at the extreme fibre from the neutral axis and the maximum shear stresses occur at the neutral axis.

The deformation of compression hoop includes bending, shear, and axial deformation under external loads. Generally, the axial and shear deformation are very small that can be ignored .

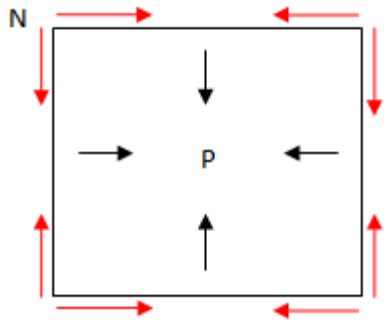

Figure 11 Cross section of a beam element under external loads

Here we suppose a simply supported beam with a point load P at the middle of the span l. The following formula can be obtained:

Flexural deformation:

$$\delta_b = \frac{Pl^3}{12EI} \tag{2.28}$$

Where EI is the flexural stiffness.

Shear deformation:

$$\delta_s = \frac{kPl}{GA} \tag{2.29}$$

Where GA is the shear stiffness, k is the coefficient of shear stress distributing along the section.

Axial deformation:

$$\delta_N = \frac{Nl}{EA} \tag{2.30}$$

Where EA is the axial stiffness, N is the axial force.

The ratio between shear and bending deformation is:

$$\eta = \frac{\delta_s}{\delta_b} = \frac{12EIk}{GAl^2} \tag{2.31}$$

Here we assume the cross section to be a solid rectangle with width b and height h, we get k=1,2, Steel will be applied as the beam material, we get G=78Gpa, E=210 GPa.

$$\eta = 3{,}23 \times \left(\frac{h}{l}\right)^2 \tag{2.32}$$

With $h \ll l$,$\eta \to 0$, which means $\delta_s \ll \delta_b$.

Thus the deformation resulted from shear can be ignored compared to that from bending. From equations above we can see that the axial and shear deformation are of the same magnitude.

In conclusion, both axial and shear deformation are very small compared to the relatively large flexural deformation.

Appendix C: Code for Plug-in GHToFem

In appendix C, the coding part for Plug-in GHToFem is introduced. These codes can be rewritten or just copy paste for the future development of plug-ins with similar functions.

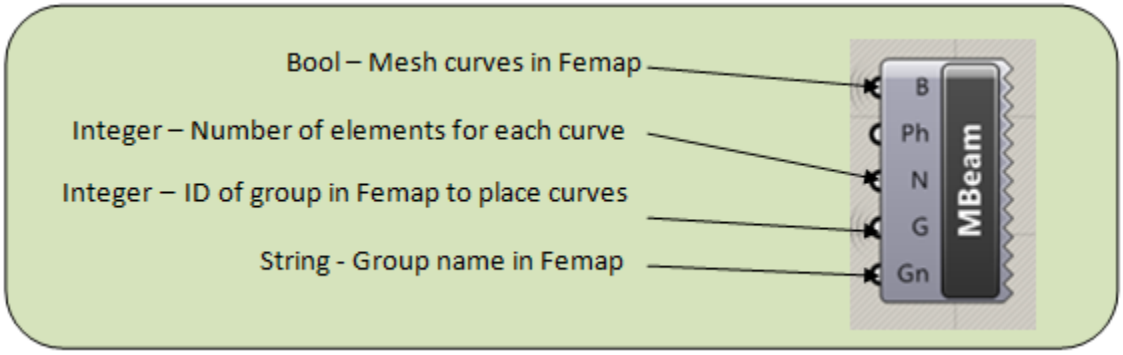


```
#Region "Coding"

    Protected Overrides Sub SolveInstance(DA As IGH_DataAccess)
        'TESTCN
        'Get and check data
        Dim Stream As New Boolean()
        If Not DA.GetData(0, Stream) Then Return

        'Check if the component is to write to femap
        If Stream Then
            'Get the aditional data
            Dim filePath As String = Nothing
            Dim NumElem As Integer = Nothing
            Dim GrID As Integer = Nothing
            Dim FemGroupName As String = Nothing
            If Not DA.GetData(1, filePath) Then Return
            If Not DA.GetData(2, NumElem) Then Return
            If Not DA.GetData(3, GrID) Then Return
            If Not DA.GetData(4, FemGroupName) Then Return

            'Optional get name

            'Set the reference to active femap
            ' Dim FemMod As femap.model =
DirectCast(System.Runtime.InteropServices.Marshal.GetActiveObject("femap.model"),
femap.model)
            'Dim FemMod As femap.model = GetObject(, "femap.model") 'Optional variation
            Dim App As femap.model
            App = GetObject(, "femap.model")
            'If supplied, open a specific file of femap for editing
            If Not filePath = "" Then App.feFileOpen(False, filePath)

            'Dim variables that are used to get results from Femap
            Dim propertyId As Integer
            Dim beamOrientation(2) As Double
            Dim curveSet As femap.Set
            curveSet = App.feSet
            If GrID = 0 Or GrID = Nothing Then
                curveSet.AddAll(zDataType.FT_CURVE)
```

```
            Else
                curveSet.AddGroup(zDataType.FT_CURVE, GrID)
            End If

            Dim beforeMeshSetElem As femap.Set = App.feSet
            Dim beforeMeshSetNode As femap.Set = App.feSet
            beforeMeshSetElem.AddAll(femap.zDataType.FT_ELEM)
            beforeMeshSetNode.AddAll(femap.zDataType.FT_NODE)
            'set mesh size for curve 1 ,amount = 1 element. It is possible use set of
curves
            App.feMeshSizeCurve(curveSet.ID, NumElem, 0, 0, 0, 0, 0, 0, 0, 0, True)
            'alternatively you can set amount of elements
            'App.feMeshSizeCurve(-curveId, 4, 0, 0, 0, 0, 0, 0, 0, 0, True)
            App.feMeshCurve(curveSet.ID, True, propertyId, beamOrientation)
            'mesh one curve (minus is used for single id)

            Dim afterMeshSetElem As femap.Set = App.feSet
            Dim afterMeshSetNode As femap.Set = App.feSet

            afterMeshSetElem.AddAll(femap.zDataType.FT_ELEM)
            afterMeshSetElem.RemoveSet(beforeMeshSetElem.ID)
            afterMeshSetNode.AddAll(femap.zDataType.FT_NODE)
            afterMeshSetNode.RemoveSet(beforeMeshSetNode.ID)


            Dim nodeSet As femap.Set
            nodeSet = App.feSet
            'merge coincident nodes
            nodeSet.AddAll(femap.zDataType.FT_NODE)
            App.feCheckCoincidentNode2(nodeSet.ID, 0,00000001, True, 0, 0, True, 0, False)

            Dim FemGroup As femap.Group = App.feGroup()
            FemGroup.SetAdd(zDataType.FT_ELEM, afterMeshSetElem.ID)
            FemGroup.SetAdd(zDataType.FT_NODE, afterMeshSetNode.ID)
            FemGroup.title = FemGroupName
            FemGroup.Put(GrID)

            App.feViewRegenerate(0)

        End If
    End Sub

#End Region
```

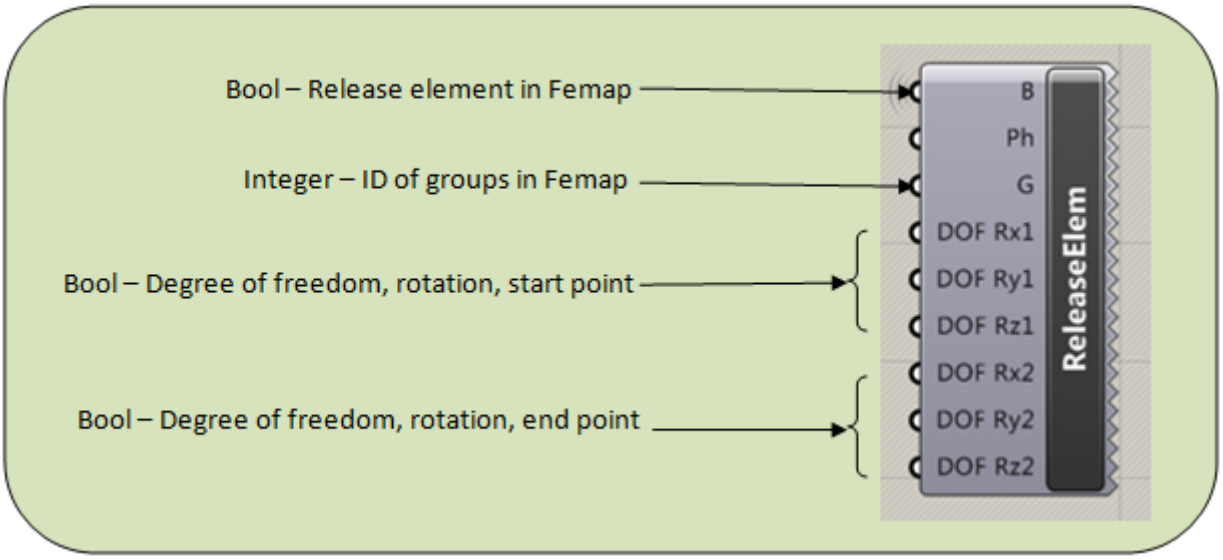


```
#Region "Coding"

    Protected Overrides Sub SolveInstance(DA As IGH_DataAccess)
        Dim Stream As New Boolean()
        If Not DA.GetData(0, Stream) Then Return
        If Stream Then
            Dim filePath As String = Nothing
            Dim GrID As Integer = Nothing
            Dim Rx1 As Integer = 0
            Dim Ry1 As Integer = 0
            Dim Rz1 As Integer = 0
            Dim Rx2 As Integer = 0
            Dim Ry2 As Integer = 0
            Dim Rz2 As Integer = 0
            Dim Tx1 As Integer = 0
            Dim Ty1 As Integer = 0
            Dim Tz1 As Integer = 0
            Dim Tx2 As Integer = 0
            Dim Ty2 As Integer = 0
            Dim Tz2 As Integer = 0

            If Not DA.GetData(1, filePath) Then Return
            If Not DA.GetData(2, GrID) Then Return
            If Not DA.GetData(3, Rx1) Then Return
            If Not DA.GetData(4, Ry1) Then Return
            If Not DA.GetData(5, Rz1) Then Return
            If Not DA.GetData(6, Rx2) Then Return
            If Not DA.GetData(7, Ry2) Then Return
            If Not DA.GetData(8, Rz2) Then Return

            Dim App As femap.model
            App = GetObject(, "femap.model")
            If Not filePath = "" Then App.feFileOpen(False, filePath)

            Dim elem As femap.Set = App.feSet
            If GrID = 0 Or Nothing Then
                elem.AddAll(zDataType.FT_ELEM)
            Else
```

```
                elem.AddGroup(zDataType.FT_ELEM, GrID)
            End If
            Dim c As Boolean() = {Tx1, Ty1, Tz1, Rx1, Ry1, Rz1}
            Dim d As Boolean() = {Tx2, Ty2, Tz2, Rx2, Ry2, Rz2}

            App.feModifyElemRelease(elem.ID, c, d)
            'App.feModifyElemRelease(elem.ID, New Boolean(False, False, False, True, True,
True), New Boolean(False, False, False, False, False, False))

            App.feViewRegenerate(0)

        End If
    End Sub


#End Region
```

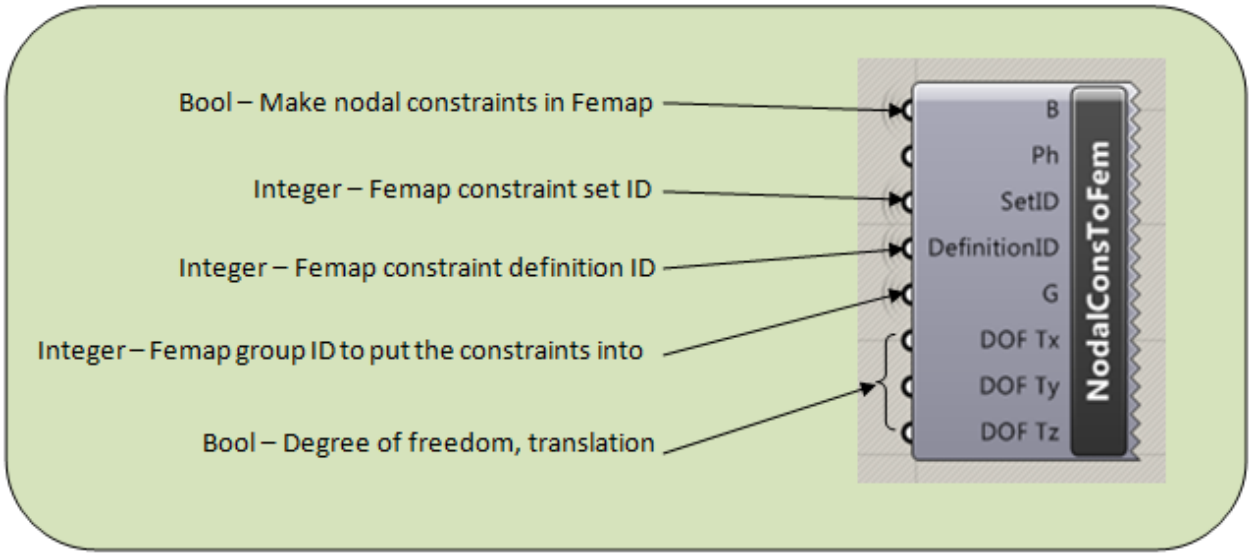


```
#Region "Coding"

    Protected Overrides Sub SolveInstance(DA As IGH_DataAccess)
        Dim Stream As New Boolean()
        If Not DA.GetData(0, Stream) Then Return
        If Stream Then
            Dim filePath As String = Nothing
            Dim constraintSetID As New Integer
            Dim constraintDefinitionID As New Integer
            Dim GrID As Integer = Nothing
            Dim Tx As New Integer
            Dim Ty As New Integer
            Dim Tz As New Integer

            If Not DA.GetData(1, filePath) Then Return
            If Not DA.GetData(2, constraintSetID) Then Return
            If Not DA.GetData(3, constraintDefinitionID) Then Return
            If Not DA.GetData(4, GrID) Then Return
            If Not DA.GetData(5, Tx) Then Return
            If Not DA.GetData(6, Ty) Then Return
            If Not DA.GetData(7, Tz) Then Return

            Dim App As femap.model =
DirectCast(System.Runtime.InteropServices.Marshal.GetActiveObject("femap.model"),
femap.model)
            If Not filePath = "" Then App.feFileOpen(False, filePath)

            'Dim variables that are used to get results from Femap

            Dim constraint As femap.BCSet = App.feBCSet
            'constraintSetID = constraint.NextEmptyID
            constraint.title = "Nodal Constraint"
            constraint.Put(constraintSetID)

            Dim constraintDefinition As femap.BCDefinition = App.feBCDefinition
            constraintDefinition.title = "Nodal Constraint"
            constraintDefinition.OnType = femap.zDataType.FT_NODE
            constraintDefinition.dataType = femap.zDataType.FT_BCO
```

```
            constraintDefinition.setID = constraintDefinitionID
            Dim definitionID As femap.zReturnCode = constraintDefinition.NextEmptyID
            constraintDefinition.Put(definitionID)

            Dim constraintNode As femap.BCNode = App.feBCNode
            constraintNode.setID = constraintSetID
            constraintNode.BCDefinitionID = constraintDefinition.ID


            Dim nodeSet As femap.Set = App.feSet
            nodeSet.AddGroup(zDataType.FT_NODE, GrID)
            constraintNode.Add(nodeSet.ID, Tx, Ty, Tz, False, False, False)


            App.feViewRegenerate(0)

        End If
    End Sub

#End Region
```

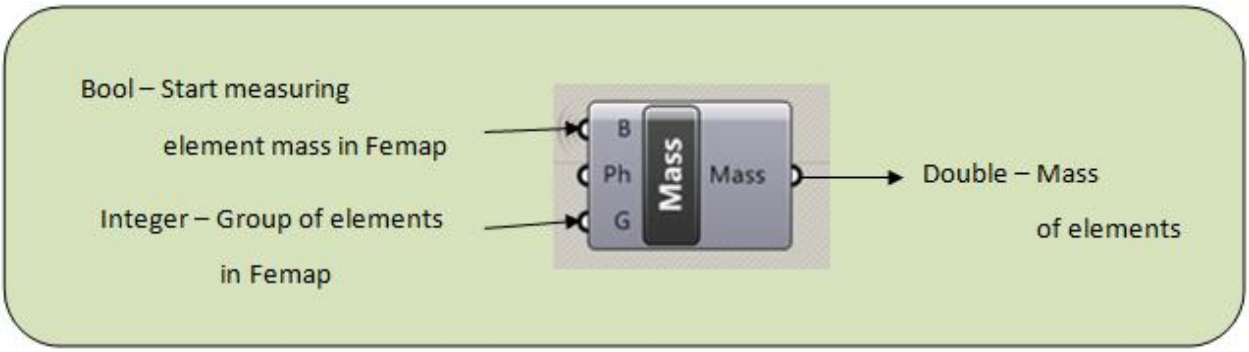


```
#Region "Coding"

    Protected Overrides Sub SolveInstance(DA As IGH_DataAccess)
        Dim Stream As New Boolean()
        If Not DA.GetData(0, Stream) Then Return
        If Stream Then
            Dim filePath As String = Nothing
            Dim GrID As Integer = Nothing
            If Not DA.GetData(1, filePath) Then Return
            If Not DA.GetData(2, GrID) Then Return
            Dim App As femap.model
            App = GetObject(, "femap.model")
            'If supplied, open a specific file of femap for editing
            If Not filePath = "" Then App.feFileOpen(False, filePath)
            Dim Mass As Double
            Dim elem As femap.Set = App.feSet
            If GrID = 0 Or GrID = Nothing Then
                elem.AddAll(zDataType.FT_ELEM)
            Else
                elem.AddGroup(zDataType.FT_ELEM, GrID)
            End If

            Dim tlen As Double
            Dim tarea As Double
            Dim tvolume As Double
            Dim tstructMass As Double
            Dim tnonstructMass As Double
            Dim ttotalMass As Double
            Dim tstructCG As Double() = Nothing
            Dim tnonstructCG As Double() = Nothing
            Dim ttotalCG As Double() = Nothing
            Dim tinertia As Double() = Nothing
            Dim tinertiaCG As Double() = Nothing

            App.feMeasureMeshMassProp(elem.ID, 0, False, False, tlen, tarea, tvolume,
tstructMass, tnonstructMass, ttotalMass, tstructCG, tnonstructCG, ttotalCG, tinertia,
tinertiaCG)
            Mass = ttotalMass
            DA.SetData(0, Mass)
            'regenerate view to see created mesh
            App.feViewRegenerate(0)

        End If
    End Sub

#End Region
```

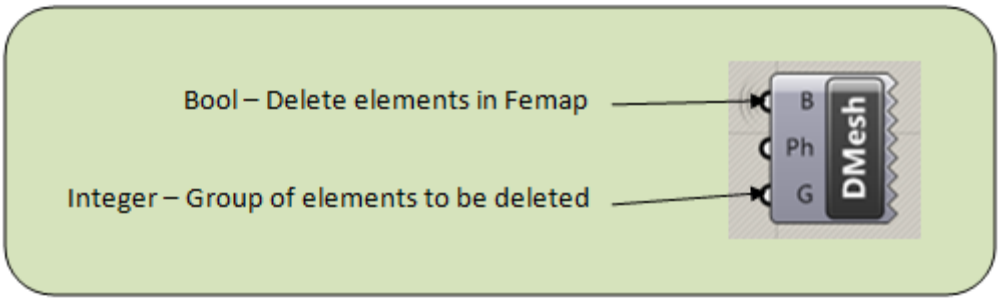


```
#Region "Coding"

    Protected Overrides Sub SolveInstance(DA As IGH_DataAccess)
        Dim Stream As New Boolean()
        If Not DA.GetData(0, Stream) Then Return
        If Stream Then
            Dim filePath As String = Nothing
            Dim GrID As Integer = Nothing
            If Not DA.GetData(1, filePath) Then Return
            If Not DA.GetData(2, GrID) Then Return

            'Optional get name

            'Set the reference to active femap
            ' Dim FemMod As femap.model =
DirectCast(System.Runtime.InteropServices.Marshal.GetActiveObject("femap.model"),
femap.model)
            'Dim FemMod As femap.model = GetObject(, "femap.model") 'Optional variation
            Dim App As femap.model
            App = GetObject(, "femap.model")
            If Not filePath = "" Then App.feFileOpen(False, filePath)
            Dim elem As femap.Set = App.feSet
            Dim crv As femap.Set = App.feSet
            Dim nod As femap.Set = App.feSet
            If GrID = 0 Or Nothing Then
                elem.AddAll(zDataType.FT_ELEM)
                nod.AddAll(zDataType.FT_NODE)
            Else
                elem.AddGroup(zDataType.FT_ELEM, GrID)
                nod.AddGroup(zDataType.FT_NODE, GrID)
            End If

            App.feDeleteAll(True, False, False, True)
            'Delete Geometry
            App.feDelete(zDataType.FT_ELEM, elem.ID)
            App.feDelete(zDataType.FT_NODE, nod.ID)
            App.feViewRegenerate(0)

        End If
    End Sub

#End Region
```

Appendix D: Fixed Joint, One Hinge, and Two Hinges for the Struts

In the beginning of the design, a simply study was done to find out the influence of the choice of connection between elements. Three types of connection for the struts were investigated, the hinges are displayed in the figures below:

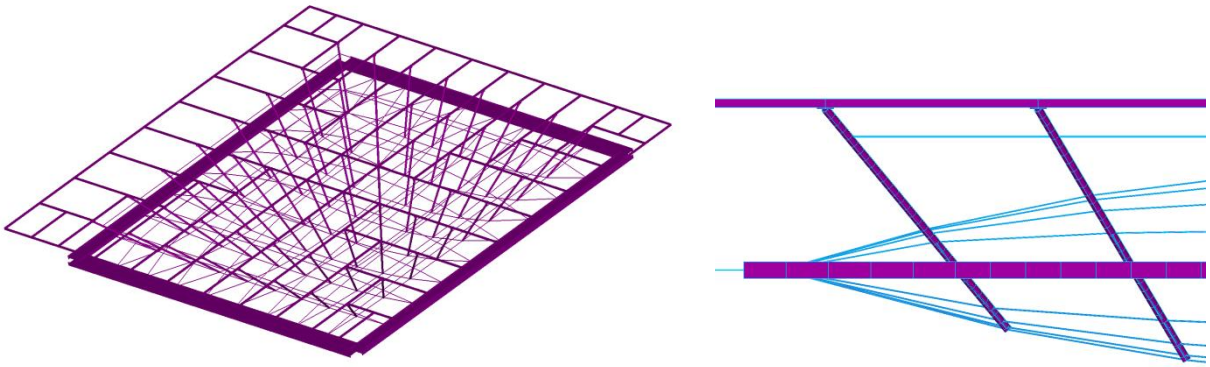

Fixed Connection

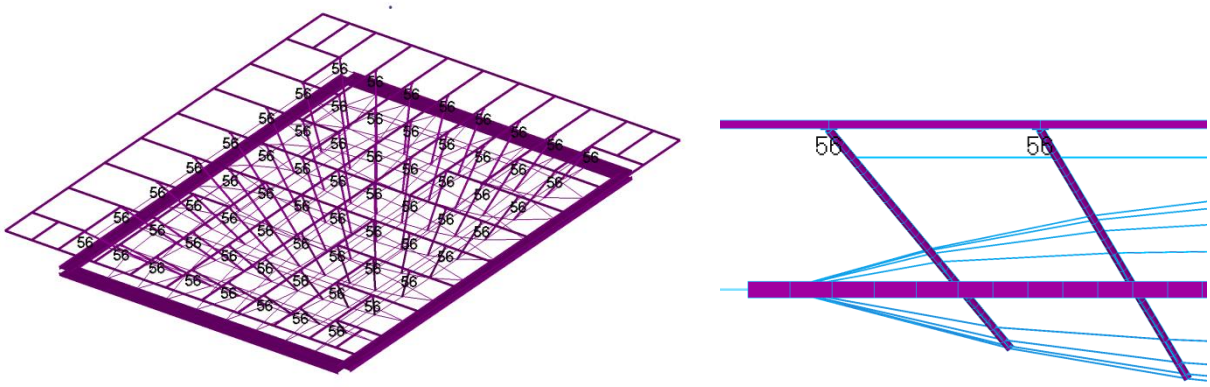

One Hinge

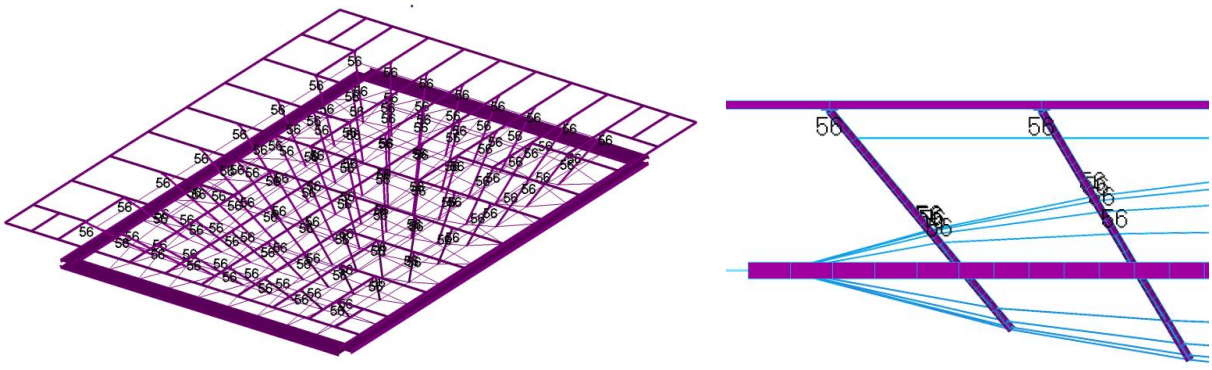

Two Hinges

Results shows that fix connections can give false impression of stability. However, making hinges at the wrong place leads to an unstable structure. To reach a good design, careful attention needs to be paid to the modelling. Results are displayed as follows:

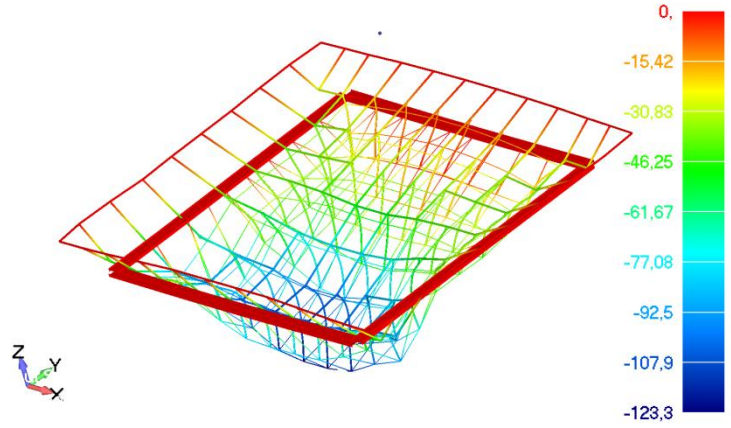

Connection

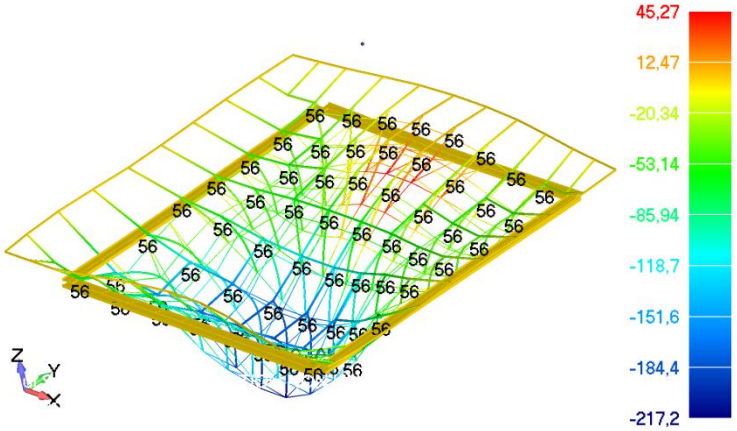

One Hinge

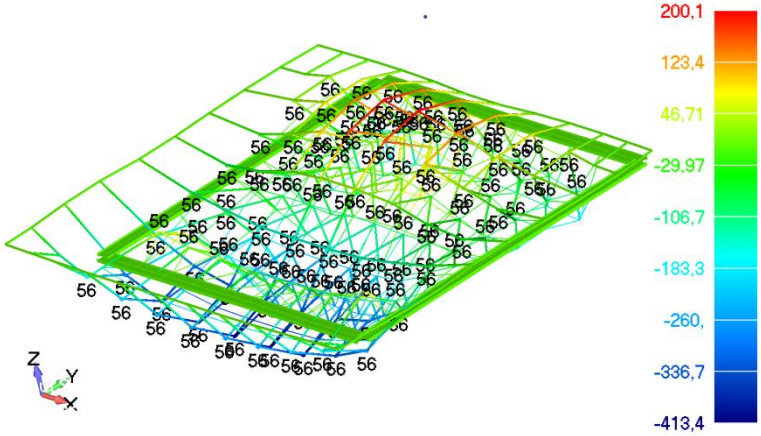

Two Hinges

Appendix E: Bolt Region and Bolt Preload in Femap

In Femap, the Bolt Region command creates individual regions of a single element or multiple elements where allows the designer to apply a bolt "preload". Bolt preload is available for FEMAP-supported Nastran Solution Sequences 101 (Linear Static Analysis), 103 (Modal Analysis), 105 (Buckling Analysis), 107 through 112 (Complex Modal Analysis and Dynamic Analysis) and 601(Advanced Nonlinear Analysis). For all these solution sequences except SOL 601 (Advanced Nonlinear Analysis), only 1 element should be in each bolt region. Bolt regions may be defined on either Beam or Bar elements, the nodes of Solid elements, or Solid elements themselves for SOL 601.

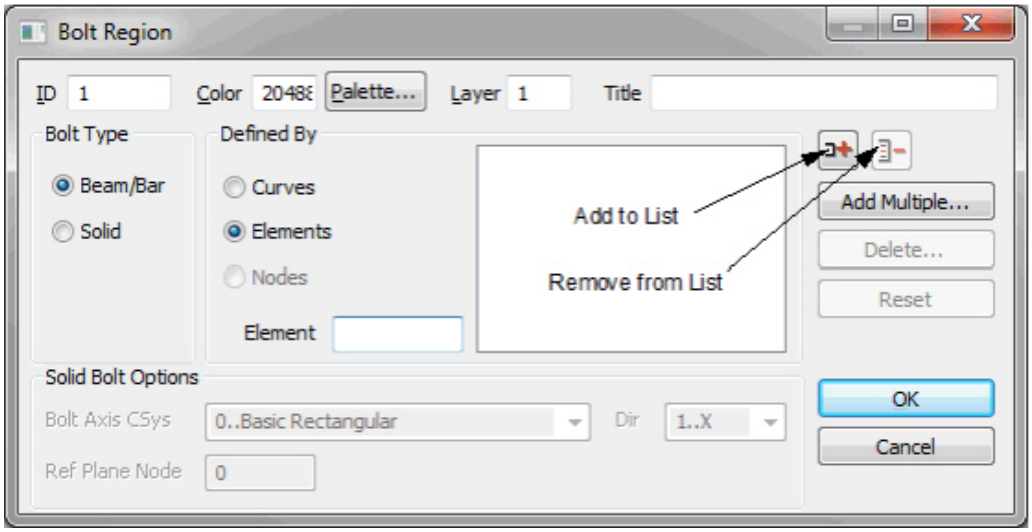

Interface for Bolt Region command

Each region represents a "bolt" and there can be multiple "bolts" in a single model, all with unique "preloads". The "preload" is a specified torque which has been translated into an axial load, arising from components in an assembly being bolted together.

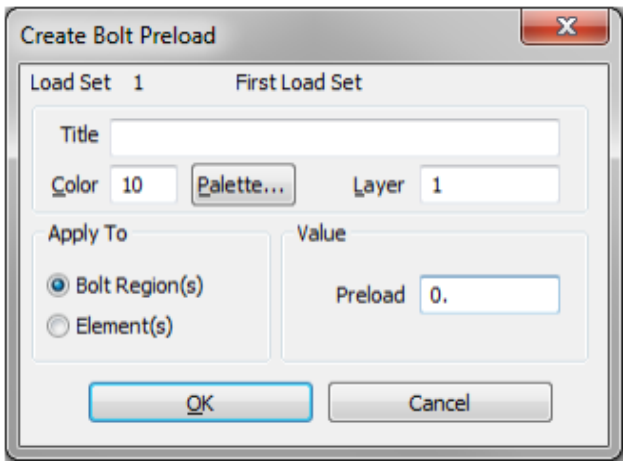

Interface for Create Bolt Preload command

The Create Bolt Preload command creates a load representing a "Bolt Preload" for NX Nastran. The Bolt Preload is available for use in Linear Static Analysis, Modal Analysis, Buckling, and Advanced Nonlinear Analysis.

Currently, Bolt Preloads can only be applied to Beam and Bar elements.

Appendix F: Translate area load to line load

In this design, the variable loads from wind and snow are described as area load which will be taken by the ETFE cushion on above the steel structure. However, it is necessary to convert these area loads into line loads in the FEM as accurate as possible to apply the correct load cases on this structure. Some assumptions are made as shown in the figure below:

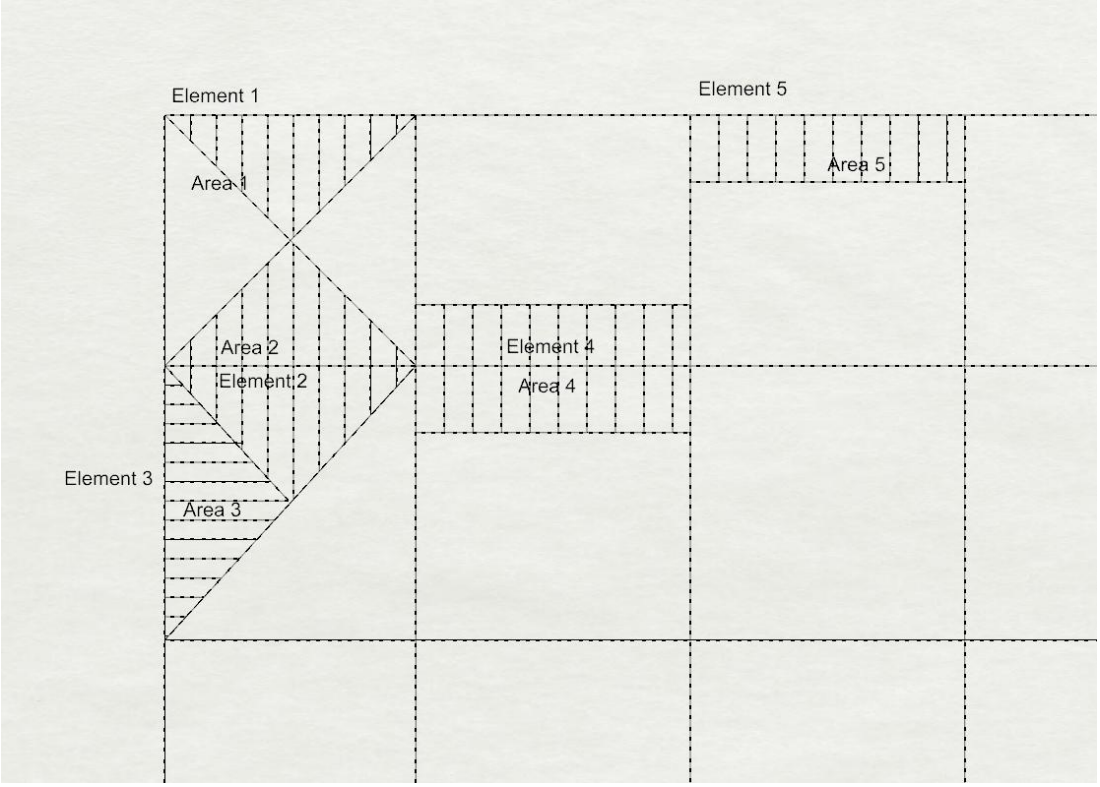

Load assumption on a single element

There are two assumptions to transfer area load into line load, the triangular shape or the rectangular shape. In both the two cases, for the elements on the grid edge, load in ¼ of the grid area is taken by the corresponding element. And for the elements in the other locations, load in ½ of the grid area is taken by the corresponding element. Thus the total amount of forces are the same in both assumptions.

The real situation is that each element shares the load in the triangular area, but it would be too laborious to model this load case in the FEM software. Therefore, it is assumed that the line load is distributed on each element, the magnitude is taken as the load from ½ of the corresponding grid area.

To calculate the right magnitude of the line load on each element, Grasshopper is used to model the variable load case. The magnitude of snow and wind load are expressed in the following 3D model. For each element, the volume lies in the corresponding rectangular area is the magnitude of this load case in the element.

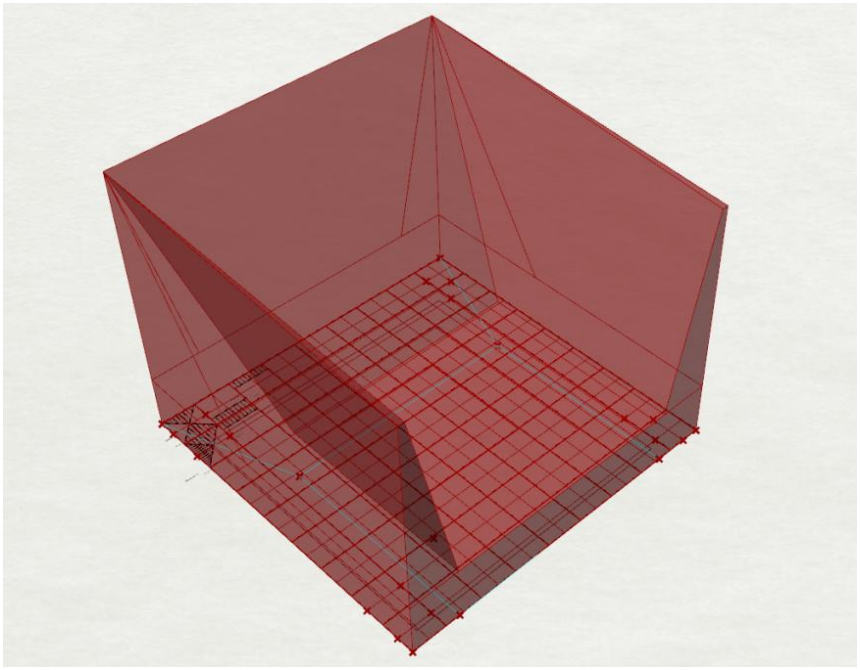

3d model for snow load

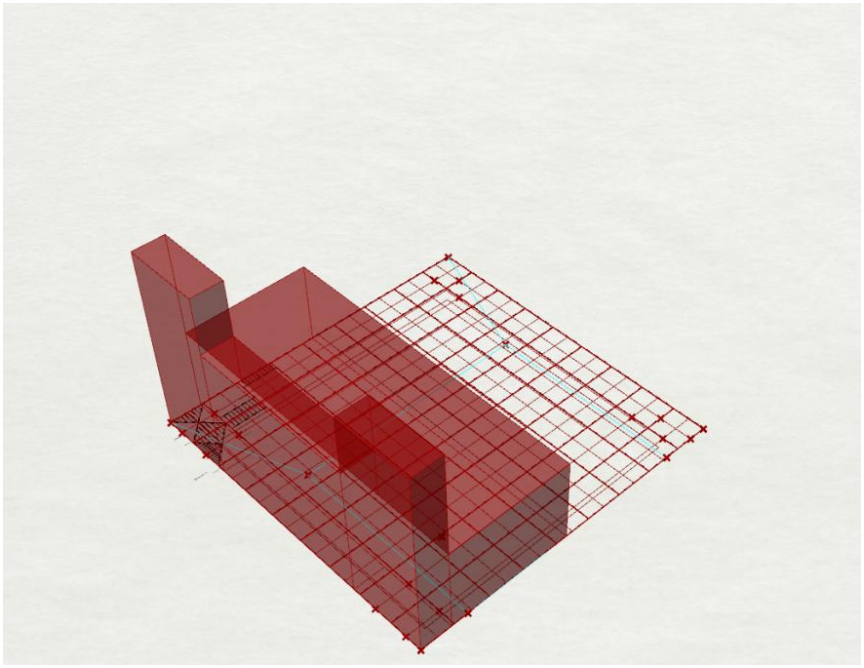

3d model for wind load

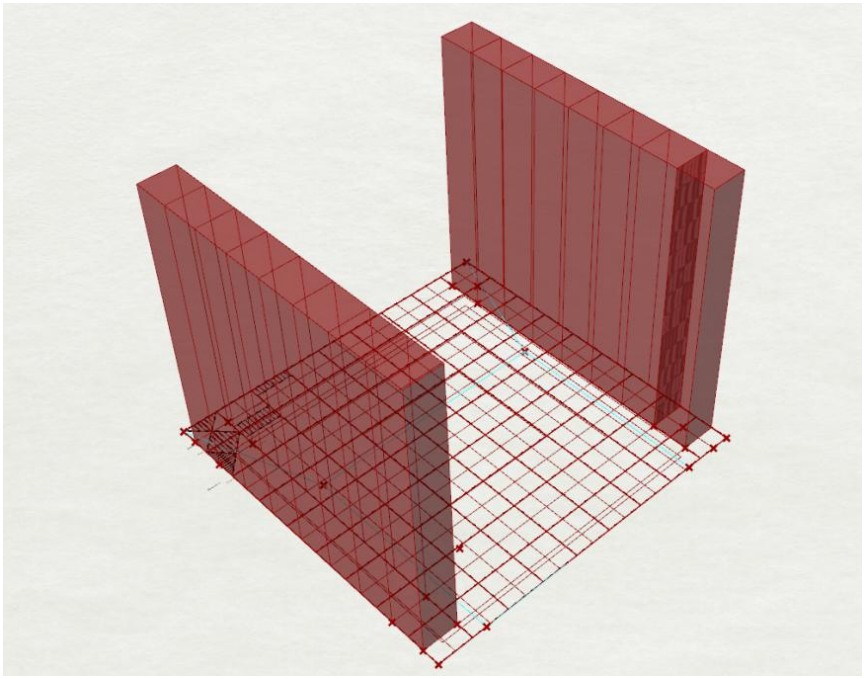

Element and corresponding cuboid in the rectangular area

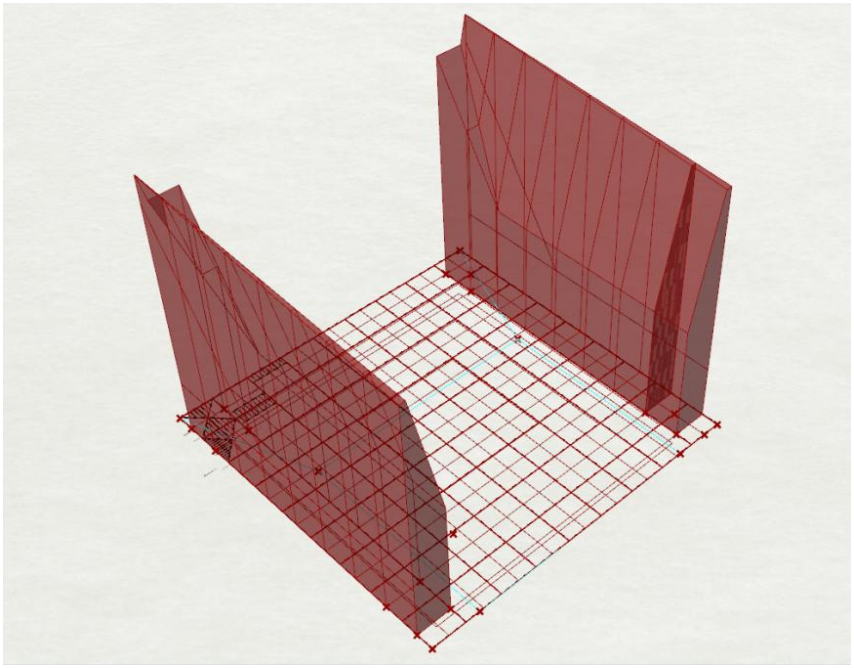

Solid difference representing the amount of snow load on elements

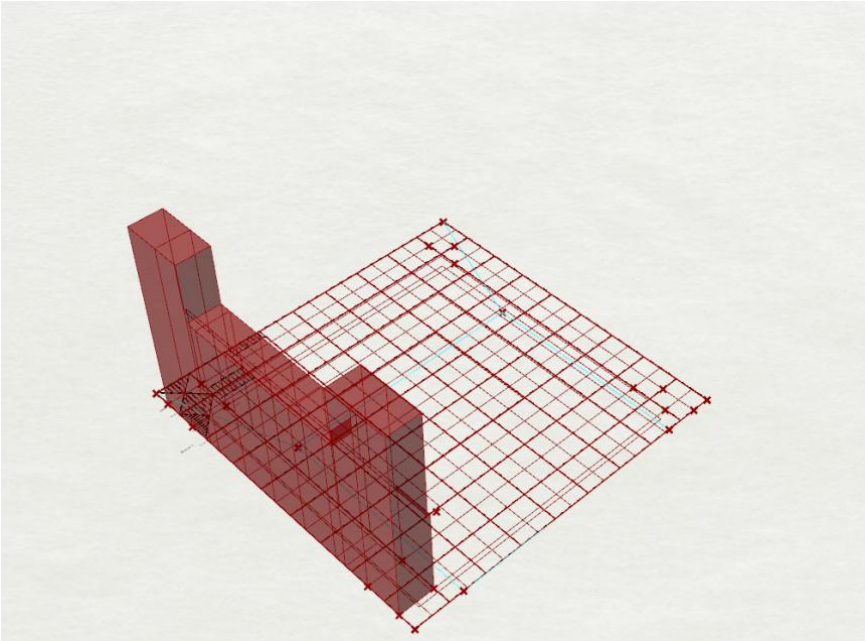

Solid difference representing the amount of wind load on elements

The volume of the solid difference is taken as the amount of variable load for the corresponding elements. Some hand calculation can be expressed as:

$$q_{line} = q_{area} \times A/2l$$

Where *A* is the area of the corresponding grid for the specific element,

l is the length of the single beam element.

Appendix G: Static analysis results of models in variable study

1. Change number of branches

6	Unity check	
Order of variable	**Topological/Geometrical**	**Choice**
1st	Number of branches	6x6
2nd	Position of intersection point	z=-13260
3rd	Height above support	2250mm
	Height below support	2350mm
4th	Way of form finding	radial pattern
5th	Pretension for top cable (kN)	230
	Pretension for bottom cable (kN)	200

Load combinations	**Displacement (mm)<143**	
	upward	downward
SLS LC1 1,0dead+1,0pre	0	-76
SLS LC2 1,0snow+1,0dead+1,0pre	3	-131
SLS LC3 1,0wind+1,0dead+1,0pre	53	-72

Type of connection	Number	Mass (kg)
ETFE beam connection	64	960
cable and strut connection	72	5760
total		6720

6th	Cross section		ULS LC2 1,5snow+1,2dead+1,0pre			ULS LC3 1,5wind+0,9dead+1,0pre		
			Stress/Load (Max)		UC	Stress/Load (Max)		UC
Group	Property	Mass (kg)	Quantity	Unit		Quantity	Unit	
ETFE beam	CHS139,7*5	9034	323	N/mm^2	91%	219	N/mm^2	62%
Strut	CHS177,8*17,5	12584	171	N/mm^2	48%	347	N/mm^2	98%
Hoop	h=1300mm,b=300mm, t_{flange}=50mm,t_{web}=15mm	43109	319	N/mm^2	90%	296	N/mm^2	83%
Rods	Circular bar d=65mm	94	317	N/mm^2	89%	314	N/mm^2	88%
Cable top	PG55 A=347mm^2	944	196	kN	60%	320	kN	98%
Cable bottom	PG90 A=572mm^2	1565	452	kN	84%	241	kN	45%
Rectangular cable	PG40 A=237mm^2	359	20	kN	9%	28	kN	13%

Mass without hoop	24580	Kg
Mass with hoop	67689	kg
Total mass	74409	kg

minimum tensile force in cable	1551N

6	Resulting forces	
Order of variable	**Topological/Geometrical**	**Choice**
1st	Number of branches	6x6
2nd	Position of intersection point	z=-13260
3rd	Height above support	2250mm
	Height below support	2350mm
4th	Way of form finding	radial pattern
5th	Pretension for top cable (kN)	230
	Pretension for bottom cable (kN)	200

Load combinations	**Displacement (mm)<143**	
	upward	downward
SLS LC1 1,0dead+1,0pre	0	-76
SLS LC2 1,0snow+1,0dead+1,0pre	3	-131
SLS LC3 1,0wind+1,0dead+1,0pre	53	-72

Type of connection	Number	Mass (kg)
ETFE beam connection	64	960
cable and strut connection	72	5760
total		6720

6th	Cross section		ULS LC2 1,5snow+1,2dead+1,0pre			ULS LC3 1,5wind+0,9dead+1,0pre		
Group	Property	Mass (kg)	N (kN)	M_y (kNm)	M_z (kNm)	N (kN)	M_y (kNm)	M_z (kNm)
ETFE beam	CHS139,7*5	9034	-	2,3	14,9	-	3,3	12,8
Strut	CHS177,8*17,5	12584	-	48,4	20,3	-	81,6	98,1
Hoop	h=1300mm,b=300mm, t_{flange}=50mm,t_{web}=15mm	43109	-	6731	91,2	-	6240	33,2
Rods	Circular bar d=65mm	94	-	6,1	6,2	-	6,8	7,8
Cable top	PG55 A=347mm^2	944	197	0	0	320	0	0
Cable bottom	PG90 A=572mm^2	1565	453	0	0	241	0	0
Rectangular cable	PG40 A=237mm^2	359	20	0	0	28	0	0

Mass without hoop	24580	Kg
Mass with hoop	67689	kg
Total mass	74409	kg

minimum tensile force in cable	1551N

7	Unity check	
Order of variable	**Topological/Geometrical**	**Choice**
1st	Number of branches	7x7
2nd	Position of intersection point	z=-13260
3rd	Height above support	2250mm
	Height below support	2350mm
4th	Way of form finding	radial pattern
5th	Pretension for top cable (kN)	180
	Pretension for bottom cable (kN)	165

Load combinations	**Displacement (mm)<143**	
	upward	downward
SLS LC1 1,0dead+1,0pre	4	-60
SLS LC2 1,0snow+1,0dead+1,0pre	5	-143
SLS LC3 1,0wind+1,0dead+1,0pre	56	-66

Type of connection	Number	Mass (kg)
ETFE beam connection	81	1215
cable and strut connection	98	7840
total		9055

6th	Cross section		ULS LC2 1,5snow+1,2dead+1,0pre			ULS LC3 1,5wind+0,9dead+1,0pre		
			Stress/Load (Max)		UC	Stress/Load (Max)		UC
Group	Property	Mass (kg)	Quantity	Unit		Quantity	Unit	
ETFE beam	CHS114,3*5	8247	302	N/mm^2	85%	174	N/mm^2	49%
Strut	CHS152,4*14,2	11793	160	N/mm^2	45%	345	N/mm^2	97%
Hoop	h=1300mm,b=300mm, t_{flange}=50mm,t_{web}=15mm	43109	301	N/mm^2	85%	284	N/mm^2	80%
Rods	Circular bar d=60mm	109	279	N/mm^2	79%	310	N/mm^2	87%
Cable top	PG55 A=347mm^2	1101	146	kN	45%	262	kN	80%
Cable bottom	PG75 A=467mm^2	1492	355	kN	81%	194	kN	44%
Rectangular cable	PG40 A=237mm^2	399	16	kN	7%	19	kN	9%

Mass without hoop	23141	Kg
Mass with hoop	66250	kg
Total mass	75305	kg

minimum tensile force in cable	769N

7	Resulting forces	
Order of variable	**Topological/Geometrical**	**Choice**
1st	Number of branches	7x7
2nd	Position of intersection point	z=-13260
3rd	Height above support	2250mm
	Height below support	2350mm
4th	Way of form finding	radial pattern
5th	Pretension for top cable (kN)	180
	Pretension for bottom cable (kN)	165

Load combinations	**Displacement (mm)<143**	
	upward	downward
SLS LC1 1,0dead+1,0pre	4	-60
SLS LC2 1,0snow+1,0dead+1,0pre	5	-143
SLS LC3 1,0wind+1,0dead+1,0pre	56	-66

Type of connection	Number	Mass (kg)
ETFE beam connection	81	1215
cable and strut connection	98	7840
total		9055

6th	Cross section		ULS LC2 1,5snow+1,2dead+1,0pre			ULS LC3 1,5wind+0,9dead+1,0pre		
Group	Property	Mass (kg)	N (kN)	M_y (kNm)	M_z (kNm)	N (kN)	M_y (kNm)	M_z (kNm)
ETFE beam	CHS114,3*5	8247	-	1,5	12,6	-	2,5	7,3
Strut	CHS152,4*14,2	11793	-	28,5	7,9	-	46,5	62
Hoop	h=1300mm,b=300mm, t_{flange}=50mm,t_{web}=15mm	43109	-	6370	57,6	-	6006	24,1
Rods	Circular bar d=60mm	109	-	4,2	4,2	-	4,8	6,4
Cable top	PG55 A=347mm^2	1101	146	0	0	262	0	0
Cable bottom	PG75 A=467mm^2	1492	355	0	0	194	0	0
Rectangular cable	PG40 A=237mm^2	399	16	0	0	19	0	0

Mass without hoop	23141	Kg
Mass with hoop	66250	kg
Total mass	75305	kg

minimum tensile force in cable	769N

8	Unity check	
Order of variable	**Topological/Geometrical**	**Choice**
1st	Number of branches	8X8
2nd	Position of intersection point	z=-13260
3rd	Height above support	2250mm
	Height below support	2350mm
4th	Way of form finding	radial pattern
5th	Pretension for top cable (kN)	175
	Pretension for bottom cable (kN)	160

Load combinations	**Displacement (mm)<143**	
	upward	downward
SLS LC1 1,0dead+1,0pre	0	-68
SLS LC2 1,0snow+1,0dead+1,0pre	3	-139
SLS LC3 1,0wind+1,0dead+1,0pre	27	-75

Type of connection	Number	Mass (kg)
ETFE beam connection	100	1500
cable and strut connection	128	10240
total		11740

6th	Cross section		ULS LC2 1,5snow+1,2dead+1,0pre			ULS LC3 1,5wind+0,9dead+1,0pre		
			Stress/Load (Max)		UC	Stress/Load (Max)		UC
Group	Property	Mass (kg)	Quantity	Unit		Quantity	Unit	
ETFE beam	CHS114,3*3,2	5961	332	N/mm^2	94%	242	N/mm^2	68%
Strut	CHS152,4*12,5	13841	146	N/mm^2	41%	323	N/mm^2	91%
Hoop	h=1300mm,b=300mm, t_{flange}=55mm,t_{web}=15mm	45669	315	N/mm^2	89%	297	N/mm^2	84%
Rods	Circular bar d=55mm	119	311	N/mm^2	88%	332	N/mm^2	94%
Cable top	PG55 A=347mm^2	1259	143	kN	44%	245	kN	75%
Cable bottom	PG75 A=467mm^2	1706	343	kN	78%	191	kN	44%
Rectangular cable	PG40 A=237mm^2	427	17	kN	8%	21	kN	9%

Mass without hoop	23313	Kg
Mass with hoop	68982	kg
Total mass	80722	kg

minimum tensile force in cable	2333N

8	Resulting forces	
Order of variable	**Topological/Geometrical**	**Choice**
1st	Number of branches	8X8
2nd	Position of intersection point	z=-13260
3rd	Height above support	2250mm
	Height below support	2350mm
4th	Way of form finding	radial pattern
5th	Pretension for top cable (kN)	175
	Pretension for bottom cable (kN)	160

Load combinations	**Displacement (mm)<143**	
	upward	downward
SLS LC1 1,0dead+1,0pre	0	-68
SLS LC2 1,0snow+1,0dead+1,0pre	3	-139
SLS LC3 1,0wind+1,0dead+1,0pre	27	-75

Type of connection	Number	Mass (kg)
ETFE beam connection	100	1500
cable and strut connection	128	10240
total		11740

6th	Cross section		ULS LC2 1,5snow+1,2dead+1,0pre			ULS LC3 1,5wind+0,9dead+1,0pre		
Group	Property	Mass (kg)	N (kN)	M_y (kNm)	M_z (kNm)	N (kN)	M_y (kNm)	M_z (kNm)
ETFE beam	CHS114,3*3,2	5961	-	1,1	9,3	-	1,8	5,9
Strut	CHS152,4*12,5	13841	-	24,1	7,6	-	40,3	52,8
Hoop	h=1300mm,b=300mm, t_{flange}=55mm,t_{web}=15mm	45669	-	7123	47,7	-	6746	16,4
Rods	Circular bar d=55mm	119	-	3,8	3,7	-	3,8	4,9
Cable top	PG55 A=347mm^2	1259	143	0	0	245	0	0
Cable bottom	PG75 A=467mm^2	1706	343	0	0	191	0	0
Rectangular cable	PG40 A=237mm^2	427	17	0	0	21	0	0

Mass without hoop	23313	Kg
Mass with hoop	68982	kg
Total mass	80722	kg

minimum tensile force in cable	2333N

9	Unity check	
Order of variable	**Topological/Geometrical**	**Choice**
1st	Number of branches	9x9
2nd	Position of intersection point	z=-13260
3rd	Height above support	2250mm
	Height below support	2350mm
4th	Way of form finding	radial pattern
5th	Pretension for top cable (kN)	160
	Pretension for bottom cable (kN)	150

Load combinations	**Displacement (mm)<143**	
	upward	downward
SLS LC1 1,0dead+1,0pre	8	-60
SLS LC2 1,0snow+1,0dead+1,0pre	3	-137
SLS LC3 1,0wind+1,0dead+1,0pre	55	-64

Type of connection	Number	Mass (kg)
ETFE beam connection	121	1815
cable and strut connection	162	12960
total		14775

6th	Cross section		ULS LC2 1,5snow+1,2dead+1,0pre			ULS LC3 1,5wind+0,9dead+1,0pre		
			Stress/Load (Max)		UC	Stress/Load (Max)		UC
Group	Property	Mass (kg)	Quantity	Unit		Quantity	Unit	
ETFE beam	CHS114,3*2,6	5356	330	N/mm^2	93%	234	N/mm^2	66%
Strut	CHS152,4*10	14142	160	N/mm^2	45%	342	N/mm^2	96%
Hoop	h=1300mm,b=300mm, t_{flange}=60mm,t_{web}=15mm	48228	310	N/mm^2	87%	292	N/mm^2	82%
Rods	Circular bar d=55mm	151	255	N/mm^2	72%	288	N/mm^2	81%
Cable top	PG40 A=237 mm^2	970	131	kN	59%	215	kN	97%
Cable bottom	PG55 A=347 mm^2	1421	315	kN	97%	176	kN	54%
Rectangular cable	PG40 A=237 mm^2	449	20	kN	9%	22	kN	10%

Mass without hoop	22489	Kg
Mass with hoop	70717	kg
Total mass	85492	kg

minimum tensile force in cable	3722N

9	Resulting forces	
Order of variable	**Topological/Geometrical**	**Choice**
1st	Number of branches	9x9
2nd	Position of intersection point	z=-13260
3rd	Height above support	2250mm
	Height below support	2350mm
4th	Way of form finding	radial pattern
5th	Pretension for top cable (kN)	160
	Pretension for bottom cable (kN)	150

Load combinations	**Displacement (mm)<143**	
	upward	downward
SLS LC1 1,0dead+1,0pre	8	-60
SLS LC2 1,0snow+1,0dead+1,0pre	3	-137
SLS LC3 1,0wind+1,0dead+1,0pre	55	-64

Type of connection	Number	Mass (kg)
ETFE beam connection	121	1815
cable and strut connection	162	12960
total		14775

6th	Cross section		ULS LC2 1,5snow+1,2dead+1,0pre			ULS LC3 1,5wind+0,9dead+1,0pre		
Group	Property	Mass (kg)	N (kN)	M_y (kNm)	M_z (kNm)	N (kN)	M_y (kNm)	M_z (kNm)
ETFE beam	CHS114,3*2,6	5356	-	1	8,2	-	1,7	5,7
Strut	CHS152,4*10	14142	-	21,8	8,5	-	38,3	42,8
Hoop	h=1300mm,b=300mm, t_{flange}=60mm,t_{web}=15mm	48228	-	7501	37,4	-	7089	11,5
Rods	Circular bar d=55mm	151	-	3,2	3,1	-	3,8	4
Cable top	PG40 A=237 mm^2	970	131	0	0	215	0	0
Cable bottom	PG55 A=347 mm^2	1421	315	0	0	176	0	0
Rectangular cable	PG40 A=237 mm^2	449	20	0	0	22	0	0

Mass without hoop	22489	Kg
Mass with hoop	70717	kg
Total mass	85492	kg

minimum tensile force in cable	3722N

10	Unity check	
Order of variable	**Topological/Geometrical**	**Choice**
1st	Number of branches	10x10
2nd	Position of intersection point	z=-13260
3rd	Height above support	2250mm
	Height below support	2350mm
4th	Way of form finding	radial pattern
5th	Pretension for top cable (kN)	145
	Pretension for bottom cable (kN)	135

Load combinations	**Displacement (mm)<143**	
	upward	downward
SLS LC1 1,0dead+1,0pre	2	67
SLS LC2 1,0snow+1,0dead+1,0pre	3	-137
SLS LC3 1,0wind+1,0dead+1,0pre	34	-73

Type of connection	Number	Mass (kg)
ETFE beam connection	144	2160
cable and strut connection	200	16000
total		18160

6th	Cross section		ULS LC2 1,5snow+1,2dead+1,0pre			ULS LC3 1,5wind+0,9dead+1,0pre		
			Stress/Load (Max)		UC	Stress/Load (Max)		UC
Group	Property	Mass (kg)	Quantity	Unit		Quantity	Unit	
ETFE beam	CHS101,6*2,6	5179	351	N/mm^2	99%	286	N/mm^2	81%
Strut	CHS152,4*8	14264	153	N/mm^2	43%	346	N/mm^2	97%
Hoop	h=1300mm,b=300mm, t_{flange}=60mm,t_{web}=15mm	48228	314	N/mm^2	88%	296	N/mm^2	83%
Rods	Circular bar d=50mm	154	327	N/mm^2	92%	324	N/mm^2	91%
Cable top	PG40 A=237 mm^2	1078	118	kN	53%	193	kN	87%
Cable bottom	PG55 A=347 mm^2	1579	283	kN	87%	161	kN	49%
Rectangular cable	PG40 A=237 mm^2	465	20	kN	9%	19	kN	9%

Mass without hoop	22719	Kg
Mass with hoop	70947	kg
Total mass	89107	kg

minimum tensile force in cable	5323N

10	Resulting forces	
Order of variable	**Topological/Geometrical**	**Choice**
1st	Number of branches	10x10
2nd	Position of intersection point	z=-13260
3rd	Height above support	2250mm
	Height below support	2350mm
4th	Way of form finding	radial pattern
5th	Pretension for top cable (kN)	145
	Pretension for bottom cable (kN)	135

Load combinations	**Displacement (mm)<143**	
	upward	downward
SLS LC1 1,0dead+1,0pre	2	67
SLS LC2 1,0snow+1,0dead+1,0pre	3	-137
SLS LC3 1,0wind+1,0dead+1,0pre	34	-73

Type of connection	Number	Mass (kg)
ETFE beam connection	144	2160
cable and strut connection	200	16000
total		18160

6th	Cross section		ULS LC2 1,5snow+1,2dead+1,0pre			ULS LC3 1,5wind+0,9dead+1,0pre		
Group	Property	Mass (kg)	N (kN)	M_y (kNm)	M_z (kNm)	N (kN)	M_y (kNm)	M_z (kNm)
ETFE beam	CHS101,6*2,6	5179	-	0,9	6,8	-	1,4	5,6
Strut	CHS152,4*8	14264	-	17,2	6,6	-	32,1	36,6
Hoop	h=1300mm,b=300mm, t_{flange}=60mm,t_{web}=15mm	48228	-	7587	30,2	-	7165	9,2
Rods	Circular bar d=50mm	154	-	2,7	2,7	-	3,2	3,6
Cable top	PG40 A=237 mm^2	1078	118	0	0	193	0	0
Cable bottom	PG55 A=347 mm^2	1579	283	0	0	161	0	0
Rectangular cable	PG40 A=237 mm^2	465	20	0	0	19	0	0

Mass without hoop	22719	Kg
Mass with hoop	70947	kg
Total mass	89107	kg

minimum tensile force in cable	5323N

2. Change converge point

Radial struts — Unity check

Order of variable	Topological/Geometrical	Choice
1st	Number of branches	8X8
2nd	Position of intersection point	z=-13260
3rd	Height above support	2250mm
	Height below support	2350mm
4th	Way of form finding	radial pattern
5th	Pretension for top cable (kN)	175
	Pretension for bottom cable (kN)	160

Load combinations	Displacement (mm)<143	
	upward	downward
SLS LC1 1,0dead+1,0pre	0	-68
SLS LC2 1,0snow+1,0dead+1,0pre	3	-139
SLS LC3 1,0wind+1,0dead+1,0pre	27	-75

Type of connection	Number	Mass (kg)
ETFE beam connection	100	1500
cable and strut connection	128	10240
total		11740

6th	Cross section		ULS LC2 1,5snow+1,2dead+1,0pre			ULS LC3 1,5wind+0,9dead+1,0pre		
			Stress/Load (Max)		UC	Stress/Load (Max)		UC
Group	Property	Mass (kg)	Quantity	Unit		Quantity	Unit	
ETFE beam	CHS114,3*3,2	5961	332	N/mm^2	94%	242	N/mm^2	68%
Strut	CHS152,4*12,5	13841	146	N/mm^2	41%	323	N/mm^2	91%
Hoop	h=1300mm,b=300mm, t_{flange}=55mm,t_{web}=15mm	45669	315	N/mm^2	89%	297	N/mm^2	84%
Rods	Circular bar d=55mm	119	311	N/mm^2	88%	332	N/mm^2	94%
Cable top	PG55 A=347mm^2	1259	143	kN	44%	245	kN	75%
Cable bottom	PG75 A=467mm^2	1706	343	kN	78%	192	kN	44%
Rectangular cable	PG40 A=237mm^2	427	17	kN	8%	21	kN	9%

Mass without hoop	23313	Kg
Mass with hoop	68982	kg
Total mass	80722	kg

minimum tensile force in cable	2333N

Radial struts Resulting forces

Order of variable	Topological/Geometrical	Choice
1st	Number of branches	8X8
2nd	Position of intersection point	z=-13260
3rd	Height above support	2250mm
	Height below support	2350mm
4th	Way of form finding	radial pattern
5th	Pretension for top cable (kN)	175
	Pretension for bottom cable (kN)	160

Load combinations	Displacement (mm)<143	
	upward	downward
SLS LC1 1,0dead+1,0pre	0	-68
SLS LC2 1,0snow+1,0dead+1,0pre	3	-139
SLS LC3 1,0wind+1,0dead+1,0pre	27	-75

Type of connection	Number	Mass (kg)
ETFE beam connection	100	1500
cable and strut connection	128	10240
total		11740

6th	Cross section		ULS LC2 1,5snow+1,2dead+1,0pre			ULS LC3 1,5wind+0,9dead+1,0pre		
Group	Property	Mass (kg)	N (kN)	M_y (kNm)	M_z (kNm)	N (kN)	M_y (kNm)	M_z (kNm)
ETFE beam	CHS114,3*3,2	5961	-	1,1	9,3	-	1,8	5,9
Strut	CHS152,4*12,5	13841	-	24,1	7,6	-	40,3	52,8
Hoop	h=1300mm,b=300mm, t_{flange}=55mm,t_{web}=15mm	45669	-	7123	47,7	-	6746	16,4
Rods	Circular bar d=55mm	119	-	3,8	3,7	-	3,8	4,9
Cable top	PG55 A=347mm^2	1259	143	0	0	245	0	0
Cable bottom	PG75 A=467mm^2	1706	343	0	0	191	0	0
Rectangular cable	PG40 A=237mm^2	427	17	0	0	21	0	0

Mass without hoop	23313	Kg
Mass with hoop	68982	kg
Total mass	80722	kg

minimum tensile force in cable	2333N

Vertical struts	Unity check	
Order of variable	**Topological/Geometrical**	**Choice**
1st	Number of branches	8X8
2nd	Position of intersection point	z=-1000000
3rd	Height above support	2250mm
	Height below support	2350mm
4th	Way of form finding	radial pattern
5th	Pretension for top cable (kN)	155
	Pretension for bottom cable (kN)	120

Load combinations	**Displacement (mm)<143**	
	upward	downward
SLS LC1 1,0dead+1,0pre	0	-46
SLS LC2 1,0snow+1,0dead+1,0pre	2	-127
SLS LC3 1,0wind+1,0dead+1,0pre	44	-79

Type of connection	Number	Mass (kg)
ETFE beam connection	100	1500
cable and strut connection	128	10240
total		11740

6th	Cross section		ULS LC2 1,5snow+1,2dead+1,0pre			ULS LC3 1,5wind+0,9dead+1,0pre		
			Stress/Load (Max)		UC	Stress/Load (Max)		UC
Group	Property	Mass (kg)	Quantity	Unit		Quantity	Unit	
ETFE beam	CHS114,3*5	9163	329	N/mm^2	93%	210	N/mm^2	59%
Strut	CHS152,4*6,3	5141	266	N/mm^2	75%	266	N/mm^2	75%
Hoop	h=1300mm,b=300mm, t_{flange}=40mm,t_{web}=15mm	37990	253	N/mm^2	71%	260	N/mm^2	73%
Rods	Circular bar d=60mm	142	177	N/mm^2	50%	266	N/mm^2	75%
Cable top	PG55 A=347mm^2	1257	133	kN	41%	237	kN	73%
Cable bottom	PG55 A=347mm^2	1258	279	kN	86%	163	kN	50%
Rectangular cable	PG40 A=237mm^2	430	9	kN	4%	16	kN	7%

Mass without hoop	17391	Kg
Mass with hoop	55381	kg
Total mass	67121	kg

minimum tensile force in cable	348N

Vertical struts Resulting forces

Order of variable	Topological/Geometrical	Choice
1st	Number of branches	8X8
2nd	Position of intersection point	z=-1000000
3rd	Height above support	2250mm
	Height below support	2350mm
4th	Way of form finding	radial pattern
5th	Pretension for top cable (kN)	155
	Pretension for bottom cable (kN)	120

Load combinations	Displacement (mm)<143	
	upward	downward
SLS LC1 1,0dead+1,0pre	0	-46
SLS LC2 1,0snow+1,0dead+1,0pre	2	-127
SLS LC3 1,0wind+1,0dead+1,0pre	44	-79

Type of connection	Number	Mass (kg)
ETFE beam connection	100	1500
cable and strut connection	128	10240
total		11740

6th	Cross section		ULS LC2 1,5snow+1,2dead+1,0pre			ULS LC3 1,5wind+0,9dead+1,0pre		
Group	Property	Mass (kg)	N (kN)	M_y (kNm)	M_z (kNm)	N (kN)	M_y (kNm)	M_z (kNm)
ETFE beam	CHS114,3*5	9163	-	5,6	14,5	-	7,6	9,2
Strut	CHS152,4*6,3	5141	-	30	11,1	-	20,1	24,7
Hoop	h=1300mm,b=300mm, t_{flange}=40mm,t_{web}=15mm	37990	-	4545	59,5	-	4678	24,5
Rods	Circular bar d=60mm	142	-	3,5	1,6	-	3,5	5,2
Cable top	PG55 A=347mm^2	1257	133	0	0	237	0	0
Cable bottom	PG55 A=347mm^2	1258	279	0	0	163	0	0
Rectangular cable	PG40 A=237mm^2	430	9	0	0	16	0	0

Mass without hoop	17391	Kg
Mass with hoop	55381	kg
Total mass	67121	kg

minimum tensile force in cable	348N

3. Change way of form-finding

Gravity	Unity check	
Order of variable	**Topological/Geometrical**	**Choice**
1st	Number of branches	8X8
2nd	Position of intersection point	z=-13260
3rd	Height above support	2250mm
	Height below support	2350mm
4th	Way of form finding	gravity
5th	Pretension for top cable (kN)	190
	Pretension for bottom cable (kN)	170

Load combinations	**Displacement (mm)<143**	
	upward	downward
SLS LC1 1,0dead+1,0pre	26	-65
SLS LC2 1,0snow+1,0dead+1,0pre	7	-138
SLS LC3 1,0wind+1,0dead+1,0pre	82	-61

Type of connection	Number	Mass (kg)
ETFE beam connection	100	1500
cable and strut connection	128	10240
total		11740

6th	Cross section		ULS LC2 1,5snow+1,2dead+1,0pre			ULS LC3 1,5wind+0,9dead+1,0pre		
			Stress/Load (Max)		UC	Stress/Load (Max)		UC
Group	Property	Mass (kg)	Quantity	Unit		Quantity	Unit	
ETFE beam	CHS114,3*3,2	5961	342	N/mm^2	96%	244	N/mm^2	69%
Strut	CHS152,4*12,5	13176	287	N/mm^2	81%	289	N/mm^2	81%
Hoop	h=1300mm,b=300mm, t_{flange}=60mm,t_{web}=15mm	48228	349	N/mm^2	98%	330	N/mm^2	93%
Rods	Circular bar d=55mm	119	246	N/mm^2	69%	355	N/mm^2	100%
Cable top	PG55 A=347mm^2	1256	154	kN	47%	269	kN	83%
Cable bottom	PG75 A=467mm^2	1701	376	kN	86%	205	kN	47%
Rectangular cable	PG40 A=237mm^2	427	16	kN	7%	22	kN	10%

Mass without hoop	22640	Kg
Mass with hoop	70868	kg
Total mass	82608	kg

minimum tensile force in cable	3813N

Gravity	Resulting forces	
Order of variable	**Topological/Geometrical**	**Choice**
1st	Number of branches	8X8
2nd	Position of intersection point	z=-13260
3rd	Height above support	2250mm
	Height below support	2350mm
4th	Way of form finding	gravity
5th	Pretension for top cable (kN)	190
	Pretension for bottom cable (kN)	170

Load combinations	**Displacement (mm)<143**	
	upward	downward
SLS LC1 1,0dead+1,0pre	26	-65
SLS LC2 1,0snow+1,0dead+1,0pre	7	-138
SLS LC3 1,0wind+1,0dead+1,0pre	82	-61

Type of connection	Number	Mass (kg)
ETFE beam connection	100	1500
cable and strut connection	128	10240
total		11740

6th	Cross section		ULS LC2 1,5snow+1,2dead+1,0pre			ULS LC3 1,5wind+0,9dead+1,0pre		
Group	Property	Mass (kg)	N (kN)	M_y (kNm)	M_z (kNm)	N (kN)	M_y (kNm)	M_z (kNm)
ETFE beam	CHS114,3*3,2	5961	-	1,1	8,6	-	1,7	7
Strut	CHS152,4*12,5	13176	-	48,4	24,3	-	36,2	46,8
Hoop	h=1300mm,b=300mm, t_{flange}=60mm,t_{web}=15mm	48228	-	7827	45,9	-	7405	16,2
Rods	Circular bar d=55mm	119	-	3	2,6	-	4,2	4,9
Cable top	PG55 A=347mm^2	1256	154	0	0	269	0	0
Cable bottom	PG75 A=467mm^2	1701	376	0	0	205	0	0
Rectangular cable	PG40 A=237mm^2	427	16	0	0	22	0	0

Mass without hoop	22640	Kg
Mass with hoop	70868	kg
Total mass	82608	kg

minimum tensile force in cable	3813N

Radial loads	Unity check	
Order of variable	**Topological/Geometrical**	**Choice**
1st	Number of branches	8X8
2nd	Position of intersection point	z=-13260
3rd	Height above support	2250mm
	Height below support	2350mm
4th	Way of form finding	radial pattern
5th	Pretension for top cable (kN)	175
	Pretension for bottom cable (kN)	160

Load combinations	**Displacement (mm)<143**	
	upward	downward
SLS LC1 1,0dead+1,0pre	0	-68
SLS LC2 1,0snow+1,0dead+1,0pre	3	-139
SLS LC3 1,0wind+1,0dead+1,0pre	27	-75

Type of connection	Number	Mass (kg)
ETFE beam connection	100	1500
cable and strut connection	128	10240
total		11740

6th	Cross section		ULS LC2 1,5snow+1,2dead+1,0pre			ULS LC3 1,5wind+0,9dead+1,0pre		
			Stress/Load (Max)		UC	Stress/Load (Max)		UC
Group	Property	Mass (kg)	Quantity	Unit		Quantity	Unit	
ETFE beam	CHS114,3*3,2	5961	332	N/mm^2	94%	242	N/mm^2	68%
Strut	CHS152,4*12,5	13841	146	N/mm^2	41%	323	N/mm^2	91%
Hoop	h=1300mm,b=300mm, t_{flange}=55mm,t_{web}=15mm	45669	315	N/mm^2	89%	297	N/mm^2	84%
Rods	Circular bar d=55mm	119	311	N/mm^2	88%	332	N/mm^2	94%
Cable top	PG55 A=347mm^2	1259	143	kN	44%	245	kN	75%
Cable bottom	PG75 A=467mm^2	1706	343	kN	78%	192	kN	44%
Rectangular cable	PG40 A=237mm^2	427	17	kN	8%	21	kN	9%

Mass without hoop	23313	Kg
Mass with hoop	68982	kg
Total mass	80722	kg

minimum tensile force in cable	2333N

Radial loads Resulting forces

Order of variable	Topological/Geometrical	Choice
1st	Number of branches	8X8
2nd	Position of intersection point	z=-13260
3rd	Height above support	2250mm
	Height below support	2350mm
4th	Way of form finding	radial pattern
5th	Pretension for top cable (kN)	175
	Pretension for bottom cable (kN)	160

Load combinations	Displacement (mm)<143	
	upward	downward
SLS LC1 1,0dead+1,0pre	0	-68
SLS LC2 1,0snow+1,0dead+1,0pre	3	-139
SLS LC3 1,0wind+1,0dead+1,0pre	27	-75

Type of connection	Number	Mass (kg)
ETFE beam connection	100	1500
cable and strut connection	128	10240
total		11740

6th	Cross section		ULS LC2 1,5snow+1,2dead+1,0pre			ULS LC3 1,5wind+0,9dead+1,0pre		
Group	Property	Mass (kg)	N (kN)	M_y (kNm)	M_z (kNm)	N (kN)	M_y (kNm)	M_z (kNm)
ETFE beam	CHS114,3*3,2	5961	-	1,1	9,3	-	1,8	5,9
Strut	CHS152,4*12,5	13841	-	24,1	7,6	-	40,3	52,8
Hoop	h=1300mm,b=300mm, t_{flange}=55mm,t_{web}=15mm	45669	-	7123	47,7	-	6746	16,4
Rods	Circular bar d=55mm	119	-	3,8	3,7	-	3,8	4,9
Cable top	PG55 A=347mm^2	1259	143	0	0	245	0	0
Cable bottom	PG75 A=467mm^2	1706	343	0	0	191	0	0
Rectangular cable	PG40 A=237mm^2	427	17	0	0	21	0	0

Mass without hoop	23313	Kg
Mass with hoop	68982	kg
Total mass	80722	kg

minimum tensile force in cable	2333N

Vertical loads | Unity check

Order of variable	Topological/Geometrical	Choice
1st	Number of branches	8X8
2nd	Position of intersection point	z=-13260
3rd	Height above support	2250mm
	Height below support	2350mm
4th	Way of form finding	vertical load
5th	Pretension for top cable (kN)	170
	Pretension for bottom cable (kN)	165

Load combinations	Displacement (mm)<143	
	upward	downward
SLS LC1 1,0dead+1,0pre	2	-73
SLS LC2 1,0snow+1,0dead+1,0pre	3	-138
SLS LC3 1,0wind+1,0dead+1,0pre	29	-86

Type of connection	Number	Mass (kg)
ETFE beam connection	100	1500
cable and strut connection	128	10240
total		11740

6th	Cross section		ULS LC2 1,5snow+1,2dead+1,0pre			ULS LC3 1,5wind+0,9dead+1,0pre		
			Stress/Load (Max)		UC	Stress/Load (Max)		UC
Group	Property	Mass (kg)	Quantity	Unit		Quantity	Unit	
ETFE beam	CHS114,3*4	7398	300	N/mm^2	85%	200	N/mm^2	56%
Strut	CHS152,4*12,5	14194	197	N/mm^2	55%	326	N/mm^2	92%
Hoop	h=1300mm,b=300mm, t_{flange}=55mm,t_{web}=15mm	45669	310	N/mm^2	87%	295	N/mm^2	83%
Rods	Circular bar d=55mm	119	343	N/mm^2	97%	345	N/mm^2	97%
Cable top	PG55 A=347mm^2	1262	143	kN	44%	236	kN	72%
Cable bottom	PG75 A=467mm^2	1710	342	kN	78%	194	kN	44%
Rectangular cable	PG40 A=237mm^2	427	16	kN	7%	20	kN	9%

Mass without hoop	25110	Kg
Mass with hoop	70779	kg
Total mass	82519	kg

minimum tensile force in cable	2192N

Vertical loads | Resulting forces

Order of variable	Topological/Geometrical	Choice
1st	Number of branches	8X8
2nd	Position of intersection point	z=-13260
3rd	Height above support	2250mm
	Height below support	2350mm
4th	Way of form finding	vertical load
5th	Pretension for top cable (kN)	170
	Pretension for bottom cable (kN)	165

Load combinations	Displacement (mm)<143	
	upward	downward
SLS LC1 1,0dead+1,0pre	2	-73
SLS LC2 1,0snow+1,0dead+1,0pre	3	-138
SLS LC3 1,0wind+1,0dead+1,0pre	29	-86

Type of connection	Number	Mass (kg)
ETFE beam connection	100	1500
cable and strut connection	128	10240
total		11740

6th	Cross section		ULS LC2 1,5snow+1,2dead+1,0pre			ULS LC3 1,5wind+0,9dead+1,0pre		
Group	Property	Mass (kg)	N (kN)	M_y (kNm)	M_z (kNm)	N (kN)	M_y (kNm)	M_z (kNm)
ETFE beam	CHS114,3*4	7398	-	1,4	11	-	2,2	6,5
Strut	CHS152,4*12,5	14194	-	33,8	15,8	-	41,3	24,3
Hoop	h=1300mm,b=300mm, t_{flange}=55mm,t_{web}=15mm	45669	-	7016	49,4	-	6693	16,1
Rods	Circular bar d=55mm	119	-	4,3	4,3	-	4,2	5,3
Cable top	PG55 A=347mm^2	1262	143	0	0	236	0	0
Cable bottom	PG75 A=467mm^2	1710	342	0	0	194	0	0
Rectangular cable	PG40 A=237mm^2	427	16	0	0	20	0	0

Mass without hoop	25110	Kg
Mass with hoop	70779	kg
Total mass	82519	kg

minimum tensile force in cable	2192N

4. Change depth of cable net

(a)Change D_{bottom}

D_{bottom}=2150mm Unity check

Order of variable	Topological/Geometrical	Choice
1st	Number of branches	8X8
2nd	Position of intersection point	z=-13260
3rd	Height above support	2250mm
	Height below support	2150mm
4th	Way of form finding	radial pattern
5th	Pretension for top cable (kN)	185
	Pretension for bottom cable (kN)	185

Load combinations	Displacement (mm)<143	
	upward	downward
SLS LC1 1,0dead+1,0pre	1	-62
SLS LC2 1,0snow+1,0dead+1,0pre	1	-135
SLS LC3 1,0wind+1,0dead+1,0pre	33	-68

Type of connection	Number	Mass (kg)
ETFE beam connection	100	1500
cable and strut connection	128	10240
total		11740

6th	Cross section		ULS LC2 1,5snow+1,2dead+1,0pre			ULS LC3 1,5wind+0,9dead+1,0pre		
			Stress/Load (Max)		UC	Stress/Load (Max)		UC
Group	Property	Mass (kg)	Quantity	Unit		Quantity	Unit	
ETFE beam	CHS114,3*3,2	5961	331	N/mm^2	93%	250	N/mm^2	70%
Strut	CHS152,4*12,5	13359	156	N/mm^2	44%	325	N/mm^2	92%
Hoop	h=1300mm,b=300mm, t_{flange}=55mm,t_{web}=15mm	45669	343	N/mm^2	97%	330	N/mm^2	93%
Rods	Circular bar d=55mm	119	305	N/mm^2	86%	349	N/mm^2	98%
Cable top	PG55 A=347mm^2	1259	152	kN	47%	257	kN	79%
Cable bottom	PG75 A=467mm^2	1702	370	kN	84%	213	kN	49%
Rectangular cable	PG40 A=237mm^2	427	17	kN	8%	23	kN	10%

Mass without hoop	22827	Kg
Mass with hoop	68496	kg
Total mass	80236	kg

minimum tensile force in cable	5655N

D_{bottom}=2150mm Resulting forces

Order of variable	Topological/Geometrical	Choice
1st	Number of branches	8X8
2nd	Position of intersection point	z=-13260
3rd	Height above support	2250mm
	Height below support	2150mm
4th	Way of form finding	radial pattern
5th	Pretension for top cable (kN)	185
	Pretension for bottom cable (kN)	185

Load combinations	Displacement (mm)<143	
	upward	downward
SLS LC1 1,0dead+1,0pre	1	-62
SLS LC2 1,0snow+1,0dead+1,0pre	1	-135
SLS LC3 1,0wind+1,0dead+1,0pre	33	-68

Type of connection	Number	Mass (kg)
ETFE beam connection	100	1500
cable and strut connection	128	10240
total		11740

6th	Cross section		ULS LC2 1,5snow+1,2dead+1,0pre			ULS LC3 1,5wind+0,9dead+1,0pre		
Group	Property	Mass (kg)	N (kN)	M_y (kNm)	M_z (kNm)	N (kN)	M_y (kNm)	M_z (kNm)
ETFE beam	CHS114,3*3,2	5961	-	1,1	9,7	-	1,8	6,1
Strut	CHS152,4*12,5	13359	-	25,3	8,1	-	41,5	51,9
Hoop	h=1300mm,b=300mm, t_{flange}=55mm,t_{web}=15mm	45669	-	7771	47,8	-	7478	16
Rods	Circular bar d=55mm	119	-	3,7	3,6	-	4,1	5,2
Cable top	PG55 A=347mm^2	1259	152	0	0	257	0	0
Cable bottom	PG75 A=467mm^2	1702	370	0	0	213	0	0
Rectangular cable	PG40 A=237mm^2	427	17	0	0	23	0	0

Mass without hoop	22827	Kg
Mass with hoop	68496	kg
Total mass	80236	kg

minimum tensile force in cable	5655N

D_{bottom}=2250mm Unity check

Order of variable	Topological/Geometrical	Choice
1st	Number of branches	8X8
2nd	Position of intersection point	z=-13260
3rd	Height above support	2250mm
	Height below support	2250mm
4th	Way of form finding	radial pattern
5th	Pretension for top cable (kN)	180
	Pretension for bottom cable (kN)	170

Load combinations	Displacement (mm)<143	
	upward	downward
SLS LC1 1,0dead+1,0pre	0	-71
SLS LC2 1,0snow+1,0dead+1,0pre	4	-143
SLS LC3 1,0wind+1,0dead+1,0pre	25	-77

Type of connection	Number	Mass (kg)
ETFE beam connection	100	1500
cable and strut connection	128	10240
total		11740

6th	Cross section		ULS LC2 1,5snow+1,2dead+1,0pre			ULS LC3 1,5wind+0,9dead+1,0pre		
			Stress/Load (Max)		UC	Stress/Load (Max)		UC
Group	Property	Mass (kg)	Quantity	Unit		Quantity	Unit	
ETFE beam	CHS114,3*3,2	5961	331	N/mm^2	93%	246	N/mm^2	69%
Strut	CHS152,4*12,5	13599	147	N/mm^2	41%	327	N/mm^2	92%
Hoop	h=1300mm,b=300mm, t_{flange}=55mm,t_{web}=15mm	45669	327	N/mm^2	92%	311	N/mm^2	88%
Rods	Circular bar d=55mm	119	311	N/mm^2	88%	339	N/mm^2	95%
Cable top	PG55 A=347mm^2	1259	148	kN	45%	251	kN	77%
Cable bottom	PG75 A=467mm^2	1704	355	kN	81%	206	kN	47%
Rectangular cable	PG40 A=237mm^2	427	17	kN	8%	22	kN	10%

Mass without hoop	23069	Kg
Mass with hoop	68738	kg
Total mass	80478	kg

minimum tensile force in cable	3949N

D_{bottom}=2250mm Resulting forces

Order of variable	Topological/Geometrical	Choice
1st	Number of branches	8X8
2nd	Position of intersection point	z=-13260
3rd	Height above support	2250mm
	Height below support	2250mm
4th	Way of form finding	radial pattern
5th	Pretension for top cable(kN)	180
	Pretension for bottom cable(kN)	170

Load combinations	Displacement (mm)<143	
	upward	downward
SLS LC1 1,0dead+1,0pre	0	-71
SLS LC2 1,0snow+1,0dead+1,0pre	4	-143
SLS LC3 1,0wind+1,0dead+1,0pre	25	-77

Type of connection	Number	Mass (kg)
ETFE beam connection	100	1500
cable and strut connection	128	10240
total		11740

6th	Cross section		ULS LC2 1,5snow+1,2dead+1,0pre			ULS LC3 1,5wind+0,9dead+1,0pre		
Group	Property	Mass (kg)	N (kN)	M_y (kNm)	M_z (kNm)	N (kN)	M_y (kNm)	M_z (kNm)
ETFE beam	CHS114,3*3,2	5961	-	1,1	9,3	-	1,8	5,9
Strut	CHS152,4*12,5	13599	-	24	7,8	-	41,5	53,2
Hoop	h=1300mm,b=300mm, t_{flange}=55mm,t_{web}=15mm	45669	-	7405	47,8	-	7061	16,2
Rods	Circular bar d=55mm	119	-	3,8	3,7	-	4	5
Cable top	PG55 A=347mm^2	1259	148	0	0	251	0	0
Cable bottom	PG75 A=467mm^2	1704	355	0	0	206	0	0
Rectangular cable	PG40 A=237mm^2	427	17	0	0	22	0	0

Mass without hoop	23069	Kg
Mass with hoop	68738	kg
Total mass	80478	kg

minimum tensile force in cable	3949N

D_{bottom}=2350mm Unity check

Order of variable	Topological/Geometrical	Choice
1st	Number of branches	8X8
2nd	Position of intersection point	z=-13260
3rd	Height above support	2250mm
	Height below support	2350mm
4th	Way of form finding	radial pattern
5th	Pretension for top cable (kN)	175
	Pretension for bottom cable (kN)	160

Load combinations	Displacement (mm)<143	
	upward	downward
SLS LC1 1,0dead+1,0pre	0	-68
SLS LC2 1,0snow+1,0dead+1,0pre	3	-139
SLS LC3 1,0wind+1,0dead+1,0pre	27	-75

Type of connection	Number	Mass (kg)
ETFE beam connection	100	1500
cable and strut connection	128	10240
total		11740

6th	Cross section		ULS LC2 1,5snow+1,2dead+1,0pre			ULS LC3 1,5wind+0,9dead+1,0pre		
			Stress/Load (Max)		UC	Stress/Load (Max)		UC
Group	Property	Mass (kg)	Quantity	Unit		Quantity	Unit	
ETFE beam	CHS114,3*3,2	5961	332	N/mm^2	94%	242	N/mm^2	68%
Strut	CHS152,4*12,5	13841	146	N/mm^2	41%	323	N/mm^2	91%
Hoop	h=1300mm,b=300mm, t_{flange}=55mm,t_{web}=15mm	45669	315	N/mm^2	89%	297	N/mm^2	84%
Rods	Circular bar d=55mm	119	311	N/mm^2	88%	332	N/mm^2	94%
Cable top	PG55 A=347mm^2	1259	143	kN	44%	245	kN	75%
Cable bottom	PG75 A=467mm^2	1706	343	kN	78%	192	kN	44%
Rectangular cable	PG40 A=237mm^2	427	17	kN	8%	21	kN	9%

Mass without hoop	23313	Kg
Mass with hoop	68982	kg
Total mass	80722	kg

minimum tensile force in cable	2333N

D_{bottom}=2350mm Resulting forces

Order of variable	Topological/Geometrical	Choice
1st	Number of branches	8X8
2nd	Position of intersection point	z=-13260
3rd	Height above support	2250mm
	Height below support	2350mm
4th	Way of form finding	radial pattern
5th	Pretension for top cable (kN)	175
	Pretension for bottom cable (kN)	160

Load combinations	Displacement (mm)<143	
	upward	downward
SLS LC1 1,0dead+1,0pre	0	-68
SLS LC2 1,0snow+1,0dead+1,0pre	3	-139
SLS LC3 1,0wind+1,0dead+1,0pre	27	-75

Type of connection	Number	Mass (kg)
ETFE beam connection	100	1500
cable and strut connection	128	10240
total		11740

6th	Cross section		ULS LC2 1,5snow+1,2dead+1,0pre			ULS LC3 1,5wind+0,9dead+1,0pre		
Group	Property	Mass (kg)	N (kN)	M_y (kNm)	M_z (kNm)	N (kN)	M_y (kNm)	M_z (kNm)
ETFE beam	CHS114,3*3,2	5961	-	1,1	9,3	-	1,8	5,9
Strut	CHS152,4*12,5	13841	-	24,1	7,6	-	40,3	52,8
Hoop	h=1300mm,b=300mm, t_{flange}=55mm,t_{web}=15mm	45669	-	7123	47,7	-	6746	16,4
Rods	Circular bar d=55mm	119	-	3,8	3,7	-	3,8	4,9
Cable top	PG55 A=347mm^2	1259	143	0	0	245	0	0
Cable bottom	PG75 A=467mm^2	1706	343	0	0	191	0	0
Rectangular cable	PG40 A=237mm^2	427	17	0	0	21	0	0

Mass without hoop	23313	Kg
Mass with hoop	68982	kg
Total mass	80722	kg

minimum tensile force in cable	2333N

D_{bottom}=2450mm Unity check

Order of variable	Topological/Geometrical	Choice
1st	Number of branches	8X8
2nd	Position of intersection point	z=-13260
3rd	Height above support	2250mm
	Height below support	2450mm
4th	Way of form finding	radial pattern
5th	Pretension for top cable (kN)	170
	Pretension for bottom cable (kN)	150

Load combinations	Displacement (mm)<143	
	upward	downward
SLS LC1 1,0dead+1,0pre	0	-69
SLS LC2 1,0snow+1,0dead+1,0pre	4	-139
SLS LC3 1,0wind+1,0dead+1,0pre	30	-76

Type of connection	Number	Mass (kg)
ETFE beam connection	100	1500
cable and strut connection	128	10240
total		11740

6th	Cross section		ULS LC2 1,5snow+1,2dead+1,0pre			ULS LC3 1,5wind+0,9dead+1,0pre		
			Stress/Load (Max)		UC	Stress/Load (Max)		UC
Group	Property	Mass (kg)	Quantity	Unit		Quantity	Unit	
ETFE beam	CHS114,3*3,2	5961	333	N/mm^2	94%	239	N/mm^2	67%
Strut	CHS152,4*12,5	14086	146	N/mm^2	41%	320	N/mm^2	90%
Hoop	h=1300mm,b=300mm, t_{flange}=55mm,t_{web}=15mm	45669	302	N/mm^2	85%	283	N/mm^2	80%
Rods	Circular bar d=55mm	119	312	N/mm^2	88%	324	N/mm^2	91%
Cable top	PG55 A=347mm^2	1259	139	kN	43%	238	kN	73%
Cable bottom	PG75 A=467mm^2	1708	332	kN	76%	182	kN	42%
Rectangular cable	PG40 A=237mm^2	427	17	kN	8%	21	kN	9%

Mass without hoop	23560	Kg
Mass with hoop	69229	kg
Total mass	80969	kg

minimum tensile force in cable	622N

D_{bottom}=2450mm Resulting forces

Order of variable	Topological/Geometrical	Choice
1st	Number of branches	8X8
2nd	Position of intersection point	z=-13260
3rd	Height above support	2250mm
	Height below support	2450mm
4th	Way of form finding	radial pattern
5th	Pretension for top cable(kN)	170
	Pretension for bottom cable(kN)	150

Load combinations	Displacement (mm)<143	
	upward	downward
SLS LC1 1,0dead+1,0pre	0	-69
SLS LC2 1,0snow+1,0dead+1,0pre	4	-139
SLS LC3 1,0wind+1,0dead+1,0pre	30	-76

Type of connection	Number	Mass (kg)
ETFE beam connection	100	1500
cable and strut connection	128	10240
total		11740

6th	Cross section		ULS LC2 1,5snow+1,2dead+1,0pre			ULS LC3 1,5wind+0,9dead+1,0pre		
Group	Property	Mass (kg)	N (kN)	M_y (kNm)	M_z (kNm)	N (kN)	M_y (kNm)	M_z (kNm)
ETFE beam	CHS114,3*3,2	5961	-	1,1	9,3	-	1,8	5,9
Strut	CHS152,4*12,5	14086	-	24,4	73,3	-	39,3	52,6
Hoop	h=1300mm,b=300mm, t_{flange}=55mm,t_{web}=15mm	45669	-	6844	47,7	-	6433	16,5
Rods	Circular bar d=55mm	119	-	3,8	3,8	-	3,7	4,8
Cable top	PG55 A=347mm^2	1259	139	0	0	238	0	0
Cable bottom	PG75 A=467mm^2	1708	332	0	0	182	0	0
Rectangular cable	PG40 A=237mm^2	427	17	0	0	21	0	0

Mass without hoop	23560	Kg
Mass with hoop	69229	kg
Total mass	80969	kg

minimum tensile force in cable	622N

D_{bottom}=2550mm Unity check

Order of variable	Topological/Geometrical	Choice
1st	Number of branches	8X8
2nd	Position of intersection point	z=-13260
3rd	Height above support	2250mm
	Height below support	2550mm
4th	Way of form finding	radial pattern
5th	Pretension for top cable (kN)	170
	Pretension for bottom cable (kN)	145

Load combinations	Displacement (mm)<143	
	upward	downward
SLS LC1 1,0dead+1,0pre	0	-69
SLS LC2 1,0snow+1,0dead+1,0pre	1	-138
SLS LC3 1,0wind+1,0dead+1,0pre	30	-76

Type of connection	Number	Mass (kg)
ETFE beam connection	100	1500
cable and strut connection	128	10240
total		11740

6th	Cross section		ULS LC2 1,5snow+1,2dead+1,0pre			ULS LC3 1,5wind+0,9dead+1,0pre		
			Stress/Load (Max)		UC	Stress/Load (Max)		UC
Group	Property	Mass (kg)	Quantity	Unit		Quantity	Unit	
ETFE beam	CHS114,3*3,2	5961	334	N/mm^2	94%	238	N/mm^2	67%
Strut	CHS152,4*12,5	14334	152	N/mm^2	43%	321	N/mm^2	90%
Hoop	h=1300mm,b=300mm, t_{flange}=55mm,t_{web}=15mm	45669	299	N/mm^2	84%	278	N/mm^2	78%
Rods	Circular bar d=55mm	119	316	N/mm^2	89%	320	N/mm^2	90%
Cable top	PG55 A=347mm^2	1259	140	kN	43%	237	kN	73%
Cable bottom	PG75 A=467mm^2	1711	325	kN	74%	178	kN	41%
Rectangular cable	PG40 A=237mm^2	427	17	kN	8%	21	kN	9%

Mass without hoop	23811	Kg
Mass with hoop	69480	kg
Total mass	81220	kg

minimum tensile force in cable	4218N

D_{bottom}=2550mm Resulting forces

Order of variable	Topological/Geometrical	Choice
1st	Number of branches	8X8
2nd	Position of intersection point	z=-13260
3rd	Height above support	2250mm
	Height below support	2550mm
4th	Way of form finding	radial pattern
5th	Pretension for top cable (kN)	170
	Pretension for bottom cable (kN)	145

Load combinations	Displacement (mm)<143	
	upward	downward
SLS LC1 1,0dead+1,0pre	0	-69
SLS LC2 1,0snow+1,0dead+1,0pre	1	-138
SLS LC3 1,0wind+1,0dead+1,0pre	30	-76

Type of connection	Number	Mass (kg)
ETFE beam connection	100	1500
cable and strut connection	128	10240
total		11740

6th	Cross section		ULS LC2 1,5snow+1,2dead+1,0pre			ULS LC3 1,5wind+0,9dead+1,0pre		
Group	Property	Mass (kg)	N (kN)	M_y (kNm)	M_z (kNm)	N (kN)	M_y (kNm)	M_z (kNm)
ETFE beam	CHS114,3*3,2	5961	-	1,1	9,3	-	1,8	5,9
Strut	CHS152,4*12,5	14334	-	25,6	76,4	-	39,7	53
Hoop	h=1300mm,b=300mm, t_{flange}=55mm,t_{web}=15mm	45669	-	6762	47,6	-	6319	16,6
Rods	Circular bar d=55mm	119	-	3,8	3,8	-	3,7	4,7
Cable top	PG55 A=347mm^2	1259	140	0	0	237	0	0
Cable bottom	PG75 A=467mm^2	1711	325	0	0	178	0	0
Rectangular cable	PG40 A=237mm^2	427	17	0	0	21	0	0

Mass without hoop	23811	Kg
Mass with hoop	69480	kg
Total mass	81220	kg

minimum tensile force in cable	4218N

(b) Change D_{top}

D_{top}=1950mm Unity check

Order of variable	Topological/Geometrical	Choice
1st	Number of branches	8X8
2nd	Position of intersection point	z=-13260
3rd	Height above support	1950mnm
	Height below support	2350mm
4th	Way of form finding	radial pattern
5th	Pretension for top cable (kN)	185
	Pretension for bottom cable (kN)	145

Load combinations	Displacement (mm)<143	
	upward	downward
SLS LC1 1,0dead+1,0pre	1	-57
SLS LC2 1,0snow+1,0dead+1,0pre	1	-136
SLS LC3 1,0wind+1,0dead+1,0pre	50	-64

Type of connection	Number	Mass (kg)
ETFE beam connection	100	1500
cable and strut connection	128	10240
total		11740

6th	Cross section		ULS LC2 1,5snow+1,2dead+1,0pre			ULS LC3 1,5wind+0,9dead+1,0pre		
			Stress/Load (Max)		UC	Stress/Load (Max)		UC
Group	Property	Mass (kg)	Quantity	Unit		Quantity	Unit	
ETFE beam	CHS114,3*3,2	5961	332	N/mm^2	94%	195	N/mm^2	55%
Strut	CHS152,4*12,5	13841	156	N/mm^2	44%	329	N/mm^2	93%
Hoop	h=1300mm,b=300mm, t_{flange}=55mm,t_{web}=15mm	45669	313	N/mm^2	88%	289	N/mm^2	81%
Rods	Circular bar d=55mm	119	310	N/mm^2	87%	207	N/mm^2	58%
Cable top	PG55 A=347mm^2	1256	149	kN	46%	250	kN	77%
Cable bottom	PG75 A=467mm^2	1706	342	kN	78%	181	kN	41%
Rectangular cable	PG40 A=237mm^2	427	17	kN	8%	18	kN	8%

Mass without hoop	23310	Kg
Mass with hoop	68979	kg
Total mass	80719	kg

minimum tensile force in cable	4012N

D_{top}=1950mm Resulting forces

Order of variable	Topological/Geometrical	Choice
1st	Number of branches	8X8
2nd	Position of intersection point	z=-13260
3rd	Height above support	1950mnm
	Height below support	2350mm
4th	Way of form finding	radial pattern
5th	Pretension for top cable(kN)	185
	Pretension for bottom cable(kN)	145

Load combinations	Displacement (mm)<143	
	upward	downward
SLS LC1 1,0dead+1,0pre	1	-57
SLS LC2 1,0snow+1,0dead+1,0pre	1	-136
SLS LC3 1,0wind+1,0dead+1,0pre	50	-64

Type of connection	Number	Mass (kg)
ETFE beam connection	100	1500
cable and strut connection	128	10240
total		11740

6th	Cross section		ULS LC2 1,5snow+1,2dead+1,0pre			ULS LC3 1,5wind+0,9dead+1,0pre		
Group	Property	Mass (kg)	N (kN)	M_y (kNm)	M_z (kNm)	N (kN)	M_y (kNm)	M_z (kNm)
ETFE beam	CHS114,3*3,2	5961	-	1,1	9,4	-	1,9	5,9
Strut	CHS152,4*12,5	13841	-	25,3	7,5	-	41,5	52,9
Hoop	h=1300mm,b=300mm, t_{flange}=55mm,t_{web}=15mm	45669	-	7090	47,4	-	6555	16,2
Rods	Circular bar d=55mm	119	-	3,7	3,7	-	2,6	3,1
Cable top	PG55 A=347mm^2	1256	149	0	0	250	0	0
Cable bottom	PG75 A=467mm^2	1706	342	0	0	181	0	0
Rectangular cable	PG40 A=237mm^2	427	17	0	0	18	0	0

Mass without hoop	23310	Kg
Mass with hoop	68979	kg
Total mass	80719	kg

minimum tensile force in cable	4012N

D_{top}=2050mm Unity check

Order of variable	Topological/Geometrical	Choice
1st	Number of branches	8X8
2nd	Position of intersection point	z=-13260
3rd	Height above support	2050mm
	Height below support	2350mm
4th	Way of form finding	radial pattern
5th	Pretension for top cable (kN)	180
	Pretension for bottom cable (kN)	150

Load combinations	Displacement (mm)<143	
	upward	downward
SLS LC1 1,0dead+1,0pre	0	-66
SLS LC2 1,0snow+1,0dead+1,0pre	4	-142
SLS LC3 1,0wind+1,0dead+1,0pre	37	-73

Type of connection	Number	Mass (kg)
ETFE beam connection	100	1500
cable and strut connection	128	10240
total		11740

6th	Cross section		ULS LC2 1,5snow+1,2dead+1,0pre			ULS LC3 1,5wind+0,9dead+1,0pre		
			Stress/Load (Max)		UC	Stress/Load (Max)		UC
Group	Property	Mass (kg)	Quantity	Unit		Quantity	Unit	
ETFE beam	CHS114,3*3,2	5961	332	N/mm^2	94%	195	N/mm^2	55%
Strut	CHS152,4*12,5	13841	149	N/mm^2	42%	331	N/mm^2	93%
Hoop	h=1300mm,b=300mm, t_{flange}=55mm,t_{web}=15mm	45669	315	N/mm^2	89%	293	N/mm^2	83%
Rods	Circular bar d=55mm	119	313	N/mm^2	88%	238	N/mm^2	67%
Cable top	PG55 A=347mm^2	1257	149	kN	46%	250	kN	77%
Cable bottom	PG75 A=467mm^2	1706	343	kN	78%	185	kN	42%
Rectangular cable	PG40 A=237mm^2	427	17	kN	8%	19	kN	9%

Mass without hoop	23311	Kg
Mass with hoop	68980	kg
Total mass	80720	kg

minimum tensile force in cable	5366N

D_{top}=2050mm Resulting forces

Order of variable	Topological/Geometrical	Choice
1st	Number of branches	8X8
2nd	Position of intersection point	z=-13260
3rd	Height above support	2050mm
	Height below support	2350mm
4th	Way of form finding	radial pattern
5th	Pretension for top cable (kN)	180
	Pretension for bottom cable (kN)	150

Load combinations	Displacement (mm)<143	
	upward	downward
SLS LC1 1,0dead+1,0pre	0	-66
SLS LC2 1,0snow+1,0dead+1,0pre	4	-142
SLS LC3 1,0wind+1,0dead+1,0pre	37	-73

Type of connection	Number	Mass (kg)
ETFE beam connection	100	1500
cable and strut connection	128	10240
total		11740

6th	Cross section		ULS LC2 1,5snow+1,2dead+1,0pre			ULS LC3 1,5wind+0,9dead+1,0pre		
Group	Property	Mass (kg)	N (kN)	M_y (kNm)	M_z (kNm)	N (kN)	M_y (kNm)	M_z (kNm)
ETFE beam	CHS114,3*3,2	5961	-	1,1	9,2	-	1,9	5,9
Strut	CHS152,4*12,5	13841	-	24,3	77,3	-	41,3	53,8
Hoop	h=1300mm,b=300mm, t_{flange}=55mm,t_{web}=15mm	45669	-	7139	47,5	-	6652	16,3
Rods	Circular bar d=55mm	119	-	3,8	3,8	-	3	3,6
Cable top	PG55 A=347mm^2	1257	149	0	0	250	0	0
Cable bottom	PG75 A=467mm^2	1706	343	0	0	185	0	0
Rectangular cable	PG40 A=237mm^2	427	17	0	0	19	0	0

Mass without hoop	23311	Kg
Mass with hoop	68980	kg
Total mass	80720	kg

minimum tensile force in cable	5366N

D_{top}=2150mm Unity check

Order of variable	Topological/Geometrical	Choice
1st	Number of branches	8X8
2nd	Position of intersection point	z=-13260
3rd	Height above support	2150mm
	Height below support	2350mm
4th	Way of form finding	radial pattern
5th	Pretension for top cable (kN)	175
	Pretension for bottom cable (kN)	155

Load combinations	Displacement (mm)<143	
	upward	downward
SLS LC1 1,0dead+1,0pre	1	-61
SLS LC2 1,0snow+1,0dead+1,0pre	4	-134
SLS LC3 1,0wind+1,0dead+1,0pre	40	-67

Type of connection	Number	Mass (kg)
ETFE beam connection	100	1500
cable and strut connection	128	10240
total		11740

6th	Cross section		ULS LC2 1,5snow+1,2dead+1,0pre			ULS LC3 1,5wind+0,9dead+1,0pre		
			Stress/Load (Max)		UC	Stress/Load (Max)		UC
Group	Property	Mass (kg)	Quantity	Unit		Quantity	Unit	
ETFE beam	CHS114,3*3,2	5961	332	N/mm^2	94%	215	N/mm^2	61%
Strut	CHS152,4*12,5	13841	154	N/mm^2	43%	322	N/mm^2	91%
Hoop	h=1300mm,b=300mm, t_{flange}=55mm,t_{web}=15mm	45669	312	N/mm^2	88%	293	N/mm^2	83%
Rods	Circular bar d=55mm	119	308	N/mm^2	87%	274	N/mm^2	77%
Cable top	PG55 A=347mm^2	1258	143	kN	44%	245	kN	75%
Cable bottom	PG75 A=467mm^2	1706	343	kN	78%	187	kN	43%
Rectangular cable	PG40 A=237mm^2	427	17	kN	8%	20	kN	9%

Mass without hoop	23312	Kg
Mass with hoop	68981	kg
Total mass	80721	kg

minimum tensile force in cable	1245N

D_{top}=2150mm Resulting forces

Order of variable	Topological/Geometrical	Choice
1st	Number of branches	8X8
2nd	Position of intersection point	z=-13260
3rd	Height above support	2150mm
	Height below support	2350mm
4th	Way of form finding	radial pattern
5th	Pretension for top cable (kN)	175
	Pretension for bottom cable (kN)	155

Load combinations	Displacement (mm)<143	
	upward	downward
SLS LC1 1,0dead+1,0pre	1	-61
SLS LC2 1,0snow+1,0dead+1,0pre	4	-134
SLS LC3 1,0wind+1,0dead+1,0pre	40	-67

Type of connection	Number	Mass (kg)
ETFE beam connection	100	1500
cable and strut connection	128	10240
total		11740

6th	Cross section		ULS LC2 1,5snow+1,2dead+1,0pre			ULS LC3 1,5wind+0,9dead+1,0pre		
Group	Property	Mass (kg)	N (kN)	M_y (kNm)	M_z (kNm)	N (kN)	M_y (kNm)	M_z (kNm)
ETFE beam	CHS114,3*3,2	5961	-	1,1	9,5	-	1,8	5,9
Strut	CHS152,4*12,5	13841	-	24,9	7,4	-	39,8	52,1
Hoop	h=1300mm,b=300mm, t_{flange}=55mm,t_{web}=15mm	45669	-	7072	47,6	-	6650	16,3
Rods	Circular bar d=55mm	119	-	3,7	3,7	-	3,4	4,2
Cable top	PG55 A=347mm^2	1258	143	0	0	245	0	0
Cable bottom	PG75 A=467mm^2	1706	343	0	0	187	0	0
Rectangular cable	PG40 A=237mm^2	427	17	0	0	20	0	0

Mass without hoop	23312	Kg
Mass with hoop	68981	kg
Total mass	80721	kg

minimum tensile force in cable	1245N

D_{top}=2250mm Unity check

Order of variable	Topological/Geometrical	Choice
1st	Number of branches	8X8
2nd	Position of intersection point	z=-13260
3rd	Height above support	2250mm
	Height below support	2350mm
4th	Way of form finding	radial pattern
5th	Pretension for top cable (kN)	175
	Pretension for bottom cable (kN)	160

Load combinations	Displacement (mm)<143	
	upward	downward
SLS LC1 1,0dead+1,0pre	0	-68
SLS LC2 1,0snow+1,0dead+1,0pre	3	-139
SLS LC3 1,0wind+1,0dead+1,0pre	27	-75

Type of connection	Number	Mass (kg)
ETFE beam connection	100	1500
cable and strut connection	128	10240
total		11740

6th	Cross section		ULS LC2 1,5snow+1,2dead+1,0pre			ULS LC3 1,5wind+0,9dead+1,0pre		
			Stress/Load (Max)		UC	Stress/Load (Max)		UC
Group	Property	Mass (kg)	Quantity	Unit		Quantity	Unit	
ETFE beam	CHS114,3*3,2	5961	332	N/mm^2	94%	242	N/mm^2	68%
Strut	CHS152,4*12,5	13841	146	N/mm^2	41%	323	N/mm^2	91%
Hoop	h=1300mm,b=300mm, t_{flange}=55mm,t_{web}=15mm	45669	315	N/mm^2	89%	297	N/mm^2	84%
Rods	Circular bar d=55mm	119	311	N/mm^2	88%	332	N/mm^2	94%
Cable top	PG55 A=347mm^2	1259	143	kN	44%	245	kN	75%
Cable bottom	PG75 A=467mm^2	1706	343	kN	78%	192	kN	44%
Rectangular cable	PG40 A=237mm^2	427	17	kN	8%	21	kN	9%

Mass without Hoop	23313	Kg
Mass with Hoop	68982	kg
Total mass	80722	kg

minimum tensile force in cable	2333N

D_{top}=2250mm Resulting forces

Order of variable	Topological/Geometrical	Choice
1st	Number of branches	8X8
2nd	Position of intersection point	z=-13260
3rd	Height above support	2250mm
	Height below support	2350mm
4th	Way of form finding	radial pattern
5th	Pretension for top cable (kN)	175
	Pretension for bottom cable (kN)	160

Load combinations	Displacement (mm)<143	
	upward	downward
SLS LC1 1,0dead+1,0pre	0	-68
SLS LC2 1,0snow+1,0dead+1,0pre	3	-139
SLS LC3 1,0wind+1,0dead+1,0pre	27	-75

Type of connection	Number	Mass (kg)
ETFE beam connection	100	1500
cable and strut connection	128	10240
total		11740

6th	Cross section		ULS LC2 1,5snow+1,2dead+1,0pre			ULS LC3 1,5wind+0,9dead+1,0pre		
Group	Property	Mass (kg)	N (kN)	M_y (kNm)	M_z (kNm)	N (kN)	M_y (kNm)	M_z (kNm)
ETFE beam	CHS114,3*3,2	5961	-	1,1	9,3	-	1,8	5,9
Strut	CHS152,4*12,5	13841	-	24,1	7,6	-	40,3	52,8
Hoop	h=1300mm,b=300mm, t_{flange}=55mm,t_{web}=15mm	45669	-	7123	47,7	-	6746	16,4
Rods	Circular bar d=55mm	119	-	3,8	3,7	-	3,8	4,9
Cable top	PG55 A=347mm^2	1259	143	0	0	245	0	0
Cable bottom	PG75 A=467mm^2	1706	343	0	0	191	0	0
Rectangular cable	PG40 A=237mm^2	427	17	0	0	21	0	0

Mass without hoop	23313	Kg
Mass with hoop	68982	kg
Total mass	80722	kg

minimum tensile force in cable	2333N

D_{top}=2350mm	Unity check	
Order of variable	**Topological/Geometrical**	**Choice**
1st	Number of branches	8X8
2nd	Position of intersection point	z=-13260
3rd	Height above support	2350mm
	Height below support	2350mm
4th	Way of form finding	radial pattern
5th	Pretension for top cable (kN)	175
	Pretension for bottom cable (kN)	170

Load combinations	**Displacement (mm)<143**	
	upward	downward
SLS LC1 1,0dead+1,0pre	3	-61
SLS LC2 1,0snow+1,0dead+1,0pre	4	-128
SLS LC3 1,0wind+1,0dead+1,0pre	34	-67

Type of connection	Number	Mass (kg)
ETFE beam connection	100	1500
cable and strut connection	128	10240
total		11740

6th	Cross section		ULS LC2 1,5snow+1,2dead+1,0pre			ULS LC3 1,5wind+0,9dead+1,0pre		
			Stress/Load (Max)		UC	Stress/Load (Max)		UC
Group	Property	Mass (kg)	Quantity	Unit		Quantity	Unit	
ETFE beam	CHS114,3*3,2	5961	333	N/mm^2	94%	276	N/mm^2	78%
Strut	CHS152,4*12,5	13841	148	N/mm^2	42%	317	N/mm^2	89%
Hoop	h=1300mm,b=300mm, t_{flange}=55mm,t_{web}=15mm	45669	320	N/mm^2	90%	306	N/mm^2	86%
Rods	Circular bar d=60mm	142	239	N/mm^2	67%	324	N/mm^2	91%
Cable top	PG55 A=347mm^2	1261	143	kN	44%	244	kN	75%
Cable bottom	PG75 A=467mm^2	1706	348	kN	79%	199	kN	45%
Rectangular cable	PG40 A=237mm^2	427	17	kN	8%	24	kN	11%

Mass without hoop	23338	Kg
Mass with hoop	69007	kg
Total mass	80747	kg

minimum tensile force in cable	3414N

D_{top}=2350mm	Resulting forces	
Order of variable	**Topological/Geometrical**	**Choice**
1st	Number of branches	8X8
2nd	Position of intersection point	z=-13260
3rd	Height above support	2350mm
	Height below support	2350mm
4th	Way of form finding	radial pattern
5th	Pretension for top cable (kN)	175
	Pretension for bottom cable (kN)	170

Load combinations	**Displacement (mm)<143**	
	upward	downward
SLS LC1 1,0dead+1,0pre	3	-61
SLS LC2 1,0snow+1,0dead+1,0pre	4	-128
SLS LC3 1,0wind+1,0dead+1,0pre	34	-67

Type of connection	Number	Mass (kg)
ETFE beam connection	100	1500
cable and strut connection	128	10240
total		11740

6th	Cross section		ULS LC2 1,5snow+1,2dead+1,0pre			ULS LC3 1,5wind+0,9dead+1,0pre		
Group	Property	Mass (kg)	N (kN)	M_y (kNm)	M_z (kNm)	N (kN)	M_y (kNm)	M_z (kNm)
ETFE beam	CHS114,3*3,2	5961	-	1,1	9,7	-	1,8	6,1
Strut	CHS152,4*12,5	13841	-	23,8	7,9	-	39,7	51,1
Hoop	h=1300mm,b=300mm, t_{flange}=55mm,t_{web}=15mm	45669	-	7255	47,8	-	6941	16,3
Rods	Circular bar d=60mm	142	-	3,8	3,7	-	5	6,1
Cable top	PG55 A=347mm^2	1261	143	0	0	244	0	0
Cable bottom	PG75 A=467mm^2	1706	349	0	0	199	0	0
Rectangular cable	PG40 A=237mm^2	427	17	0	0	24	0	0

Mass without hoop	23338	Kg
Mass with hoop	69007	kg
Total mass	80747	kg

minimum tensile force in cable	3414N

Appendix H: Buckling check for Structs

In the buckling sheet, all the load inputs are the maximum value in the struts, and the length should be the minimum value of the struts. Element in this most critical situation fulfills the buckling verification, thus no buckling is expected in compression struts. All the formulas are from EN 1993-1-1.

Buckling sheet

Structural system: Axial compressed beam, with possible bending moment, y=strong axes of cross section
Part: Part..

EN 1993-1-1, art. 6.2 and 6.3
National Annex: Dutch

Loads:

N;Ed;1 =	49556	N		gamma;M0 =	1,00	
N;Ed;0 =	49556	N		gamma;M1 =	1,00	
N;Ed;max =	**49556**	**N**	**(=49,56 kN)**	gamma;M2 =	1,25	
e =	20	mm				
M;y,Ed;1 =	0	Nmm				
M;y,Ed;0,5 =	38492652	Nmm				
M;y,Ed;0 =	0	Nmm				
M;y,Ed;max =	**39483772**	**Nmm**	**(=39,48 kNm)**			
M;z,Ed;1 =	0	Nmm				
M;z,Ed;0,5 =	46921384	Nmm				
M;z,Ed;0 =	0	Nmm				
M;z,Ed;max =	**47912504**	**Nmm**	**(=47,91 kNm)**			
g;ev,k =	0,907	N/mm				

Type of profile:

chs	hot-rolled		Type of profile	CHS	
			h =	152,4	mm
Diameter =	152,4	mm	b =	152,4	mm
Thickness Flange (t;f) =	0,0	mm	t;f =	0,0	mm
Thickness Web (t;w) =	12,5	mm	t;w =	12,5	mm
			A =	5494	mm^2
S355			I;y =	13548038	mm^4
E;d =	210000	N/mm^2	I;z =	13548038	mm^4
G;d =	81000	N/mm^2	I;t =	26881471	mm^4
f;y =	355	N/mm^2	I;w =	0	mm^6
Vol. Mass	0,0000785	N/mm^3	W;y,el =	177796	mm^3
			W;z,el =	177796	mm^3

Buckling Length Factor:

	L =	5000	mm	W;y,pl =	245301	mm^3
0,7	L;y,cr =	3500	mm	W;z,pl =	245301	mm^3
1	L;z,cr =	5000	mm			
0,5	L;cr,LT =	2500	mm			
	Lateral-torsional buckl.	relevant	(6.3.1.4, 6.3.2.1)			
	Cross section class:	1	(Table 5.2)			
	Buckling curve y-y:	a	(Table 6.2)	C;my =	1,00	(Table B.3)
	Buckling curve z-z:	a	(Table 6.2)	C;mz =	1,00	(Table B.3)
	Table choice 6.3.3 (4)	B.1	(Annex B, Methode 2)	C;mLT =	1,00	(Table B.3)

Verification:

1 - Compression :	0,03	<= 1	OK	(6.2.4)
2 - Bending moment strong axis:	0,45	<= 1	OK	(6.2.5)
3 - Bending moment weak axis:	0,55	<= 1	OK	(6.2.5)
4 - Bending moment and axial force:	0,51	<= 1	OK	(6.2.9)
5 - Buckling strong axis:	0,04	<= 1	OK	(6.3.1.1)
6 - Buckling weak axis:	0,06	<= 1	OK	(6.3.1.1)
7 - Lateral-torsional buckling:	0,45	<= 1	OK	(6.3.2.1)
8 - Bending and axial force, Check 1 :	0,85	<= 1	OK	(6.3.3)
9 - Bending and axial force, Check 2 :	0,91	<= 1	OK	(6.3.3)

Appendix I: Different designs for cable and strut connection

In this roof system, design the way for cable and strut connection is of great importance. This connection functions in three ways:

1) To guarantee that the cables and struts stay in the right position.
2) To transfer axial force between cables and struts
3) To take the largest bending moments in struts

This requires the connection to be strong enough to withstand external loads and to restrict sliding between cable and strut. Strength of the connection is not tested in this thesis work, but the concept for a efficient design is derived.

Besides, the connection should allow cables go through without change of direction. As is displayed in the figure below, if the cable go through strut with direction changed, additional bending moment occurs due to eccentricity, resulting in rotation in the system.

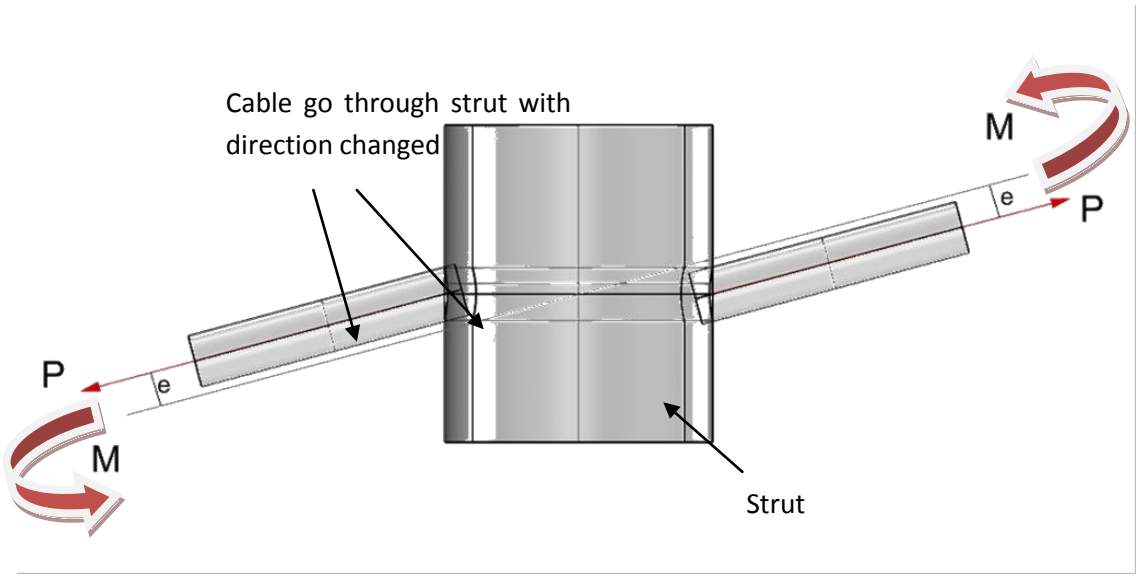

To avoid this rotation, first idea is to design the connection with holes of different angles. The tensegrity of this roof design is double symmetric, thus connections in only ¼ area of the roof need to be designed with holes of different angles. And for each branch of the cable net, one continuous cable is applied for the span. Based on this idea, three clamp systems are designed to restrict the sliding between cable and strut.

However, considering adjustability of the cable angle and the difference between computational model and real construction, in the end cable segments are used and bolted with struts rather than go though them. In this way only one type of connector is applied for all the cable and strut connections.

Version 1

Idea of this connection is to design the holes according to the direction of cables. This clamp is composed of four parts, by tightening the bolts friction is applied on cables to restrict sliding.

However, considering that the largest bending moment in strut occurs at the connection, this design may not be efficient for withstanding bending.

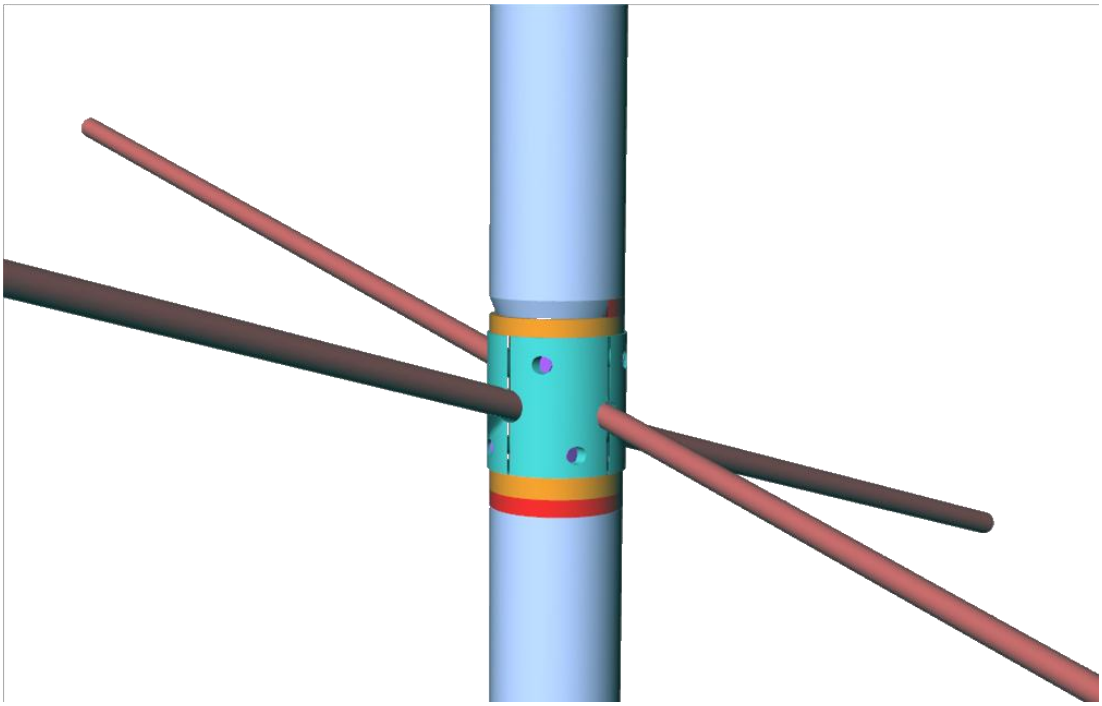

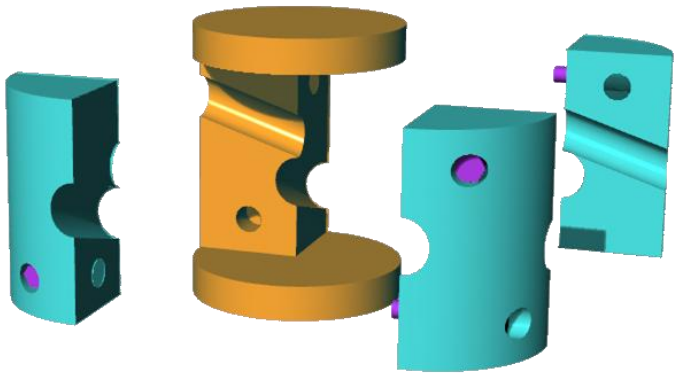

Version 2

The connector designed is composed of two parts, the circular hollow section with the same property of strut, and clamps for tightening the cables. Cable go through the connector, outside the connector two clamps are applied for each cable, in such a way to restrict sliding between cable and strut.

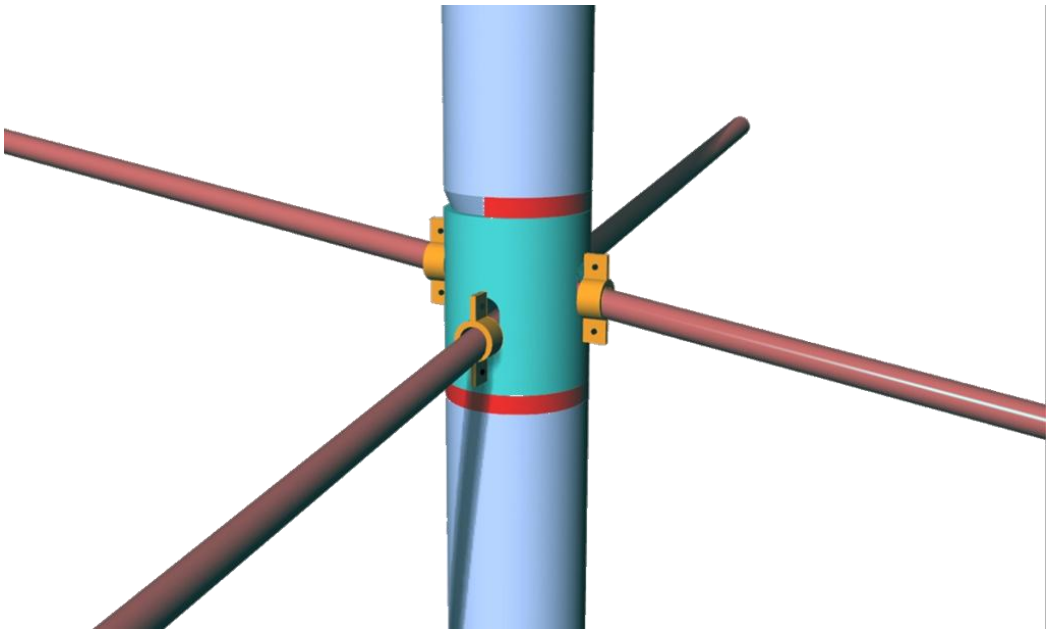

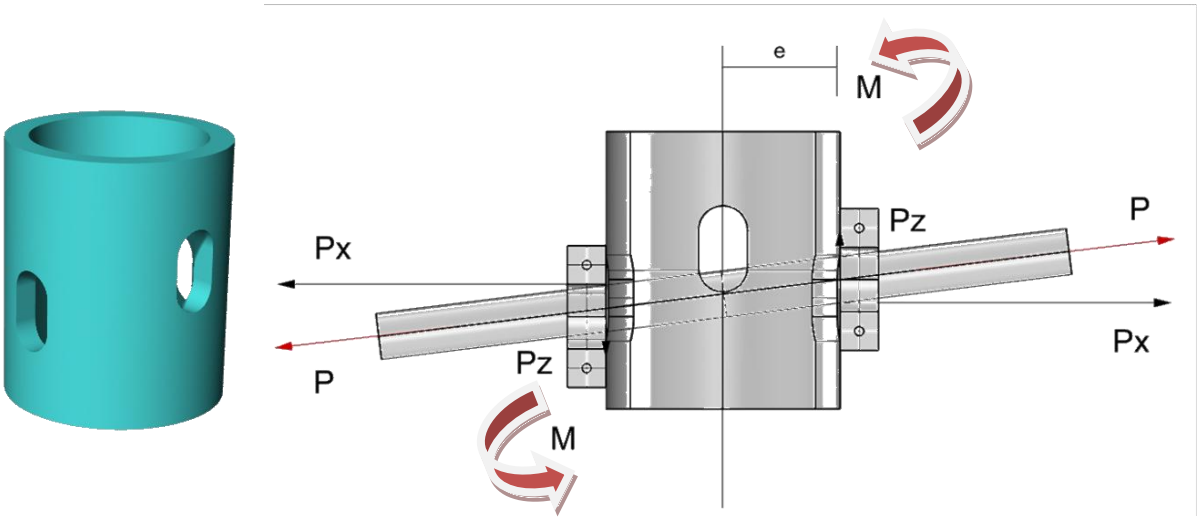

The slotted holes are made on the connector with an intention to allow adjustment of cable angles. However, although the slotted holes allow cable go through strut in a straight line, bending moment still exists in this design. Plus the clamp outside the strut need to be strengthened.

Version 3

By making some improvements of the connection in version two, a similar design is made. In this design, circular holes of different height replaced slotted holes. The cone-shapes clamps are used instead of the two-ear clamps. Still connections in ¼ of the roof area need to be designed differently considering the angles of cables.

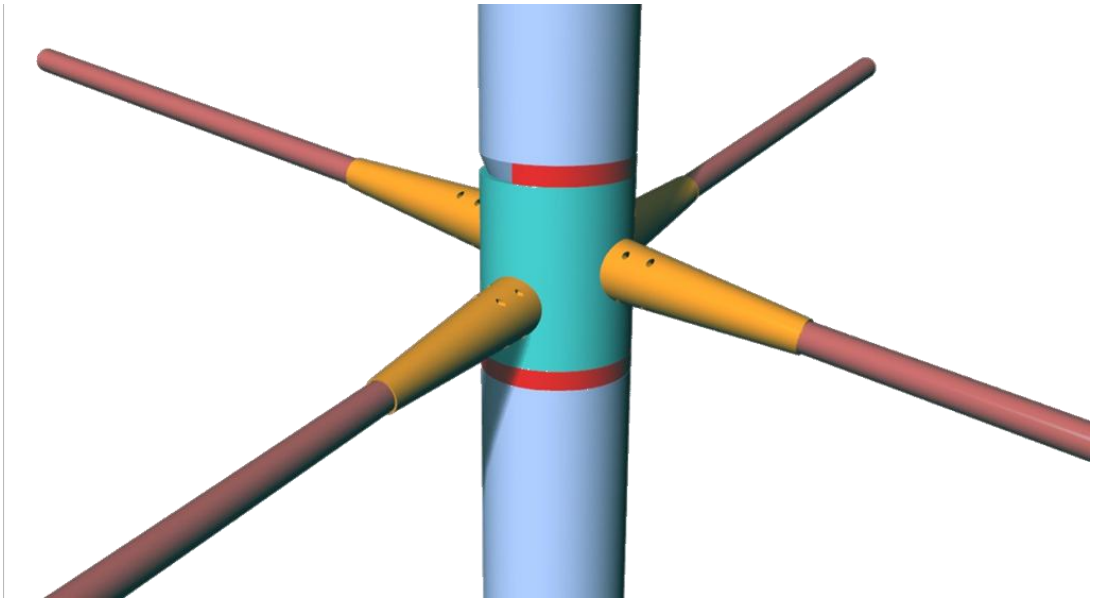

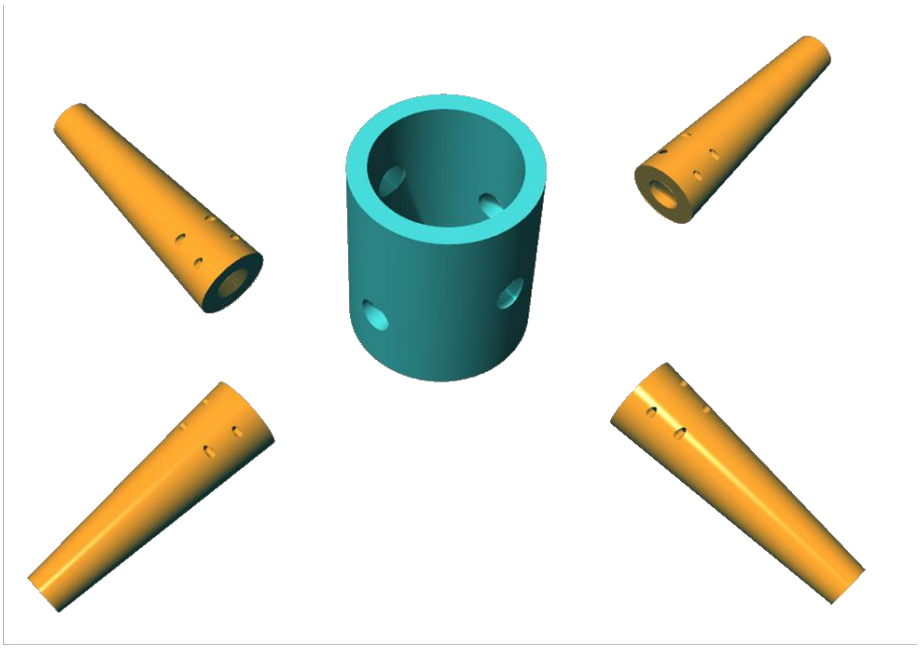

Theoretically this connection should work well on condition that 100% accuracy can be achieved in real construction.

Final version

In this final version, cable segments are used and bolted to a special connector in between two strut elements. Cable angles are adjustable thus only one type of connector is applied for all the cable and strut connections.

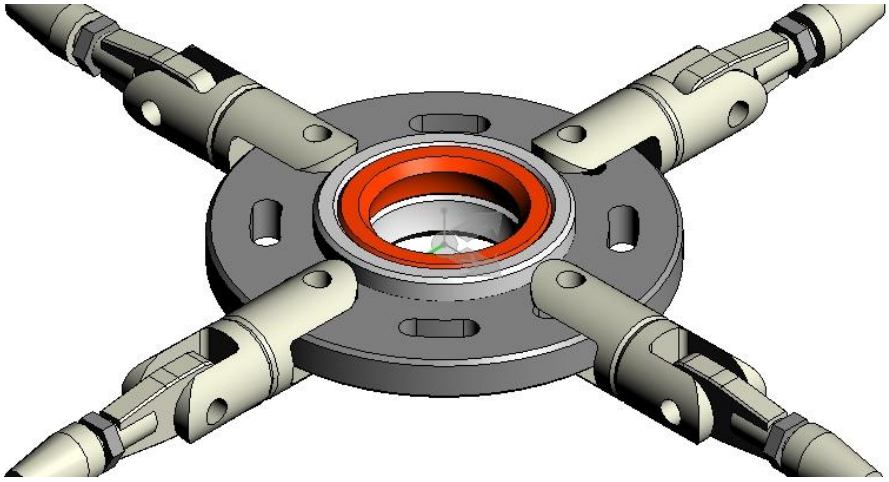

Appendix J : Section view of Het Gelders Huis

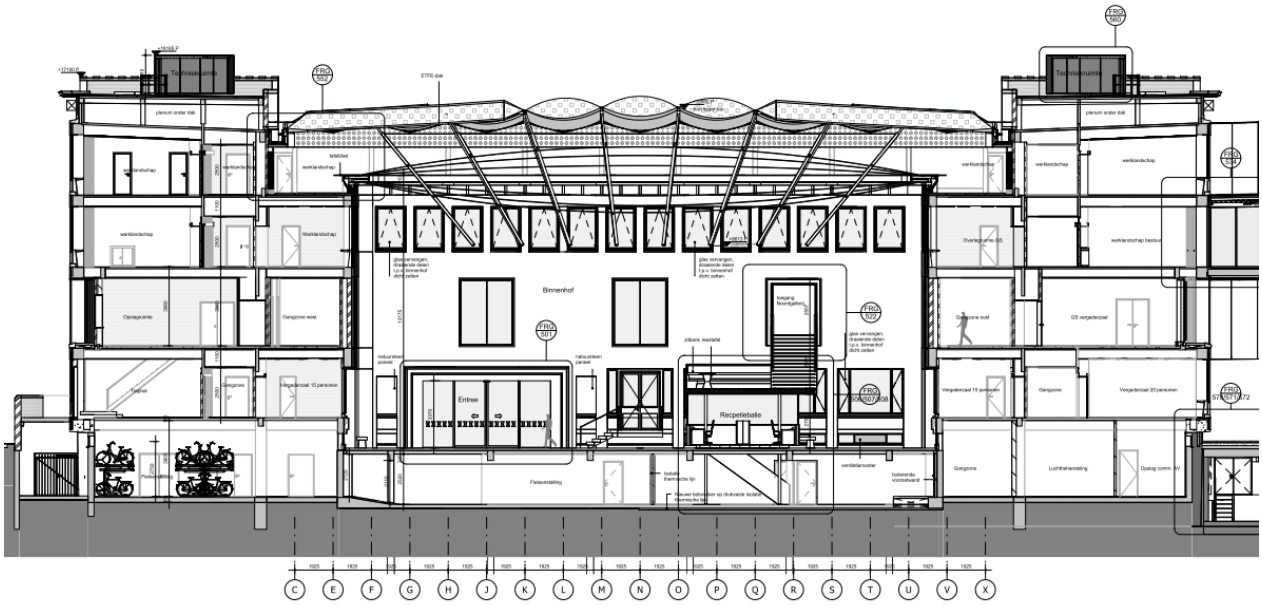

Front view

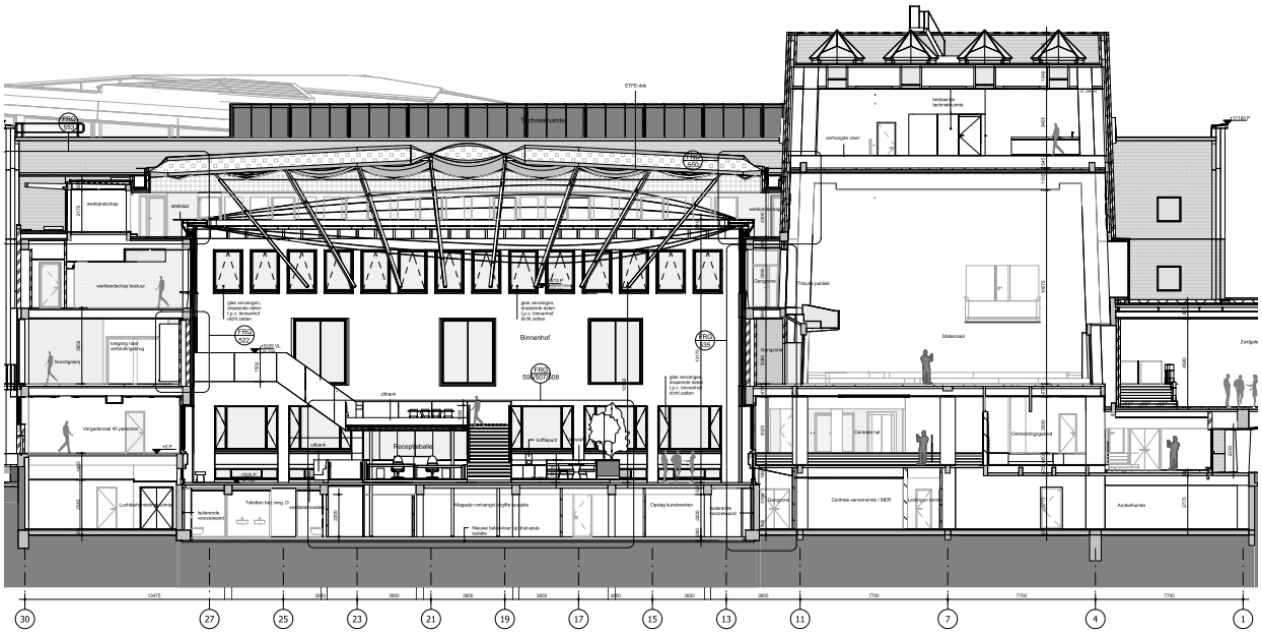

Right view